Cerebral Mitochondrial Dysfunction and the Development of Targeted Therapeutics

Karlsson, Michael

2017

Document Version:
Publisher's PDF, also known as Version of record

Cerebral Mitochondrial Dysfunction and the Development of Targeted Therapeutics

Michael Karlsson

LUND
UNIVERSITY

DOCTORAL DISSERTATION
by due permission of the Faculty of Medicine, Lund University, Sweden.
To be defended at Belfrage Lecture Hall, Biomedical Center,
Lund University, Sweden on December 8th at 1:00 p.m.

Faculty opponent
Professor Patrick Sullivan
Department of Neuroscience,
The Spinal Cord & Brain Injury Research Center,
The University of Kentucky Chandler College of Medicine,
Lexington, KY, USA

Organization LUND UNIVERSITY Faculty of Medicine Department of Clinical Sciences, Lund Mitochondrial Medicine	Document name DOCTORAL DISSERTATION Date of issue December 8th, 2017 Sponsoring organization
Author(s) Michael Karlsson	

Title and subtitle

Cerebral Mitochondrial Dysfunction and the Development of Targeted Therapeutics

Abstract

Mitochondria are indispensable for cerebral energy metabolism and mitochondrial respiratory dysfunction may have immediate and detrimental consequences on brain function and cell survival. Acute mitochondrial dysfunction has been suggested to play a role in the pathophysiology of sepsis and the secondary injury cascade following traumatic brain injury.

In the first part of this thesis we used two distinct animal models of traumatic brain injury, as well as a model of sepsis, to characterize alterations in the electron transport chain in brain tissue. We demonstrated specific alterations in the relative contribution of complex I and complex II of the electron transport chain, as well as varying degree of mitochondrial uncoupling with an associated decrease in mitochondrial respiratory efficiency.

We then developed novel cell-permeable succinate prodrugs that can bypass a mitochondrial complex I deficiency and designed an animal model of acute complex I dysfunction. We concluded that the developed model may be well suited for future in vivo assessment of the cell-permeable succinate prodrugs.

In the final part of this thesis we evaluated the neuroprotective properties of cyclosporine, a drug known to target the mitochondrial permeability transition pore, in a large animal model of focal traumatic brain injury. The randomized blinded placebo-controlled large animal trial demonstrated that cyclosporine decreased the volume of brain injury by 35% assessed using MRI.

In conclusion, we demonstrated that mitochondrial respiration, as an integrative measure of mitochondrial function, displays a wide range of distinct alterations depending on the specific type of injury. Targeting the mitochondria may be a promising treatment strategy.

Key words: mitochondria, brain, animal models, sepsis, traumatic brain injury, neuroprotection, cyclosporine

Classification system and/or index termes (if any):

Supplementary bibliographical information: Doctoral Dissertation Series 2017:174	Language English
ISSN and key title: 1652-8220	ISBN 978-91-7619-556-7
Recipient's notes	Number of pages 85 / Price
	Security classification

Cerebral Mitochondrial Dysfunction and the Development of Targeted Therapeutics

Michael Karlsson

LUND
UNIVERSITY

DOCTORAL DISSERTATION
Mitochondrial Medicine
Department of Clinical Sciences, Lund
Faculty of Medicine
Lund University
2017

Cover by Sofia Lundeholm

Mitochondrial Medicine
Department of Clinical Sciences, Lund

Lund University Faculty of Medicine
Doctoral Dissertation Series 2017:174

ISBN 978-91-7619-556-7
ISSN 1652-8220

Printed in Sweden by Media-Tryck, Lund University
Lund 2017

To Kobayashi

Content

Original articles

This thesis is based on the following papers, referred to in the text by their respective Roman numerals:

I. Karlsson M, Hara N, Morota S, Sjövall F, Kilbaugh T, Hansson MJ, Uchino H, Elmér E. Diverse and tissue-specific mitochondrial respiratory response in a mouse model of sepsis-induced multiple organ failure. *Shock*. 2016;45(4):404-10.

II. Kilbaugh TJ, Karlsson M, Byro M, Bebee A, Ralston J, Sullivan S, Duhaime AC, Hansson MJ, Elmér E, Margulies SS. Mitochondrial bioenergetic alterations after focal traumatic brain injury in the immature brain. *Experimental neurology*. 2015;271:136-44.

III. Kilbaugh TJ, Karlsson M, Duhaime AC, Hansson MJ, Elmér E, Margulies SS. Mitochondrial response in a toddler-aged swine model following diffuse non-impact traumatic brain injury. *Mitochondrion*. 2015;26:19-25.

IV. Ehinger JK, Piel S, Ford R, Karlsson M, Sjövall F, Frostner EA, Morota S, Taylor RW, Turnbull DM, Cornell C, Moss SJ, Metzsch C, Hansson MJ, Fliri H, Elmér E. Cell-permeable succinate prodrugs bypass mitochondrial complex I deficiency. *Nature Communications*. 2016;7:12317.

V. Karlsson M*, Ehinger JK*, Piel S, Sjövall F, Henriksnäs J, Höglund U, Hansson MJ, Elmér E. Changes in energy metabolism due to acute rotenone-induced mitochondrial complex I dysfunction - An in vivo large animal model. *Mitochondrion*. 2016;31:56-62.

VI. Karlsson M, Pukenas B, Plyler R, Stolow M, Byro M, Ehinger JK, Hugerth M, Elmér E, Hansson MJ, Margulies SS, Kilbaugh TJ. Neuroprotective effects of cyclosporine in a porcine model of focal traumatic brain injury. *Manuscript.*

* Contributed equally

The following papers are of relevance to this thesis, but are not formally included in the thesis:

- Kilbaugh TJ, Lvova M, Karlsson M, Zhang Z, Leipzig J, Wallace DC, Margulies SS. Peripheral blood mitochondrial DNA as a biomarker of cerebral mitochondrial dysfunction following traumatic brain injury in a porcine model. *PLoS One*. 2015;10(6):e0130927.
- Hara N, Chijiiwa M, Yara M, Ishida Y, Ogiwara Y, Inazu M, Kuroda M, Karlsson M, Sjovall F, Elmer E, Uchino H. Metabolomic analyses of brain tissue in sepsis induced by cecal ligation reveal specific redox alterations – protective effects of the oxygen radical scavenger edaravone. *Shock*. 2015;44(6):578-84.
- Kilbaugh TJ, Sutton RM, Karlsson M, Hansson MJ, Naim MY, Morgan RW, Bratinov G, Lampe JW, Nadkarni VM, Becker LB, Margulies SS, Berg RA. Persistently altered brain mitochondrial bioenergetics after apparently successful resuscitation from cardiac arrest. *Journal of the American Heart Association*. 2015;4(9):e002232.
- Karlsson M, Hempel C, Sjovall F, Hansson MJ, Kurtzhals JA, Elmer E. Brain mitochondrial function in a murine model of cerebral malaria and the therapeutic effects of rhEPO. *The International Journal of Biochemistry & Cell Biology*. 2013;45(1):151-5.

List of abbreviations

$^{\bullet}OH$	Hydroxyl radical
ADP	Adenosine diphosphate
ANT	Adenine nucleotide translocase
ATP	Adenosine triphosphate
CCI	Controlled cortical impact
CDE	Common data elements
CE-MS	Capillary electrophoresis mass spectrometry
CI	Complex I
CII	Complex II
CIII	Complex III
CIV	Complex IV
CLP	Cecal ligation and puncture
CS	Citrate synthase
CypD	Cyclophilin D
DAI	Diffuse axonal injury
DMF	Dimethyl fumarate
DMSO	Dimethyl sulfoxide
DNA	Deoxyribonucleic acid
DTI	Diffusion tensor imaging
ER	Endoplasmic reticulum
ETC	Electron transport chain
FAD	Flavin adenine dinucleotide
FADH2	1,5-dihydro-flavin adenine dinucleotide
FCCP	Carbonyl cyanide p-(trifluoromethoxy) phenylhydrazone
GCS	Glasgow coma scale
GDP	Guanosine diphosphate
GOS-E	Glasgow outcome scale – Extended
GSH	Reduced glutathione
GSSG	Oxidized glutathione
H_2O_2	Hydrogen peroxide
KO	Knock-out
MiR05	Mitochondrial respiration medium
mPT	Mitochondrial permeability transition
mPTP	Mitochondrial permeability transition pore
MRI	Magnetic resonance imaging
mtDNA	Mitochondrial DNA
NAD^+	Nicotinamide adenine dinucleotide, oxidized form
$FADH_2$	1,5-dihydro-flavin adenine dinucleotide
NADH	Nicotinamide adenine dinucleotide, reduced form
nDNA	Nuclear DNA
O_2^-	Superoxide
$ONOO^-$	Peroxynitrite
PBMC	Peripheral blood mononuclear cells
PDH	Pyruvate dehydrogenase
PK	Pharmacokinetics
PRP	Platelet-rich plasma
RET	Reverse electron transfer
RNR	Rapid non-impact rotational
ROS	Reactive oxygen species
ROX	Residual oxygen consumption
siRNA	Small interfering RNA
SOD	Superoxide dismutase
SUIT	Substrate, uncoupler, inhibitor titration
TBI	Traumatic brain injury
TCA	Tricarboxylic acid
TMPD	N,N,N′,N′-tetramethyl-pphenylenediamine
UCP	Uncoupling protein
VDAC	Voltage dependent anion channel

Summary

Mitochondria are indispensable for cerebral energy metabolism and mitochondrial respiratory dysfunction may have immediate and detrimental consequences on brain function and cell survival. Acute mitochondrial dysfunction has been suggested to play a role in the pathophysiology of sepsis and the secondary injury cascade following traumatic brain injury.

In the first part of this thesis we used two distinct animal models of traumatic brain injury, as well as a model of sepsis, to characterize alterations in the electron transport chain in brain tissue. We demonstrated specific alterations in the relative contribution of complex I and complex II of the electron transport chain, as well as varying degree of mitochondrial uncoupling with an associated decrease in mitochondrial respiratory efficiency.

We then developed novel cell-permeable succinate prodrugs that can bypass a mitochondrial complex I deficiency and designed an animal model of acute complex I dysfunction. We concluded that the developed model may be well suited for future *in vivo* assessment of the cell-permeable succinate prodrugs.

In the final part of this thesis we evaluated the neuroprotective properties of cyclosporine, a drug known to target the mitochondrial permeability transition pore, in a large animal model of focal traumatic brain injury. The randomized blinded placebo-controlled large animal trial demonstrated that cyclosporine decreased the volume of brain injury by 35% assessed using MRI.

In conclusion, we demonstrated that mitochondrial respiration, as an integrative measure of mitochondrial function, displays a wide range of distinct alterations depending on the specific type of injury. Targeting the mitochondria may be a promising treatment strategy.

Background

An introduction to the mitochondrion

The mitochondrion is thought to have a bacterial origin and the endosymbiotic theory suggests that billions of years ago a prokaryotic cell, specialized in oxidative energy metabolism, merged with a non-respiring prokaryotic cell and integrated into the cytoplasm (1-4). This endosymbiotic relationship provided a clear evolutionary advantage, allowing for respiration, in addition to glycolysis, as a source of energy. Reflecting this evolutionary origin, the mitochondrion has its own DNA, with many similarities to bacterial DNA, but throughout evolutionary history most genes with prokaryotic origins have been transferred to the nucleus and only a minor percentage of the total mitochondrial proteome are encoded by mitochondrial DNA (5-9).

The ultrastructure of the mitochondrion with its double membrane is integral to its function. The outer and inner membranes are composed of a phospholipid bilayer and the composition of the inner membrane reflects its bacterial origin. The inner mitochondrial membrane is folded to increase the membrane surface area and these grooves form the cristae. The outer membrane is freely permeable to small molecules, but the inner membrane is highly impermeable to even small ions, and membrane transporters or carriers are necessary for permeation. The common depiction of the mitochondrion as an oval shaped and static organelle is incorrect. Mitochondria are highly dynamic structures that continuously undergo fission and fusion, and also interact with other organelles such as the endoplasmic reticulum (ER). To maintain a vigorous population of mitochondria, the removal and destruction of damaged mitochondria is tightly regulated by a process called mitophagy (10, 11).

Cellular chemical energy is stored as adenosine triphosphate (ATP) and the main task of the mitochondrion is to generate ATP. This stored energy can be released by ATP hydrolysis and utilized by energy-requiring enzymes to support various functions throughout the cell. In the electron transport chain (ETC) of the inner mitochondrial membrane, electrons derived from dietary nutrients are passed down a series of protein complexes that act as a pumps translocating protons from the matrix to the intermembrane space, while generating a proton gradient. The ATP synthase then utilizes this gradient to phosphorylate adenosine diphosphate (ADP), as the protons flow back in the opposite direction (12, 13). This process ultimately converts dietary

nutrients to CO_2 and H_2O, while consuming O_2. The indirect coupling between ATP generation and electron transfer was first proposed by Peter D. Mitchell in 1961 and he was later awarded the Nobel prize for this discovery (14).

Feeding the tricarboxylic acid cycle

Food nutrients, in the form of carbohydrates, fatty acids and amino acids are primarily oxidized in the mitochondria through the tricarboxylic acid (TCA) cycle, as a common pathway for energy metabolism (15). Under aerobic conditions, pyruvate is the end product of glycolysis and the pyruvate dehydrogenase (PDH) complex converts pyruvate to acetyl CoA, which feeds into the TCA cycle. The regulation of the PDH complex is important for overall metabolism and it is regulated by the energy status of the cell reflected in the levels of ATP, acetyl CoA and nicotinamide adenine dinucleotide (NADH). While the PDH complex is technically not part of the TCA cycle it is nonetheless integral to its function.

It is the oxidation of acetyl CoA in the TCA cycle, together with the ETC and oxidative phosphorylation, that produces the majority of the ATP that is generated in the cell. Pyruvate can also be reduced to lactate in a reaction coupled to the oxidization of NADH, which allows glycolysis to proceed under anaerobic conditions in order to generate a limited amount of ATP. The reduction of pyruvate to lactate by lactate dehydrogenase is therefore important under ischemic conditions, when the NADH/NAD+ ratio is elevated as the ETC and oxidative phosphorylation are halted. Lactate that reaches the bloodstream can also be converted back to glucose by the liver through the Cori cycle (16). Recent data even suggests that circulating lactate may, indirectly, be a primary contributor of carbons to the TCA cycle in all tissues except the brain (17).

Our main fuel storage is fatty acids in adipose tissue and during fasting these fatty acids are released into the blood stream. They can then be oxidized, primarily in the muscles and the liver, to provide energy. Fatty acids are metabolized through β-oxidation which takes place in the mitochondrial matrix. β-oxidation involves four reactions and results in two carbons being removed for each round, sequentially shortening the fatty acid chain, and for every round generating acetyl CoA, NADH, and 1,5-dihydro-flavin adenine dinucleotide ($FADH_2$) (18-20).

Ketone bodies are an alternative energy source for cells. Mitochondria in the liver can transfer acetyl CoA derived from fatty acids to ketone bodies, i.e. acetone, acetoacetate, and β-hydroxybutyrate. The brain can utilize ketone bodies during periods of prolonged fasting when fatty acids are mobilized from adipose tissue to produce ketone bodies in the liver. The metabolism of specific amino acids is also

integral to ATP generation in the mitochondria, as their catabolism can generate intermediates to the TCA cycle, as well as pyruvate and acetyl CoA that can feed into the TCA cycle. These amino acids may also enter other pathways resulting in the synthesis of glucose or lipids that indirectly contribute to ATP generation.

The first step of the TCA cycle is the synthesis of citrate from oxaloacetate and acetyl CoA, catalyzed by CS. CS is regulated by substrate availability, as well as citrate, through conformational changes (21). Citrate also inhibits phosphofructokinase, an enzyme in glycolysis, acting as feedback and controlling the supply of acetyl CoA to the TCA cycle. Citrate is then isomerized to isocitrate by the enzyme aconitase. Isocitrate dehydrogenase catalyzes the oxidative decarboxylation of isocitrate to α-ketoglutarate. This is an important rate-limiting step of the TCA cycle that is regulated by the energy status of the cell. High ADP levels and Ca^{2+} activates the enzyme, whereas it is inhibited by NADH and ATP. This step also yields the first of the three NADH molecules, as well as the release of CO_2. The conversion of α-ketoglutarate to succinyl CoA, releasing the second NADH of the TCA cycle, is catalyzed by α-ketoglutarate dehydrogenase. This rate-limiting enzymatic reaction is activated by Ca^{2+} and inhibited by its products succinyl CoA and NADH. Thereafter, succinyl CoA synthetase cleaves the high-energy thioester bond of succinyl CoA in a reversible reaction, generating succinate. This reaction is coupled to the phosphorylation of guanosine diphosphate (GDP). Succinate dehydrogenase oxidizes succinate to fumarate, coupled to the reduction of ubiquinone, also called coenzyme Q, to ubiquinol, via the reduction of FAD to $FADH_2$. Succinate dehydrogenase is located at the inner mitochondrial membrane and is also referred to as complex II (CII) of the ETC. Fumarate is then hydrated to malate, in a reversible reaction catalyzed by fumarate hydratase. Malate dehydrogenase reversibly catalyzes the oxidization of malate to oxaloacetate while simultaneously producing the final NADH molecule. Thereafter the cycle starts all over again (15). The addition of each acetyl CoA to the TCA cycle does not consume nor produce any intermediates and for every two carbons entering as acetyl CoA, two carbons exits as CO_2. The summation of the TCA cycle is that for every turn, three pairs of electrons reduce three NAD+ to NADH and one pair of electrons reduces flavin adenine dinucleotide (FAD) to $FADH_2$.

The electron transport chain and oxidative phosphorylation

The metabolism described above is in essence a series of reactions to produce redox energy that is to be transferred to the ETC, where NADH donates electrons to

complex I (CI), and succinate donates electrons to CII and reduces FAD to $FADH_2$. Electrons are then transferred down the ETC with oxygen as the final electron acceptor. The need for oxygen as an electron acceptor in the ETC accounts for the vast majority of the body's use of oxygen and is thus in essence, along with extrusion of CO_2, the reason why we need to breathe in order to stay alive.

The ETC takes place in the inner mitochondrial membrane and consists of four protein complexes. Ubiquinone and cytochrome c receive electrons from the donating complexes and subsequently donate the electrons further down the chain. These reactions are coupled to oxidation-driven proton pumps, at CI, complex III (CIII) and complex IV (CIV), pumping protons from the matrix to the intermembrane space. The complexes are not randomly distributed, but may be assembled into supercomplexes. The majority of CI for example, seems to be assembled into supercomplexes together with CIII and CIV, rather than existing as individual and discrete complexes (22). The flow of electrons and the coupled proton pumping creates an electrochemical gradient across the inner mitochondrial membrane and it is this gradient that then drives ATP synthesis. The ATP synthase can also go in reverse and instead hydrolyze ATP to maintain the electrochemical gradient (5).

An important group of proteins relevant to the electrochemical gradient over the inner mitochondrial membrane are the so-called uncoupling proteins. These are responsible for a proton leak across the inner mitochondrial membrane that does not contribute to ATP generation. The first uncoupling protein that was discovered was thermogenin, also referred to as uncoupling protein (UCP) 1 and is found in brown adipose tissue (23). It is unclear what role UCP1 plays in adult human physiology, but it is known to play an important role in neonates because of its ability to generate heat. The significance of UCP2, as well as the other proposed uncoupling proteins, is not as clear but seems to be very different from that of UCP1. UCP2, which is expressed in various tissues including the brain, does not seem to be involved in heat generation. Instead its primary function may be that of handling reactive oxygen species (ROS) in pathological states by inhibiting cell death through mild uncoupling. Preclinical data suggests that neuronal survival correlates with increased expression of UCP2 and, more specifically, overexpression of UCP2 seems to be neuroprotective in animal models of traumatic brain injury (TBI) (24, 25). There is also an endogenous mild proton leak in all mitochondria that is independent of the uncoupling proteins (5). This may be a protective mechanism related to the fact that a high electrochemical gradient is linked to more production of ROS and a basal proton leak may thus be a way to control oxidative stress (26).

Mitochondrial generation and handling of reactive oxygen species

ROS are oxygen-derived molecules with a free unpaired electron and are potentially damaging to cellular structures, including the mitochondrion. ROS generation is not only a pathological mechanism, as it is also of importance for normal cellular processes such as intracellular signaling, including the adaptation to cellular stress by regulating metabolism and mitochondrial dynamics (27). Mitochondria, and more specifically the ETC, are responsible for the majority of the ROS generation. In the ETC there are numerous sites where a two-electron carrier donates electrons to one-electron carriers and these sites are potential sources of ROS (5, 28, 29).

Mitochondria generate ROS by incomplete reduction of O_2 and the primary ROS produced under these circumstances is superoxide (O_2^-), although this depends on the cellular context. O_2^- can in turn generate peroxynitrite when nitric oxide (NO) is present as well as hydroxyl radicals ($^{\bullet}OH$) in the presence of Fe^{2+}. CI and CIII are considered to be the major sources of ROS production, but under physiological conditions the generation of O_2^- by CIII is low compared with that of CI (5, 30). The electron-transferring flavoprotein and glycerophosphate dehydrogenase are also thought to be major sites of ROS production (31, 32). Previously, it has been argued that ROS from the ETC can only be produced at CI and CIII, but new data indicate that also CII may be a direct source of ROS (33-35).

CII may also play an indirect role in ROS generation through reverse electron transfer (RET), when electrons flow from succinate to O_2 with RET through CI, this however is the subject of an ongoing debate. Under physiological conditions it is unclear if RET occurs because succinate is generated by NAD-dependent dehydrogenases in the TCA cycle (36, 37). It has, however, been suggested to play a role in the pathophysiology of ischemia-reperfusion injury. Reperfusion is essential for survival but it also initiates oxidative damage through the generation of ROS (38). This burst in ROS during the reperfusion phase may be due to the rapid metabolism of succinate and the reversal of CII, driving extensive ROS generation at CI (39). This theory regarding succinate-fueled RET driven O_2^- production was however recently disputed and it was argued that conditions are unfavorable for RET during early reperfusion and that the rapid loss of accumulated succinate can be explained by its efflux. Measurements of ROS during the reperfusion phase detected major increases in ROS only after mitochondrial permeability transition pore (mPTP) opening was first detected, most likely triggered by increased concentrations of Ca^{2+} rather than triggered directly by ROS (40), and this explanation is in line with earlier data (41).

The concentration of ROS is tightly regulated by antioxidant defense systems and it is only when the antioxidant capacity is overwhelmed, with dramatic increases in ROS

concentrations, that there is oxidative damage to the cell (31). The effective removal of O_2^- is therefore critical for cell survival. Animals deficient in mitochondrial SOD die at a very young age, illustrating the necessity of this endogenous antioxidant mechanism (42). Most O_2^- will immediately and spontaneously dismutate to O_2 and hydrogen peroxide (H_2O_2), but the process is accelerated by superoxide dismutase (SOD). SODs are thus the first line of defense against oxidative damage, converting O_2^- to H_2O_2, which is then converted to H_2O by glutathione peroxidase. There are three different SODs, the primarily cytoplasmic SOD1, the mitochondrial SOD2 found in the matrix, and SOD3 which is located extracellularly (43).

Since most O_2^- is converted to H_2O_2 and since H_2O_2 is reasonably stable and permeates membranes, H_2O_2 is often utilized as a proxy for overall ROS generation and is measurable with various probes (31). The data presented above regarding ROS have primarily been elucidated by work performed on isolated mitochondria, as it is difficult to provide accurate and quantitative results using tissue and intact cells (44). The translatability and *in vivo* relevance of this data is unclear and one must be cautious not to over-interpret the data (31, 45).

Mitochondrial calcium buffering

The cellular concentration of Ca^{2+} is tightly controlled as Ca^{2+} plays an important role in cell signaling. In the context of mitochondrial bioenergetics, it should be noted that the Ca^{2+} levels are also a mechanism through which mitochondrial bioenergetics and oxidative stress is regulated. Calcium homeostasis is dependent on the mitochondrial membrane potential and is therefore linked to a functioning ETC (46). Ca^{2+} also has the ability to regulate enzymes in the TCA cycle and calcium homeostasis is thus fundamental to overall metabolism (47, 48).

Mitochondria play a key role in calcium homeostasis and may act as a cytosolic buffer that transiently takes up Ca^{2+} from the cytosol and then holds it as inactive calcium phosphate complexes. Ca^{2+} levels in the cytoplasm are kept at a concentration that is 1000-10000 times lower than that of the extracellular space and this difference in Ca^{2+} levels is upheld by sodium-calcium exchangers and Ca^{2+} ATPases in the plasma membrane, in addition to the buffering capacities of the ER and mitochondria. The most substantial storage site of Ca^{2+} is the ER, however there is a significant interplay between the ER and the mitochondria (49).

The mitochondrial permeability transition pore and cyclosporine

Even though mitochondria can take up large amounts of Ca^{2+}, a threshold is eventually reached and the inner mitochondrial membrane will suddenly lose its membrane integrity and undergo permeability transition through the opening of the mitochondrial permeability transition pore (mPTP), with a subsequent loss of ATP production, a spike in ROS generation, and the release of pro-apoptotic factors. The sudden increase in permeability has detrimental effects for the cell. When protons flow back into the mitochondrial matrix, they cause an osmotic influx of water, which in turn results in the rupturing of the outer mitochondrial membrane (50-53). This phenomenon was observed in early studies of mitochondrial physiology during the isolation process of mitochondria, but was considered a non-specific methodological artifact (54). In the late 1970s it was suggested that mitochondrial permeability transition (mPT) was in fact the result of a pore formation and that it was both tightly regulated and reversible (55-58).

Several factors can sensitize or desensitize the mitochondria to mPT. Calcium concentration is the most important aspect and may independently, at sufficient concentrations, activate mPT regardless of other factors. Opening of the mPTP in a specific mitochondrion also results in the flow of Ca^{2+} out of that mitochondrion, resulting in elevated cytosolic Ca^{2+} concentrations, which may lead to a vicious chain of reactions with calcium overload activating mPT in other mitochondria. Excessive ROS generation and an oxidized redox status of glutathione may also stimulate mPTP opening. Inorganic phosphate and certain fatty acids decreases the Ca^{2+} concentration threshold for activation of mPT, but will not independently activate it (59-61). Cations such as Mg^{2+} counteract the Ca^{2+} effect through competitive binding. Finally, high levels of ATP, ADP, and a reduced NADH/ NAD+ ratio also decrease the activation threshold for mPT (56, 59, 62, 63).

The exact configuration of the mPTP is a controversial topic, but regardless of the exact conformation it is established that the opening of the mPTP can be inhibited, or at least delayed, by cyclosporine (64). Cyclosporine was discovered as a metabolite from the fungi *Tolypocladium inflatum Gams*, isolated from soil samples collected from the Hardanger Vidda in southern Norway in 1969 and was later discovered to have remarkable immunosuppressive properties. It has been used for immunosuppression in transplant medicine since the early 1980s (65-67). Cyclosporine acts as an immunosuppressant through inhibition of calcineurin, which in turn blocks T cell activation. Cyclosporine's interaction with the mPTP is distinct from its ability to inhibit calcineurin.

A key component of the mPTP is thought to be cyclophilin D (CypD). Cyclosporine binds to CypD in the mitochondrial matrix and consequently inhibits mPTP formation (68-70). Cyclosporine is not a blocker of mPT, but rather acts as a regulator and desensitizer of mPTP formation. Cyclosporine's ability to inhibit the mPTP can be overridden by increasing concentrations of Ca^{2+} (71). This ability of cyclosporine to significantly increase the calcium retention capacity has been shown in mitochondria isolated from rodent heart, liver and brain, as well as mitochondria isolated from the corresponding human tissues (41, 72-76).

It was shown that mitochondria isolated from $Ppif^{-/-}$ KO mutant mice become insensitive to Ca^{2+} induced mPTP, while still having normal development (77). Ppif is the gene that codes for CypD and these mice thus lack CypD (5, 77). The $Ppif^{-/-}$ mice also seem to be somewhat protected *in vivo* from ischemia-reperfusion injury (77). Specifically, in the context of neuronal cell death following cerebral ischemia, it has been shown that $Ppif^{-/-}$ mice have a decreased brain infarct size in a middle cerebral artery occlusion and reperfusion model (78). Further underlining the importance of CypD in mPTP formation, it has been shown that mitochondria from mice overexpressing CypD exhibits mitochondrial swelling, together with subsequent spontaneous cell death (68).

In addition to CypD, many other components of the mPTP have been proposed (79, 80). For example, it was suggested that the voltage dependent anion channel (VDAC) may be part of the mPTP (81, 82). However, subsequent KO studies ($VDAC^{-/-}$) using mice showed that VDAC was not necessary for mPTP formation (83, 84). It has also been suggested that the Adenine Nucleotide Translocase (ANT) may be involved in the formation of the mPTP (85-87). CypD was shown to bind to ANT and that this binding is sensitive to cyclosporine (82, 88). Furthermore, ATP and ADP, i.e. substrates transported by the ANT can inhibit mPT (55, 89). However, the ANT hypothesis has also been disputed, as it was shown in KO studies that liver cells from mice lacking ANT1 and ANT2, may still undergo cyclosporine-sensitive mPT (90). ANT is perhaps not a critical component of mPT but may still have a regulating role as the required calcium dose was considerably higher compared to controls. These mice also have the ANT4 homolog that could explain this phenomenon, or perhaps other mitochondrial carriers can replace the role of ANT (91, 92).

It has also been argued that the ATP synthase, and more specifically the c-subunit ring in the F_o subunit of the ATP synthase, may contribute to the formation of the mPTP. It has been shown that it can form a voltage-sensitive channel, and that its opening leads to rapid and uncontrolled depolarization of the inner mitochondrial membrane. Depletion of the c-subunit with small interfering RNA (siRNA) attenuates Ca^{2+} induced inner mitochondrial membrane depolarization and cell death, while increasing the expression of the c-subunit promotes cell death and it has thus been argued that the c-subunit is required for mPT (80, 93-97). Halestrap et al.

however argued that this may be due an indirect effect related to decreased ATP generation (79).

The particularities of cerebral metabolism

The adult brain makes up a mere 1-2% of the total body weight, but at rest the brain accounts for approximately 20% of basal oxygen consumption (98). Plasma glucose is the primary energy substrate for the brain in the normal fed state (99). The brain is given metabolic priority over other organs as the brain has a need for unimpaired oxidative phosphorylation for its energy supply and is also very sensitive to acidosis. The fact that the brain's GLUT-3 transporter is insulin-insensitive highlights the importance of brain metabolism. Energy substrates for the brain must be able to cross the blood-brain barrier and circulating fatty acids do not contribute in any meaningful way to brain metabolism since they are bound to albumin and do not cross the blood-brain barrier efficiently. If the blood concentration of glucose falls below a certain threshold, cerebral function is impaired, as the brain does not contain any significant stores of glycogen and is thus completely dependent on a continuous supply of glucose from the blood. The interrupted supply of glucose is an often neglected part of brain ischemia. As discussed earlier, ketone bodies can supply the brain with fuel during prolonged fasting, but if the hypoglycemia is rapid, irreversible brain damage may occur.

The early work on elucidating the configuration and function of the mPTP was primarily executed in mitochondria derived from liver and heart, and it was initially suggested that the brain may possess distinctive characteristics in regards to the mPTP. Early studies even suggested that brain mitochondria are relatively resistant to mPT (100-102). It was suggested that cyclosporine is a less potent inhibitor in brain-derived mitochondria compared to mitochondria derived from the liver (103, 104). It was furthermore argued that brain mitochondria may be more heterogeneous in their response to calcium overload (105), but these findings were later disputed and it was demonstrated that brain mitochondria do in fact undergo homogenous mPT when exposed to calcium overload (74, 106, 107). Importantly, the ability of cyclosporine to significantly increase the calcium retention capacity has been demonstrated in mitochondria isolated from human brain tissue (41).

Mitochondria in excitable tissues, such as the brain, are important for calcium homeostasis, as uninterrupted cerebral metabolism and oxidative phosphorylation is essential to uphold the ion gradients over the cell membrane that are required for synaptic transmission. Excitotoxicity is important in the context of cerebral metabolism and mitochondrial dysfunction. Excitotoxicity aggravates the calcium

induced mPTP formation in brain injury, in addition to activating mPTP by ischemia-reperfusion injury (108, 109). During excitotoxicity, NMDA and AMPA receptors are over-activated by excessive glutamate, which is the primary excitatory neurotransmitter (108, 109). Glutamate binding depolarizes the membrane, resulting in opening of Ca^{2+} channels with subsequent dramatic increases in Ca^{2+}. Since the regulation of Ca^{2+} homeostasis is highly dependent on ATP, a bioenergetic dysfunction further exacerbates Ca^{2+} toxicity (110).

Sepsis and mitochondrial dysfunction

The clinical presentation of sepsis is highly variable and dependent on underlying factors related to the infection, as well as the *a priori* status of the patient. Sepsis was extremely lethal before the advent of modern intensive care and, as recently as 30 years ago, the rates of in-hospital death from septic shock exceeded 80% (111, 112). With improvements in clinical management the 28-day mortality in septic shock is now reported to be 24-60% (113-117). This variation in the reported mortality may be related to problems with the previous definition of sepsis, which was implemented differently.

Sepsis is not a disease, but rather a syndrome. The definition of sepsis was recently updated and should now be defined as *a life-threatening organ dysfunction caused by a dysregulated host response to infection* (118). From a clinical perspective, organ dysfunction can be defined as an increase of 2 points or more on the Sequential Organ Failure Assessment (SOFA) score in patients with confirmed or suspected infection. Septic shock is *a subset of patients with profound circulatory, cellular, and metabolic abnormalities* (118). Patients with septic shock are defined by a vasopressor requirement in the absence of hypovolemia, to maintain a minimum mean arterial pressure of 65 mm Hg and a serum lactate level greater than 2 mmol/L (118). Patients with sepsis can also be diagnosed with a more rapid bedside clinical score termed qSOFA, if they have a respiratory rate of 22 per min or above, altered mentation, or a systolic blood pressure of 100 mm Hg or less (118).

Unfortunately, there is not a clear understanding of the pathophysiology of sepsis. However, it is thought to involve a dysregulated immune response, activated coagulation, and a pathophysiological role of the endothelium (112). Mitochondrial dysfunction has also been suggested to play a role in the pathophysiology (119). Elevated levels of blood lactate, which are undoubtedly a hallmark of sepsis, may theoretically be partially due to a dysfunctional ETC irrespective of oxygen availability. However, organ hypo-perfusion and decreased O_2 delivery certainly also contributes to a significant portion of elevated lactate levels (120, 121).

Oxygen concentrations in organs during sepsis can be normal or higher than normal, and this does not seem to be related to ischemia as the failing organs do not exhibit major cell death and are able to recover when sepsis resolves (122-125). The data on mitochondrial dysfunction in sepsis are seemingly contradictory. Multiple studies have indicated altered mitochondrial function (126-129). Most studies come to the conclusion that there is a reduced mitochondrial respiratory function, but a few studies have seemingly indicated increased respiration (130, 131). The conflicting data may be due to, variability of model system, the specific organ, and the time of observation.

Encephalopathy is a frequent manifestation of sepsis and is also an independent predictor of mortality (117). It has been shown that sepsis can induce increased uncoupling of the oxidative phosphorylation system in brain homogenates from a rodent model of sepsis and there is evidence that links a bioenergetic dysfunction to oxidative stress in septic encephalopathy (117, 132). Septic encephalopathy also involves a dysregulated inflammatory response, neurotransmission disturbances, and vascular dysfunction (117).

The incomplete understanding of the pathophysiological mechanisms behind sepsis may explain the fact that there are currently no targeted therapeutics specifically for sepsis. Multiple therapeutics have shown promise in early development, but to date all large phase III trials have failed (133). Based on preclinical data, mitochondrially targeted drugs have been suggested as possible therapeutics for sepsis (134).

Traumatic brain injury and mitochondrial dysfunction

TBI is caused by a blow to the head or penetrating trauma and is a serious public health problem globally. In the US alone, the Center for Disease Control estimated that in 2010 2.5 million TBI occurred as an isolated injury or in combination with other injuries. Almost one third of all civilian trauma-related deaths are related to TBI. The burden of TBI is greatest in low- and middle-income countries with more trauma overall and also over doubled risk of dying from severe TBI (135). TBI can cause a wide range of symptoms affecting memory, balance, as well as causing emotional disturbance, including depression, anxiety and aggressive behavior. Patients who have suffered from a TBI also have an increased risk of drug and alcohol abuse together with a subsequent increased risk of suicide (136, 137). There is also a growing awareness about the long term risk related to neurodegenerative brain disorders following TBI.

TBI is classified as mild, moderate or severe based on the Glasgow Coma Scale (GCS), which is often the primary classification of patients in clinical trials. However,

TBI encompasses a number of different phenotypes under one term and can, in addition to the GCS, be classified into subtypes based on neuroimaging and pathoanatomic features. The injury can be closed or penetrating and furthermore classified as focal or diffuse. Additionally, it is common for both types of injury to exist alongside (138-140). Focal injuries are inherently heterogeneous and the symptoms are related to the anatomical location of the injury. Blast injuries seem to have distinct characteristics (138). Diffuse axonal injury (DAI) manifests with little apparent damage on neuroimaging and is difficult to detect noninvasively (140), but may be observed with MRI, especially when utilizing diffusion tensor imaging (DTI) (141). There may also be hemorrhage caused by the trauma which can be classified according to location and vascular origin.

From a pathophysiological perspective TBI occurs in two phases. First, there is the primary injury associated with structural damage to the brain, which is then followed by a secondary injury. Altered metabolism and energy deficits are prominent characteristics post injury (142, 143) and more specifically, mitochondrial dysfunction is thought to play a pivotal role in the secondary injury (144-146). Since the brain needs unimpaired oxidative phosphorylation for its energy supply, mitochondrial dysfunction and a subsequent energy deficit will have rapid detrimental effects. Mitochondrial function is thus extremely important for cell survival following TBI (144).

The opening of the mPTP following TBI has been proposed to be a decisive pathophysiological mechanism in the secondary injury cascade and cyclosporine has thus been proposed as a treatment for TBI. More than 20 independent experimental *in vivo* studies, in a multitude of TBI models with various outcome metrics, have demonstrated the neuroprotective effects of cyclosporine (145, 147-169). There are a few studies that have failed to show efficacy with cyclosporine, primarily when screening multiple drugs in a high-throughput study design (170, 171). The majority of the preclinical efficacy studies has however been performed in rodent models and utilized endpoints that are not directly translatable to humans.

In addition to the robust pre-clinical data supporting the positive treatment effect, two clinical studies with cyclosporine in TBI has have been completed. These studies illustrate an appropriate safety profile in a specific patient population, as well as showing data indicating a positive treatment effect (172-174). There is also a third clinical study that was recently completed and where the results are pending (175).

Mitochondrial complex I dysfunction in acquired and inherited disease

CI is also the most commonly observed dysfunctional mitochondrial protein complex in inherited mitochondrial disease. These genetic diseases occur due to a variety of genetic mutations in the nuclear and mitochondrial DNA (176). These primarily pediatric disorders present with failure to thrive, as well as a variety of symptoms from organs with high energy requirements, such as the brain.

These patients might be able to cope with everyday life, but during an infection they may become severely ill when their mitochondria cannot cope with the increased energy demand, and as a result may suffer from metabolic decompensation and organ failure (177). Unfortunately, there are no evidence based treatments for these patients. As described previously, most food derived nutrients provide energy through oxidation in the TCA cycle, primarily generating NADH that feeds into CI. Succinate on the other hand donates electrons to CII. Succinate administration has been suggested as a therapeutic strategy to bypass CI dysfunction for both inherited mitochondrial disease and acute acquired CI dysfunction (134, 178), but exogenously delivered succinate has extremely poor cell permeability and its usage as a therapeutic is therefore uncertain.

Objectives

The overall objective of this thesis was to characterize acute cerebral mitochondrial dysfunction and to develop targeted therapeutics. The specific aims were as follows:

1. Evaluate mitochondrial bioenergetics in a mouse model of sepsis and assess the feasibility of mitochondrial respiration as a therapeutic target (Paper I).

2. Perform a detailed evaluation of mitochondrial bioenergetics in a porcine traumatic brain injury model of both focal controlled cortical impact injury and diffuse rapid non-impact rotational injury (Paper II-III).

3. Develop a cell membrane-permeable succinate prodrug that can increase ATP output in cells and tissues with mitochondrial CI dysfunction (Paper IV).

4. Develop an *in vivo* pig model of acute mitochondrial CI dysfunction with associated changes in metabolism (Paper V).

5. Evaluate the efficacy of cyclosporine in a large animal model of focal TBI using a translational study design (Paper VI).

Methods

Rodent cecal ligation and puncture model of sepsis

The study described in paper I was approved by the ethical committee of animal experiments at Tokyo Medical University. Eight week old male C57BL/6 mice were used and kept with *ad libitum* access to food and water and maintained on a 12 h day and night cycle. Sepsis was induced by cecal ligation and puncture (CLP) (179). The mice were anesthetized using continuous inhalation of isoflurane and a laparotomy was performed. The cecum was exposed using anatomical forceps and the cecum was ligated right below the ileocecal valve. Feces was gently relocated toward the distal cecum and the cecum was perforated by a single through and through puncture using a 21 G needle and a small droplet of feces was gently squeezed through the perforation. The cecum was then returned to the peritoneal cavity with careful attention so that feces did not contaminate the margins of the wound and the incision was closed with sutures. Postoperatively the animals were resuscitated with a subcutaneous injection of saline. Controls were sham operated and underwent the same procedure for everything except the ligation and the puncture. The mice were terminated, at either 6 h or 24 h after surgery, by cervical dislocation and body temperature as well as blood glucose were measured directly afterwards. Beginning with the brain, the organs were rapidly harvested and immediately transferred to ice-cold buffer solution (IB) (320 mM sucrose, 2 mM EGTA, 10 mM Trizma base, pH 7.4).

Porcine models of traumatic brain injury

The procedures described in papers II, III and VI were all approved by the Institutional Animal Care and Use Committee of the University of Pennsylvania. Four-week-old (7–9 kg) female Yorkshire piglets were used for both the controlled cortical impact (CCI) injury model and the rapid non-impact rotational (RNR) injury model. Piglets were premedicated with an intramuscular injection of ketamine and xylazine. After induction with isoflurane via snout mask the subjects were intubated. Anesthesia was maintained with approximately 1% inhaled isoflurane via

endotracheal tube with the fraction of inspired oxygen set at 0.21. Prior to injury cefazolin and buprenorphine were administered intramuscularly. A rectal probe was used to monitor the core body temperature and a circulating water blanket was used to keep the temperature constant between 36°C and 38°C throughout the experiment. Blood pressure, oxygen saturation, respiratory rate, heart rate, and end-tidal CO_2 were continuously monitored. Piglets maintained spontaneous ventilation, if possible, otherwise mechanical ventilation was adjusted to maintain normoxia and normocarbia. To allow for a continuous drug infusion and blood pharmacokinetic (PK) sampling, as in the study described in paper VI, tunneled central venous catheter lines were placed into the bilateral cephalic veins and the lines were tunneled between the animals' scapula. The central venous catheter line was connected to an ambulatory Bluetooth pump (3D BT mini infusion, Strategic Applications Inc., Infusion Technologies, Lake Villa, IL, USA) for continuous drug delivery.

For the focal CCI injury model used in paper II and VI, a spring-loaded CCI device was utilized that produces a lesion volume of approximately 8% of the hemisphere. The head was shaved and cleaned with chlorhexidine. The right coronal suture was exposed and a craniectomy was performed over the rostral gyrus. The dura was opened to reveal the cortical surface. The device was stabilized against the skull with screws and the device then rapidly (4 ms) depressed the cortical surface to a depth of 0.7 cm. The device was subsequently removed and the surgical flap closed with sutures.

For the RNR injury model in paper III, TBI was induced using a rapid head rotation technique (180-182). While under anesthesia, the subjects head was secured to a bite plate by a snout strap. Anesthesia was withdrawn immediately prior to injury, and the head was rotated rapidly ventral-to-dorsal in the sagittal plane with the center of rotation at the cervical spine. The animals were removed from the device immediately afterwards.

For both models the piglets were extubated after emergence from anesthesia when they had return of pinch reflex, spontaneously breathing, maintaining appropriate ventilation and oxygenation, and had stable vitals including blood pressure, heart rate and respiratory rate. Animals were continuously monitored during recovery and they all displayed initial depressed activity and gait instability. Subjects were returned to the animal housing facility when they were able to vocalize without squealing, able to ambulate, exhibited no aggression or avoidance behavior, had absence of piloerection, and also had proper feeding and drinking behaviors. For the sample acquisition animals were re-anesthetized as described above. A bilateral craniectomy was performed to expose the brain, tissue was rapidly extracted while the animal simultaneously received a pentobarbital overdose. Tissue was removed within seconds and placed in ice-cold buffer solution (IB).

Porcine rotenone model of complex I dysfunction

The regional ethics committee of Stockholm approved the study described in paper V. Ten female Yorkshire/landrace hybrid pigs were included in the study. Animals were pre-medicated with intramuscular administration of Zoletil (tiletamine and zolazepam), Domitor (medetomidine hydrochloride) and atropin. The pigs were put under anesthesia and maintained by a continuous infusion of fentanyl and pentobarbital. The animals were intubated and supplied with mechanical ventilation. The rate and tidal volume of the ventilator was kept constant during the experiment and arterial blood pO_2 was also kept constant by adjusting the inspired oxygen concentration (FiO_2) accordingly. Ringer-Acetate was infused and the rate was adjusted according to the clinical assessment of urinary output and mean arterial pressure. Heparin was administered to prevent blood clots. Rotenone was administered through a single lumen catheter in the left jugular vein to half of the animal cohort. The dose was 0.25 mg/kg/h for 3 h and was increased thereafter to 0.5 mg/kg/h for the final hour of the experiment. The remaining half of the animals received vehicle.

Arterial blood pressure was measured continuously through a catheter in the femoral artery. A Swan-Ganz catheter was inserted through the right external jugular vein into the pulmonary artery. Central venous pressure, pulmonary artery pressure and pulmonary wedge pressure were measured. Cardiac output was measured by thermo-dilution from the Swan-Ganz catheter. Animals were also monitored by ECG during the experiment. Arterial blood samples were collected from the femoral artery and venous blood samples were collected from the Swan-Ganz catheter in the pulmonary artery. Continuous indirect calorimetry was performed using a Quark RMR ICU (Cosmed, Rome, Italy), measuring whole animal oxygen consumption (VO_2) and carbon dioxide production (VCO_2). Measurement of *in vivo* oxygen tension in skeletal muscle was conducted with large area surface (LAS)™oxygen-sensing luminescent optodes in *m. pectineus* and *m. sternocleidomastoideus* for continuous monitoring of tissue PO_2 (183).

Acquisition and preparation of samples for mitochondrial analysis

Brain and liver tissue, as applicable for each respective study, was harvested rapidly and placed in ice-cold buffer solution (IB). The tissue was dissected gently and subsequently placed quickly on drying paper to absorb excess buffer, then weighed. Brain and liver tissue was homogenized on ice in mitochondrial respiration medium

(MiR05) (110 mM sucrose, 0.5 mM EGTA, 3.0 mM MgCl2, 60 mM K-lactobionate, 10 mM KH2PO4, 20 mM taurine, 20 mM HEPES and 1.0 g/l fatty acid-free BSA) using a 5 ml Potter–Elvehjem Teflon glass homogenizer.

Porcine skeletal muscle biopsies for paper V were obtained using a 14 G micro-biopsy needle from *m. pectineus*. Human atrial heart muscle biopsies for paper IV were obtained from patients undergoing elective open-heart surgery, such as mitral valve repair, or the maze procedure. Pre-surgery informed consent was obtained and the cardiothoracic surgeon harvested superfluous tissue that was located behind the suture line for the cannulation catheter or tissue that would have been discarded. Porcine skeletal muscle biopsies and human atrial heart biopsies were immediately transferred to ice-cold biopsy preservation solution (BIOPS) (10 mMCa-EGTA buffer, 0.1 µM free calcium, 20 mM imidazole, 20 mM taurine, 50 mM KMES, 0.5 mMDTT, 6.56 mMMgCl2, 5.77 mMATP, 15 mM phosphocreatine, pH 7.1). The fibers were thereafter dissected using forceps under microscope to separate the fibers and remove fat and connective tissue (184).

For the human blood samples collected from healthy volunteers for paper IV, written informed consent was acquired, and blood was subsequently collected through a standard venous puncture. Porcine blood samples for paper V were collected using the existing catheter in the femoral artery. Platelets were prepared by 15 min centrifugation at 300 g resulting in a platelet-rich plasma (PRP). This PRP was collected and centrifuged for 5 min at 4600 g, producing nearly cell-free plasma and a platelet pellet. The pellet was resuspended in 1 to 3 mL of plasma by gentle pipetting to obtain a suspension of highly enriched PRP (185). Peripheral blood mononuclear cells (PBMC) were isolated using Lymphoprep™ (Axis-shield PoC AS, Oslo, Norway) (186). After removing the platelet-rich plasma (PRP) from whole blood as described above, the remaining part containing PBMCs and erythrocytes was resuspended in saline, layered on a Ficoll gradient and centrifuged 30 min at 800 g. Then the layer containing PBMC was collected, resuspended in saline and pelleted at 250 g for 10 min. The supernatant was removed and the pellet was finally resuspended in 100-200 µl of saline and 50-100 µl of plasma. Final concentrations of the suspensions were determined using a Swelab Alfa hematology analyzer (Boule Medical AB, Stockholm, Sweden).

For paper IV control cell lines from healthy donors as well as a cell line from a patient with Leigh syndrome, were provided by the Wellcome Trust Centre for Mitochondrial Research at Newcastle University. The fibroblasts were cultured at 37°C and 5% CO_2 using minimum essential medium (MEM) supplemented with 10% fetal bovine serum, 1% MEM vitamins, 1% MEM non-essential amino acids, 2 mM L-glutamine, 50 ug ml^{-1} streptomycin, 50 U ml^{-1} penicillin, 50 ug ml^{-1} uridine and 1 mM sodium pyruvate. Cells were collected using trypsin and used for analysis at 70–80% confluence. The fibroblasts were counted using an automated cell counter

(TC20, Bio-Rad, Hercules, USA). Fibroblasts were seeded out in cell growth medium in collagen-coated 96-well plates and kept at 37°C and 5% CO_2 overnight. The growth medium was replaced by XF-Base Medium (2 mM L-glutamine, 5 mM sodium pyruvate and 10 mM glucose, pH 7.4) and incubated for 1 hour at 37°C prior to experiment.

Mitochondrial respirometry

Mitochondrial respiration was measured in most tissue types and cells using high-resolution respirometry (Oroboros O2k, Oroboros Instruments, Innsbruck, Austria). A substrate, uncoupler, inhibitor titration (SUIT) protocol was used that extends conventional bioenergetic protocols that utilize only NADH-linked substrates (184, 187), with the addition of succinate, to assess maximal oxidative phosphorylation capacity through convergent flow through the Q-junction (184, 187). The SUIT protocol also provides data on maximal uncoupled oxidative phosphorylation capacity, CIV respiration, and LEAK respiration (mitochondrial inner membrane proton leak). Measurements in fibroblasts were performed using the Seahorse Bioscience XFe 96 Extracellular Flux Analyzer (Seahorse Bioscience, North Billerica, USA).

The specific protocol for the high-resolution respirometry performed in the Oroboros O2k (Oroboros Instruments, Innsbruck, Austria) differed depending on tissue and cell type. Digitonin was used, when applicable, to permeabilize the plasma membranes. Digitonin was also used in brain homogenates to access the subpopulations of mitochondria trapped within synaptosomes that form during the preparation. Malate and pyruvate was added, followed by ADP and glutamate, to measure the oxidative phosphorylation capacity of CI, driven by the NADH-related substrates. In the presence of ADP this would correspond to state 3 respiration in established bioenergetics terminology. Succinate was added to stimulate maximal phosphorylating respiration capacity via convergent electron input through complexes I and II.

Oligomycin, an inhibitor of the ATP synthase, was used to induce mitochondrial respiration independent of ATP production across the inner mitochondrial membrane, referred to as LEAK respiration. Maximal convergent non-phosphorylating respiration of the ETC was evaluated by titrating the protonophore, carbonyl cyanide p-(trifluoromethoxy) phenylhydrazone (FCCP) until no further increase in respiration was detected. Non-phosphorylating respiration through CII was achieved through the addition of rotenone with oligomycin present. The CIII inhibitor antimycin-A was added to measure the residual oxygen consumption (ROX)

that is independent of the ETC. The ROX value was subsequently subtracted from each of the previously measured respiratory states. CIV activity was determined by the addition of ascorbate and N,N,N′,N′-tetramethyl-pphenylenediamine (TMPD), an electron donor to CIV. TMPD has a high level of auto-oxidation and the CIV inhibitor sodium azide was subsequently added and the remaining chemical background was subtracted from the TMPD value to assess CIV activity.

The chamber contents from the high-resolution respirometry measurements were frozen for subsequent citrate synthase (CS) activity quantification. CS activity (µmol/mL/min) was used as a marker of mitochondrial content (188). At a later time point the samples were thawed and a commercially available kit (Citrate Synthase Assay Kit, CS0720, Sigma) was used according to the manufacturer's instructions to determine CS activity.

Fluorometry and the measurement of reactive oxygen species

Measurement of ROS production in brain homogenates was utilized in papers II, II and VI. It was carried out using the add-on O2k-Flourescence LED2 module (Oroboros Instruments, Innsbruck, Austria) to allow simultaneous measurement alongside mitochondrial respiration. The Amplex UltraRed H_2O_2 assay was used. In the presence of horseradish peroxidase Amplex UltraRed (N-acetyl-3,7 dihydroxyphenoxazine) reacts with H_2O_2 to produce the fluorescent compound resorufin. The addition of SOD ensures that all $O_2^{\cdot-}$ is converted into H_2O_2. Calibration of the fluorometric signal was conducted prior to each measurement by the addition of 100 nM H_2O_2. This method was only used in brain homogenates, because liver homogenates have a high content of endogenous cytosolic antioxidants that interfere with the assay and the measurement of H_2O_2 production. For muscle fibers and intact cells measurements using this technique is problematic due to diffusion and gradient challenges.

Metabolomics

Metabolomics was performed in muscle biopsies as described in paper V, as well as in blood cells as part of the development of the succinate prodrugs described in paper IV. A quantitative analysis of 116 metabolites was performed using capillary electrophoresis time-of-flight mass spectrometry (CE-TOF-MS) for cationic

compounds and capillary electrophoresis tandem mass spectrometry (CE-MS/MS) for anionic compounds. The analysis was carried out by Human Metabolome Technologies Inc. (HMT, Tsoruka, Japan).

Neuroimaging

For paper VI, Magnetic Resonance Imaging (MRI) was obtained on a 3T MRI research magnet on day 5 post injury. MRI measurements were taken from the series with a TR of 2500 ms and TE 38 ms. Anatomic images were assessed for presence of hemorrhage, edema, and other structural abnormalities. The injury was defined as the area of signal abnormality when compared to contralateral brain. Volume of injury was traced by free hand on each individual slice, and then the volume was calculated using Terarecon software. The MRI protocol included T1 weighted images (T1WI), T2 weighted images (T2WI), and T2 weighted short time image of inversion recovery (STIR) using repeat time (TR) and echo time (TE).

The protocol also included MRI diffusion-weighted imaging (DWI)-Apparent Diffusion Coefficient (ADC) and Magnetic Resonance Spectroscopic Imaging (MRSI) sequencing, as well as fast spin-echo proton density-weighted imaging (PDWI) and DTI, which was performed using selective radiofrequency (RF) excitation in single-shot echoplanar imaging sequence (30 directions, repetition time: 3.200 ms, echo time: 55 ms). To improve the signal to noise ratio, the scans were acquired over 3 averages. Fractional anisotropy (FA) maps were constructed from the region of interest. Tractography was performed using custom-modified software. Data analysis for these additional neuroimaging techniques is ongoing and the data is thus not included in the manuscript referred to as paper VI in this thesis.

Cerebral microdialysis

For the study in paper VI cerebral microdialysis was performed on day 5 post injury in the ipsilateral hemisphere to the injury, approximately 10 mm from the contusion (CMA 71 Elite mDialysis, Sweden). While under anesthesia the scalp was reopened and the probe was placed approximately 1 cm deep to reach the junction of cortex and subcortical white matter, following needle puncture of the dura. Sterile saline was perfused at 1 µL/min and after a 30 min equilibration period, for which the collected sample was discarded, the samples were collected over the succeeding 30 min. Samples were immediately frozen at -80°C for subsequent analysis in batch using the ISCUS Flex™ Microdialysis Analyzer (mDialysis, Sweden).

Additional methods utilized

Isotope labelling of the succinate prodrugs was utilized in paper IV. Compounds were synthesized that incorporated all four carbons in the central succinate structure with [13C] isotopes. The isotope-labelled compound was added in two boluses to a final concentration of 0.5 mM and the samples were incubated for 15, 30, 120 or 240 min at 37°C in MiR05 buffer with added glucose (5 mM). Measurements were carried out by Human Metabolome Technology Inc. (Tsuruoka, Japan).

For the lactate measurements, platelets were incubated for 4 hours in PBS at 37 °C at a stirrer speed of 750 r.p.m, with either only rotenone, rotenone and antimycin A combined, or with dimethyl sulfoxide (DMSO) vehicle. Additions of the succinate prodrugs or vehicle was initiated at 60 min and repeated every 30 min thereafter. Lactate levels were measured every 30 min using a Lactate ProTM 2 blood lactate meter (Arkray, Alere AB, Lidingo, Sweden).

Mitochondrial membrane potential in isolated human platelets was measured using a flow cytometer FACSAria III (BD, Franklin Lakes, USA) with Diva version 7.0 software using TMRM (Life Techologies, Ref: T668) in non-quench mode. CD41a-APC (BD Pharmingen, Clone HIP8, Ref: 559777) was used to assess platelet activation. Samples were incubated with the probes in MiR05 at room temperature for 30 min. CI was inhibited using rotenone and the succinate prodrug or DMSO was added followed by oligomycin. FCCP and antimycin A were added as internal controls. FlowJo 10 software (Tree Star, Ashland, USA) was used for data analysis.

Results and conclusions

The mitochondrial respiratory response to sepsis is organ-specific (Paper I)

In this paper we examined the mitochondrial respiratory response to a septic insult in two different organs. The CS activity, as a measure of mitochondrial mass, was not altered in either tissue. The brain tissue displayed a slightly impaired mitochondrial respiratory efficiency in the septic mice that was mainly due to increased uncoupling. The maximal non-phosphorylating capacity of the ETC did not differ significantly compared to controls. There was no difference in ROS generation between the groups.

In the liver tissue there was, contrary to the brain, a significant increase in the mitochondrial respiratory efficiency. The maximal non-phosphorylating capacity of the ETC was comparable between the two groups, but the insult dramatically increased the phosphorylating capacity in the septic mice. The ETC capacity was thus less restricted by the ATP synthase in the septic mice.

The conclusion of the paper was that the mitochondrial respiratory response to a septic insult seems to be organ specific. The brain displayed an impaired mitochondrial respiratory efficiency, whereas the liver displayed an increase in the respiratory efficiency. This may be an adaptive response related to ROS handling in the brain and an increased metabolic demand in the liver. Future therapeutic approaches targeting mitochondrial function needs to be organ specific.

Focal traumatic brain injury induces a bilateral decrease in complex I-driven mitochondrial respiration and a contralateral increase in complex II-driven respiration (Paper II)

In this study we examined mitochondrial function following focal TBI in a large animal model. Mitochondrial respiration was measured in the ipsilateral and contralateral side relative to the injury. The ipsilateral side to the injury exhibited a significant reduction in CS activity, indicating loss of mitochondrial mass. When expressed per mg of tissue, CI-driven respiration was significantly decreased bilaterally, while the contralateral side exhibited a significantly increased convergent

maximal phosphorylating respiration, as well as an increase in non-phosphorylating CII-driven respiration compared to sham and the ipsilateral brain. The alterations in convergent electron flow resulted in significantly lower maximal coupled respiration in the ipsilateral side compared to the contralateral side, while the contralateral side displayed an increased mitochondrial respiratory efficiency compared to the ipsilateral side, as well as to sham animals.

In conclusion, the study reports a bilateral decrease in CI-driven respiration and a contralateral increase in CII-driven respiration after focal TBI. These results were most likely primarily the result of a reduced mitochondrial mass demonstrated by a significant reduction in CS activity by almost 50% in the ipsilateral brain. When respiration was normalized to CS activity the overall changes became less significant. The decrease in CI respiration and increase in CII respiration nonetheless offers opportunities for the therapeutic approach presented in paper IV. This work also illustrates the difficulties of normalizing mitochondrial respiration and the implications it may have for data interpretation.

Diffuse non-impact traumatic brain injury induces uncoupling of oxidative phosphorylation as well as reduced mitochondrial respiratory efficiency (Paper III)

In this study we examined mitochondrial function following diffuse non-impact TBI in a large animal model. Mitochondrial respiration was measured in the cortex and hippocampus. Diffuse non-impact TBI did not result in a significant overall reduction in CS activity compared to controls. The most robust finding was a significantly decreased mitochondrial respiratory efficiency in both the cortex and hippocampus in response to injury, associated with significantly increased uncoupling in both regions, regardless of normalization method. Furthermore, the study suggests alterations in the proportionate contribution of CI and CII to convergent mitochondrial respiration and that this differs by brain region.

Cell-permeable succinate prodrugs can bypass a mitochondrial complex I dysfunction (Paper IV)

In a therapeutic drug development program, more than 50 prodrugs of succinate were designed, synthesized and evaluated for cell-permeability. Three compounds, NV118, NV189 and NV241, were identified and further characterized in more extensive assays, using a variety of human cells and tissues, to show proof of concept using these cell-permeable succinate prodrugs.

It was shown that cell-permeable succinate can increase mitochondrial oxygen consumption in intact cells with rotenone-induced inhibition of CI. The addition of oligomycin decreased respiration and thus indicating that the increased respiration was coupled to ATP generation. The addition of cell-permeable succinate prodrugs increased the mitochondrial membrane potential. Furthermore, the cell-permeable succinate prodrugs attenuated lactate production in platelets incubated with the CI toxin rotenone. Metabolomics, using quantitative capillary electrophoresis mass spectrometry (CE-MS), including the use of ^{13}C labelled succinate prodrug, confirmed delivery of succinate to the TCA cycle and its downstream metabolism.

In conclusion, the cell-permeable succinate prodrugs demonstrated proof of concept *in vitro* and *ex vivo*. It was demonstrated that the prodrugs can deliver succinate and bypass a CI dysfunction. However, they lacked sufficient plasma stability for *in vivo* studies. A 2nd generation of compounds with improved plasma stability has now been generated. These drugs are primarily being developed for pediatric genetic diseases with mitochondrial CI dysfunction. However, a cell-permeable succinate prodrug may also be a suitable as therapeutic for TBI.

Intravenous infusion of rotenone decreases mitochondrial utilization of oxygen *in vivo* and causes a switch from aerobic to anaerobic metabolism (Paper V)

In this study we developed a large animal model of acute rotenone-induced mitochondrial CI dysfunction. This model was developed to test the compounds developed in paper IV. To allow for adequate clinical monitoring with invasive measurements and to precisely control ventilation, a large-animal model was preferable. It also made it possible to collect multiple blood samples in a longitudinal design, where the blood volume of a smaller animal would be insufficient.

Rotenone infusion caused a switch from oxidative phosphorylation to glycolysis with a corresponding progressive increase in lactate formation due to a shift towards non-mitochondrial metabolism. These changes were not due to tissue hypoperfusion or other secondary cardiovascular effects of rotenone, as there was a corresponding increase in oxygen tension in venous blood and skeletal muscle. The major hemodynamic parameters remained reasonably stable throughout the lower infusion rate, but with the higher infusion rate the clinical status of the pigs treated with rotenone deteriorated. Continuous indirect calorimetry showed that rotenone caused a decrease in whole body O_2 consumption and initially a decrease in CO_2 production. Analysis of mitochondrial function *ex vivo* in platelets from rotenone-treated animals displayed a statistically non-significant inhibition of phosphorylating capacity. In

muscle biopsies from rotenone-treated animals the levels of succinate were decreased, while other intermediates of glycolysis and the TCA cycle were increased.

In conclusion, the composite data indicate that intravenous rotenone infusion decreases mitochondrial utilization of oxygen due to CI inhibition and causes a switch from aerobic to anaerobic metabolism. The model may be well suited for future studies of therapeutic interventions aimed at counteracting acute changes in energy metabolism due to mitochondrial CI dysfunction. Furthermore, an attenuation of lactate production may be used as an endpoint to evaluate therapeutic interventions.

Cyclosporine is neuroprotective in a large animal model of focal traumatic brain injury (Paper VI)

In this study, we evaluated the neuroprotective properties of cyclosporine in the large animal model of focal TBI used in paper II. As a first step, we performed a bioequivalence study comparing the NeuroSTAT formulation to the Sandimmune formulation of cyclosporine and it was indicated that they have equivalent brain exposure. The second step was a dose-escalation study using the NeuroSTAT formulation. Cyclosporine brain concentrations significantly increased with each escalation from 5 to 40 mg/kg/day and the dose of 20 mg/kg/day was determined to be optimal.

Finally, a randomized blinded placebo controlled study was conducted as a third step in this study. The results confirmed the neuroprotective properties of cyclosporine, by demonstrating a treatment response that included a reduction of the volume of injury in cortical and subcortical tissue by 35% compared to placebo, measured by MRI on day 5 following injury.

In addition, a number of other outcome metrics indicated an overall positive treatment effect. Pericontusional cortical glucose levels were significantly increased and there was a non-significant decrease in lactate:pyruvate ratio in the cyclosporine group. The overall mitochondrial response displayed a non-significant but consistent trend towards a beneficial effect with cyclosporine treatment with a higher capacity of oxidative phosphorylation and lower ROS generation.

In conclusion, this randomized, blinded, and placebo-controlled large animal model trial demonstrated the neuroprotective effect of IV cyclosporine administration in the context of focal traumatic brain injury. This finding is consistent with existing literature and warrants further studies in clinical trials. The efficacy demonstrated in a translational neuroimaging endpoint in this large animal model should be of high relevance for the predicted effect in human clinical trials.

Discussion

The threshold effect and complexities of data interpretation

The papers in this thesis demonstrate that mitochondrial respiration, as an integrative measure of mitochondrial function, show a wide range of specific alterations, depending on time, localization, and the specific type of injury. One has to ask the question; what do these changes in mitochondrial respiration mean and how do they translate into changes in patient outcome related to morbidity and mortality? Since there is a several-fold spare capacity for each step downstream in the ETC, a statistically significant enzymatic defect, of for example 20%, in a specific complex e*x vivo* does not necessarily translate to decreased ATP output *in vivo*. Furthermore, even if this specific enzymatic decrease did in fact translate to a decreased ATP output, it is unclear how this would affect morbidity and mortality. One also has to remember that in the *ex vivo* assays, substrates are added at saturating levels and fuel depletion is thus not a problem. The supply of TCA cycle intermediates is not thought to be rate limiting under physiological conditions, however, it is unclear what happens during starvation, such as during early phases of sepsis before a patient reaches medical care. During this phase there could be alterations in the anaplerotic reactions that replenishes the pool of metabolites in the TCA cycle.

The alterations observed may also be part of an adaptive response, rather than a mitochondrial dysfunction *per se*. It is not necessarily the case that a lower maximal phosphorylating capacity or an increased uncoupling of the mitochondria resulting in decreased ATP output, are harmful to the cell. In fact, the opposite may very well be true. The perceived mitochondrial dysfunction might instead be a potentially protective adaptive response (125). Many critical illnesses such as sepsis produce a biphasic response, both in regards to the inflammatory and metabolic response. The acute phase, associated with stress hormone release, is often associated with an increased metabolic and mitochondrial activity. The subsequent phase, on the other hand, is associated with a decreased metabolic rate and, in the case of sepsis, associated with multiple organ failure. It has been argued that this second phase is in fact a protective mechanism and that a reduced cellular metabolism could increase cell survival in the face of an overwhelming insult (125). We also have preliminary data

indicating that there is a biphasic mitochondrial respiratory response to TBI (data not shown).

Mitochondria that are more uncoupled, as seen in both the septic model described in paper I, and the TBI model described in paper III, results in less efficient mitochondrial respiration and this may be interpreted as a pathological response. However, as discussed in the background, there is a proton leak in all mitochondria, with an endogenous basal leak that is independent of uncoupling proteins and this may be due to the fact that a high membrane potential would generate more ROS, and a proton leak may therefore be a way to limit oxidative damage (5, 26). The increased uncoupling of oxidative phosphorylation, seen as a response to sepsis and TBI, might therefore be an adaptive response to improve the ROS handling capacity.

A moderate increase in ROS generation might not be detrimental to cell survival, but may instead be an important signal that triggers an adaptive response (27). Therapeutics that depresses this endogenous signaling pathway may increase morbidity and mortality . The therapeutic approach should also differ depending on the time-course and the specific circumstances. An example may be the inhibition of CII with the competitive inhibitor malonate, which has been suggested to be protective against ischemia-reperfusion injury when delivered during the ischemic phase by inhibiting RET, as discussed earlier (39, 189). If the hypothesis presented holds true, the same therapeutic given only minutes later during the reperfusion phase would conceivably have a negative effect on ischemia-reperfusion injury. When generating a hypothesis for a suitable therapeutic approach targeting the mitochondria one must have an understanding of these complexities.

Normalizing mitochondrial respiration

Measuring mitochondrial content of a tissue sample through calculating the mitochondrial fractional area from transmission electron microscopy has been suggested to be the gold standard for determining mitochondrial mass (188). This is, however, extremely labor-intensive and requires specific preparation following tissue collection. CS activity is a commonly used marker of mitochondrial content that can be easily measured in frozen tissue homogenates. Several other biochemical measures have also been proposed, such as mtDNA copy number (190), cardiolipin content (191), as well as activity of the individual complexes (188, 192, 193). In a study by Larsen et al., skeletal muscle mitochondrial content was assessed using a number of different alternatives and correlated to mitochondrial content determined by transmission electron microscopy (188). Results showed that cardiolipin, followed by CS activity, and CI activity were the biomarkers that correlated best with

mitochondrial content determined by transmission electron microscopy, whereas mtDNA was found to be a poor biomarker of mitochondrial content. The fact that mtDNA showed such a poor correlation might be related to methodological problems with the specific genes used for mtDNA copy number determination. Other studies have suggested that mtDNA is a good marker (194) and in fact it has been shown that CS and mtDNA exhibit a remarkable correlation in platelets acquired from septic patients as well as controls (195). This finding of an excellent correlation in platelets may be due to the fact that platelets do not have a nucleus and therefore lack nuclear genes that can interfere with the assay. Most of the research in this field has been conducted in skeletal muscle biopsies and is evidently not applicable to all tissue types.

It is also unknown how these surrogate markers change in pathological states relative to the measured variable, i.e. for example mitochondrial respiration. Cardiolipin has for example been suggested as a marker (188), but it has been shown that myocardial ischemia selectively depletes cardiolipin in a specific subpopulation of mitochondria (196). In the same study it was illustrated that these mitochondrial subpopulations, including subsarcolemmal mitochondria and interfibrillar mitochondria, responded to the insult differently. The content of cardiolipin decreased only in subsarcolemmal mitochondria, whereas it was preserved in interfibrillar mitochondria (196). This highlights the issues with surrogate markers in a specific pathological state, which have been shown to correlate in healthy controls. Further adding to the complexity in the context of TBI is the fact that the injury in itself will also alter the water content of the brain, especially in the pericontusional area. A swelling of the brain could result in a decrease in mitochondrial respiration per wet weight of tissue, simply because of an increase in water content. The observed decrease in mitochondrial respiration in that specific situation would thus not be the result of a mitochondrial dysfunction whatsoever.

Porcine and rodent models of human disease

Rodent models are essential to modern biomedical research. Working with rodents is practical and essential for elucidating pathways and basic pathophysiological mechanisms such as the mPTP. Until very recently, genetic KO studies were possible only in rodents. However, the failures of translating preclinical discoveries to human therapeutics in the field of neuroscience, as well as in inflammatory diseases such a sepsis, have been attributed to the extensive use of rodents in preclinical research. The track record for clinical trials of investigative drugs for the treatment of sepsis is disappointing, with over 150 failures to date (197). In a provocative paper published by Seok et al. in 2013 it was illustrated that acute inflammatory stress, including

endotoxemia, blunt trauma, and burn, resulted in genomic responses in the rodent orthologs that were close to random in matching their human counterparts (198). This article sparked a debate, especially within the field of sepsis research (197, 199-206), but also in neuroscience (207). The findings were disputed in subsequent studies by other groups that reevaluated and performed meta-analyses of the same dataset (206, 208). Irrespective of the validity of the conclusions made by Seok et al., care needs to be taken when extrapolating the findings from rodent preclinical studies into the human clinical setting. In regards to sepsis, it should be noted that mice respond to infection, contrary to what is commonly the case in humans, with a decreased body temperature.

In the context of TBI, the biomechanical aspects add another layer of complexity as rodents obviously have much smaller brains, with very little white matter, making it difficult to characterize DAI. Pigs, on the other hand, have a similar gyral pattern and distribution of gray and white matter making them more similar to humans. The pig brain resembles the human brain more anatomically, as well as by its development pattern than that of rodents (209). Rodent data does not seem to follow a similar time course and magnitude of alterations in bioenergetic response as gyrencephalic animals do (146, 210, 211). The article by Seok et al. also alarmed the stroke community as the adaptive immune system is believed to contribute significantly to the pathophysiology of stroke and may also be of relevance to TBI (212).

About 90% of therapeutics with efficacy in animal models, and published in high profile journals, ultimately fail in clinical trials (213). This is perhaps not surprising given the fact that approximately 75 million years have passed since humans and mice shared a common ancestor (214). These failures are not only a problem because of resources wasted on developing drugs for mice, that never had any possibility of succeeding in humans. It is also an enormous problem when looking at it from the opposite direction, failed rodent studies may also have blocked the development of compounds that might ultimately have proven to be successful in humans. While we need not to deny that rodent studies are important and allow large throughput as well as early mechanism development. However, large animal studies should be used as a bridge to clinical trials, but also in parallel as a complement to rodent studies to increase the success rate of therapeutics in human clinical trials.

Related to paper VI and preclinical efficacy studies in general, it should be noted that brain exposure of the studied drug is often not measured. Cyclosporine possesses pharmacokinetic properties that makes this shortcoming problematic because of a challenging dose-response curve and poor blood-brain barrier penetration. At a sufficiently high dose the p-glycoprotein transporter will be saturated and cyclosporine will thus inhibit the efflux of itself and steady state can be reached (172, 215, 216). With sufficient biomechanical forces, TBI may also affect the

microvasculature and cause micro-hemorrhages with subsequent blood-brain barrier disruption, but this may be model specific.

The rotenone pig model developed in paper V was primarily established for the purpose of testing the cell permeable succinate prodrugs presented in paper IV. The objective was to establish an *in vivo* pig model of acute mitochondrial CI dysfunction with associated changes in metabolism. The model should not be viewed as refined porcine version of existing mouse models for mitochondrial diseases (217-223). Additional models are certainly warranted specifically for mitochondrial disease, conceivably by generating porcine KO models corresponding to the existing mouse models (217-223).

Metabolic support with cell permeable succinate

The therapeutic concept of cell permeable succinate prodrugs may be a double-edged sword. As mentioned in the background, exogenously delivered succinate may generate ROS from CI through RET (39). It is also possible that by increasing the membrane potential through normal forward electron transfer will also result in increased ROS generation downstream in the ETC. Mice with a mitochondrial DNA (mtDNA) missense mutation in the CI ND6 gene (ND6 nucleotide mtDNA ND6 13997G>A, P25L) (ND6P25L), a mutation also present in the human population, have a 30% reduction in CI and a general increase in ROS generation. These mice develop a rather severe phenotype over time (223). These mice, however, seem to be resistant to ROS production through RET and may therefore be less prone to IR injury (223). A pathological state with an acquired acute CI dysfunction may also generate less ROS through RET. The timing and precise dosing of the cell permeable succinate prodrugs may be critical to direct metabolism towards ATP-generation rather than ROS-generation.

Mitochondria as a therapeutic target in sepsis

The interpretation of the data will obviously have implications on the pursued strategy for therapeutic development, should the alterations in mitochondrial bioenergetics be interpreted as a dysfunction or as part of an adaptive response? Perhaps a combination strategy is needed, with distinct approaches during the initial phase and the later recovery phase. The intervention also needs to be tissue-focused since a specific approach might be beneficial in one organ while detrimental to another.

Mitochondrial dysfunction in sepsis, with apparent inhibition of CI, has been described by others, including downregulated synthesis of CI (128, 129, 224-226), with CII usually unaffected (128, 129, 224, 225). Providing metabolic support through cell permeable succinate could therefore be a successful therapeutic approach for sepsis, especially since it has been suggested that succinate can recover mitochondrial function in septic skeletal muscle (134). In a study by Protti et al., respiration with NADH related substrates was low in septic animals, while the addition of succinate *ex vivo* restored respiration. In animal models, it has also been shown that infusion of a succinate dimethyl ester prolonged survival and also provided positive changes in liver ATP content (227, 228).

Thiamine administration is another example of a mitochondrial targeted therapeutic with possible viability as a treatment for sepsis. PDH is the rate-limiting mitochondrial enzyme linking glycolysis to the TCA cycle (229, 230). PDH catalyzes oxidative decarboxylation of pyruvate to form acetyl-CoA, which may then be used in the TCA cycle. PDH inhibition can therefore cause mitochondrial and metabolic dysfunction (231). Inadequate PDH function limits pyruvate from entering the TCA Cycle. It is the essential co-enzyme thiamine pyrophosphate that regulates the activity of PDH, several other enzymes in the TCA cycle, and metabolism through the pentose phosphate shuttle (231). In a randomized, double-blind, placebo-controlled trial thiamine was investigated as a metabolic resuscitator for septic shock, with lactate as the primary outcome (232). Even though the primary outcome was not reached in those with thiamine deficiency at baseline, which was a predefined subgroup, the treated group had significantly lower lactate levels at 24 hours, as well as a significant decrease in mortality over time (232).

Mitochondrial targeted therapeutics for traumatic brain injury

After focal TBI there is a decrease in CI-driven respiration and an increase in CII-driven respiration. Similarly, in the diffuse model of TBI, convergent respiration via succinate-supported CII respiration is stimulated at 24h post-TBI. In both models, despite dependence on CII activity following injury, convergent CI- and CII-driven respiration is limited in its ability to maintain oxidative phosphorylation. Alterations in CI-driven respiration in focal and diffuse TBI identify opportunities for therapeutic interventions aimed at limiting the secondary injury and supporting bioenergetic demand by substrate-directed mitochondrial resuscitation. It has already been shown that focally perfused succinate through a microdialysis catheter improves brain metabolism in TBI patients (233). The same group also recently showed that

succinate supplementation *in vitro* improves the metabolism of glial cells with mitochondrial dysfunction (234). Future studies are therefore warranted to test the cell permeable succinate prodrugs *in vivo* in animal models of TBI.

Dysregulated brain glucose metabolism and lactate accumulation is present following TBI. Similar to sepsis, thiamine may also improve outcomes after TBI through activation and restoration of PDH activity. PDH plays a critical role in maintaining homeostasis of brain glucose metabolism. Following TBI there seems to be an altered expression and phosphorylation of PDH (235). Administering thiamine has been shown to improve neurological outcome and survival in mice after ischemic brain injury along with improved mitochondrial oxygen consumption and normalized PDH activity (231). Thiamine seems to be effective independently of deficiency. Thiamine may therefore be a suitable therapeutic to stimulate mitochondrial function and ATP output following TBI.

It is well established that there is an increase in ROS generation following TBI contributing to the secondary injury. An important pathway and a master regulator of the antioxidant defenses is the Nuclear factor (erythroid-derived 2)-like 2 (Nrf2), regulating hundreds of cytoprotective proteins. Activation and regulation of the Nrf2 pathway might therefore attenuate the secondary injury following TBI. It has been shown that TBI activates the Nrf2-ARE pathway (236) as part of the endogenous response, and it has also been shown that the absence of Nrf2 function in mice may result in exacerbated injury (237). Many different drugs have been proposed to attenuate brain injury via activation of Nrf2 (238-246). Dimethyl fumarate (DMF) which is in clinical use for the treatment of multiple sclerosis, has not been tested as a treatment for TBI. The mechanism of action for DMF is not completely understood, but it is known to activate the Nrf2 pathway. Furthermore, it has recently been shown that DMF mediates Nrf2-dependent mitochondrial biogenesis in a dose-dependent manner (247). DMF is the first drug to demonstrate increased mitochondrial biogenesis *in vivo* in humans and is in development for different diseases with mitochondrial dysfunction as part of the pathophysiology (247).

Uncoupling of mitochondrial respiration could be a potential novel treatment for TBI. Following TBI there is a calcium influx and subsequent detrimental increase in ROS generation. Since calcium homeostasis is linked to the membrane potential, a reduction in the membrane potential may reduce excitotoxicity associated cell death by reducing mitochondrial Ca^{2+} loading. It has been shown that upregulation of UCP can reduce ROS production and excitotoxicity related cell death (248, 249). Studies have also shown that that the therapeutic uncoupler 2,4-dinitrophenol (DNP), as well as FCCP can protect neurons, brain tissue and improve behavioral outcomes in a cortical impact model of TBI (250, 251). The timing and dosing of these therapeutics may be of key importance, as the beneficial effect with decreased ROS may be counteracted by simultaneously also decreasing ATP output. Perhaps decreased ROS

generation is beneficial in the acute phase, while bioenergetic support to increase ATP output is beneficial in the recovery phase.

The failures of therapeutic development for traumatic brain injury

All previous attempts to find an effective therapeutic treatment for TBI have failed. The list spans over 100 clinical trials and include drugs like, Selfotel, CP-101-606, D-CPP-ene, Cortocosteroids, Tirilazad, PEG-SOD, Nimodipine, Bradycor, Dexanabinol, SNX-111 and Progesterone (252-254). Progesterone was the most recent therapeutic to fail in two large phase III trials (255, 256). Over 180 preclinical studies, conducted in over twenty different models by twenty different research groups indicated altogether that progesterone should have a beneficial treatment effect. Nonetheless, the two phase III clinical trials showed no clinical benefit of progesterone. Many of these failed clinical trials have largely ignored the underlying inter-individual heterogeneity and have not stratified for the type of injury (257). Most previous TBI studies have based the selection of patients primarily on Glasgow Outcome Scale – Extended (GOS/GOS-E). In an analogy to cancer, *it is extremely unlikely that any of the new target specific cancer drugs that have reached patients in the last decade would have been successful if cancer had only been categorized as mild, moderate and severe*. GOS/GOS-E is a very blunt tool to assess these patients. It is not reasonable to stratify TBI as only mild-moderate-severe.

The development of standardized injury classifications and validation of novel endpoints is being addressed by ongoing large multicenter studies, such as TRACK-TBI and TBI Endpoints Development (TED). Part of the problem may also be related to the quality and translatability of preclinical studies, with a lack of standard scientific rigor in regards to randomization, blinding, and the necessity of pre-determined outcome metrics. This rigor needs to be applied to preclinical studies. The use of outcome metrics that are directly translatable to human clinical trials is imperative for the clinical trial design (258). As a response to this lack of translatability, common data elements (CDE) for preclinical research have been defined to assist collaborations and allow for easier meta-analysis of preclinical data and generate a common language for TBI research, as there are corresponding CDEs for clinical TBI research. The National Institute of Neurological Disorders and Stroke (NINDS) CDEs are subdivided into a core module for data elements as well as injury- and model-specific modules (259).

Targeted therapeutics and sex differences

Developing targeted therapeutics for cerebral mitochondrial dysfunction requires an understanding of the complexities and variabilities between individuals within the population. One important aspect regarding therapeutic development for TBI could be sex differences. There is evidence suggesting that gender influences mitochondrial bioenergetics following cerebral stress and TBI (260, 261). ROS production is higher in males in stroke models and the female brain is equipped with higher levels of endogenous anti-oxidant defense systems (262-265). Finally, mitochondrial dynamics following brain injury may differ between the genders (266-269). There is a general male-bias in medical research. Learning from the stroke field, Tirilazad mesylate, a non-glucocorticoid, 21-aminosteroid, that inhibits lipid peroxidation, was almost exclusively evaluated in male rodents during the preclinical studies, and subsequently failed in clinical trials, showing worse outcome in females (270).

Tirilazad mesylate was also evaluated in trials for TBI and likewise failed to show a significant beneficial effect. However, a subgroup analysis of male TBI patients with traumatic subarachnoid hemorrhage revealed a significantly reduced mortality in the treated group (271). Sex differences have also been shown in cerebral blood flow, related to cerebral ischemia (272) and could be of importance post TBI. It has also been shown that cell death pathways may be influenced by estrogen levels and testosterone levels have been implicated in the regulation of inflammatory pathways giving a stronger immune response in females (207, 273-276). The literature also suggests that under metabolic stress, the metabolism in neuronal cells may differ between the sexes (260, 274).

The pediatric perspective

Epidemiological and clinical data show that an individual's age at the time of TBI is negatively correlated with outcome (277). Evidence specifically suggests that age-specific mitochondrial differences between the myelinated adult and the pre-myelinated young brain may be related to outcome following TBI (278-280). Critical mitochondrial characteristics related to the ETC and ROS, may differ depending on age (281, 282). We have preliminary data indicating that age and brain development influence mitochondrial response to TBI in pigs and others have also shown age-related changes in mitochondrial bioenergetics in rodent models of TBI with significant declines in mitochondrial efficiency and limited ability to respond to oxidative stress in aged rats (280). Mitochondrial uncoupling protein-2, as mentioned previously, has furthermore been shown to protect the immature brain from

excitotoxic neuronal death (283). These differences could have implications on the therapeutic approach.

An evolutionary perspective on mitochondrial function

It has been suggested that a patient's *a priori* mitochondrial function related to their mitochondrial genetic makeup, may affect disease outcome. Humans have a wide range of functional mtDNA variation that subtly alter mitochondrial function and thus a person's mitochondrial genetic variation may have a significant effect on his or her ability to cope with cellular stress. Evidence suggests that these genetic variants linked within mtDNA haplogroups can modify the susceptibility to and outcome of a variety of diseases, including sepsis and TBI (278, 284-287). These mtDNA polymorphisms have been shown to alter mitochondrial respiration and ROS generation, as well as to influence more universal functions such as inflammation (288, 289). The theory is that a specific mtDNA variant that proved to be adaptive in a specific geographic environment would increase in frequency and give rise to a haplogroup (289-292). While haplogroups associated with functional mitochondrial variants can be beneficial in one context, they can be deleterious in another.

For example, a mtDNA mutation that increases ROS production may provide resistance to infection. The same mtDNA mutation may cause a worse outcome following TBI, even with similar biomechanical forces, as these discrete mtDNA variations may predispose patients to a varying degree of secondary brain injury following TBI (288, 289). An increasing number of studies have reported associations between mtDNA haplogroups and differing outcomes following sepsis as well as TBI (278, 285-287). As an example, haplogroup H has been reported to have a decreased susceptibility to sepsis (287), but at increased risk for neurodegenerative diseases (293, 294). Haplogroup K on the other hand was shown to have better outcomes following TBI. However, the theory linking mtDNA haplogroups to disease outcomes and how it is related to distinct alterations in mitochondrial respiration and ROS generation has been disputed altogether and it has been suggested that the differences are related to the influence of nuclear genes (295). As stated in the introduction, only a small part of the mitochondrial proteome is coded by mtDNA and the relative importance of genes coded by nuclear DNA (nDNA) and mtDNA related to distinct mitochondrial characteristics may need to be explored further. Regardless, the inherited functional mitochondrial characteristics defined by both nDNA and mtDNA may be of critical importance to the clinical outcome.

Future perspectives

A future clinical trial in traumatic brain injury

Some of the therapies that have been tested in clinical trials and failed may have been truly ineffective, but may also have been inappropriately discarded due to limitations in the study designs. Part of this problem may have been due to inadequate endpoints. Peripheral blood/CSF biomarkers and novel neuroimaging are two promising approaches that may be useful for initial patient stratification and classification, as well as being used as efficacy endpoints. Blood and CSF biomarkers in the pipeline include those of glial injury (GFAP, glial fibrillary acidic protein and S100β), axonal injury (pNF-H, Phosphorylated Axonal Form of the Neurofilament Subunit NF-H and SBDP150/SBDP120), neuronal cell body injury (UCH-L1, Ubiquitin C-terminal hydrolase and NSE, Neuron-specific enolase), demyelination markers (MBP, Myelin Basic Proteins), and plasma tau profiles (296-298). Biomarker assays are promising as potential diagnostic and prognostic predictors of persistent symptoms after TBI (299-301).

Advanced neuroimaging is also being validated in the TBI population as novel endpoints that correlates to functional outcome metrics. These imaging modalities include for example, DTI, diffusion kurtosis imaging (DKI), resting state functional MRI (rsfMRI), and arterial spin labeling (ASL). The Quantitative Imaging Biomarkers Alliance (QIBA) is working on validating neuroimaging as a biomarker by essentially counting pixels as an objective comparison. Sequential imaging should also be employed and even if an immediate baseline MRI is perhaps not feasible in the moderate to severe TBI patient population, an MRI should be conducted as soon as possible to be used for stratification and as baseline that can then be compared to a follow up MRI to assess longitudinal changes (302).

One has to differentiate between biomarkers that can be used as outcome metrics and those that can be used for patient stratification to decrease heterogeneity and identify a more unified subject population. One advantage of biomarkers is that the same biomarker could theoretically be used in pre-clinical trials and inform injury-specific translation. Preclinical and clinical endpoints must be developed in parallel and we should use the same biomarkers in the preclinical studies and in clinical trials, truly embracing a bidirectional bench to bedside development. This would be in stark

contrast to the Morris water maze, often used as a functional behavioral outcome metric in preclinical studies, and its poor translatability to GOS/GOS-E used in clinical trials. A functional outcome metric such as the GOS/GOS-E may however still be suitable for a large phase III trial, especially in the moderate to severe TBI patient population, given proper patient stratification.

Metabolic support for treatment of chemical toxins and warfare agents

Development of the cell permeable succinate prodrugs (Paper IV) and the rotenone pig model (Paper V) led to the idea of expanding the target indication to treat chemically-induced mitochondrial dysfunction. Inhibition of CI is one of the more commonly reported toxic effect of chemicals, and over sixty different families of compounds are known to inhibit CI (303). These chemicals include pesticides and insecticides, such as glyphosate (304), benzimidazole (305), atrazine (306), fenazaquin (307), fenpyroximate (308), cyhalothrin (309) and chlorpyrifos (310). Pesticides of the organophosphate class to which chlorpyrifos belongs are the main cause of death from poisoning in the developing world (311).

Chemical warfare agents such as the highly lethal nerve gasses, Sarin, Soman, Tabun and VX belong to the same class of chemicals as the organophosphate pesticides (312). The lethal potential of these chemical warfare agents is due to their acetylcholinesterase inhibitory effects. However, an increasing body of evidence indicates that changes in mitochondrial function may partially account for long-term effects of nerve gases (313). Lewisite, another important chemical warfare agent, inhibits the PDH complex and results in decreased ATP production and a metabolic shift to anaerobic metabolism (314). The related compounds arsine and phosgene have similar effects.

Sodium fluoroacetate, commonly known as compound 1080, decreases ATP production by inhibiting aconitase, an enzyme in the TCA cycle. A secondary effect of sodium fluoroacetate is a feedback loop that also inhibits glycolysis, compounding the inhibition of cellular respiration (315). The exposure to all these chemical agents that inhibit mitochondrial respiration at CI or upstream, are potential treatment indications for the cell-permeable succinate prodrug described in paper IV.

In addition, the drug may also limit toxicity of any chemical agent that decreases ATP output due to downstream toxic effects, such as the respiratory chain CIV inhibitors cyanide, cyanogen chloride, carbon monoxide and sodium azide (316). Preliminary data show that the succinate prodrugs also enhance cellular respiration in partial CIV

inhibition. Since the drug does not act on the chemical agent itself, but acts as a countermeasure to compensate for decreased mitochondrial respiration and prevent subsequent organ failure, the succinate prodrugs may be beneficial to patients for hours and days after exposure.

Metabolic support to prevent brain injury following cardiac arrest

Resuscitation from cardiac arrest is invariably accompanied by ischemia-reperfusion injury and subsequent neurological impairment (317). The brain is particularly susceptible to severe and permanent injury. Initial survival of cardiac arrest is about effective CPR, but in the subsequent hours and days there is a reduction in oxidative phosphorylation in the brain (318, 319). ETC function, particularly of CI, is significantly reduced immediately after ischemia-reperfusion injury and for the following hours and days (318, 319). Several studies suggest that CII-driven respiration is critical and rescues ATP generation in the first several hours following cerebral ischemia (320, 321). Administering cell-permeable succinate to bypass a dysfunctional CI and thereby reduce the bioenergetic crisis may improve survival and neurologic outcomes after cardiac arrest.

Acknowledgements

If I have seen further, it is by standing on the shoulders of giants.

I want to begin by thanking all my fellow scientists who have made the discoveries on which this thesis builds. Secondly, I want to thank my supervisor Eskil Elmér. He is a bright and eccentric scientist who sees only solutions, never problems—the personification of thinking outside the box. My brilliant assistant supervisor Magnus Hansson is of equal importance. A scientist at heart, his rigorous approach to everything forced me to tackle problems in my methodology and data interpretation.

I also want to thank all of my other colleagues and collaborators: Eleonor Åsander-Frostner, our lab manager, without whom everything would literally have fallen apart, Sarah Piel who made me look like a procrastinating teenager, Saori Morota, whose work ethic is in a league of its own, Fredrik Sjövall, whose sociable and easygoing personality made science seem less daunting, Hiroyuki Uchino, a tremendously generous collaborator, and Johannes Ehinger, my closest friend in the lab. While in all honesty, a terrible PhD student (in Philadelphia he was known as Professor Ehinger), Johannes possesses capabilities that will no doubt lead him to success as a principal investigator.

Another person I must thank is Todd Kilbaugh, my mentor and friend in Philadelphia with whom I have accomplished, and will continue to accomplish, many great things. My first visit to Todd's lab six years ago changed the trajectory of my life. Thank you to all my other colleagues in Philadelphia as well, and especially Melissa Gabello who deserves a special thanks for her inspiring tenacity. She got run over by a car in front of our eyes, broke her pelvis and jaw (which meant she had to eat through a straw for months), but she was nonetheless back in the lab after only a few days.

I also want to thank my parents, Kerstin and Ingemar, as well as my four older brothers, Andreas, Johannes, Lukas and Samuel. Growing up, I was always encouraged to view the world with a scientific mindset. My first intellectual challenges as a teenager were related to metaphysical questions such as, *what is life?* Having completed this thesis, I think I finally have the answer: Life is the membrane

potential over the inner mitochondrial membrane. That is the only thing that differentiates those who are alive from those who are deceased—it's that simple.

Finally, I want to thank my wonderful and brilliant wife Sofia. She is able to remind me of what is truly important in life while simultaneously encouraging me to work hard and strive to accomplish all my professional goals. She is not easily impressed, so whenever she is, I know I have actually accomplished something extraordinary. Sofia, I hope you are impressed when you read this!

Svensk populärvetenskaplig sammanfattning

Mitokondrien brukar oftast liknas vid cellens kraftverk. Majoriteten av den energi vi får i oss via maten omvandlas i mitokondrien till den energirika molekylen ATP. Denna molekyl kan liknas vid cellens energivaluta och när cellen utför energikrävande uppgifter kan ATP frigöra den energi som behövs. ATP produceras i elektrontransportkedjan som är lokaliserad i mitokondriens innermembran. Elektrontransportkedjan består av fyra proteinkomplex benämnda I, II, III och IV.

Energin i till exempel kolhydrater, som succesivt brutits ner till mindre beståndsdelar via glykolysen och citronsyrecykeln, doneras i form av elektroner till elektrontransportkedjan. Energin i elektronerna används sedan för att pumpa protoner över mitokondriens innermembran. Detta skapar en protongradient över membranet som sedan används av det så kallade ATP-syntaset, som protonerna flödar tillbaka igenom i motsatt riktning, samtidigt som ATP produceras. ATP-syntaset kan därmed liknas vid en turbin i ett vattenkraftverk som omvandlar den energi som finns lagrad i vattnets potentiella energi till elektricitet.

Hjärnan hos en vuxen person utgör endast någon enstaka procent av den totala kroppsvikten men konsumerar syrgas som motsvarar ungefär en femtedel av kroppens totala syrgaskonsumtion. Hjärnan är helt beroende av mitokondrien för dess energiförsörjning och är ytterst känslig för störningar. Denna avhandling fokuserar på en eventuell mitokondriell dysfunktion i hjärnan vid två olika sjukdomstillstånd. Vid både dessa tillstånd har andra forskare sedan tidigare föreslagit att mitokondriens funktion kan vara av avgörande betydelse för sjukdomsutvecklingen. I arbetet med denna avhandling så har vi huvudsakligen använt oss av en metod där man i detalj mäter mitokondriernas syrgaskonsumtion för att kartlägga funktionen i elektrontransportkedjan.

Blodförgiftning, även kallat sepsis, är ett syndrom som kännetecknas av en organdysfunktion som inte bara är orsakad av den underliggande infektionen utan också av en generell och oreglerad inflammatorisk reaktion. Den kliniska bilden skiljer sig mycket åt beroende på den specifika infektionen samt hur patientens tillstånd var före insjuknandet. Sjukdomsprocessen tros vara multifaktoriell men det har föreslagits att mitokondriell dysfunktion kan spela en avgörande roll. Andra

forskargrupper har tidigare bland annat påvisat att mitokondrierna i hjärnan blir mindre effektiva som en del i sjukdomsprocessen. Förutom antibiotika så finns det finns inga läkemedel utöver allmänt stödjande behandling som angriper de underliggande sjukdomsprocesserna.

Traumatisk hjärnskada orsakas av ett yttre fysiskt våld mot huvudet. Den initiala skadan kan medföra omedelbar vävnadsdöd och förlust av hjärnvävnad som givetvis inte kan behandlas med läkemedel. Efter skadeögonblicket så fortgår dock en sekundär sjukdomsprocess under de efterföljande timmarna och dagarna. I denna sekundära sjukdomsprocess så tror man att mitokondriell dysfunktion spelar en betydande roll för den slutgiltiga utbredningen av hjärnskadan. Utöver allmänt stödjande behandling så finns det, i likhet med sepsis, inga tillgängliga läkemedel som angriper de underliggande sjukdomsprocesserna.

I det första delarbetet undersöktes hur den mitokondriella funktionen påverkas av sepsis. I en djurmodell undersöktes funktionen i elektronstrasportkedjan i detalj i både hjärnan och levern. Resultaten visade att dessa två organ reagerar väldigt olika på sepsis. Funktionen i hjärnan kan enklast beskrivas som att mitokondrien blir mindre effektiv och att en mindre andel av syrgaskonsumtionen går till att producera ATP. I levern däremot så pekade funktionen i elektrontransportkedjan på att ATP-syntaset ökade som svar på sepsis. På grund av att vi såg denna skillnad i hur organen reagerade så kan man argumentera för att detta är en adaptiv respons och inte nödvändigtvis en dysfunktion, vilket även andra forskare argumenterat för tidigare.

I de följande två delarbetena undersöktes den mitokondriella funktionen efter traumatisk hjärnskada, både i en skademodell som ger en fokalt lokaliserad skada, samt i en modell som ger en mer generell och diffus skada. I den fokala modellen påvisades en bilateralt sänkt funktion i komplex I i elektrontransportkedjan och en kontralateral, relativt skadan, ökning i komplex II. Sänkningen i komplex I på samma sida som skadan tycks främst beror på att mitokondrier går under och att man således får färre mitokondrier.

I den generella diffusa skademodellen så var det primära fyndet en sänkt effektivitet hos mitokondrierna som främst var relaterad till att en mindre andel av syrgaskonsumtionen går till att producera ATP. Även i denna modell tycks det relativa bidraget av komplex I respektive komplex II ändras som ett resultat av skadan. I båda dessa delarbeten som berör traumatisk hjärnskada exemplifieras också svårigheten med att normalisera den mitokondriella funktionen. Enkelt förklarat så kan man antingen normalisera den mitokondriella funktionen per viktenhet eller med olika mått på hur många mitokondrier där finns. Genom att använda sig av de olika metoderna kan konklusionerna skilja sig diametralt åt.

Det fjärde delarbetet beskriver utvecklingen av en helt ny och innovativ läkemedelsklass. Som beskrivet kan komplex I vara dysfunktionellt på grund av akut

skada, men komplex I kan också fungera dåligt på grund av genetiskt nedärvda sjukdomar. Huvuddelen av den energi vi får i oss via maten utvinns via nedbrytningsvägar som går via komplex I i elektrontransportkedjan. Succinat, även kallat bärnstenssyra, donerar däremot sina elektroner till komplex II och administrering av succinat har därför föreslagits som läkemedelsstrategi för sjukdomar som innefattar en dysfunktion i komplex I. Problemet är dock att succinat inte kan passera över cellens membran och är därför sannolikt inte användbart som läkemedel. Vi utvecklade dock ett antal så kallade prodroger av succinat som gjorde dem cellpermeabla. Enkelt beskrivet så modifierade vi den kemiska strukturen genom att koppla på molekylgrupper som gjorde succinat cellpermeabelt. När läkemedlet väl kommer in i cellen klyvs dessa påkopplade molekylstrukturer av, genom enzymer som finns i alla celler, och succinat frigörs. Vi visade att läkemedelskonceptet fungerar i en mängd olika mänskliga celler, samt hjärtbiopsier från patienter.

I det femte delarbetet utvecklades en djurmodell för utvärdering av läkemedelskandidaterna som utvecklades i det fjärde delarbetet. Administration av ett toxin som specifikt inhiberar komplex I resulterade i en markant laktatstegring i blodet. Laktat, även kallat mjölksyra, kan öka på grund av antingen dålig mitokondriell funktion alternativt dålig syrgastillförsel på grund av sekundära effekter. De sammantagna resultaten i det femte delarbetet visade att laktatstegringen specifikt berodde på en mitokondriell dysfunktion i komplex I och inte på grund av att vävnaden var dåligt syresatt. Konklusionen är att modellen kan användas för att utvärdera läkemedelskandidater som har till syfte att motverka eller överbrygga en dysfunktion i komplex I.

Det sista delarbetet i denna avhandling utvärderar ett läkemedel som heter ciklosporin, som redan idag används vid transplantationer för att trycka ner kroppens immunförsvar. Man har dock tidigare även visat att läkemedlet verkar på en sjukdomsprocess relaterat till mitokondrien samt, främst i studier på främst möss och råttor, påvisat att läkemedlet kan skydda hjärnan efter traumatisk hjärnskada. Vi utförde en avancerad studie i grisar enligt en standard som oftast bara tillämpas i kliniska studier på människa och kunde påvisa en minskad volym på hjärnskadan på hela 35%.

Sammanfattningsvis så handlar avhandlingen om förändringar i hjärnans mitokondriella funktion relaterat till elektrontransportkedjan och dess roll vid sepsis och traumatisk hjärnskada. Forskningen visar att nya läkemedel som verkar på mitokondrierna kan vara en lovande strategi. Utöver de sjukdomsprocesser som denna avhandling handlar om så har mitokondriell dysfunktion i komplex I föreslagits i en mängd olika sjukdomsprocesser. Man kan därför tänka sig att de läkemedelskandidaterna som beskrivs i delarbete IV även kan användas vid andra sjukdomstillstånd.

References

1. Lane N, Martin W. The energetics of genome complexity. Nature. 2010;467(7318):929-34. doi: 10.1038/nature09486. PubMed PMID: 20962839.
2. Sagan L. On the origin of mitosing cells. J Theor Biol. 1967;14(3):255-74. Epub 1967/03/01. PubMed PMID: 11541392.
3. Rivera MC, Lake JA. The ring of life provides evidence for a genome fusion origin of eukaryotes. Nature. 2004;431(7005):152-5. Epub 2004/09/10. doi: 10.1038/nature02848. PubMed PMID: 15356622.
4. Cox CJ, Foster PG, Hirt RP, Harris SR, Embley TM. The archaebacterial origin of eukaryotes. Proc Natl Acad Sci U S A. 2008;105(51):20356-61. Epub 2008/12/17. doi: 10.1073/pnas.0810647105. PubMed PMID: 19073919; PMCID: PMC2629343.
5. Choi SW, Gerencser AA, Lee DW, Rajagopalan S, Nicholls DG, Andersen JK, Brand MD. Intrinsic bioenergetic properties and stress sensitivity of dopaminergic synaptosomes. J Neurosci. 2011;31(12):4524-34. doi: 10.1523/JNEUROSCI.5817-10.2011. PubMed PMID: 21430153; PMCID: PMC3083118.
6. Nass MM, Nass S. Intramitochondrial Fibers with Dna Characteristics. I. Fixation and Electron Staining Reactions. J Cell Biol. 1963;19:593-611. Epub 1963/12/01. PubMed PMID: 14086138; PMCID: PMC2106331.
7. Nass S, Nass MM. Intramitochondrial Fibers with Dna Characteristics. Ii. Enzymatic and Other Hydrolytic Treatments. J Cell Biol. 1963;19:613-29. Epub 1963/12/01. PubMed PMID: 14086139; PMCID: PMC2106332.
8. DiMauro S, Garone C. Historical perspective on mitochondrial medicine. Dev Disabil Res Rev. 2010;16(2):106-13. Epub 2010/09/08. doi: 10.1002/ddrr.102. PubMed PMID: 20818724; PMCID: PMC3839238.
9. Gray MW. Mosaic nature of the mitochondrial proteome: Implications for the origin and evolution of mitochondria. Proc Natl Acad Sci U S A. 2015;112(33):10133-8. Epub 2015/04/08. doi: 10.1073/pnas.1421379112. PubMed PMID: 25848019; PMCID: PMC4547279.
10. Twig G, Elorza A, Molina AJ, Mohamed H, Wikstrom JD, Walzer G, Stiles L, Haigh SE, Katz S, Las G, Alroy J, Wu M, Py BF, Yuan J, Deeney JT, Corkey BE, Shirihai OS. Fission and selective fusion govern mitochondrial segregation and elimination by autophagy. Embo J. 2008;27(2):433-46. Epub 2008/01/18. doi: 10.1038/sj.emboj.7601963. PubMed PMID: 18200046; PMCID: PMC2234339.
11. Deas E, Wood NW, Plun-Favreau H. Mitophagy and Parkinson's disease: the PINK1-parkin link. Biochim Biophys Acta. 2011;1813(4):623-33. Epub 2010/08/26. doi: 10.1016/j.bbamcr.2010.08.007. PubMed PMID: 20736035; PMCID: PMC3925795.

12. Kagawa Y, Racker E. Partial resolution of the enzymes catalyzing oxidative phosphorylation. IX. Reconstruction of oligomycin-sensitive adenosine triphosphatase. J Biol Chem. 1966;241(10):2467-74. Epub 1966/05/25. PubMed PMID: 4223641.
13. Abrahams JP, Leslie AG, Lutter R, Walker JE. Structure at 2.8 A resolution of F1-ATPase from bovine heart mitochondria. Nature. 1994;370(6491):621-8. Epub 1994/08/25. doi: 10.1038/370621a0. PubMed PMID: 8065448.
14. Mitchell P. Coupling of phosphorylation to electron and hydrogen transfer by a chemi-osmotic type of mechanism. Nature. 1961;191:144-8. Epub 1961/07/08. PubMed PMID: 13771349.
15. Krebs HA, Johnson WA. Metabolism of ketonic acids in animal tissues. Biochem J. 1937;31(4):645-60. Epub 1937/04/01. PubMed PMID: 16746382; PMCID: PMC1266984.
16. Cori CC, Gerty. Glycogen formation in the liver with d- and l-lactic acid Journal of Biological Chemistry. 1929;81(402).
17. Hui S, Ghergurovich JM, Morscher RJ, Jang C, Teng X, Lu W, Esparza LA, Reya T, Le Z, Yanxiang Guo J, White E, Rabinowitz JD. Glucose feeds the TCA cycle via circulating lactate. Nature. 2017. Epub 2017/10/19. doi: 10.1038/nature24057. PubMed PMID: 29045397.
18. Knoop F. Der Abbau aromatischer Fettsäuren im Tierkörper. Beitr Chem Physiol Pathol. 1904(6):150–62.
19. Simoni RD, Hill RL, Vaughan M. Comparative studies of the mode of oxidation of phenyl derivatives of fatty acids by the animal organism and by hydrogen peroxide (Dakin, H. D. (1908) J. Biol. Chem. 4, 419-435). J Biol Chem. 2002;277(15):e4-5. Epub 2002/04/09. PubMed PMID: 11937515.
20. Kresge N, Hanson RW, Simoni RD, Hill RL. Sidney Weinhouse and the mechanism of ketone body synthesis from fatty acids. J Biol Chem. 2005;280(23):e20. Epub 2005/06/07. PubMed PMID: 15937341.
21. Bayer E, Bauer B, Eggerer H. Evidence from inhibitor studies for conformational changes of citrate synthase. Eur J Biochem. 1981;120(1):155-60. Epub 1981/11/01. PubMed PMID: 7308213.
22. Schagger H, Pfeiffer K. Supercomplexes in the respiratory chains of yeast and mammalian mitochondria. Embo J. 2000;19(8):1777-83. Epub 2000/04/25. doi: 10.1093/emboj/19.8.1777. PubMed PMID: 10775262; PMCID: PMC302020.
23. Rial E, Nicholls DG. The uncoupling protein from brown adipose tissue mitochondria. Revis Biol Celular. 1987;11:75-104. Epub 1987/01/01. PubMed PMID: 3324211.
24. Mattiasson G, Sullivan PG. The emerging functions of UCP2 in health, disease, and therapeutics. Antioxid Redox Signal. 2006;8(1-2):1-38. Epub 2006/02/21. doi: 10.1089/ars.2006.8.1. PubMed PMID: 16487034.
25. Mattiasson G, Shamloo M, Gido G, Mathi K, Tomasevic G, Yi S, Warden CH, Castilho RF, Melcher T, Gonzalez-Zulueta M, Nikolich K, Wieloch T. Uncoupling protein-2 prevents neuronal death and diminishes brain dysfunction after stroke and brain trauma. Nat Med. 2003;9(8):1062-8. Epub 2003/07/15. doi: 10.1038/nm903. PubMed PMID: 12858170.

26. Brand MD, Chien LF, Ainscow EK, Rolfe DF, Porter RK. The causes and functions of mitochondrial proton leak. Biochim Biophys Acta. 1994;1187(2):132-9. Epub 1994/08/30. PubMed PMID: 8075107.
27. Sena LA, Chandel NS. Physiological roles of mitochondrial reactive oxygen species. Mol Cell. 2012;48(2):158-67. Epub 2012/10/30. doi: 10.1016/j.molcel.2012.09.025. PubMed PMID: 23102266; PMCID: PMC3484374.
28. Murphy MP. How mitochondria produce reactive oxygen species. Biochem J. 2009;417(1):1-13. Epub 2008/12/09. doi: 10.1042/BJ20081386. PubMed PMID: 19061483; PMCID: PMC2605959.
29. Handy DE, Loscalzo J. Redox regulation of mitochondrial function. Antioxid Redox Signal. 2012;16(11):1323-67. Epub 2011/12/08. doi: 10.1089/ars.2011.4123. PubMed PMID: 22146081; PMCID: PMC3324814.
30. Quinlan CL, Gerencser AA, Treberg JR, Brand MD. The mechanism of superoxide production by the antimycin-inhibited mitochondrial Q-cycle. J Biol Chem. 2011;286(36):31361-72. Epub 2011/06/29. doi: 10.1074/jbc.M111.267898. PubMed PMID: 21708945; PMCID: PMC3173136.
31. Makrecka-Kuka M, Krumschnabel G, Gnaiger E. High-Resolution Respirometry for Simultaneous Measurement of Oxygen and Hydrogen Peroxide Fluxes in Permeabilized Cells, Tissue Homogenate and Isolated Mitochondria. Biomolecules. 2015;5(3):1319-38. doi: 10.3390/biom5031319. PubMed PMID: 26131977; PMCID: PMC4598754.
32. Brand MD. The sites and topology of mitochondrial superoxide production. Exp Gerontol. 2010;45(7-8):466-72. Epub 2010/01/13. doi: 10.1016/j.exger.2010.01.003. PubMed PMID: 20064600; PMCID: PMC2879443.
33. Guzy RD, Sharma B, Bell E, Chandel NS, Schumacker PT. Loss of the SdhB, but Not the SdhA, subunit of complex II triggers reactive oxygen species-dependent hypoxia-inducible factor activation and tumorigenesis. Mol Cell Biol. 2008;28(2):718-31. Epub 2007/10/31. doi: 10.1128/MCB.01338-07. PubMed PMID: 17967865; PMCID: PMC2223429.
34. Dong LF, Freeman R, Liu J, Zobalova R, Marin-Hernandez A, Stantic M, Rohlena J, Valis K, Rodriguez-Enriquez S, Butcher B, Goodwin J, Brunk UT, Witting PK, Moreno-Sanchez R, Scheffler IE, Ralph SJ, Neuzil J. Suppression of tumor growth in vivo by the mitocan alpha-tocopheryl succinate requires respiratory complex II. Clin Cancer Res. 2009;15(5):1593-600. Epub 2009/02/19. doi: 10.1158/1078-0432.CCR-08-2439. PubMed PMID: 19223492.
35. Bezawork-Geleta A, Rohlena J, Dong L, Pacak K, Neuzil J. Mitochondrial Complex II: At the Crossroads. Trends Biochem Sci. 2017;42(4):312-25. Epub 2017/02/12. doi: 10.1016/j.tibs.2017.01.003. PubMed PMID: 28185716.
36. Pryde KR, Hirst J. Superoxide is produced by the reduced flavin in mitochondrial complex I: a single, unified mechanism that applies during both forward and reverse electron transfer. J Biol Chem. 2011;286(20):18056-65. Epub 2011/03/12. doi: 10.1074/jbc.M110.186841. PubMed PMID: 21393237; PMCID: PMC3093879.
37. Treberg JR, Quinlan CL, Brand MD. Evidence for two sites of superoxide production by mitochondrial NADH-ubiquinone oxidoreductase (complex I). J Biol Chem.

2011;286(31):27103-10. Epub 2011/06/11. doi: 10.1074/jbc.M111.252502. PubMed PMID: 21659507; PMCID: PMC3149303.
38. Eltzschig HK, Eckle T. Ischemia and reperfusion--from mechanism to translation. Nat Med. 2011;17(11):1391-401. Epub 2011/11/09. doi: 10.1038/nm.2507. PubMed PMID: 22064429; PMCID: PMC3886192.
39. Chouchani ET, Pell VR, Gaude E, Aksentijevic D, Sundier SY, Robb EL, Logan A, Nadtochiy SM, Ord EN, Smith AC, Eyassu F, Shirley R, Hu CH, Dare AJ, James AM, Rogatti S, Hartley RC, Eaton S, Costa AS, Brookes PS, Davidson SM, Duchen MR, Saeb-Parsy K, Shattock MJ, Robinson AJ, Work LM, Frezza C, Krieg T, Murphy MP. Ischaemic accumulation of succinate controls reperfusion injury through mitochondrial ROS. Nature. 2014;515(7527):431-5. doi: 10.1038/nature13909. PubMed PMID: 25383517; PMCID: 4255242.
40. Andrienko TN, Pasdois P, Pereira GC, Ovens MJ, Halestrap AP. The role of succinate and ROS in reperfusion injury - A critical appraisal. J Mol Cell Cardiol. 2017. doi: 10.1016/j.yjmcc.2017.06.016. PubMed PMID: 28689004.
41. Hansson MJ, Mansson R, Morota S, Uchino H, Kallur T, Sumi T, Ishii N, Shimazu M, Keep MF, Jegorov A, Elmer E. Calcium-induced generation of reactive oxygen species in brain mitochondria is mediated by permeability transition. Free Radic Biol Med. 2008;45(3):284-94. Epub 2008/05/10. doi: S0891-5849(08)00208-6 [pii]

10.1016/j.freeradbiomed.2008.04.021. PubMed PMID: 18466779.
42. Li Y, Huang TT, Carlson EJ, Melov S, Ursell PC, Olson JL, Noble LJ, Yoshimura MP, Berger C, Chan PH, Wallace DC, Epstein CJ. Dilated cardiomyopathy and neonatal lethality in mutant mice lacking manganese superoxide dismutase. Nat Genet. 1995;11(4):376-81. doi: 10.1038/ng1295-376. PubMed PMID: 7493016.
43. Murphy MP. Mitochondrial thiols in antioxidant protection and redox signaling: distinct roles for glutathionylation and other thiol modifications. Antioxid Redox Signal. 2012;16(6):476-95. Epub 2011/10/01. doi: 10.1089/ars.2011.4289. PubMed PMID: 21954972.
44. Starkov AA. Measurement of mitochondrial ROS production. Methods Mol Biol. 2010;648:245-55. Epub 2010/08/12. doi: 10.1007/978-1-60761-756-3_16. PubMed PMID: 20700717; PMCID: 3057530.
45. Kowaltowski AJ, de Souza-Pinto NC, Castilho RF, Vercesi AE. Mitochondria and reactive oxygen species. Free Radic Biol Med. 2009;47(4):333-43. Epub 2009/05/12. doi: 10.1016/j.freeradbiomed.2009.05.004. PubMed PMID: 19427899.
46. Chalmers S, Nicholls DG. The relationship between free and total calcium concentrations in the matrix of liver and brain mitochondria. J Biol Chem. 2003;278(21):19062-70. Epub 2003/03/28. doi: 10.1074/jbc.M212661200. PubMed PMID: 12660243.
47. Ivannikov MV, Macleod GT. Mitochondrial free Ca(2)(+) levels and their effects on energy metabolism in Drosophila motor nerve terminals. Biophys J. 2013;104(11):2353-61. Epub 2013/06/12. doi: 10.1016/j.bpj.2013.03.064. PubMed PMID: 23746507; PMCID: PMC3672877.
48. Schwarzlander M, Logan DC, Johnston IG, Jones NS, Meyer AJ, Fricker MD, Sweetlove LJ. Pulsing of membrane potential in individual mitochondria: a stress-induced mechanism to regulate respiratory bioenergetics in Arabidopsis. Plant Cell.

2012;24(3):1188-201. Epub 2012/03/08. doi: 10.1105/tpc.112.096438. PubMed PMID: 22395486; PMCID: PMC3336130.
49. Pizzo P, Pozzan T. Mitochondria-endoplasmic reticulum choreography: structure and signaling dynamics. Trends Cell Biol. 2007;17(10):511-7. Epub 2007/09/14. doi: 10.1016/j.tcb.2007.07.011. PubMed PMID: 17851078.
50. Lemasters JJ, Nieminen AL, Qian T, Trost LC, Elmore SP, Nishimura Y, Crowe RA, Cascio WE, Bradham CA, Brenner DA, Herman B. The mitochondrial permeability transition in cell death: a common mechanism in necrosis, apoptosis and autophagy. Biochim Biophys Acta. 1998;1366(1-2):177-96. PubMed PMID: 9714796.
51. Lemasters JJ. V. Necrapoptosis and the mitochondrial permeability transition: shared pathways to necrosis and apoptosis. Am J Physiol. 1999;276(1 Pt 1):G1-6. PubMed PMID: 9886971.
52. Lemasters JJ, Qian T, Bradham CA, Brenner DA, Cascio WE, Trost LC, Nishimura Y, Nieminen AL, Herman B. Mitochondrial dysfunction in the pathogenesis of necrotic and apoptotic cell death. J Bioenerg Biomembr. 1999;31(4):305-19. PubMed PMID: 10665521.
53. Crompton M. The mitochondrial permeability transition pore and its role in cell death. Biochem J. 1999;341 (Pt 2):233-49. PubMed PMID: 10393078; PMCID: PMC1220352.
54. Hunter FE, Jr., Ford L. Inactivation of oxidative and phosphorylative systems in mitochondria by preincubation with phosphate and other ions. J Biol Chem. 1955;216(1):357-69. Epub 1955/09/01. PubMed PMID: 13252035.
55. Hunter DR, Haworth RA. The Ca2+-induced membrane transition in mitochondria. I. The protective mechanisms. Arch Biochem Biophys. 1979;195(2):453-9. Epub 1979/07/01. PubMed PMID: 383019.
56. Hunter DR, Haworth RA. The Ca2+-induced membrane transition in mitochondria. III. Transitional Ca2+ release. Arch Biochem Biophys. 1979;195(2):468-77. Epub 1979/07/01. PubMed PMID: 112926.
57. Hunter DR, Haworth RA, Southard JH. Relationship between configuration, function, and permeability in calcium-treated mitochondria. J Biol Chem. 1976;251(16):5069-77. Epub 1976/08/25. PubMed PMID: 134035.
58. Haworth RA, Hunter DR. The Ca2+-induced membrane transition in mitochondria. II. Nature of the Ca2+ trigger site. Arch Biochem Biophys. 1979;195(2):460-7. Epub 1979/07/01. PubMed PMID: 38751.
59. Brustovetsky N, Brustovetsky T, Purl KJ, Capano M, Crompton M, Dubinsky JM. Increased susceptibility of striatal mitochondria to calcium-induced permeability transition. J Neurosci. 2003;23(12):4858-67. Epub 2003/07/02. PubMed PMID: 12832508.
60. Nicholls DG, Brand MD. The nature of the calcium ion efflux induced in rat liver mitochondria by the oxidation of endogenous nicotinamide nucleotides. Biochem J. 1980;188(1):113-8. Epub 1980/04/15. PubMed PMID: 7406874; PMCID: PMC1162544.
61. Gunter TE, Gunter KK, Sheu SS, Gavin CE. Mitochondrial calcium transport: physiological and pathological relevance. Am J Physiol. 1994;267(2 Pt 1):C313-39. Epub 1994/08/01. PubMed PMID: 8074170.

62. Doczi J, Turiak L, Vajda S, Mandi M, Torocsik B, Gerencser AA, Kiss G, Konrad C, Adam-Vizi V, Chinopoulos C. Complex contribution of cyclophilin D to Ca2+-induced permeability transition in brain mitochondria, with relation to the bioenergetic state. J Biol Chem. 2011;286(8):6345-53. Epub 2010/12/22. doi: 10.1074/jbc.M110.196600. PubMed PMID: 21173147; PMCID: PMC3057831.
63. Beutner G, Ruck A, Riede B, Brdiczka D. Complexes between porin, hexokinase, mitochondrial creatine kinase and adenylate translocator display properties of the permeability transition pore. Implication for regulation of permeability transition by the kinases. Biochim Biophys Acta. 1998;1368(1):7-18. Epub 1998/02/12. PubMed PMID: 9459579.
64. Crompton M, Ellinger H, Costi A. Inhibition by cyclosporin A of a Ca2+-dependent pore in heart mitochondria activated by inorganic phosphate and oxidative stress. Biochem J. 1988;255(1):357-60. Epub 1988/10/01. PubMed PMID: 3196322; PMCID: PMC1135230.
65. Borel JF, Feurer C, Gubler HU, Stahelin H. Biological effects of cyclosporin A: a new antilymphocytic agent. Agents Actions. 1976;6(4):468-75. Epub 1976/07/01. PubMed PMID: 8969.
66. Borel J. Cyclosporine: historical perspectives. Transplant Proc. 1983;15:2219–29.
67. Borel J. History of cyclosporin A and its significance in immunology DJG W, editor. Amsterdam: Elsevier Biomedical Press; 1982.
68. Baines CP, Kaiser RA, Purcell NH, Blair NS, Osinska H, Hambleton MA, Brunskill EW, Sayen MR, Gottlieb RA, Dorn GW, Robbins J, Molkentin JD. Loss of cyclophilin D reveals a critical role for mitochondrial permeability transition in cell death. Nature. 2005;434(7033):658-62. Epub 2005/04/01. doi: 10.1038/nature03434. PubMed PMID: 15800627.
69. Bernardi P. The permeability transition pore. Control points of a cyclosporin A-sensitive mitochondrial channel involved in cell death. Biochim Biophys Acta. 1996;1275(1-2):5-9. Epub 1996/07/18. PubMed PMID: 8688451.
70. Bernardi P, Colonna R, Costantini P, Eriksson O, Fontaine E, Ichas F, Massari S, Nicolli A, Petronilli V, Scorrano L. The mitochondrial permeability transition. Biofactors. 1998;8(3-4):273-81. Epub 1999/01/23. PubMed PMID: 9914829.
71. Bernardi P, Krauskopf A, Basso E, Petronilli V, Blachly-Dyson E, Di Lisa F, Forte MA. The mitochondrial permeability transition from in vitro artifact to disease target. FEBS J. 2006;273(10):2077-99. Epub 2006/05/03. doi: 10.1111/j.1742-4658.2006.05213.x. PubMed PMID: 16649987.
72. Halestrap AP, Davidson AM. Inhibition of Ca2(+)-induced large-amplitude swelling of liver and heart mitochondria by cyclosporin is probably caused by the inhibitor binding to mitochondrial-matrix peptidyl-prolyl cis-trans isomerase and preventing it interacting with the adenine nucleotide translocase. Biochem J. 1990;268(1):153-60. Epub 1990/05/15. PubMed PMID: 2160810; PMCID: PMC1131405.
73. Hansson MJ, Persson T, Friberg H, Keep MF, Rees A, Wieloch T, Elmer E. Powerful cyclosporin inhibition of calcium-induced permeability transition in brain mitochondria. Brain Res. 2003;960(1-2):99-111. PubMed PMID: 12505662.

74. Hansson MJ, Mansson R, Mattiasson G, Ohlsson J, Karlsson J, Keep MF, Elmer E. Brain-derived respiring mitochondria exhibit homogeneous, complete and cyclosporin-sensitive permeability transition. J Neurochem. 2004;89(3):715-29. doi: 10.1111/j.1471-4159.2004.02400.x. PubMed PMID: 15086528.
75. Hansson MJ, Morota S, Chen L, Matsuyama N, Suzuki Y, Nakajima S, Tanoue T, Omi A, Shibasaki F, Shimazu M, Ikeda Y, Uchino H, Elmer E. Cyclophilin D-sensitive mitochondrial permeability transition in adult human brain and liver mitochondria. J Neurotrauma. 2011;28(1):143-53. Epub 2010/12/03. doi: 10.1089/neu.2010.1613. PubMed PMID: 21121808; PMCID: 3025768.
76. Morota S, Manolopoulos T, Eyjolfsson A, Kimblad PO, Wierup P, Metzsch C, Blomquist S, Hansson MJ. Functional and pharmacological characteristics of permeability transition in isolated human heart mitochondria. PLoS One. 2013;8(6):e67747. Epub 2013/07/11. doi: 10.1371/journal.pone.0067747. PubMed PMID: 23840770; PMCID: PMC3695980.
77. Nakagawa T, Shimizu S, Watanabe T, Yamaguchi O, Otsu K, Yamagata H, Inohara H, Kubo T, Tsujimoto Y. Cyclophilin D-dependent mitochondrial permeability transition regulates some necrotic but not apoptotic cell death. Nature. 2005;434(7033):652-8. Epub 2005/04/01. doi: 10.1038/nature03317. PubMed PMID: 15800626.
78. Schinzel AC, Takeuchi O, Huang Z, Fisher JK, Zhou Z, Rubens J, Hetz C, Danial NN, Moskowitz MA, Korsmeyer SJ. Cyclophilin D is a component of mitochondrial permeability transition and mediates neuronal cell death after focal cerebral ischemia. Proc Natl Acad Sci U S A. 2005;102(34):12005-10. Epub 2005/08/17. doi: 10.1073/pnas.0505294102. PubMed PMID: 16103352; PMCID: PMC1189333.
79. Halestrap AP, Richardson AP. The mitochondrial permeability transition: a current perspective on its identity and role in ischaemia/reperfusion injury. J Mol Cell Cardiol. 2015;78:129-41. Epub 2014/09/03. doi: 10.1016/j.yjmcc.2014.08.018. PubMed PMID: 25179911.
80. Bernardi P, Rasola A, Forte M, Lippe G. The Mitochondrial Permeability Transition Pore: Channel Formation by F-ATP Synthase, Integration in Signal Transduction, and Role in Pathophysiology. Physiol Rev. 2015;95(4):1111-55. Epub 2015/08/14. doi: 10.1152/physrev.00001.2015. PubMed PMID: 26269524; PMCID: PMC4600949.
81. Szabo I, De Pinto V, Zoratti M. The mitochondrial permeability transition pore may comprise VDAC molecules. II. The electrophysiological properties of VDAC are compatible with those of the mitochondrial megachannel. FEBS Lett. 1993;330(2):206-10. Epub 1993/09/13. PubMed PMID: 7689984.
82. Crompton M, Virji S, Ward JM. Cyclophilin-D binds strongly to complexes of the voltage-dependent anion channel and the adenine nucleotide translocase to form the permeability transition pore. Eur J Biochem. 1998;258(2):729-35. Epub 1999/01/05. PubMed PMID: 9874241.
83. Krauskopf A, Eriksson O, Craigen WJ, Forte MA, Bernardi P. Properties of the permeability transition in VDAC1(-/-) mitochondria. Biochim Biophys Acta. 2006;1757(5-6):590-5. Epub 2006/04/22. doi: 10.1016/j.bbabio.2006.02.007. PubMed PMID: 16626625.
84. Baines CP, Kaiser RA, Sheiko T, Craigen WJ, Molkentin JD. Voltage-dependent anion channels are dispensable for mitochondrial-dependent cell death. Nat Cell

Biol. 2007;9(5):550-5. Epub 2007/04/10. doi: 10.1038/ncb1575. PubMed PMID: 17417626; PMCID: PMC2680246.
85. Brustovetsky N, Klingenberg M. Mitochondrial ADP/ATP carrier can be reversibly converted into a large channel by Ca2+. Biochemistry. 1996;35(26):8483-8. Epub 1996/07/02. doi: 10.1021/bi960833v. PubMed PMID: 8679608.
86. Brustovetsky N, Tropschug M, Heimpel S, Heidkamper D, Klingenberg M. A large Ca2+-dependent channel formed by recombinant ADP/ATP carrier from Neurospora crassa resembles the mitochondrial permeability transition pore. Biochemistry. 2002;41(39):11804-11. Epub 2002/09/25. PubMed PMID: 12269823.
87. Halestrap AP. What is the mitochondrial permeability transition pore? J Mol Cell Cardiol. 2009;46(6):821-31. Epub 2009/03/07. doi: 10.1016/j.yjmcc.2009.02.021. PubMed PMID: 19265700.
88. Woodfield K, Ruck A, Brdiczka D, Halestrap AP. Direct demonstration of a specific interaction between cyclophilin-D and the adenine nucleotide translocase confirms their role in the mitochondrial permeability transition. Biochem J. 1998;336 (Pt 2):287-90. PubMed PMID: 9820802; PMCID: PMC1219869.
89. Zoratti M, Szabo I. The mitochondrial permeability transition. Biochim Biophys Acta. 1995;1241(2):139-76. Epub 1995/07/17. PubMed PMID: 7640294.
90. Kokoszka JE, Waymire KG, Levy SE, Sligh JE, Cai J, Jones DP, MacGregor GR, Wallace DC. The ADP/ATP translocator is not essential for the mitochondrial permeability transition pore. Nature. 2004;427(6973):461-5. doi: 10.1038/nature02229. PubMed PMID: 14749836; PMCID: PMC3049806.
91. Halestrap AP, Clarke SJ, Khaliulin I. The role of mitochondria in protection of the heart by preconditioning. Biochim Biophys Acta. 2007;1767(8):1007-31. Epub 2007/07/17. doi: 10.1016/j.bbabio.2007.05.008. PubMed PMID: 17631856; PMCID: PMC2212780.
92. Da Cruz S, Xenarios I, Langridge J, Vilbois F, Parone PA, Martinou JC. Proteomic analysis of the mouse liver mitochondrial inner membrane. J Biol Chem. 2003;278(42):41566-71. Epub 2003/07/17. doi: 10.1074/jbc.M304940200. PubMed PMID: 12865426.
93. Beutner G, Alavian KN, Jonas EA, Porter GA, Jr. The Mitochondrial Permeability Transition Pore and ATP Synthase. Handb Exp Pharmacol. 2017;240:21-46. Epub 2016/09/04. doi: 10.1007/164_2016_5. PubMed PMID: 27590224.
94. Mnatsakanyan N, Beutner G, Porter GA, Alavian KN, Jonas EA. Physiological roles of the mitochondrial permeability transition pore. J Bioenerg Biomembr. 2017;49(1):13-25. Epub 2016/02/13. doi: 10.1007/s10863-016-9652-1. PubMed PMID: 26868013; PMCID: PMC4981558.
95. Jonas EA, Porter GA, Jr., Beutner G, Mnatsakanyan N, Alavian KN. Cell death disguised: The mitochondrial permeability transition pore as the c-subunit of the F(1)F(O) ATP synthase. Pharmacol Res. 2015;99:382-92. Epub 2015/05/10. doi: 10.1016/j.phrs.2015.04.013. PubMed PMID: 25956324; PMCID: PMC4567435.
96. Alavian KN, Beutner G, Lazrove E, Sacchetti S, Park HA, Licznerski P, Li H, Nabili P, Hockensmith K, Graham M, Porter GA, Jr., Jonas EA. An uncoupling channel within the c-subunit ring of the F1FO ATP synthase is the mitochondrial permeability

transition pore. Proc Natl Acad Sci U S A. 2014;111(29):10580-5. Epub 2014/07/01. doi: 10.1073/pnas.1401591111. PubMed PMID: 24979777; PMCID: PMC4115574.
97. Bonora M, Bononi A, De Marchi E, Giorgi C, Lebiedzinska M, Marchi S, Patergnani S, Rimessi A, Suski JM, Wojtala A, Wieckowski MR, Kroemer G, Galluzzi L, Pinton P. Role of the c subunit of the FO ATP synthase in mitochondrial permeability transition. Cell Cycle. 2013;12(4):674-83. Epub 2013/01/25. doi: 10.4161/cc.23599. PubMed PMID: 23343770; PMCID: PMC3594268.
98. Erecinska M, Silver IA. ATP and brain function. J Cereb Blood Flow Metab. 1989;9(1):2-19. Epub 1989/02/01. doi: 10.1038/jcbfm.1989.2. PubMed PMID: 2642915.
99. Gibbs E. L. LWG, Nims L. F., Gibbs F. A. ARTERIAL AND CEREBRAL VENOUS BLOOD: ARTERIAL-VENOUS DIFFERENCES IN MAN. The Journal of Biological Chemistry. 1942(144):325-32.
100. Berman SB, Watkins SC, Hastings TG. Quantitative biochemical and ultrastructural comparison of mitochondrial permeability transition in isolated brain and liver mitochondria: evidence for reduced sensitivity of brain mitochondria. Exp Neurol. 2000;164(2):415-25. Epub 2000/08/01. doi: 10.1006/exnr.2000.7438. PubMed PMID: 10915580.
101. Andreyev A, Fiskum G. Calcium induced release of mitochondrial cytochrome c by different mechanisms selective for brain versus liver. Cell Death Differ. 1999;6(9):825-32. Epub 1999/10/08. doi: 10.1038/sj.cdd.4400565. PubMed PMID: 10510464.
102. Andreyev AY, Fahy B, Fiskum G. Cytochrome c release from brain mitochondria is independent of the mitochondrial permeability transition. FEBS Lett. 1998;439(3):373-6. Epub 1998/12/09. PubMed PMID: 9845356.
103. Brustovetsky N, Dubinsky JM. Limitations of cyclosporin A inhibition of the permeability transition in CNS mitochondria. J Neurosci. 2000;20(22):8229-37. Epub 2000/11/09. PubMed PMID: 11069928.
104. Kristal BS, Staats PN, Shestopalov AI. Biochemical characterization of the mitochondrial permeability transition in isolated forebrain mitochondria. Dev Neurosci. 2000;22(5-6):376-83. Epub 2000/12/09. doi: 17463. PubMed PMID: 11111153.
105. Kristian T, Weatherby TM, Bates TE, Fiskum G. Heterogeneity of the calcium-induced permeability transition in isolated non-synaptic brain mitochondria. J Neurochem. 2002;83(6):1297-308. Epub 2002/12/11. PubMed PMID: 12472884.
106. Friberg H, Connern C, Halestrap AP, Wieloch T. Differences in the activation of the mitochondrial permeability transition among brain regions in the rat correlate with selective vulnerability. J Neurochem. 1999;72(6):2488-97. Epub 1999/06/01. PubMed PMID: 10349859.
107. Friberg H, Ferrand-Drake M, Bengtsson F, Halestrap AP, Wieloch T. Cyclosporin A, but not FK 506, protects mitochondria and neurons against hypoglycemic damage and implicates the mitochondrial permeability transition in cell death. J Neurosci. 1998;18(14):5151-9. PubMed PMID: 9651198.
108. Schinder AF, Olson EC, Spitzer NC, Montal M. Mitochondrial dysfunction is a primary event in glutamate neurotoxicity. J Neurosci. 1996;16(19):6125-33. Epub 1996/10/01. PubMed PMID: 8815895.

109. White RJ, Reynolds IJ. Mitochondrial depolarization in glutamate-stimulated neurons: an early signal specific to excitotoxin exposure. J Neurosci. 1996;16(18):5688-97. Epub 1996/09/15. PubMed PMID: 8795624.
110. Nicholls DG. Oxidative stress and energy crises in neuronal dysfunction. Ann N Y Acad Sci. 2008;1147:53-60. Epub 2008/12/17. doi: 10.1196/annals.1427.002. PubMed PMID: 19076430.
111. Friedman G, Silva E, Vincent JL. Has the mortality of septic shock changed with time. Crit Care Med. 1998;26(12):2078-86. Epub 1999/01/06. PubMed PMID: 9875924.
112. Angus DC, van der Poll T. Severe sepsis and septic shock. N Engl J Med. 2013;369(9):840-51. Epub 2013/08/30. doi: 10.1056/NEJMra1208623. PubMed PMID: 23984731.
113. Annane D, Sebille V, Charpentier C, Bollaert PE, Francois B, Korach JM, Capellier G, Cohen Y, Azoulay E, Troche G, Chaumet-Riffaud P, Bellissant E. Effect of treatment with low doses of hydrocortisone and fludrocortisone on mortality in patients with septic shock. JAMA. 2002;288(7):862-71. Epub 2002/08/21. PubMed PMID: 12186604.
114. Russell JA, Walley KR, Singer J, Gordon AC, Hebert PC, Cooper DJ, Holmes CL, Mehta S, Granton JT, Storms MM, Cook DJ, Presneill JJ, Ayers D, Investigators V. Vasopressin versus norepinephrine infusion in patients with septic shock. N Engl J Med. 2008;358(9):877-87. Epub 2008/02/29. doi: 10.1056/NEJMoa067373. PubMed PMID: 18305265.
115. Sprung CL, Annane D, Keh D, Moreno R, Singer M, Freivogel K, Weiss YG, Benbenishty J, Kalenka A, Forst H, Laterre PF, Reinhart K, Cuthbertson BH, Payen D, Briegel J, Group CS. Hydrocortisone therapy for patients with septic shock. N Engl J Med. 2008;358(2):111-24. Epub 2008/01/11. doi: 10.1056/NEJMoa071366. PubMed PMID: 18184957.
116. Ranieri VM, Thompson BT, Barie PS, Dhainaut JF, Douglas IS, Finfer S, Gardlund B, Marshall JC, Rhodes A, Artigas A, Payen D, Tenhunen J, Al-Khalidi HR, Thompson V, Janes J, Macias WL, Vangerow B, Williams MD, Group P-SS. Drotrecogin alfa (activated) in adults with septic shock. N Engl J Med. 2012;366(22):2055-64. Epub 2012/05/24. doi: 10.1056/NEJMoa1202290. PubMed PMID: 22616830.
117. Bozza FA, D'Avila JC, Ritter C, Sonneville R, Sharshar T, Dal-Pizzol F. Bioenergetics, mitochondrial dysfunction, and oxidative stress in the pathophysiology of septic encephalopathy. Shock. 2013;39(7 Suppl 1):10-6. Epub 2013/03/14. doi: 10.1097/SHK.0b013e31828fade1. PubMed PMID: 23481496.
118. Singer M, Deutschman CS, Seymour CW, Shankar-Hari M, Annane D, Bauer M, Bellomo R, Bernard GR, Chiche JD, Coopersmith CM, Hotchkiss RS, Levy MM, Marshall JC, Martin GS, Opal SM, Rubenfeld GD, van der Poll T, Vincent JL, Angus DC. The Third International Consensus Definitions for Sepsis and Septic Shock (Sepsis-3). JAMA. 2016;315(8):801-10. Epub 2016/02/24. doi: 10.1001/jama.2016.0287. PubMed PMID: 26903338; PMCID: PMC4968574.
119. Singer M, Brealey D. Mitochondrial dysfunction in sepsis. Biochem Soc Symp. 1999;66:149-66. Epub 2000/09/16. PubMed PMID: 10989665.
120. Robin ED. Special report: dysoxia. Abnormal tissue oxygen utilization. Arch Intern Med. 1977;137(7):905-10. PubMed PMID: 879930.

121. Abraham E, Singer M. Mechanisms of sepsis-induced organ dysfunction. Crit Care Med. 2007;35(10):2408-16. Epub 2007/10/20. PubMed PMID: 17948334.
122. Boekstegers P, Weidenhofer S, Pilz G, Werdan K. Peripheral oxygen availability within skeletal muscle in sepsis and septic shock: comparison to limited infection and cardiogenic shock. Infection. 1991;19(5):317-23. Epub 1991/09/01. PubMed PMID: 1800370.
123. Rosser DM, Stidwill RP, Jacobson D, Singer M. Oxygen tension in the bladder epithelium rises in both high and low cardiac output endotoxemic sepsis. J Appl Physiol. 1995;79(6):1878-82. Epub 1995/12/01. PubMed PMID: 8847247.
124. Hotchkiss RS, Swanson PE, Freeman BD, Tinsley KW, Cobb JP, Matuschak GM, Buchman TG, Karl IE. Apoptotic cell death in patients with sepsis, shock, and multiple organ dysfunction. Crit Care Med. 1999;27(7):1230-51. Epub 1999/08/14. PubMed PMID: 10446814.
125. Singer M, De Santis V, Vitale D, Jeffcoate W. Multiorgan failure is an adaptive, endocrine-mediated, metabolic response to overwhelming systemic inflammation. Lancet. 2004;364(9433):545-8. Epub 2004/08/11. doi: 10.1016/S0140-6736(04)16815-3. PubMed PMID: 15302200.
126. Kozlov AV, van Griensven M, Haindl S, Kehrer I, Duvigneau JC, Hartl RT, Ebel T, Jafarmadar M, Calzia E, Gnaiger E, Redl H, Radermacher P, Bahrami S. Peritoneal inflammation in pigs is associated with early mitochondrial dysfunction in liver and kidney. Inflammation. 2010;33(5):295-305. Epub 2010/02/25. doi: 10.1007/s10753-010-9185-4. PubMed PMID: 20180005.
127. Crouser ED. Mitochondrial dysfunction in septic shock and multiple organ dysfunction syndrome. Mitochondrion. 2004;4(5-6):729-41. Epub 2005/08/27. doi: 10.1016/j.mito.2004.07.023. PubMed PMID: 16120428.
128. Brealey D, Karyampudi S, Jacques TS, Novelli M, Stidwill R, Taylor V, Smolenski RT, Singer M. Mitochondrial dysfunction in a long-term rodent model of sepsis and organ failure. Am J Physiol Regul Integr Comp Physiol. 2004;286(3):R491-7. Epub 2003/11/08. doi: 10.1152/ajpregu.00432.2003. PubMed PMID: 14604843.
129. Brealey D, Brand M, Hargreaves I, Heales S, Land J, Smolenski R, Davies NA, Cooper CE, Singer M. Association between mitochondrial dysfunction and severity and outcome of septic shock. Lancet. 2002;360(9328):219-23. Epub 2002/07/23. doi: 10.1016/S0140-6736(02)09459-X. PubMed PMID: 12133657.
130. Taylor DE, Kantrow SP, Piantadosi CA. Mitochondrial respiration after sepsis and prolonged hypoxia. Am J Physiol. 1998;275(1 Pt 1):L139-44. Epub 1998/08/05. PubMed PMID: 9688945.
131. Sjovall F, Morota S, Hansson MJ, Friberg H, Gnaiger E, Elmer E. Temporal increase of platelet mitochondrial respiration is negatively associated with clinical outcome in patients with sepsis. Crit Care. 2010;14(6):R214. doi: 10.1186/cc9337. PubMed PMID: 21106065; PMCID: PMC3219983.
132. d'Avila JC, Santiago AP, Amancio RT, Galina A, Oliveira MF, Bozza FA. Sepsis induces brain mitochondrial dysfunction. Crit Care Med. 2008;36(6):1925-32. Epub 2008/05/23. doi: 10.1097/CCM.0b013e3181760c4b. PubMed PMID: 18496362.

133. Deans KJ, Haley M, Natanson C, Eichacker PQ, Minneci PC. Novel therapies for sepsis: a review. J Trauma. 2005;58(4):867-74. Epub 2005/04/13. PubMed PMID: 15824673.
134. Protti A, Carre J, Frost MT, Taylor V, Stidwill R, Rudiger A, Singer M. Succinate recovers mitochondrial oxygen consumption in septic rat skeletal muscle. Crit Care Med. 2007;35(9):2150-5. Epub 2007/09/15. PubMed PMID: 17855829.
135. De Silva MJ, Roberts I, Perel P, Edwards P, Kenward MG, Fernandes J, Shakur H, Patel V, Collaborators CT. Patient outcome after traumatic brain injury in high-, middle- and low-income countries: analysis of data on 8927 patients in 46 countries. International journal of epidemiology. 2009;38(2):452-8. Epub 2008/09/11. doi: 10.1093/ije/dyn189. PubMed PMID: 18782898.
136. Jorge RE, Robinson RG, Moser D, Tateno A, Crespo-Facorro B, Arndt S. Major depression following traumatic brain injury. Arch Gen Psychiatry. 2004;61(1):42-50. Epub 2004/01/07. doi: 10.1001/archpsyc.61.1.42. PubMed PMID: 14706943.
137. Vasterling JJ, Brailey K, Proctor SP, Kane R, Heeren T, Franz M. Neuropsychological outcomes of mild traumatic brain injury, post-traumatic stress disorder and depression in Iraq-deployed US Army soldiers. Br J Psychiatry. 2012;201(3):186-92. Epub 2012/06/30. doi: 10.1192/bjp.bp.111.096461. PubMed PMID: 22743844.
138. Maas AI, Stocchetti N, Bullock R. Moderate and severe traumatic brain injury in adults. Lancet Neurol. 2008;7(8):728-41. Epub 2008/07/19. doi: 10.1016/S1474-4422(08)70164-9. PubMed PMID: 18635021.
139. Saatman KE, Duhaime AC, Bullock R, Maas AI, Valadka A, Manley GT, Workshop Scientific T, Advisory Panel M. Classification of traumatic brain injury for targeted therapies. J Neurotrauma. 2008;25(7):719-38. Epub 2008/07/17. doi: 10.1089/neu.2008.0586. PubMed PMID: 18627252; PMCID: PMC2721779.
140. Smith DH, Meaney DF, Shull WH. Diffuse axonal injury in head trauma. J Head Trauma Rehabil. 2003;18(4):307-16. Epub 2005/10/14. PubMed PMID: 16222127.
141. Kumar R, Husain M, Gupta RK, Hasan KM, Haris M, Agarwal AK, Pandey CM, Narayana PA. Serial changes in the white matter diffusion tensor imaging metrics in moderate traumatic brain injury and correlation with neuro-cognitive function. J Neurotrauma. 2009;26(4):481-95. Epub 2009/02/07. doi: 10.1089/neu.2008.0461. PubMed PMID: 19196176.
142. Xing G, Ren M, Watson WD, O'Neill JT, Verma A. Traumatic brain injury-induced expression and phosphorylation of pyruvate dehydrogenase: a mechanism of dysregulated glucose metabolism. Neurosci Lett. 2009;454(1):38-42. doi: 10.1016/j.neulet.2009.01.047. PubMed PMID: 19429050.
143. Marcoux J, McArthur DA, Miller C, Glenn TC, Villablanca P, Martin NA, Hovda DA, Alger JR, Vespa PM. Persistent metabolic crisis as measured by elevated cerebral microdialysis lactate-pyruvate ratio predicts chronic frontal lobe brain atrophy after traumatic brain injury. Crit Care Med. 2008;36(10):2871-7. Epub 2008/09/04. doi: 10.1097/CCM.0b013e318186a4a0. PubMed PMID: 18766106.
144. Robertson CL, Scafidi S, McKenna MC, Fiskum G. Mitochondrial mechanisms of cell death and neuroprotection in pediatric ischemic and traumatic brain injury. Experimental neurology. 2009;218(2):371-80. Epub 2009/05/12. doi: 10.1016/j.expneurol.2009.04.030. PubMed PMID: 19427308; PMCID: 3096876.

145. Sullivan PG, Rabchevsky AG, Waldmeier PC, Springer JE. Mitochondrial permeability transition in CNS trauma: cause or effect of neuronal cell death? J Neurosci Res. 2005;79(1-2):231-9. doi: 10.1002/jnr.20292. PubMed PMID: 15573402.
146. Singh IN, Sullivan PG, Deng Y, Mbye LH, Hall ED. Time course of post-traumatic mitochondrial oxidative damage and dysfunction in a mouse model of focal traumatic brain injury: implications for neuroprotective therapy. J Cereb Blood Flow Metab. 2006;26(11):1407-18. doi: 10.1038/sj.jcbfm.9600297. PubMed PMID: 16538231.
147. Sullivan PG, Thompson MB, Scheff SW. Cyclosporin A attenuates acute mitochondrial dysfunction following traumatic brain injury. Exp Neurol. 1999;160(1):226-34. Epub 2000/01/12. doi: S0014-4886(99)97197-2 [pii]

10.1006/exnr.1999.7197. PubMed PMID: 10630207.
148. Sullivan PG, Thompson M, Scheff SW. Continuous infusion of cyclosporin A postinjury significantly ameliorates cortical damage following traumatic brain injury. Exp Neurol. 2000;161(2):631-7. doi: 10.1006/exnr.1999.7282. PubMed PMID: 10686082.
149. Vink R, Van Den Heuvel C. Recent advances in the development of multifactorial therapies for the treatment of traumatic brain injury. Expert Opin Investig Drugs. 2004;13(10):1263-74. doi: 10.1517/13543784.13.10.1263. PubMed PMID: 15461556.
150. Alessandri B, Rice AC, Levasseur J, DeFord M, Hamm RJ, Bullock MR. Cyclosporin A improves brain tissue oxygen consumption and learning/memory performance after lateral fluid percussion injury in rats. J Neurotrauma. 2002;19(7):829-41. Epub 2002/08/20. doi: 10.1089/08977150260190429. PubMed PMID: 12184853.
151. Brophy GM, Mazzeo AT, Brar S, Alves OL, Bunnell K, Gilman C, Karnes T, Hayes RL, Bullock R. Exposure of cyclosporin A in whole blood, cerebral spinal fluid, and brain extracellular fluid dialysate in adults with traumatic brain injury. Journal of neurotrauma. 2013;30(17):1484-9. Epub 2013/04/02. doi: 10.1089/neu.2012.2524. PubMed PMID: 23540442; PMCID: 3751213.
152. Buki A, Okonkwo DO, Povlishock JT. Postinjury cyclosporin A administration limits axonal damage and disconnection in traumatic brain injury. J Neurotrauma. 1999;16(6):511-21. Epub 1999/07/03. PubMed PMID: 10391367.
153. Colley BS, Phillips LL, Reeves TM. The effects of cyclosporin-A on axonal conduction deficits following traumatic brain injury in adult rats. Exp Neurol. 2010;224(1):241-51. Epub 2010/04/07. doi: 10.1016/j.expneurol.2010.03.026. PubMed PMID: 20362574; PMCID: PMC2885519.
154. Gabbita SP, Scheff SW, Menard RM, Roberts K, Fugaccia I, Zemlan FP. Cleaved-tau: a biomarker of neuronal damage after traumatic brain injury. J Neurotrauma. 2005;22(1):83-94. Epub 2005/01/25. doi: 10.1089/neu.2005.22.83. PubMed PMID: 15665604.
155. Kilbaugh TJ, Bhandare S, Lorom DH, Saraswati M, Robertson CL, Margulies SS. Cyclosporin A preserves mitochondrial function after traumatic brain injury in the immature rat and piglet. Journal of neurotrauma. 2011;28(5):763-74. Epub 2011/01/22. doi: 10.1089/neu.2010.1635. PubMed PMID: 21250918; PMCID: 3125546.
156. Margulies SS, Kilbaugh T, Sullivan S, Smith C, Propert K, Byro M, Saliga K, Costine BA, Duhaime AC. Establishing a Clinically Relevant Large Animal Model Platform for TBI Therapy Development: Using Cyclosporin A as a Case Study. Brain Pathol.

2015;25(3):289-303. doi: 10.1111/bpa.12247. PubMed PMID: 25904045; PMCID: PMC4459790.
157. Mbye LH, Singh IN, Carrico KM, Saatman KE, Hall ED. Comparative neuroprotective effects of cyclosporin A and NIM811, a nonimmunosuppressive cyclosporin A analog, following traumatic brain injury. J Cereb Blood Flow Metab. 2009;29(1):87-97. Epub 2008/08/21. doi: 10.1038/jcbfm.2008.93. PubMed PMID: 18714331; PMCID: PMC2755489.
158. Mbye LH, Singh IN, Sullivan PG, Springer JE, Hall ED. Attenuation of acute mitochondrial dysfunction after traumatic brain injury in mice by NIM811, a non-immunosuppressive cyclosporin A analog. Exp Neurol. 2008;209(1):243-53. Epub 2007/11/21. doi: 10.1016/j.expneurol.2007.09.025. PubMed PMID: 18022160.
159. Okonkwo DO, Povlishock JT. An intrathecal bolus of cyclosporin A before injury preserves mitochondrial integrity and attenuates axonal disruption in traumatic brain injury. J Cereb Blood Flow Metab. 1999;19(4):443-51. Epub 1999/04/10. doi: 10.1097/00004647-199904000-00010. PubMed PMID: 10197514.
160. Okonkwo DO, Melon DE, Pellicane AJ, Mutlu LK, Rubin DG, Stone JR, Helm GA. Dose-response of cyclosporin A in attenuating traumatic axonal injury in rat. Neuroreport. 2003;14(3):463-6. Epub 2003/03/14. doi: 10.1097/01.wnr.0000058958.85541.d3. PubMed PMID: 12634504.
161. Riess P, Bareyre FM, Saatman KE, Cheney JA, Lifshitz J, Raghupathi R, Grady MS, Neugebauer E, McIntosh TK. Effects of chronic, post-injury Cyclosporin A administration on motor and sensorimotor function following severe, experimental traumatic brain injury. Restor Neurol Neurosci. 2001;18(1):1-8. Epub 2001/10/24. PubMed PMID: 11673665.
162. Scheff SW, Sullivan PG. Cyclosporin A significantly ameliorates cortical damage following experimental traumatic brain injury in rodents. J Neurotrauma. 1999;16(9):783-92. Epub 1999/10/16. PubMed PMID: 10521138.
163. Signoretti S, Marmarou A, Tavazzi B, Dunbar J, Amorini AM, Lazzarino G, Vagnozzi R. The protective effect of cyclosporin A upon N-acetylaspartate and mitochondrial dysfunction following experimental diffuse traumatic brain injury. J Neurotrauma. 2004;21(9):1154-67. Epub 2004/09/30. doi: 10.1089/neu.2004.21.1154. PubMed PMID: 15453986.
164. Staal JA, Dickson TC, Chung RS, Vickers JC. Cyclosporin-A treatment attenuates delayed cytoskeletal alterations and secondary axotomy following mild axonal stretch injury. Dev Neurobiol. 2007;67(14):1831-42. Epub 2007/08/19. doi: 10.1002/dneu.20552. PubMed PMID: 17702000.
165. Suehiro E, Povlishock JT. Exacerbation of traumatically induced axonal injury by rapid posthypothermic rewarming and attenuation of axonal change by cyclosporin A. J Neurosurg. 2001;94(3):493-8. Epub 2001/03/10. doi: 10.3171/jns.2001.94.3.0493. PubMed PMID: 11235956.
166. Sullivan PG, Sebastian AH, Hall ED. Therapeutic window analysis of the neuroprotective effects of cyclosporine A after traumatic brain injury. J Neurotrauma. 2011;28(2):311-8. doi: 10.1089/neu.2010.1646. PubMed PMID: 21142667; PMCID: PMC3037811.

167. Turkoglu OF, Eroglu H, Gurcan O, Bodur E, Sargon MF, Oner L, Beskonakli E. Local administration of chitosan microspheres after traumatic brain injury in rats: a new challenge for cyclosporine--a delivery. Br J Neurosurg. 2010;24(5):578-83. Epub 2010/09/28. doi: 10.3109/02688697.2010.487126. PubMed PMID: 20868245.
168. Van Den Heuvel C, Donkin JJ, Finnie JW, Blumbergs PC, Kuchel T, Koszyca B, Manavis J, Jones NR, Reilly PL, Vink R. Downregulation of amyloid precursor protein (APP) expression following post-traumatic cyclosporin-A administration. J Neurotrauma. 2004;21(11):1562-72. Epub 2005/02/03. doi: 10.1089/neu.2004.21.1562. PubMed PMID: 15684649.
169. Yin WD, Xu BN, Wang XG. [Neurobehavior changes of rats after diffuse axonal injury and the treatment effect with cyclosporin A]. Zhongguo Wei Zhong Bing Ji Jiu Yi Xue. 2004;16(4):214-7. Epub 2004/04/08. PubMed PMID: 15068712.
170. Abdel Baki SG, Schwab B, Haber M, Fenton AA, Bergold PJ. Minocycline synergizes with N-acetylcysteine and improves cognition and memory following traumatic brain injury in rats. PLoS One. 2010;5(8):e12490. Epub 2010/09/09. doi: 10.1371/journal.pone.0012490. PubMed PMID: 20824218; PMCID: PMC2930858.
171. Dixon CE, Bramlett HM, Dietrich WD, Shear DA, Yan HQ, Deng-Bryant Y, Mondello S, Wang KK, Hayes RL, Empey PE, Povlishock JT, Tortella FC, Kochanek PM. Cyclosporine Treatment in Traumatic Brain Injury: Operation Brain Trauma Therapy. J Neurotrauma. 2016;33(6):553-66. doi: 10.1089/neu.2015.4122. PubMed PMID: 26671075.
172. Hatton J, Rosbolt B, Empey P, Kryscio R, Young B. Dosing and safety of cyclosporine in patients with severe brain injury. Journal of neurosurgery. 2008;109(4):699-707. Epub 2008/10/02. doi: 10.3171/JNS/2008/109/10/0699. PubMed PMID: 18826358; PMCID: 2770729.
173. Mazzeo AT, Alves OL, Gilman CB, Hayes RL, Tolias C, Niki Kunene K, Ross Bullock M. Brain metabolic and hemodynamic effects of cyclosporin A after human severe traumatic brain injury: a microdialysis study. Acta Neurochir (Wien). 2008;150(10):1019-31; discussion 31. Epub 2008/09/11. doi: 10.1007/s00701-008-0021-7. PubMed PMID: 18781275.
174. Mazzeo AT, Brophy GM, Gilman CB, Alves OL, Robles JR, Hayes RL, Povlishock JT, Bullock MR. Safety and tolerability of cyclosporin a in severe traumatic brain injury patients: results from a prospective randomized trial. Journal of neurotrauma. 2009;26(12):2195-206. Epub 2009/07/23. doi: 10.1089/neu.2009.1012. PubMed PMID: 19621985; PMCID: 2824218.
175. Copenhagen Head Injury Ciclosporin (CHIC) Study [cited 2017 10/29]. Available from: https://clinicaltrials.gov/ct2/show/NCT01825044.
176. Darin N, Oldfors A, Moslemi AR, Holme E, Tulinius M. The incidence of mitochondrial encephalomyopathies in childhood: clinical features and morphological, biochemical, and DNA anbormalities. Ann Neurol. 2001;49(3):377-83. Epub 2001/03/23. PubMed PMID: 11261513.
177. Chinnery PF, Turnbull DM. Clinical features, investigation, and management of patients with defects of mitochondrial DNA. J Neurol Neurosurg Psychiatry. 1997;63(5):559-63. Epub 1998/01/04. PubMed PMID: 9408091; PMCID: 2169824.
178. Shoffner JM, Lott MT, Voljavec AS, Soueidan SA, Costigan DA, Wallace DC. Spontaneous Kearns-Sayre/chronic external ophthalmoplegia plus syndrome associated

with a mitochondrial DNA deletion: a slip-replication model and metabolic therapy. Proc Natl Acad Sci U S A. 1989;86(20):7952-6. PubMed PMID: 2554297; PMCID: 298190.
179. Rittirsch D, Huber-Lang MS, Flierl MA, Ward PA. Immunodesign of experimental sepsis by cecal ligation and puncture. Nat Protoc. 2009;4(1):31-6. Epub 2009/01/10. doi: 10.1038/nprot.2008.214. PubMed PMID: 19131954; PMCID: 2754226.
180. Weeks D, Sullivan S, Kilbaugh T, Smith C, Margulies SS. Influences of developmental age on the resolution of diffuse traumatic intracranial hemorrhage and axonal injury. J Neurotrauma. 2014;31(2):206-14. doi: 10.1089/neu.2013.3113. PubMed PMID: 23984914; PMCID: PMC3901955.
181. Eucker SA, Smith C, Ralston J, Friess SH, Margulies SS. Physiological and histopathological responses following closed rotational head injury depend on direction of head motion. Exp Neurol. 2011;227(1):79-88. doi: 10.1016/j.expneurol.2010.09.015. PubMed PMID: 20875409; PMCID: PMC3021173.
182. Raghupathi R, Margulies SS. Traumatic axonal injury after closed head injury in the neonatal pig. J Neurotrauma. 2002;19(7):843-53. doi: 10.1089/08977150260190438. PubMed PMID: 12184854.
183. Dyson A, Simon F, Seifritz A, Zimmerling O, Matallo J, Calzia E, Radermacher P, Singer M. Bladder tissue oxygen tension monitoring in pigs subjected to a range of cardiorespiratory and pharmacological challenges. Intensive Care Med. 2012;38(11):1868-76. Epub 2012/10/12. doi: 10.1007/s00134-012-2712-z. PubMed PMID: 23052956.
184. Pesta D, Gnaiger E. High-resolution respirometry: OXPHOS protocols for human cells and permeabilized fibers from small biopsies of human muscle. Methods Mol Biol. 2012;810:25-58. Epub 2011/11/08. doi: 10.1007/978-1-61779-382-0_3. PubMed PMID: 22057559.
185. Sjovall F, Ehinger JK, Marelsson SE, Morota S, Frostner EA, Uchino H, Lundgren J, Arnbjornsson E, Hansson MJ, Fellman V, Elmer E. Mitochondrial respiration in human viable platelets--methodology and influence of gender, age and storage. Mitochondrion. 2013;13(1):7-14. Epub 2012/11/21. doi: 10.1016/j.mito.2012.11.001. PubMed PMID: 23164798.
186. Sjovall F, Morota S, Persson J, Hansson MJ, Elmer E. Patients with sepsis exhibit increased mitochondrial respiratory capacity in peripheral blood immune cells. Crit Care. 2013;17(4):R152. doi: 10.1186/cc12831. PubMed PMID: 23883738; PMCID: PMC4056763.
187. Picard M, Taivassalo T, Ritchie D, Wright KJ, Thomas MM, Romestaing C, Hepple RT. Mitochondrial structure and function are disrupted by standard isolation methods. PLoS One. 2011;6(3):e18317. Epub 2011/04/23. doi: 10.1371/journal.pone.0018317. PubMed PMID: 21512578; PMCID: 3065478.
188. Larsen S, Nielsen J, Hansen CN, Nielsen LB, Wibrand F, Stride N, Schroder HD, Boushel R, Helge JW, Dela F, Hey-Mogensen M. Biomarkers of mitochondrial content in skeletal muscle of healthy young human subjects. J Physiol. 2012;590(Pt 14):3349-60. Epub 2012/05/16. doi: 10.1113/jphysiol.2012.230185. PubMed PMID: 22586215; PMCID: 3459047.
189. Chouchani ET, Methner C, Nadtochiy SM, Logan A, Pell VR, Ding S, James AM, Cocheme HM, Reinhold J, Lilley KS, Partridge L, Fearnley IM, Robinson AJ,

Hartley RC, Smith RA, Krieg T, Brookes PS, Murphy MP. Cardioprotection by S-nitrosation of a cysteine switch on mitochondrial complex I. Nat Med. 2013;19(6):753-9. Epub 2013/05/28. doi: 10.1038/nm.3212. PubMed PMID: 23708290; PMCID: PMC4019998.
190. Boushel R, Gnaiger E, Schjerling P, Skovbro M, Kraunsoe R, Dela F. Patients with type 2 diabetes have normal mitochondrial function in skeletal muscle. Diabetologia. 2007;50(4):790-6. Epub 2007/03/06. doi: 10.1007/s00125-007-0594-3. PubMed PMID: 17334651; PMCID: PMC1820754.
191. Ritov VB, Menshikova EV, Kelley DE. Analysis of cardiolipin in human muscle biopsy. J Chromatogr B Analyt Technol Biomed Life Sci. 2006;831(1-2):63-71. Epub 2005/12/13. doi: 10.1016/j.jchromb.2005.11.031. PubMed PMID: 16337440.
192. Rustin P, Chretien D, Bourgeron T, Gerard B, Rotig A, Saudubray JM, Munnich A. Biochemical and molecular investigations in respiratory chain deficiencies. Clin Chim Acta. 1994;228(1):35-51. Epub 1994/07/01. PubMed PMID: 7955428.
193. Renner K, Amberger A, Konwalinka G, Kofler R, Gnaiger E. Changes of mitochondrial respiration, mitochondrial content and cell size after induction of apoptosis in leukemia cells. Biochim Biophys Acta. 2003;1642(1-2):115-23. Epub 2003/09/16. PubMed PMID: 12972300.
194. Cormio A, Guerra F, Cormio G, Pesce V, Fracasso F, Loizzi V, Resta L, Putignano G, Cantatore P, Selvaggi LE, Gadaleta MN. Mitochondrial DNA content and mass increase in progression from normal to hyperplastic to cancer endometrium. BMC Res Notes. 2012;5:279. Epub 2012/06/09. doi: 10.1186/1756-0500-5-279. PubMed PMID: 22676897; PMCID: PMC3502111.
195. Sjovall F, Morota S, Asander Frostner E, Hansson MJ, Elmer E. Cytokine and nitric oxide levels in patients with sepsis - temporal evolvement and relation to platelet mitochondrial respiratory function. PLoS One. 2014;9(5):e97673. doi: 10.1371/journal.pone.0097673. PubMed PMID: 24828117; PMCID: 4020920.
196. Lesnefsky EJ, Slabe TJ, Stoll MS, Minkler PE, Hoppel CL. Myocardial ischemia selectively depletes cardiolipin in rabbit heart subsarcolemmal mitochondria. Am J Physiol Heart Circ Physiol. 2001;280(6):H2770-8. Epub 2001/05/18. PubMed PMID: 11356635.
197. Drake AC. Of mice and men: what rodent models don't tell us. Cell Mol Immunol. 2013;10(4):284-5. Epub 2013/05/21. doi: 10.1038/cmi.2013.21. PubMed PMID: 23686228; PMCID: PMC4003210.
198. Seok J, Warren HS, Cuenca AG, Mindrinos MN, Baker HV, Xu W, Richards DR, McDonald-Smith GP, Gao H, Hennessy L, Finnerty CC, Lopez CM, Honari S, Moore EE, Minei JP, Cuschieri J, Bankey PE, Johnson JL, Sperry J, Nathens AB, Billiar TR, West MA, Jeschke MG, Klein MB, Gamelli RL, Gibran NS, Brownstein BH, Miller-Graziano C, Calvano SE, Mason PH, Cobb JP, Rahme LG, Lowry SF, Maier RV, Moldawer LL, Herndon DN, Davis RW, Xiao W, Tompkins RG, Inflammation, Host Response to Injury LSCRP. Genomic responses in mouse models poorly mimic human inflammatory diseases. Proc Natl Acad Sci U S A. 2013;110(9):3507-12. Epub 2013/02/13. doi: 10.1073/pnas.1222878110. PubMed PMID: 23401516; PMCID: PMC3587220.
199. Osuchowski MF, Remick DG, Lederer JA, Lang CH, Aasen AO, Aibiki M, Azevedo LC, Bahrami S, Boros M, Cooney R, Cuzzocrea S, Jiang Y, Junger WG, Hirasawa H, Hotchkiss RS, Li XA, Radermacher P, Redl H, Salomao R, Soebandrio A, Thiemermann C,

Vincent JL, Ward P, Yao YM, Yu HP, Zingarelli B, Chaudry IH. Abandon the mouse research ship? Not just yet! Shock. 2014;41(6):463-75. Epub 2014/02/27. doi: 10.1097/SHK.0000000000000153. PubMed PMID: 24569509; PMCID: PMC4139038.
200. Karumanchi SA, Parikh SM. Moving forward in sepsis research. Am J Respir Crit Care Med. 2013;188(10):1264-5. Epub 2013/11/19. doi: 10.1164/rccm.201305-0810LE. PubMed PMID: 24236592; PMCID: PMC3863731.
201. Remick D. Use of animal models for the study of human disease-a shock society debate. Shock. 2013;40(4):345-6. Epub 2013/09/21. doi: 10.1097/SHK.0b013e3182a2aee0. PubMed PMID: 24045419.
202. Cauwels A, Vandendriessche B, Brouckaert P. Of mice, men, and inflammation. Proc Natl Acad Sci U S A. 2013;110(34):E3150. Epub 2013/07/16. doi: 10.1073/pnas.1308333110. PubMed PMID: 23852732; PMCID: PMC3752222.
203. Osterburg AR, Hexley P, Supp DM, Robinson CT, Noel G, Ogle C, Boyce ST, Aronow BJ, Babcock GF. Concerns over interspecies transcriptional comparisons in mice and humans after trauma. Proc Natl Acad Sci U S A. 2013;110(36):E3370. Epub 2013/07/13. doi: 10.1073/pnas.1306033110. PubMed PMID: 23847210; PMCID: PMC3767557.
204. Tompkins RG, Warren HS, Mindrinos MN, Xiao W, Davis RW. Reply to Osterburg et al.: To study human inflammatory diseases in humans. Proc Natl Acad Sci U S A. 2013;110(36):E3371. Epub 2013/10/19. PubMed PMID: 24137798; PMCID: PMC3767510.
205. Warren HS, Tompkins RG, Mindrinos MN, Xiao W, Davis RW. Reply to Cauwels et al.: Of men, not mice, and inflammation. Proc Natl Acad Sci U S A. 2013;110(34):E3151. Epub 2013/10/19. PubMed PMID: 24137663; PMCID: PMC3752239.
206. Shay T, Lederer JA, Benoist C. Genomic responses to inflammation in mouse models mimic humans: we concur, apples to oranges comparisons won't do. Proc Natl Acad Sci U S A. 2015;112(4):E346. Epub 2014/12/30. doi: 10.1073/pnas.1416629111. PubMed PMID: 25540423; PMCID: PMC4313855.
207. Offner H. Modeling immunity and inflammation in stroke: don't be afraid of mice? Stroke. 2014;45(9):e181-2. Epub 2014/07/26. doi: 10.1161/STROKEAHA.114.005642. PubMed PMID: 25061079; PMCID: PMC4146705.
208. Takao K, Miyakawa T. Genomic responses in mouse models greatly mimic human inflammatory diseases. Proc Natl Acad Sci U S A. 2015;112(4):1167-72. Epub 2014/08/06. doi: 10.1073/pnas.1401965111. PubMed PMID: 25092317; PMCID: PMC4313832.
209. Lind NM, Moustgaard A, Jelsing J, Vajta G, Cumming P, Hansen AK. The use of pigs in neuroscience: modeling brain disorders. Neurosci Biobehav Rev. 2007;31(5):728-51. doi: 10.1016/j.neubiorev.2007.02.003. PubMed PMID: 17445892.
210. Hovda DA, Yoshino A, Kawamata T, Katayama Y, Becker DP. Diffuse prolonged depression of cerebral oxidative metabolism following concussive brain injury in the rat: a cytochrome oxidase histochemistry study. Brain Res. 1991;567(1):1-10. Epub 1991/12/13. PubMed PMID: 1667742.

211. Yamaki T, Imahori Y, Ohmori Y, Yoshino E, Hohri T, Ebisu T, Ueda S. Cerebral hemodynamics and metabolism of severe diffuse brain injury measured by PET. J Nucl Med. 1996;37(7):1166-70. Epub 1996/07/01. PubMed PMID: 8965189.
212. Hurn PD, Subramanian S, Parker SM, Afentoulis ME, Kaler LJ, Vandenbark AA, Offner H. T- and B-cell-deficient mice with experimental stroke have reduced lesion size and inflammation. J Cereb Blood Flow Metab. 2007;27(11):1798-805. Epub 2007/03/30. doi: 10.1038/sj.jcbfm.9600482. PubMed PMID: 17392692; PMCID: PMC2592689.
213. van der Worp HB, Howells DW, Sena ES, Porritt MJ, Rewell S, O'Collins V, Macleod MR. Can animal models of disease reliably inform human studies? PLoS Med. 2010;7(3):e1000245. Epub 2010/04/03. doi: 10.1371/journal.pmed.1000245. PubMed PMID: 20361020; PMCID: PMC2846855.
214. Mouse Genome Sequencing C, Waterston RH, Lindblad-Toh K, Birney E, Rogers J, Abril JF, Agarwal P, Agarwala R, Ainscough R, Alexandersson M, An P, Antonarakis SE, Attwood J, Baertsch R, Bailey J, Barlow K, Beck S, Berry E, Birren B, Bloom T, Bork P, Botcherby M, Bray N, Brent MR, Brown DG, Brown SD, Bult C, Burton J, Butler J, Campbell RD, Carninci P, Cawley S, Chiaromonte F, Chinwalla AT, Church DM, Clamp M, Clee C, Collins FS, Cook LL, Copley RR, Coulson A, Couronne O, Cuff J, Curwen V, Cutts T, Daly M, David R, Davies J, Delehaunty KD, Deri J, Dermitzakis ET, Dewey C, Dickens NJ, Diekhans M, Dodge S, Dubchak I, Dunn DM, Eddy SR, Elnitski L, Emes RD, Eswara P, Eyras E, Felsenfeld A, Fewell GA, Flicek P, Foley K, Frankel WN, Fulton LA, Fulton RS, Furey TS, Gage D, Gibbs RA, Glusman G, Gnerre S, Goldman N, Goodstadt L, Grafham D, Graves TA, Green ED, Gregory S, Guigo R, Guyer M, Hardison RC, Haussler D, Hayashizaki Y, Hillier LW, Hinrichs A, Hlavina W, Holzer T, Hsu F, Hua A, Hubbard T, Hunt A, Jackson I, Jaffe DB, Johnson LS, Jones M, Jones TA, Joy A, Kamal M, Karlsson EK, Karolchik D, Kasprzyk A, Kawai J, Keibler E, Kells C, Kent WJ, Kirby A, Kolbe DL, Korf I, Kucherlapati RS, Kulbokas EJ, Kulp D, Landers T, Leger JP, Leonard S, Letunic I, Levine R, Li J, Li M, Lloyd C, Lucas S, Ma B, Maglott DR, Mardis ER, Matthews L, Mauceli E, Mayer JH, McCarthy M, McCombie WR, McLaren S, McLay K, McPherson JD, Meldrim J, Meredith B, Mesirov JP, Miller W, Miner TL, Mongin E, Montgomery KT, Morgan M, Mott R, Mullikin JC, Muzny DM, Nash WE, Nelson JO, Nhan MN, Nicol R, Ning Z, Nusbaum C, O'Connor MJ, Okazaki Y, Oliver K, Overton-Larty E, Pachter L, Parra G, Pepin KH, Peterson J, Pevzner P, Plumb R, Pohl CS, Poliakov A, Ponce TC, Ponting CP, Potter S, Quail M, Reymond A, Roe BA, Roskin KM, Rubin EM, Rust AG, Santos R, Sapojnikov V, Schultz B, Schultz J, Schwartz MS, Schwartz S, Scott C, Seaman S, Searle S, Sharpe T, Sheridan A, Shownkeen R, Sims S, Singer JB, Slater G, Smit A, Smith DR, Spencer B, Stabenau A, Stange-Thomann N, Sugnet C, Suyama M, Tesler G, Thompson J, Torrents D, Trevaskis E, Tromp J, Ucla C, Ureta-Vidal A, Vinson JP, Von Niederhausern AC, Wade CM, Wall M, Weber RJ, Weiss RB, Wendl MC, West AP, Wetterstrand K, Wheeler R, Whelan S, Wierzbowski J, Willey D, Williams S, Wilson RK, Winter E, Worley KC, Wyman D, Yang S, Yang SP, Zdobnov EM, Zody MC, Lander ES. Initial sequencing and comparative analysis of the mouse genome. Nature. 2002;420(6915):520-62. Epub 2002/12/06. doi: 10.1038/nature01262. PubMed PMID: 12466850.
215. Redell JB, Zhao J, Dash PK. Acutely increased cyclophilin a expression after brain injury: a role in blood-brain barrier function and tissue preservation. J Neurosci Res. 2007;85(9):1980-8. Epub 2007/04/28. doi: 10.1002/jnr.21324. PubMed PMID: 17461417.

216. Schinkel AH, Wagenaar E, Mol CA, van Deemter L. P-glycoprotein in the blood-brain barrier of mice influences the brain penetration and pharmacological activity of many drugs. J Clin Invest. 1996;97(11):2517-24. Epub 1996/06/01. doi: 10.1172/JCI118699. PubMed PMID: 8647944; PMCID: PMC507337.
217. Kruse SE, Watt WC, Marcinek DJ, Kapur RP, Schenkman KA, Palmiter RD. Mice with mitochondrial complex I deficiency develop a fatal encephalomyopathy. Cell Metab. 2008;7(4):312-20. Epub 2008/04/09. doi: 10.1016/j.cmet.2008.02.004. PubMed PMID: 18396137; PMCID: 2593686.
218. Koene S, Willems PH, Roestenberg P, Koopman WJ, Smeitink JA. Mouse models for nuclear DNA-encoded mitochondrial complex I deficiency. J Inherit Metab Dis. 2011;34(2):293-307. Epub 2010/01/29. doi: 10.1007/s10545-009-9005-x. PubMed PMID: 20107904.
219. Tyynismaa H, Suomalainen A. Mouse models of mitochondrial DNA defects and their relevance for human disease. EMBO Rep. 2009;10(2):137-43. Epub 2009/01/17. doi: 10.1038/embor.2008.242. PubMed PMID: 19148224; PMCID: 2637315.
220. Wallace DC, Fan W. The pathophysiology of mitochondrial disease as modeled in the mouse. Genes Dev. 2009;23(15):1714-36. Epub 2009/08/05. doi: 10.1101/gad.1784909. PubMed PMID: 19651984; PMCID: 2720256.
221. Roestenberg P, Manjeri GR, Valsecchi F, Smeitink JA, Willems PH, Koopman WJ. Pharmacological targeting of mitochondrial complex I deficiency: the cellular level and beyond. Mitochondrion. 2012;12(1):57-65. Epub 2011/07/16. doi: 10.1016/j.mito.2011.06.011. PubMed PMID: 21757032.
222. Ke BX, Pepe S, Grubb DR, Komen JC, Laskowski A, Rodda FA, Hardman BM, Pitt JJ, Ryan MT, Lazarou M, Koleff J, Cheung MM, Smolich JJ, Thorburn DR. Tissue-specific splicing of an Ndufs6 gene-trap insertion generates a mitochondrial complex I deficiency-specific cardiomyopathy. Proc Natl Acad Sci U S A. 2012;109(16):6165-70. doi: 10.1073/pnas.1113987109. PubMed PMID: 22474353; PMCID: PMC3341001.
223. Lin CS, Sharpley MS, Fan W, Waymire KG, Sadun AA, Carelli V, Ross-Cisneros FN, Baciu P, Sung E, McManus MJ, Pan BX, Gil DW, Macgregor GR, Wallace DC. Mouse mtDNA mutant model of Leber hereditary optic neuropathy. Proc Natl Acad Sci U S A. 2012;109(49):20065-70. doi: 10.1073/pnas.1217113109. PubMed PMID: 23129651; PMCID: PMC3523873.
224. Svistunenko DA, Davies N, Brealey D, Singer M, Cooper CE. Mitochondrial dysfunction in patients with severe sepsis: an EPR interrogation of individual respiratory chain components. Biochim Biophys Acta. 2006;1757(4):262-72. Epub 2006/04/22. doi: 10.1016/j.bbabio.2006.03.007. PubMed PMID: 16626626.
225. Callahan LA, Supinski GS. Sepsis induces diaphragm electron transport chain dysfunction and protein depletion. Am J Respir Crit Care Med. 2005;172(7):861-8. Epub 2005/07/05. doi: 10.1164/rccm.200410-1344OC. PubMed PMID: 15994462.
226. Cathebras PJ, Robbins JM, Kirmayer LJ, Hayton BC. Fatigue in primary care: prevalence, psychiatric comorbidity, illness behavior, and outcome. J Gen Intern Med. 1992;7(3):276-86. Epub 1992/05/01. PubMed PMID: 1613608.
227. Malaisse WJ, Nadi AB, Ladriere L, Zhang TM. Protective effects of succinic acid dimethyl ester infusion in experimental endotoxemia. Nutrition. 1997;13(4):330-41. Epub 1997/04/01. PubMed PMID: 9178284.

228. Ferreira FL, Ladriere L, Vincent JL, Malaisse WJ. Prolongation of survival time by infusion of succinic acid dimethyl ester in a caecal ligation and perforation model of sepsis. Horm Metab Res. 2000;32(8):335-6. Epub 2000/09/13. doi: 10.1055/s-2007-978647. PubMed PMID: 10983631.
229. Martin E, Rosenthal RE, Fiskum G. Pyruvate dehydrogenase complex: metabolic link to ischemic brain injury and target of oxidative stress. J Neurosci Res. 2005;79(1-2):240-7. doi: 10.1002/jnr.20293. PubMed PMID: 15562436; PMCID: PMC2570320.
230. Bogaert YE, Rosenthal RE, Fiskum G. Postischemic inhibition of cerebral cortex pyruvate dehydrogenase. Free Radic Biol Med. 1994;16(6):811-20. PubMed PMID: 8070685.
231. Ikeda K, Liu X, Kida K, Marutani E, Hirai S, Sakaguchi M, Andersen LW, Bagchi A, Cocchi MN, Berg KM, Ichinose F, Donnino MW. Thiamine as a neuroprotective agent after cardiac arrest. Resuscitation. 2016;105:138-44. doi: 10.1016/j.resuscitation.2016.04.024. PubMed PMID: 27185216.
232. Donnino MW, Andersen LW, Chase M, Berg KM, Tidswell M, Giberson T, Wolfe R, Moskowitz A, Smithline H, Ngo L, Cocchi MN, Center for Resuscitation Science Research G. Randomized, Double-Blind, Placebo-Controlled Trial of Thiamine as a Metabolic Resuscitator in Septic Shock: A Pilot Study. Crit Care Med. 2016;44(2):360-7. doi: 10.1097/CCM.0000000000001572. PubMed PMID: 26771781; PMCID: PMC4754670.
233. Jalloh I, Helmy A, Howe DJ, Shannon RJ, Grice P, Mason A, Gallagher CN, Stovell MG, van der Heide S, Murphy MP, Pickard JD, Menon DK, Carpenter TA, Hutchinson PJ, Carpenter KL. Focally perfused succinate potentiates brain metabolism in head injury patients. J Cereb Blood Flow Metab. 2016:271678X16672665. doi: 10.1177/0271678X16672665. PubMed PMID: 27798266.
234. Giorgi-Coll S, Amaral AI, Hutchinson PJA, Kotter MR, Carpenter KLH. Succinate supplementation improves metabolic performance of mixed glial cell cultures with mitochondrial dysfunction. Sci Rep. 2017;7(1):1003. doi: 10.1038/s41598-017-01149-w. PubMed PMID: 28432362; PMCID: PMC5430749.
235. Xing G, Ren M, O'Neill JT, Verma A, Watson WD. Controlled cortical impact injury and craniotomy result in divergent alterations of pyruvate metabolizing enzymes in rat brain. Exp Neurol. 2012;234(1):31-8. doi: 10.1016/j.expneurol.2011.12.007. PubMed PMID: 22193111.
236. Yan W, Wang HD, Hu ZG, Wang QF, Yin HX. Activation of Nrf2-ARE pathway in brain after traumatic brain injury. Neurosci Lett. 2008;431(2):150-4. doi: 10.1016/j.neulet.2007.11.060. PubMed PMID: 18162315.
237. Jin W, Wang H, Yan W, Zhu L, Hu Z, Ding Y, Tang K. Role of Nrf2 in protection against traumatic brain injury in mice. J Neurotrauma. 2009;26(1):131-9. doi: 10.1089/neu.2008.0655. PubMed PMID: 19125683.
238. Jin W, Ni H, Dai Y, Wang H, Lu T, Wu J, Jiang J, Liang W. Effects of tert-butylhydroquinone on intestinal inflammatory response and apoptosis following traumatic brain injury in mice. Mediators Inflamm. 2010;2010:502564. doi: 10.1155/2010/502564. PubMed PMID: 21274455; PMCID: PMC3025385.
239. Ding K, Wang H, Xu J, Li T, Zhang L, Ding Y, Zhu L, He J, Zhou M. Melatonin stimulates antioxidant enzymes and reduces oxidative stress in experimental

traumatic brain injury: the Nrf2-ARE signaling pathway as a potential mechanism. Free Radic Biol Med. 2014;73:1-11. doi: 10.1016/j.freeradbiomed.2014.04.031. PubMed PMID: 24810171.
240. Xu J, Wang H, Ding K, Zhang L, Wang C, Li T, Wei W, Lu X. Luteolin provides neuroprotection in models of traumatic brain injury via the Nrf2-ARE pathway. Free Radic Biol Med. 2014;71:186-95. doi: 10.1016/j.freeradbiomed.2014.03.009. PubMed PMID: 24642087.
241. Li Z, Dong X, Zhang J, Zeng G, Zhao H, Liu Y, Qiu R, Mo L, Ye Y. Formononetin protects TBI rats against neurological lesions and the underlying mechanism. J Neurol Sci. 2014;338(1-2):112-7. doi: 10.1016/j.jns.2013.12.027. PubMed PMID: 24411660.
242. Ding H, Wang H, Zhu L, Wei W. Ursolic Acid Ameliorates Early Brain Injury After Experimental Traumatic Brain Injury in Mice by Activating the Nrf2 Pathway. Neurochem Res. 2017;42(2):337-46. doi: 10.1007/s11064-016-2077-8. PubMed PMID: 27734181.
243. Li X, Wang H, Gao Y, Li L, Tang C, Wen G, Zhou Y, Zhou M, Mao L, Fan Y. Protective Effects of Quercetin on Mitochondrial Biogenesis in Experimental Traumatic Brain Injury via the Nrf2 Signaling Pathway. PLoS One. 2016;11(10):e0164237. doi: 10.1371/journal.pone.0164237. PubMed PMID: 27780244; PMCID: PMC5079551.
244. Yang Y, Wang H, Li L, Li X, Wang Q, Ding H, Wang X, Ye Z, Wu L, Zhang X, Zhou M, Pan H. Sinomenine Provides Neuroprotection in Model of Traumatic Brain Injury via the Nrf2-ARE Pathway. Front Neurosci. 2016;10:580. doi: 10.3389/fnins.2016.00580. PubMed PMID: 28066165; PMCID: PMC5179594.
245. Lu XY, Wang HD, Xu JG, Ding K, Li T. Pretreatment with tert-butylhydroquinone attenuates cerebral oxidative stress in mice after traumatic brain injury. J Surg Res. 2014;188(1):206-12. doi: 10.1016/j.jss.2013.11.1106. PubMed PMID: 24387843.
246. Miller DM, Singh IN, Wang JA, Hall ED. Nrf2-ARE activator carnosic acid decreases mitochondrial dysfunction, oxidative damage and neuronal cytoskeletal degradation following traumatic brain injury in mice. Exp Neurol. 2015;264:103-10. doi: 10.1016/j.expneurol.2014.11.008. PubMed PMID: 25432068; PMCID: PMC4323924.
247. Hayashi G, Jasoliya M, Sacca F, Pane C, Filla A, Marsili A, Puorro G, Lanzillo R, Brescia Morra V, Cortopassi G. Dimethyl Fumarate Mediates Nrf2-dependent Mitochondrial Biogenesis in Mice and Humans. Hum Mol Genet. 2017. doi: 10.1093/hmg/ddx167. PubMed PMID: 28460056.
248. Sullivan PG, Springer JE, Hall ED, Scheff SW. Mitochondrial uncoupling as a therapeutic target following neuronal injury. J Bioenerg Biomembr. 2004;36(4):353-6. Epub 2004/09/21. doi: 10.1023/B:JOBB.0000041767.30992.19. PubMed PMID: 15377871.
249. Pandya JD, Pauly JR, Sullivan PG. The optimal dosage and window of opportunity to maintain mitochondrial homeostasis following traumatic brain injury using the uncoupler FCCP. Exp Neurol. 2009;218(2):381-9. Epub 2009/05/30. doi: 10.1016/j.expneurol.2009.05.023. PubMed PMID: 19477175.
250. Pandya JD, Pauly JR, Nukala VN, Sebastian AH, Day KM, Korde AS, Maragos WF, Hall ED, Sullivan PG. Post-Injury Administration of Mitochondrial Uncouplers Increases Tissue Sparing and Improves Behavioral Outcome following Traumatic

Brain Injury in Rodents. J Neurotrauma. 2007;24(5):798-811. Epub 2007/05/24. doi: 10.1089/neu.2006.3673. PubMed PMID: 17518535.
251. Geisler JG, Marosi K, Halpern J, Mattson MP. DNP, mitochondrial uncoupling, and neuroprotection: A little dab'll do ya. Alzheimers Dement. 2017;13(5):582-91. Epub 2016/09/07. doi: 10.1016/j.jalz.2016.08.001. PubMed PMID: 27599210; PMCID: PMC5337177.
252. Lu J, Gary KW, Neimeier JP, Ward J, Lapane KL. Randomized controlled trials in adult traumatic brain injury. Brain Inj. 2012;26(13-14):1523-48. Epub 2012/11/21. doi: 10.3109/02699052.2012.722257. PubMed PMID: 23163248.
253. Narayan RK, Michel ME, Ansell B, Baethmann A, Biegon A, Bracken MB, Bullock MR, Choi SC, Clifton GL, Contant CF, Coplin WM, Dietrich WD, Ghajar J, Grady SM, Grossman RG, Hall ED, Heetderks W, Hovda DA, Jallo J, Katz RL, Knoller N, Kochanek PM, Maas AI, Majde J, Marion DW, Marmarou A, Marshall LF, McIntosh TK, Miller E, Mohberg N, Muizelaar JP, Pitts LH, Quinn P, Riesenfeld G, Robertson CS, Strauss KI, Teasdale G, Temkin N, Tuma R, Wade C, Walker MD, Weinrich M, Whyte J, Wilberger J, Young AB, Yurkewicz L. Clinical trials in head injury. Journal of neurotrauma. 2002;19(5):503-57. Epub 2002/06/04. doi: 10.1089/089771502753754037. PubMed PMID: 12042091; PMCID: 1462953.
254. Menon DK. Unique challenges in clinical trials in traumatic brain injury. Crit Care Med. 2009;37(1 Suppl):S129-35. Epub 2009/01/06. doi: 10.1097/CCM.0b013e3181921225. PubMed PMID: 19104212.
255. Wright DW, Yeatts SD, Silbergleit R, Palesch YY, Hertzberg VS, Frankel M, Goldstein FC, Caveney AF, Howlett-Smith H, Bengelink EM, Manley GT, Merck LH, Janis LS, Barsan WG. Very early administration of progesterone for acute traumatic brain injury. N Engl J Med. 2014;371(26):2457-66. Epub 2014/12/11. doi: 10.1056/NEJMoa1404304. PubMed PMID: 25493974; PMCID: 4303469.
256. Skolnick BE, Maas AI, Narayan RK, van der Hoop RG, MacAllister T, Ward JD, Nelson NR, Stocchetti N. A clinical trial of progesterone for severe traumatic brain injury. N Engl J Med. 2014;371(26):2467-76. Epub 2014/12/11. doi: 10.1056/NEJMoa1411090. PubMed PMID: 25493978.
257. Maas AI, Menon DK. Traumatic brain injury: rethinking ideas and approaches. Lancet Neurol. 2012;11(1):12-3. doi: 10.1016/S1474-4422(11)70267-8. PubMed PMID: 22172614.
258. Diaz-Arrastia R, Kochanek PM, Bergold P, Kenney K, Marx CE, Grimes CJ, Loh LT, Adam LT, Oskvig D, Curley KC, Salzer W. Pharmacotherapy of traumatic brain injury: state of the science and the road forward: report of the Department of Defense Neurotrauma Pharmacology Workgroup. J Neurotrauma. 2014;31(2):135-58. doi: 10.1089/neu.2013.3019. PubMed PMID: 23968241; PMCID: PMC3900003.
259. Smith DH, Hicks RR, Johnson VE, Bergstrom DA, Cummings DM, Noble LJ, Hovda D, Whalen M, Ahlers ST, LaPlaca M, Tortella FC, Duhaime AC, Dixon CE. Pre-Clinical Traumatic Brain Injury Common Data Elements: Toward a Common Language Across Laboratories. J Neurotrauma. 2015;32(22):1725-35. doi: 10.1089/neu.2014.3861. PubMed PMID: 26058402; PMCID: PMC4651035.

260. Demarest TG, McCarthy MM. Sex differences in mitochondrial (dys)function: Implications for neuroprotection. J Bioenerg Biomembr. 2015;47(1-2):173-88. doi: 10.1007/s10863-014-9583-7. PubMed PMID: 25293493; PMCID: PMC4988325.
261. Demarest TG, Schuh RA, Waite EL, Waddell J, McKenna MC, Fiskum G. Sex dependent alterations in mitochondrial electron transport chain proteins following neonatal rat cerebral hypoxic-ischemia. J Bioenerg Biomembr. 2016;48(6):591-8. doi: 10.1007/s10863-016-9678-4. PubMed PMID: 27683241.
262. Bayir H, Marion DW, Puccio AM, Wisniewski SR, Janesko KL, Clark RS, Kochanek PM. Marked gender effect on lipid peroxidation after severe traumatic brain injury in adult patients. J Neurotrauma. 2004;21(1):1-8. Epub 2004/02/28. doi: 10.1089/089771504772695896. PubMed PMID: 14987460.
263. Costa LG, de Laat R, Dao K, Pellacani C, Cole TB, Furlong CE. Paraoxonase-2 (PON2) in brain and its potential role in neuroprotection. Neurotoxicology. 2014;43:3-9. Epub 2013/09/10. doi: 10.1016/j.neuro.2013.08.011. PubMed PMID: 24012887; PMCID: PMC3942372.
264. Di Domenico F, Casalena G, Jia J, Sultana R, Barone E, Cai J, Pierce WM, Cini C, Mancuso C, Perluigi M, Davis CM, Alkayed NJ, Butterfield DA. Sex differences in brain proteomes of neuron-specific STAT3-null mice after cerebral ischemia/reperfusion. J Neurochem. 2012;121(4):680-92. Epub 2012/03/08. doi: 10.1111/j.1471-4159.2012.07721.x. PubMed PMID: 22394374; PMCID: PMC3325362.
265. Saeed U, Karunakaran S, Meka DP, Koumar RC, Ramakrishnan S, Joshi SD, Nidadavolu P, Ravindranath V. Redox activated MAP kinase death signaling cascade initiated by ASK1 is not activated in female mice following MPTP: novel mechanism of neuroprotection. Neurotox Res. 2009;16(2):116-26. Epub 2009/06/16. doi: 10.1007/s12640-009-9058-5. PubMed PMID: 19526288.
266. Sharma J, Johnston MV, Hossain MA. Sex differences in mitochondrial biogenesis determine neuronal death and survival in response to oxygen glucose deprivation and reoxygenation. BMC Neurosci. 2014;15:9. Epub 2014/01/15. doi: 10.1186/1471-2202-15-9. PubMed PMID: 24410996; PMCID: PMC3898007.
267. Mohagheghi F, Ahmadiani A, Rahmani B, Moradi F, Romond N, Khalaj L. Gemfibrozil pretreatment resulted in a sexually dimorphic outcome in the rat models of global cerebral ischemia-reperfusion via modulation of mitochondrial pro-survival and apoptotic cell death factors as well as MAPKs. J Mol Neurosci. 2013;50(3):379-93. Epub 2013/01/05. doi: 10.1007/s12031-012-9932-0. PubMed PMID: 23288702.
268. Andrabi SA, Dawson TM, Dawson VL. Mitochondrial and nuclear cross talk in cell death: parthanatos. Ann N Y Acad Sci. 2008;1147:233-41. Epub 2008/12/17. doi: 10.1196/annals.1427.014. PubMed PMID: 19076445; PMCID: PMC4454457.
269. Djebaili M, Guo Q, Pettus EH, Hoffman SW, Stein DG. The neurosteroids progesterone and allopregnanolone reduce cell death, gliosis, and functional deficits after traumatic brain injury in rats. J Neurotrauma. 2005;22(1):106-18. Epub 2005/01/25. doi: 10.1089/neu.2005.22.106. PubMed PMID: 15665606.
270. Tirilazad mesylate in acute ischemic stroke: A systematic review. Tirilazad International Steering Committee. Stroke. 2000;31(9):2257-65. Epub 2000/09/08. PubMed PMID: 10978061.

271. Marshall LF, Maas AI, Marshall SB, Bricolo A, Fearnside M, Iannotti F, Klauber MR, Lagarrigue J, Lobato R, Persson L, Pickard JD, Piek J, Servadei F, Wellis GN, Morris GF, Means ED, Musch B. A multicenter trial on the efficacy of using tirilazad mesylate in cases of head injury. J Neurosurg. 1998;89(4):519-25. Epub 1998/10/07. doi: 10.3171/jns.1998.89.4.0519. PubMed PMID: 9761043.
272. Ahnstedt H, Cao L, Krause DN, Warfvinge K, Saveland H, Nilsson OG, Edvinsson L. Male-female differences in upregulation of vasoconstrictor responses in human cerebral arteries. PLoS One. 2013;8(4):e62698. Epub 2013/05/10. doi: 10.1371/journal.pone.0062698. PubMed PMID: 23658641; PMCID: PMC3639206.
273. Gibson CL. Cerebral ischemic stroke: is gender important? J Cereb Blood Flow Metab. 2013;33(9):1355-61. Epub 2013/06/13. doi: 10.1038/jcbfm.2013.102. PubMed PMID: 23756694; PMCID: PMC3764377.
274. Furman D, Hejblum BP, Simon N, Jojic V, Dekker CL, Thiebaut R, Tibshirani RJ, Davis MM. Systems analysis of sex differences reveals an immunosuppressive role for testosterone in the response to influenza vaccination. Proc Natl Acad Sci U S A. 2014;111(2):869-74. Epub 2013/12/25. doi: 10.1073/pnas.1321060111. PubMed PMID: 24367114; PMCID: PMC3896147.
275. Du L, Bayir H, Lai Y, Zhang X, Kochanek PM, Watkins SC, Graham SH, Clark RS. Innate gender-based proclivity in response to cytotoxicity and programmed cell death pathway. J Biol Chem. 2004;279(37):38563-70. Epub 2004/07/06. doi: 10.1074/jbc.M405461200. PubMed PMID: 15234982.
276. Li H, Pin S, Zeng Z, Wang MM, Andreasson KA, McCullough LD. Sex differences in cell death. Ann Neurol. 2005;58(2):317-21. Epub 2005/07/01. doi: 10.1002/ana.20538. PubMed PMID: 15988750.
277. Utomo WK, Gabbe BJ, Simpson PM, Cameron PA. Predictors of in-hospital mortality and 6-month functional outcomes in older adults after moderate to severe traumatic brain injury. Injury. 2009;40(9):973-7. Epub 2009/06/23. doi: 10.1016/j.injury.2009.05.034. PubMed PMID: 19540490.
278. Bulstrode H, Nicoll JA, Hudson G, Chinnery PF, Di Pietro V, Belli A. Mitochondrial DNA and traumatic brain injury. Ann Neurol. 2014;75(2):186-95. doi: 10.1002/ana.24116. PubMed PMID: 24523223; PMCID: PMC4112718.
279. Gilmer LK, Ansari MA, Roberts KN, Scheff SW. Age-related mitochondrial changes after traumatic brain injury. J Neurotrauma. 2010;27(5):939-50. Epub 2010/02/24. doi: 10.1089/neu.2009.1181. PubMed PMID: 20175672; PMCID: PMC2943941.
280. Gilmer LK, Ansari MA, Roberts KN, Scheff SW. Age-related changes in mitochondrial respiration and oxidative damage in the cerebral cortex of the Fischer 344 rat. Mech Ageing Dev. 2010;131(2):133-43. Epub 2010/01/19. doi: 10.1016/j.mad.2009.12.011. PubMed PMID: 20080122; PMCID: PMC2834189.
281. Del Maestro R, McDonald W. Distribution of superoxide dismutase, glutathione peroxidase and catalase in developing rat brain. Mech Ageing Dev. 1987;41(1-2):29-38. PubMed PMID: 3431167.
282. Bates TE, Almeida A, Heales SJ, Clark JB. Postnatal development of the complexes of the electron transport chain in isolated rat brain mitochondria. Dev Neurosci. 1994;16(5-6):321-7. PubMed PMID: 7768212.

283. Sullivan PG, Dube C, Dorenbos K, Steward O, Baram TZ. Mitochondrial uncoupling protein-2 protects the immature brain from excitotoxic neuronal death. Ann Neurol. 2003;53(6):711-7. Epub 2003/06/05. doi: 10.1002/ana.10543. PubMed PMID: 12783416; PMCID: PMC2930774.
284. Chinnery PF, Elliott HR, Syed A, Rothwell PM, Oxford Vascular S. Mitochondrial DNA haplogroups and risk of transient ischaemic attack and ischaemic stroke: a genetic association study. Lancet Neurol. 2010;9(5):498-503. doi: 10.1016/S1474-4422(10)70083-1. PubMed PMID: 20362514; PMCID: PMC2855429.
285. Lorente L, Iceta R, Martin MM, Lopez-Gallardo E, Sole-Violan J, Blanquer J, Labarta L, Diaz C, Borreguero-Leon JM, Jimenez A, Montoya J, Ruiz-Pesini E. Severe septic patients with mitochondrial DNA haplogroup JT show higher survival rates: a prospective, multicenter, observational study. PLoS One. 2013;8(9):e73320. doi: 10.1371/journal.pone.0073320. PubMed PMID: 24069186; PMCID: PMC3772099.
286. Conley YP, Okonkwo DO, Deslouches S, Alexander S, Puccio AM, Beers SR, Ren D. Mitochondrial polymorphisms impact outcomes after severe traumatic brain injury. J Neurotrauma. 2014;31(1):34-41. doi: 10.1089/neu.2013.2855. PubMed PMID: 23883111; PMCID: PMC3880110.
287. Baudouin SV, Saunders D, Tiangyou W, Elson JL, Poynter J, Pyle A, Keers S, Turnbull DM, Howell N, Chinnery PF. Mitochondrial DNA and survival after sepsis: a prospective study. Lancet. 2005;366(9503):2118-21. Epub 2005/12/20. doi: 10.1016/S0140-6736(05)67890-7. PubMed PMID: 16360789.
288. Wallace DC. A mitochondrial bioenergetic etiology of disease. J Clin Invest. 2013;123(4):1405-12. doi: 10.1172/JCI61398. PubMed PMID: 23543062; PMCID: PMC3614529.
289. Wallace DC. Mitochondrial DNA variation in human radiation and disease. Cell. 2015;163(1):33-8. doi: 10.1016/j.cell.2015.08.067. PubMed PMID: 26406369; PMCID: PMC4743751.
290. Mishmar D, Ruiz-Pesini E, Golik P, Macaulay V, Clark AG, Hosseini S, Brandon M, Easley K, Chen E, Brown MD, Sukernik RI, Olckers A, Wallace DC. Natural selection shaped regional mtDNA variation in humans. Proc Natl Acad Sci U S A. 2003;100(1):171-6. doi: 10.1073/pnas.0136972100. PubMed PMID: 12509511; PMCID: PMC140917.
291. Ruiz-Pesini E, Mishmar D, Brandon M, Procaccio V, Wallace DC. Effects of purifying and adaptive selection on regional variation in human mtDNA. Science. 2004;303(5655):223-6. doi: 10.1126/science.1088434. PubMed PMID: 14716012.
292. Ruiz-Pesini E, Wallace DC. Evidence for adaptive selection acting on the tRNA and rRNA genes of human mitochondrial DNA. Hum Mutat. 2006;27(11):1072-81. doi: 10.1002/humu.20378. PubMed PMID: 16947981.
293. Ghezzi D, Marelli C, Achilli A, Goldwurm S, Pezzoli G, Barone P, Pellecchia MT, Stanzione P, Brusa L, Bentivoglio AR, Bonuccelli U, Petrozzi L, Abbruzzese G, Marchese R, Cortelli P, Grimaldi D, Martinelli P, Ferrarese C, Garavaglia B, Sangiorgi S, Carelli V, Torroni A, Albanese A, Zeviani M. Mitochondrial DNA haplogroup K is associated with a lower risk of Parkinson's disease in Italians. Eur J Hum Genet. 2005;13(6):748-52. doi: 10.1038/sj.ejhg.5201425. PubMed PMID: 15827561.

294. Shoffner JM, Brown MD, Torroni A, Lott MT, Cabell MF, Mirra SS, Beal MF, Yang CC, Gearing M, Salvo R, et al. Mitochondrial DNA variants observed in Alzheimer disease and Parkinson disease patients. Genomics. 1993;17(1):171-84. PubMed PMID: 8104867.
295. Amo T, Yadava N, Oh R, Nicholls DG, Brand MD. Experimental assessment of bioenergetic differences caused by the common European mitochondrial DNA haplogroups H and T. Gene. 2008;411(1-2):69-76. Epub 2008/02/19. doi: 10.1016/j.gene.2008.01.007. PubMed PMID: 18280061; PMCID: PMC2270349.
296. Olivera A, Lejbman N, Jeromin A, French LM, Kim HS, Cashion A, Mysliwiec V, Diaz-Arrastia R, Gill J. Peripheral Total Tau in Military Personnel Who Sustain Traumatic Brain Injuries During Deployment. JAMA Neurol. 2015;72(10):1109-16. Epub 2015/08/04. doi: 10.1001/jamaneurol.2015.1383. PubMed PMID: 26237304.
297. Shively S, Scher AI, Perl DP, Diaz-Arrastia R. Dementia resulting from traumatic brain injury: what is the pathology? Archives of neurology. 2012;69(10):1245-51. Epub 2012/07/11. doi: 10.1001/archneurol.2011.3747. PubMed PMID: 22776913; PMCID: PMC3716376.
298. Stern RA, Tripodis Y, Baugh CM, Fritts NG, Martin BM, Chaisson C, Cantu RC, Joyce JA, Shah S, Ikezu T, Zhang J, Gercel-Taylor C, Taylor DD. Preliminary Study of Plasma Exosomal Tau as a Potential Biomarker for Chronic Traumatic Encephalopathy. J Alzheimers Dis. 2016;51(4):1099-109. Epub 2016/02/19. doi: 10.3233/JAD-151028. PubMed PMID: 26890775; PMCID: PMC4833534.
299. Kochanek PM, Bell MJ. Making an IMPACT in traumatic brain injury research. The Lancet Neurology. 2013;12(12):1132-3. Epub 2013/10/22. doi: 10.1016/S1474-4422(13)70245-X. PubMed PMID: 24139679.
300. Diaz-Arrastia R, Wang KK, Papa L, Sorani MD, Yue JK, Puccio AM, McMahon PJ, Inoue T, Yuh EL, Lingsma HF, Maas AI, Valadka AB, Okonkwo DO, Manley GT, Investigators T-T. Acute biomarkers of traumatic brain injury: relationship between plasma levels of ubiquitin C-terminal hydrolase-L1 and glial fibrillary acidic protein. J Neurotrauma. 2014;31(1):19-25. doi: 10.1089/neu.2013.3040. PubMed PMID: 23865516; PMCID: PMC3880090.
301. Okonkwo DO, Yue JK, Puccio AM, Panczykowski DM, Inoue T, McMahon PJ, Sorani MD, Yuh EL, Lingsma HF, Maas AI, Valadka AB, Manley GT, Transforming R, Clinical Knowledge in Traumatic Brain Injury I. GFAP-BDP as an acute diagnostic marker in traumatic brain injury: results from the prospective transforming research and clinical knowledge in traumatic brain injury study. J Neurotrauma. 2013;30(17):1490-7. doi: 10.1089/neu.2013.2883. PubMed PMID: 23489259; PMCID: PMC3751263.
302. Warner MA, Youn TS, Davis T, Chandra A, Marquez de la Plata C, Moore C, Harper C, Madden CJ, Spence J, McColl R, Devous M, King RD, Diaz-Arrastia R. Regionally selective atrophy after traumatic axonal injury. Archives of neurology. 2010;67(11):1336-44. Epub 2010/07/14. doi: 10.1001/archneurol.2010.149. PubMed PMID: 20625067; PMCID: PMC3465162.
303. Degli Esposti M. Inhibitors of NADH-ubiquinone reductase: an overview. Biochim Biophys Acta. 1998;1364(2):222-35. PubMed PMID: 9593904.
304. Mesnage R, Arno M, Costanzo M, Malatesta M, Seralini GE, Antoniou MN. Transcriptome profile analysis reflects rat liver and kidney damage following chronic ultra-low

dose Roundup exposure. Environ Health. 2015;14:70. doi: 10.1186/s12940-015-0056-1. PubMed PMID: 26302742; PMCID: PMC4549093.
305. Friedrich T, van Heek P, Leif H, Ohnishi T, Forche E, Kunze B, Jansen R, Trowitzsch-Kienast W, Hofle G, Reichenbach H, et al. Two binding sites of inhibitors in NADH: ubiquinone oxidoreductase (complex I). Relationship of one site with the ubiquinone-binding site of bacterial glucose:ubiquinone oxidoreductase. Eur J Biochem. 1994;219(1-2):691-8. PubMed PMID: 8307034.
306. Lim S, Ahn SY, Song IC, Chung MH, Jang HC, Park KS, Lee KU, Pak YK, Lee HK. Chronic exposure to the herbicide, atrazine, causes mitochondrial dysfunction and insulin resistance. PLoS One. 2009;4(4):e5186. doi: 10.1371/journal.pone.0005186. PubMed PMID: 19365547; PMCID: PMC2664469.
307. Hollingworth RM, Ahammadsahib KI, Gadelhak G, McLaughlin JL. New inhibitors of complex I of the mitochondrial electron transport chain with activity as pesticides. Biochem Soc Trans. 1994;22(1):230-3. PubMed PMID: 8206238.
308. Satoh T, Miyoshi H, Sakamoto K, Iwamura H. Comparison of the inhibitory action of synthetic capsaicin analogues with various NADH-ubiquinone oxidoreductases. Biochim Biophys Acta. 1996;1273(1):21-30. PubMed PMID: 8573592.
309. Gassner B, Wuthrich A, Scholtysik G, Solioz M. The pyrethroids permethrin and cyhalothrin are potent inhibitors of the mitochondrial complex I. J Pharmacol Exp Ther. 1997;281(2):855-60. PubMed PMID: 9152394.
310. Lee JE, Park JH, Shin IC, Koh HC. Reactive oxygen species regulated mitochondria-mediated apoptosis in PC12 cells exposed to chlorpyrifos. Toxicol Appl Pharmacol. 2012;263(2):148-62. doi: 10.1016/j.taap.2012.06.005. PubMed PMID: 22714038.
311. Eddleston M. Patterns and problems of deliberate self-poisoning in the developing world. QJM. 2000;93(11):715-31. PubMed PMID: 11077028.
312. Buckley NA, Roberts D, Eddleston M. Overcoming apathy in research on organophosphate poisoning. Bmj. 2004;329(7476):1231-3. doi: 10.1136/bmj.329.7476.1231. PubMed PMID: 15550429; PMCID: PMC529372.
313. Terry AV, Jr. Functional consequences of repeated organophosphate exposure: potential non-cholinergic mechanisms. Pharmacol Ther. 2012;134(3):355-65. doi: 10.1016/j.pharmthera.2012.03.001. PubMed PMID: 22465060; PMCID: PMC3366364.
314. Peters RA, Sinclair HM, Thompson RH. An analysis of the inhibition of pyruvate oxidation by arsenicals in relation to the enzyme theory of vesication. Biochem J. 1946;40(4):516-24. PubMed PMID: 20273636.
315. Proudfoot AT, Bradberry SM, Vale JA. Sodium fluoroacetate poisoning. Toxicol Rev. 2006;25(4):213-9. PubMed PMID: 17288493.
316. Stannard JN, Horecker BL. The in vitro inhibition of cytochrome oxidase by azide and cyanide. J Biol Chem. 1948;172(2):599-608. PubMed PMID: 18901179.
317. Young GB. Clinical practice. Neurologic prognosis after cardiac arrest. N Engl J Med. 2009;361(6):605-11. doi: 10.1056/NEJMcp0903466. PubMed PMID: 19657124.
318. Kilbaugh TJ, Sutton RM, Karlsson M, Hansson MJ, Naim MY, Morgan RW, Bratinov G, Lampe JW, Nadkarni VM, Becker LB, Margulies SS, Berg RA. Persistently Altered Brain Mitochondrial Bioenergetics After Apparently Successful Resuscitation From

Cardiac Arrest. J Am Heart Assoc. 2015;4(9):e002232. doi: 10.1161/JAHA.115.002232. PubMed PMID: 26370446; PMCID: PMC4599507.
319. Han F, Da T, Riobo NA, Becker LB. Early mitochondrial dysfunction in electron transfer activity and reactive oxygen species generation after cardiac arrest. Crit Care Med. 2008;36(11 Suppl):S447-53. PubMed PMID: 20449909; PMCID: PMC3315374.
320. Almeida A, Brooks KJ, Sammut I, Keelan J, Davey GP, Clark JB, Bates TE. Postnatal development of the complexes of the electron transport chain in synaptic mitochondria from rat brain. Dev Neurosci. 1995;17(4):212-8. PubMed PMID: 8575340.
321. Ayoub IM, Radhakrishnan J, Gazmuri RJ. Targeting mitochondria for resuscitation from cardiac arrest. Crit Care Med. 2008;36(11 Suppl):S440-6. PubMed PMID: 20449908; PMCID: PMC2865162.

Paper I

SHOCK, Vol. 45, No. 4, pp. 404–410, 2016

DIVERSE AND TISSUE-SPECIFIC MITOCHONDRIAL RESPIRATORY RESPONSE IN A MOUSE MODEL OF SEPSIS-INDUCED MULTIPLE ORGAN FAILURE

Michael Karlsson,[*] Naomi Hara,[†] Saori Morata,[‡] Fredrik Sjövall,[*§] Todd Kilbaugh,[¶] Magnus J. Hansson,[*] Hiroyoki Uchino,[†] and Eskil Elmér[*]

[*]Mitochondrial Medicine, Department of Clinical Sciences, Lund University, Lund, Sweden; [†]Department of Anesthesiology, Tokyo Medical University; [‡]Department of Human Genetics, National Center for Child Health and Development, Tokyo, Japan; [§]Intensive Care Unit, University Hospital of Copenhagen, Copenhagen, Denmark; and [¶]Perelman School of Medicine at the University of Pennsylvania, Anesthesiology and Critical Care Medicine, Children's Hospital of Philadelphia, Philadelphia, Pennsylvania

Received 16 Aug 2015; first review completed 15 Sep 2015; accepted in final form 26 Oct 2015

ABSTRACT—Mitochondrial function is thought to play a role in sepsis-induced multiple organ failure. However, the temporal and organ-specific alterations in mitochondrial function have yet to be fully elucidated. Many studies show reduced phosphorylating capacity, while others have indicated that mitochondrial respiration is enhanced. The objective of this study was to evaluate the temporal dynamics of brain and liver mitochondrial function in a mouse model of sepsis. Sepsis was induced by cecal ligation and puncture. Controls were sham operated. Using high-resolution respirometry, brain and liver homogenates from 31 C57BL/6 mice were analyzed at either 6 or 24 h. Reactive oxygen species (ROS) production was simultaneously measured in brain samples using fluorometry. Septic brain tissue exhibited an early increased uncoupling of respiration. Temporal changes between the two time points were diminutive and no difference in ROS production was detected. Liver homogenate from the septic mice displayed a significant increase in the respiratory control ratio at 6 h. In the 24-h group, the rate of maximal oxidative phosphorylation, as well as LEAK respiration, was significantly increased compared with controls and the resultant respiratory control ratio was also significantly increased. Maximal protonophore-induced respiratory (uncoupled) capacity was similar between the two treatment groups. The present study suggests a diverse and tissue-specific mitochondrial respiratory response to sepsis. The brain displayed an early impaired mitochondrial respiratory efficiency. In the liver the primary finding was a substantial activation of the maximal phosphorylating capacity.

KEYWORDS—Brain, fluorometry, liver, respirometry, rodent

INTRODUCTION

The pathogenesis of sepsis-induced multiple organ failure (MOF) is complex and our understanding of the pathophysiology is incomplete. There is an ongoing controversy regarding O_2 delivery in MOF and hypoperfusion of the organs certainly plays a role. However, it has been argued that perhaps the problem does not only relate to O_2 delivery and tissue hypoxia. Tissue oxygen levels can apparently be normal or even higher than normal in organ failure, and it has been shown that failing organs show limited cell death and failed organs have the potential for recovery (1–3). Elevated tissue oxygenation may compound organ failure due to the production of reactive oxygen species (ROS). The majority of the oxygen delivered to cells is consumed by mitochondria for oxidative phosphorylation and mitochondrial respiratory dysfunction has been suggested to play a role in the pathogenesis of sepsis-induced multiple organ failure, although the precise pathological mechanisms are not clear (4).

One proposed theory is that of cytopathic hypoxia, which suggests that mitochondrial dysfunction is caused by an inability to utilize available oxygen (5). However, the composed data on the subject are seemingly contradictory. Studies have indicated altered mitochondrial respiratory function in human muscle tissue as well as in diverse animal models examining various tissues and different tissues seem to respond differently to sepsis (6–10). Many studies show reduced phosphorylating capacity (11), whereas other studies have indicated enhanced mitochondrial respiration in sepsis (12, 13). Further, as a framework for this study, it has previously been shown in a rodent model that sepsis can induce increased uncoupling of the oxidative phosphorylation system in brain homogenates (14, 15).

The somewhat contradictory results obtained not only seem to depend on the model used but also on the specific organ from which the mitochondria are obtained as well as the studied time-point during the disease progression. The pathogenesis is multifaceted and sepsis is clearly a dynamic process. Mitochondrial biogenesis occurs together with the respiratory alterations and we have previously demonstrated, in human platelets, that an early increase in uncoupling is followed by a gradual increase in respiration during the first week of sepsis and that the increase was most pronounced in non-survivors, likely correlated to the severity of the septic insult (13).

Address reprint requests to Michael Karlsson, MD, Lund University, 221 84 Lund, Sweden. E-mail michael.karlsson@med.lu.se

This work was supported by the Swedish Research Council (2011-3470) and the Swedish government project and salary funding for clinically oriented medical research (ALF grants). MK, MJH, and EE have equity interests in and/or have received salary support from NeuroVive Pharmaceutical AB, a public company developing pharmaceuticals in the field of mitochondrial medicine. This project was, however, not initiated or supported by NeuroVive Pharmaceutical AB. The remaining authors declare no financial or commercial conflicts of interest.

DOI: 10.1097/SHK.0000000000000525

The aim of the present study was to evaluate the mitochondrial respiratory function in two different organs commonly affected in sepsis and the subsequent multiple organ failure, the brain and the liver. By also analyzing two different time-points we wanted to evaluate the temporal dynamics of mitochondrial function. In addition, the tissue generation of ROS was evaluated in the brain tissues simultaneously to respiratory measurements.

MATERIALS AND METHODS

Chemicals used were purchased from Wako Pure Chemical Industries, Ltd. (Osaka, Japan) if not stated otherwise.

Animals and study design

The ethical committee of animal experiments at Tokyo Medical University (H-24013) approved the study. Animals were kept under standard conditions with *ad libitum* access to food and water and maintained at a 12-h day and night cycle. The population consisted of 31 pathogen-free 8-week-old male C57BL/6 mice. Sepsis was induced by cecal ligation and puncture (CLP) as previously described, but with a few alterations (16). In short, the mice were anesthetized using continuous inhalation of isofluorane. Laparotomy was performed with a 10-mm incision. After the cecum was exposed using blunt anatomical forceps, 75% of the cecum was ligated right below the ileocecal valve. Before perforation, feces was gently relocated toward the distal cecum. The cecum was perforated by a single through and through (mesenteric to antimesenteric) puncture using a 21-G needle at half way from tip to ligation. A small droplet of feces was then gently squeezed through the punctures. The cecum was then returned to the peritoneal cavity with careful attention so that feces did not contaminate the margins of the abdominal and skin wound. The muscle and skin incisions were closed using 4-0 interrupted sutures. This method represents a high-grade sepsis with a 100% mortality in 72 h (16). The animals were resuscitated directly postoperatively by 1.0-mL subcutaneous injection of saline (37°C). Controls were sham operated and underwent the same procedure, except the ligation and the puncture of the cecum.

Termination and preparation of homogenates

The mice were selected at a predetermined time point, regardless of symptoms, at either 6 h (±15 min) or 24 h (±30 min) after surgery. The mice were video filmed for later unbiased evaluation of clinical status. The clinical parameters assessed included convulsions, loss of balance, loss of gripping reflex, paralysis, ruffled fur, and a score was assigned from the clinical assessment table (Table 1). The mice were subsequently terminated by cervical dislocation. Body temperature was measured directly after cervical dislocation using a digital rectal probe (BWT-100, Bio Research Center Co, Ltd., Nagoya, Japan) and blood glucose was measured (Terumo Finetouch, Tokyo, Japan). The organs for analysis were harvested, beginning with the brain, by rapid but gentle dissection and then immediately transferred into ice-cold buffer solution (320 mM sucrose, 2 mM EGTA, 10 mM Trizma base, pH 7.4). The tissues were weighed and manually homogenized in a 5-mL Potter-Elvehjem teflon-glass homogenizer to a concentration of 1 mg wet weight tissue/10 μL MiR05 buffer (0.5 mM EGTA, 3 mM $MgCl_2$, 60 mM K-lactobionate, 20 mM Taurine, 10 mM KH_2P0_4, 20 mM HEPES, 110 mM sucrose, 1 g/L BSA, pH 7.1). The entire procedure was performed on ice and all buffer solutions were ice-cold.

TABLE 1. **Clinical scoring criteria**

Score	Observation
0	No discernible clinical signs
1	Hunched back, slightly ruffled fur
2	Very ruffled fur, reduced rate of movement, developing motor impairments
3	Very ruffled fur, impaired balance/coordination, severe motor impairments such as ataxia, hemiplegia and paraplegia, convulsions, fitting
4	Very little movement, convulsions, fitting
5	Loss of consciousness/coma

High-resolution respirometry

Mitochondrial respiration was measured using a high-resolution Oxygraph-2k (Oroboros Instruments, Innsbruck, Austria). Mitochondrial respiration was corrected for instrumental oxygen flux, measured separately for automatic correction. Calibration was performed daily with air-saturated MilliQ water. An oxygen solubility factor relative to H_2O was set to 0.92 for MiR05. Experiments were carried out at a controlled constant temperature of 37°C. Experiments were started by the addition of 22 μL of brain homogenate (2.2 mg wet weight brain tissue) into chamber prefilled with MiR05 to a final concentration in the closed chamber of 1 mg/mL. Oxygen concentration and oxygen flux were monitored and recorded in real-time using DatLab 5.1 software (Oroboros Instruments).

Fluorometric measurements of ROS

Measurement of ROS production in brain homogenates was carried out using the add-on module O2k-Flourescence LED2 (Oroboros Instruments) to allow simultaneous measurement of ROS production and mitochondrial respiration. ROS production was detected using the Amplex Red (*N*-acetyl-3,7 dihydroxyphenoxazine) hydrogen peroxide (H_2O_2) assay. In the presence of horseradish peroxidase, Amplex Red reacts with H_2O_2 to produce the fluorescent compound resorufin. The addition of superoxide dismutase ensures that all superoxide is converted into H_2O_2.

Amplex red (5 μM), horseradish peroxidase (1 U/mL), and Superoxide dismutase (10 U/mL) were added to the chamber prior to adding homogenates. Calibration of fluorometric signal was conducted prior to each measurement by the addition of 100 nM H_2O_2. Hydrogen peroxide for calibration was diluted daily from 1 M stock solution. Measurements of ROS were not performed in liver homogenates due to the high content of endogenous cytosolic antioxidants that interfere with the Amplex red assay and the measurement of H_2O_2 production.

Protocol for assessment of mitochondrial respiratory function

A substrate, uncoupler and inhibitor titration (SUIT) protocol with consecutive additions was utilized as previously described, but with a few modifications (17). By using complex-specific substrates and inhibitors it is possible to examine the respiratory capacities with electron flow through both Complex I (CI) and Complex II (CII), as well as the convergent electron input through the Q-junction (CI + II). The maximal phosphorylating and non-phosphorylating respiration were measured as stimulated by combined NADH-linked substrates and succinate. Digitonin was added to brain homogenates for permeabilization of the synaptosomes. The homogenates were then allowed to stabilize at basal respiration without exogenous substrates in MiR05 when calibration of the fluorometric signal was conducted in the brain homogenate. The remaining protocol was identical for both brain and liver homogenates as follows. Malate (5 mM) and pyruvate (5 mM) were added followed by ADP (1 mM) and glutamate (5 mM) attaining oxidative phosphorylation (OXPHOS) capacity supported through CI ($OXPHOS_{CI}$), driven by the NADH-related substrates. OXPHOS respiration is an ATP-producing state where the electron flow is controlled by the ATP synthase. Subsequently, succinate (20 mM) was added stimulating maximal OXPHOS capacity by convergent input through CI and CII ($OXPHOS_{CI+II}$). Oxidative phosphorylation was inhibited by oligomycin, an ATP-synthase inhibitor, inducing LEAK respiration state ($LEAK_{CI+II}$), i.e., mitochondrial respiration independent of ATP production. LEAK respiration reveals the respiration related to electron flow through the electron transport system (ETS) necessary to uphold the membrane potential compensating for leakage of protons independent of the ATP synthase. Maximal convergent respiratory capacity of the ETS (ETS_{CI+II}) was then evaluated by titrating the protonophore, carbonyl cyanide p-(trifluoromethoxy) phenylhydrazone (FCCP) until no further increase in respiration was detected. ETS_{CI+II} reveals respiration related to electron flow, through both CI and CII, when it is not restricted by the ATP synthase. To measure the ETS capacity supported by succinate alone through CII (ETS_{CII}) rotenone was added to inhibit CI. The complete electron flow through the ETS was inhibited by the addition of the complex III (CIII) inhibitor antimycin-A (1 μg/mL) revealing the residual oxygen consumption not related to the ETS. This value was subtracted from the different respiratory states in the final analysis. Finally, an addition was made of ascorbate and *N*,*N*,*N*′,*N*′-Tetramethyl-*p*-phenylenediamine dihydrochloride (TMPD), which is an artificial substrate for reducing cytochrome c, to measure the activity of cytochrome c oxidase (CIV). Sodium azide was subsequently added for evaluation of the level of auto-oxidation which was subtracted from the TMPD value. Respiratory control ratios were calculated for $OXPHOS_{CI}$, the convergent $OXPHOS_{CI+II}$, and max ETS by dividing each separate rate with LEAK respiration rate. Control ratios were also calculated for ETS divided by

$OXPHOS_{CI}$ and $OXPHOS_{CI+II}$. The duration of the complete titration protocol was approximately 1 h.

Measurements of citrate synthase

Citrate synthase activity was used as a marker for mitochondrial content (18). After sonication of samples, citrate synthase activity was measured in a spectrophotometric plate-reader using a commercially available kit according to the manufacturer's instructions (Citrate Synthase Assay Kit, CS0720, Sigma).

Statistical analysis

The data from two control mice in the original design of 33 mice were excluded altogether due to evident laboratory error related to contamination. One analysis of liver tissue from a 24-h control was removed due to technical laboratory error related to substrate titration. Statistical analysis was carried out using PRISM 6.0 software (GraphPad Software Inc, La Jolla, CA, USA). To calculate if the differences in separate respiratory states between the treatment groups were statistically significant Student *t* test was used. The respiratory control ratios, clinical scores, and temperatures were not considered to be normally distributed and a Mann–Whitney non-parametric test was used. Differences were considered significant where $P < 0.05$.

RESULTS

Clinical signs of sepsis

The CLP-treated mice developed clinical signs of sepsis and lowered body temperatures compared with controls. The median temperature dropped from 36.8° to 31.7° ($P < 0.001$) in the 6-h group and from 37.6° to 30.8° ($P < 0.01$) in the 24-h group. The median clinical score went from 0 in both controls to 2 in the 6-h group ($P < 0.001$) and to 3 in the 24-h group ($P < 0.01$). Clinical parameters are summarized in Table 2.

Mitochondrial function in brain homogenates following sepsis

No statistically significant differences were detected in citrate synthase activity between the groups (data not shown). The respiratory capacities of $OXPHOS_{CI}$, $OXPHOS_{CI+CII}$, $LEAK_{CI+CII}$, ETS_{CI+CII}, ETS_{CII}, and CIV were evaluated for each treatment group, as illustrated in Table 3. All respiratory data were normalized to wet weight of tissue.

As shown in Figure 1A the respiratory control ratio (RCR) of $OXPHOS_{CI+II}$ and $LEAK_{CI+CII}$ was significantly ($P < 0.05$) decreased in the septic mice in the 6-h group compared with controls. This was mainly due to an underlying increase in the oligomycin-induced $LEAK_{CI+CII}$ state in septic mice compared with controls ($P < 0.05$) (Table 3).

At the 24-h time point there was a non-significant decreased respiratory control ratio of $OXPHOS_{CI+II}$ and $LEAK_{CI+II}$ ($P = 0.055$) in the septic mice (Fig. 1B). $OXPHOS_{CI}$, $OXPHOS_{CI+CII}$, and $LEAK_{CI+II}$ separately all showed similar trends at both time points of decreased oxidative phosphorylation and increased LEAK respiration. ETS_{CI+CII}, ETS_{CII}, and CIV did not differ significantly between septic mice and controls at each separate time-point. FCCP titration (ETS_{CI+CII}) did not increase respiration further compared with OXPHOS (Table 3).

The maximal phosphorylating capacity as a ratio of maximal uncoupled ETS capacity ($OXPHOS_{CI+II}/ETS_{CI+II}$) was just above 1.0 for both groups at both time-points (Table 3), suggesting that the respiratory capacity was not restricted by the ATP synthase. Despite being similar at 6 h the median difference of the ratio (control 1.06; sepsis 1.03, i.e., 2.8% decrease) was statistically significant (Fig. 1, C and D).

ROS production was in control mice significantly altered at different respiratory states and inhibiting the ATP synthase increased ROS production dramatically. However, there were no differences in ROS production between septic mice and controls at either time-point, neither were there any differences in ROS production between the time-points of the two septic groups (Fig. 2).

Mitochondrial function in liver homogenates following sepsis

The liver samples displayed no statistically significant changes in citrate synthase activity between the groups (data not shown). The respiratory capacities of $OXPHOS_{CI}$, $OXPHOS_{CI+CII}$, $LEAK_{CI+CII}$, ETS_{CI+CII}, ETS_{CII}, and CIV were evaluated for each treatment group, as illustrated in Table 4. All respiratory data presented were normalized to wet weight.

Contrary to the brain, the RCR of $OXPHOS_{CI+CII}$ and $LEAK_{CI+CII}$ was increased ($P < 0.001$) at 6 h (Fig. 3A). In the 6-h group there was also a general trend toward lower rates of respiration in the septic mice for all respiration states, except $OXPHOS_{CI+CII}$ (e.g., $P = 0.054$ for $OXPHOS_{CI}$). LEAK state respiration also tended to be, differing to the brain, lower in septic mice ($P = 0.11$) at 6 h.

At 24 h the RCR of $OXPHOS_{CI+CII}$ and LEAK was also increased ($P < 0.05$), as shown in Figure 3B. The respiration associated with oxidative phosphorylation using CI ($OXPHOS_{CI}$) and CI+II substrates ($OXPHOS_{CI+CII}$) in liver from septic mice was dramatically increased compared with controls at 24 h (Table 4) ($P < 0.01$ and $P < 0.0001$ respectively). There was also an increased LEAK in the septic mice ($P < 0.001$) compared with control at 24 h (Table 4).

The maximal uncoupled ETS capacity (ETS_{CI+CII}) was comparable between control and septic mice at both time-points. When comparing the phosphorylating capacity as a ratio of maximal uncoupled ETS capacity ($OXPHOS_{CI+II}/ETS_{CI+II}$), at 6 h the septic mice exhibited a trend toward an increased ratio ($P = 0.072$) (Fig. 3C) and at 24 h the median ratio of the controls was 0.44, whereas the septic mice had a median ratio of 0.75 ($P < 0.001$) (Fig. 3D). The respiratory

TABLE 2. **Clinical characteristics at termination**

	6 h		24 h	
	Control (n = 8)	Sepsis (n = 7)	Control (n = 7)	Sepsis (n = 9)
Clinical score	0 (0–1)	2 (2–3)	0 (0)	3 (1–4)
Blood glucose	8.65 mmol/L (7.90–9.00)	9.30 mmol/L (6.80–10.2)	9.50 mmol/L (7.90–9.70)	5.30 mmol/L (4.15–5.65)
Temperature	36.8° (36.2–37.4)	31.7° (29.6–33.1)	37.6° (36.9–38.0)	30.8° (26.4–36.4)

Clinical score presented as median (range). Blood glucose and temperature presented as median (IQR).

TABLE 3. **Brain homogenates—mitochondrial respiration**

	6 h		24 h	
Respiratory parameters	Control (n = 8)	Sepsis (n = 7)	Control (n = 7)	Sepsis (n = 9)
$OXPHOS_{CI}$	87.74 ± 10.3	76.88 ± 15.1	95.61 ± 9.72	84.37 ± 13.0
$OXPHOS_{CI+CII}$	152.1 ± 10.9	147.6 ± 14.1	158.5 ± 9.81	150.7 ± 15.4
$LEAK_{CI+CII}$	24.64 ± 1.84	27.29 ± 2.56*	25.24 ± 1.67	26.40 ± 2.17
ETS_{CI+CII}	142.1 ± 12.0	143.6 ± 12.5	152.9 ± 9.80	144.7 ± 15.0
ETS_{CII}	74.83 ± 4.59	76.88 ± 7.39	75.20 ± 3.87	75.08 ± 6.49
CIV	240.6 ± 23.4	256.1 ± 22.5	246.1 ± 15.6	250.8 ± 25.1
$RCR_{OXPHOS\ CI}$	3.64 (3.12–3.74)	3.04 (2.25–3.42)*	3.57 (3.38–4.21)	3.04 (2.85–3.74)*
$RCR_{OXPHOS\ CI+II}$	6.16 (5.74–6.49)	5.66 (5.05–5.94)*	6.11 (5.90–6.60)	5.53 (5.29–6.21)
$OXPHOS_{CI+CII}/ETS_{CI+CII}$	1.06 (1.05–1.10)	1.03 (0.99–1.08)*	1.03 (1.01–1.06)	1.05 (1.02–1.06)

Values presented as mean ± SD. Ratios presented as median (IQR). OXPHOS respiration associated with ATP synthesis by oxidative phosphorylation, ETS respiration associated with maximal protonophore stimulated flux through the electron transport system, LEAK idle respiration without ATP-synthase activity, RCR indicates respiratory control ratio. CI, complex I, CII, complex II, CIV, complex IV. Statistical comparison to control at the same time-point.
* = $P < 0.05$.

capacity was thus to a lesser extent restricted by the phosphorylating capacity in the septic mice.

DISCUSSION

The present study indicates a diverse and tissue-specific mitochondrial respiratory response to sepsis-induced multiple organ failure. The brain tissue displayed a slightly impaired mitochondrial respiratory efficiency already at an early stage of sepsis, but the temporal dynamics of the brain mitochondrial function were diminutive. The most interesting finding is that there seems to be an activation of the phosphorylating capacity in the liver by the septic insult, most evidently, after 24 h. The maximal uncoupled ETS capacity was comparable between the two groups, whereas the insult dramatically increased the phosphorylating capacity in the septic mice. It is not the difference between the treatment groups in the same tissue that is the main finding, a difference that indeed is quite small with significant overlap in the data. The main finding is the fact that the tissues respond very differently to the septic insult. We therefore argue that the mitochondrial respiratory response in sepsis is clearly organ specific and that we need to move beyond a simplistic view of a mitochondrial dysfunction in sepsis when directing further preclinical research toward the clinical setting.

In this study, we chose to analyze homogenates instead of isolated mitochondria to reveal possible short acting factors affecting mitochondrial respiration. In isolated mitochondria it is also possible that defective mitochondria are, to a higher extent, removed in the isolation process and the process may also affect the structure and function of the mitochondria (19). A previous study of mitochondrial respiratory function in both brain and liver found that homogenates were comparable to that of isolated mitochondria (20). In brain homogenates formation of synaptosomes takes place. For substrate access to mitochondria trapped within synaptosomes digitonin was used to permeate the plasma membrane. However, it has been demonstrated that digitonin produces swelling and cytochrome c release in brain mitochondria (21). Therefore, careful titration of digitonin was conducted before setting the protocol to find the appropriate dose. Exogenously administered cytochrome c did not induce any significant effect on respiration with the digitonin dose used in the present study, indicating intact integrity of the outer mitochondrial membrane.

Brain and liver specifically were selected for both methodological and clinical purposes. Brain mitochondrial respiratory alterations have previously been shown in a rodent model using similar techniques and could therefore be used as a benchmark (14, 15). Furthermore, our group recently published that sepsis alters cerebral redox status (22). Both organs are also

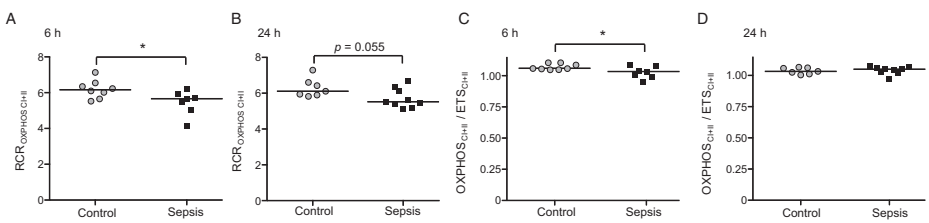

FIG. 1. **Brain mitochondrial function.** A, Brain: 6 h. The respiratory control ratio (RCR) at 6 h of $OXPHOS_{CI+II}/LEAK_{CI+CII}$ was significantly decreased ($P < 0.05$) in septic mice compared with controls. B, Brain: 24 h. At 24 h there was a similar trend that however did not reach significance ($P = 0.055$). $OXPHOS_{CI+II}$ was measured using the NADH-linked substrates malate, pyruvate, and glutamate as well as CII substrate succinate. $LEAK_{CI+II}$ respiration, i.e., mitochondrial respiration independent of ATP production, was induced by the ATP-synthase inhibitor oligomycin. C, Brain: 6 h. At 6 h the $OXPHOS_{CI+II}/ETS_{CI+II}$ ratio was significantly decreased, but both groups displayed ratios just above 1.0. D, Brain: 24 h. At 24 h there was no statistical difference in $OXPHOS_{CI+II}/ETS_{CI+II}$ ratio and likewise both groups displayed ratios just above 1.0, indicating that the respiratory capacity was not restricted by the phosphorylating capacity. The maximal uncoupled ETS capacity (ETS_{CI+CII}) was induced by FCCP titration. Line at median. *=$P < 0.05$.

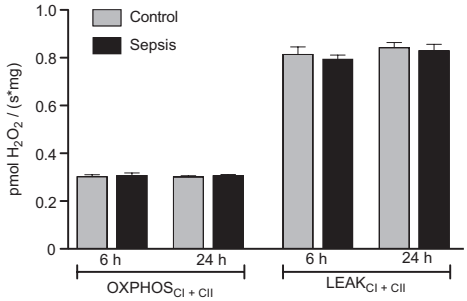

FIG. 2. **ROS production in brain homogenates.** Fluorescent measurement of ROS production using the Amplex Red assay. H_2O_2 levels measured in the presence of superoxide dismutase that ensures that all superoxide is converted into H_2O_2. Comparing ROS production under convergent CI + CII respiration and LEAK respiration state. Inhibiting ATP synthase increases ROS production dramatically as expected. No statistical significant differences between the groups. Data presented as pmol H_2O_2/(s*mg).

unquestionably of key relevance to MOF. Due to technical aspects of the Oroboros Oxygraph-2k, which is limited to only two chambers per machine, it is not possible to measure additional organs when using fresh tissue. Previous experience in our group, as well as pilots specifically for this project, has indicated that it is not feasible to store tissue for sequential analysis. Another advantage of analyzing brain and liver specifically, in contrast to most other tissues, is that almost identical methods and protocols for tissue preparation and analysis could be used, therefore decreasing the influence of confounding factors.

In a protocol with consecutive titrations the order of additions may affect the absolute values of the respiratory states obtained. However, by measuring these different respiratory states, it is possible to determine more specifically how and where the mitochondrial respiration is effected. The protocol used was designed to include evaluation of maximal OXPHOS and ETS capacities, and complex I, II, and IV function, as well as LEAK respiration.

The present data indicated that there was no difference in ROS production in the brain between the groups. A previous study indicated lower ROS production in brain from septic mice (14). Higher LEAK will most likely also mean a lower proton motive force, which could decrease ROS production. Strength in the present study is that ROS-production measurements were done simultaneously to the respiratory measurements in the same sample. ROS production was therefore also measured during respiration with electron flow through both CI and the convergent electron input through the Q-junction (CI + II).

Increased LEAK will be detrimental to ATP production and at a certain level the cell will no longer be able to uphold its energy demand. But perhaps increased LEAK respiration should not necessarily be viewed as a pathological mechanism but rather as an adaptive and protective metabolic response to conceivably decrease ROS production and increase heat production (23).

The increased phosphorylating capacity seen in the liver seems to be adaptive to the insult and is possibly caused by increased levels of catecholamines. A previous study showed that norepinephrine increased the activity of hepatic succinate dehydrogenase (24) and in another study epinephrine has been shown to enhance the activity of mitochondrial phosphorylation and ATP production, increasing oxygen consumption (25). There are, however, apparently conflicting data in the literature, using isolated swine liver mitochondria it has also been shown that catecholamines impair the efficiency of mitochondrial complex I respiration *in vitro* (26). Regardless of mechanism, the organ-specific response with increased oxidative phosphorylation in the liver is noteworthy and is also supported by previous research. In an equivalent study but with heart and liver mitochondria, in rats that responded to endotoxin, the heart mitochondria showed decreased oxidative activity, whereas the liver mitochondria showed increased oxidative phosphorylation compared with both non-responders and controls (27).

The two separate groups of controls of liver at 6 and 24 h, respectively, displayed some differences. All 6-h mice were consistently done at a different time during the day than the 24-hour mice, although the septic and control mice at each time point were performed at the same time during the day. The differences observed in the controls could be due to post-translational circadian and nocturnal metabolic changes.

TABLE 4. **Liver homogenates—mitochondrial respiration**

	6 h		24 h	
Respiratory parameters	Control (n = 8)	Sepsis (n = 7)	Control (n = 6)	Sepsis (n = 9)
$OXPHOS_{CI}$	65.13 ± 11.7	53.17 ± 9.90	36.93 ± 3.15	56.86 ± 12.2*
$OXPHOS_{CI+CII}$	157.6 ± 39.2	174.8 ± 17.1	112.6 ± 20.2	180.6 ± 21.4*
$LEAK_{CI+CII}$	40.45 ± 5.53	36.34 ± 3.30	28.04 ± 3.14	38.47 ± 5.46*
ETS_{CI+CII}	284.4 ± 21.6	264.1 ± 22.1	244.6 ± 13.3	249.8 ± 17.2
ETS_{CII}	251.7 ± 30.1	236.6 ± 9.41	228.2 ± 12.9	227.4 ± 15.4
CIV	390.0 ± 36.8	388.8 ± 34.7	359.5 ± 25.6	353.1 ± 34.5
$RCR_{OXPHOS\ CI}$	1.71 (1.32–1.85)	1.54 (1.41–1.68)	1.28 (1.20–1.43)	1.39 (1.24–1.76)
$RCR_{OXPHOS\ CI+II}$	4.17 (3.59–4.33)	4.76 (4.63–4.98)*	3.85 (3.62–4.62)	4.90 (4.25–5.12)*
$OXPHOS_{CI+CII}/ETS_{CI+CII}$	0.57 (0.47–0.64)	0.65 (0.63–0.72)	0.44 (0.41–0.50)	0.75 (0.68–0.78)*

Values presented as mean ± SD. Ratios presented as median (IQR). OXPHOS respiration associated with ATP synthesis by oxidative phosphorylation, ETS respiration associated with maximal protonophore-stimulated flux through the electron transport system, LEAK idle respiration without ATP-synthase activity, RCR indicates respiratory control ratio. CI, complex I, CII, complex II, CIV, complex IV. Statistical comparison to control at the same time-point.
* = $P < 0.05$.

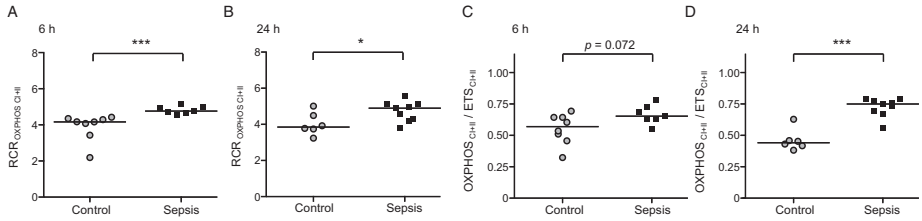

Fig. 3. **Liver mitochondrial function.** A, Liver: 6 h. The respiratory control ratio (RCR) at 6 h of $OXPHOS_{CI+II}/LEAK_{CI+CII}$ was significantly increased ($P < 0.001$) in septic mice compared with controls. B, Liver: 24 h. At 24 h there was likewise an increase compared with controls ($P < 0.05$). $OXPHOS_{CI+II}$ was measured using the NADH-linked substrates malate, pyruvate, and glutamate as well as CII substrate succinate. $LEAK_{CI+II}$ respiration, i.e., mitochondrial respiration independent of ATP production, was induced by the ATP-synthase inhibitor oligomycin. C, Liver: 6 h. At 6 h the $OXPHOS_{CI+II}/ETS_{CI+II}$ ratio displayed a trend toward increased phosphorylating capacity ($P = 0.072$). D, Liver: 24 h. At 24 h the $OXPHOS_{CI+II}/ETS_{CI+II}$ ratio was dramatically increased ($P < 0.001$) with a median of 0.75 in septic mice and 0.44 in the controls. The maximal uncoupled ETS capacity (ETS_{CI+CII}) was induced by FCCP titration. Line at median. $^{*}P < 0.05$. $^{***}P < 0.001$.

Changes in rodent mitochondrial respiratory function due to nocturnal changes have been known for a long time, in one study the rate of succinate oxidation in liver mitochondria from rats was 40% greater at night (28). One study indicated that the activity oscillations of succinic dehydrogenase showed a tendency to 24-h rhythmicity (29). In another study, they found that darkness induces a more efficient phosphorylation, as indicated by a higher ratio of ATP synthase/ATPase activity (30). Another pivotal study on circadian changes in metabolism revealed the influence of clock-driven acetylation on multiple mitochondrial proteins involved in metabolic pathways in both glycolysis and the citric acid cycle demonstrating how the circadian clock can regulate the metabolic state of the cell (31). One important finding of this study is that the circadian alterations seem to affect primarily the ATP synthase, as ETS capacity was similar, but not OXPHOS capacity. These alterations could perhaps be modulated by PGC-1β, as in one study using PGC-1β KO mice an altered expression in a number of nuclear-encoded genes governing mitochondrial and metabolic functions was detected in both brain and liver. The PGC-1β KO mice showed decreased activity during the dark cycle and also had altered thermoregulation and developed abnormal hypothermia when exposed to cold compared with wild type, perhaps because of an inability to increase uncoupling. Interestingly when involuntary subjected to exercise on a treadmill they showed equivalent endurance (32). The animals in this study had *ad libitum* access to food and water, which could also have implications for liver mitochondrial function (33). These changes are perhaps not surprising as the liver plays an important role as a metabolic pacemaker, changing full body metabolism back and forth, from anabolic to catabolic states in an oscillatory manner. For these reasons we chose to only compare the data to each respective control.

The cecal ligation and puncture (CLP) method to induce sepsis in rodents is widely used and is considered to be the gold standard, corresponding to a bowel perforation with a subsequent peritonitis and polymicrobial sepsis. Small alterations in needle size, number of punctures, etc., will drastically change mortality rates. The precise procedure used was chosen to avoid unwanted selection between the groups due to mortality, but still ensuring that the animals would also be severely affected at the 24-h endpoint (16,34). The effects of anesthetics are a major concern of mitochondrial research as studies have shown interference with mitochondrial function (35). For ethical and practical reasons anesthetics must be used for the CLP procedure. In the present study, continuous gas anesthesia using isoflurane was chosen. Also isoflurane may interfere with mitochondrial respiration by, for example, opening the mitochondrial permeability transition pore (mPTP) (36). This is one of the reasons why it was important to use separate controls for each time point as the effects of isoflurane could possibly be short acting.

Care needs to be taken when extrapolating the findings of altered respiratory function in this mouse model to humans in a clinical setting. Mice do not respond to infection with a rise in temperature but with a decreased body temperature. Septic mice, in general, had higher LEAK than controls and this could be an adaptive response to low body temperature, with an up regulation of uncoupling proteins to produce more heat. Therefore, interpreting the data related to uncoupling (LEAK) and the hypothermic response is challenging. For obvious reasons obtaining brain and liver samples from septic patients is not feasible. But, nonetheless, animal models can indeed only complement human data and the present data need to be viewed in the context of previous human data.

Concerning the controversy regarding O_2 delivery in MOF, the present study does not resolve this issue. Preferably venous O_2 saturation and lactate, for example, should have been measured to provide basic information related to oxygen delivery. The lack of these data, including other functional parameters, is a limitation. However, one can also argue that this type of data would not be sufficient to fully answer a question related to O_2 delivery. Venous O_2 saturation and lactate does not necessarily reflect the tissue oxygenation and microcirculation of the organs. An increase in lactate could reflect a mitochondrial inhibition and an increased anaerobic glycolysis.

The theory one embraces regarding mitochondrial respiration in sepsis will have implications on which strategy one should pursue for pharmaceutical development. As indicated by the results in this study, the target needs to be organ specific. One strategy could be to find methods to support and restore function by optimized and specific substrate supply and

essentially increasing respiration and the phosphorylating capacity (37). Another strategy could be to help protect the mitochondria and a possible adaptive metabolic change during the insult. Sepsis is a dynamic process and perhaps a combination of strategies is best suited during the initial development and hopefully later recovery from sepsis. Nonetheless, the mitochondria seem to be affected and therefore might be a suitable pharmaceutical target for the treatment of sepsis.

In conclusion, the present study suggests a diverse and tissue-specific mitochondrial respiratory response to sepsis-induced multiple organ failure. The brain displayed an early impaired mitochondrial respiratory efficiency. Interestingly, as a possible response to an increased metabolic demand, the liver increased the phosphorylating capacity as a response to the septic insult. The liver also displayed increased uncoupling of oxidative phosphorylation at 24 h.

ACKNOWLEDGMENTS

The authors thank Eleonor Åsander Frostner for administrative support.

REFERENCES

1. Boekstegers P, Weidenhofer S, Pilz G, Werdan K: Peripheral oxygen availability within skeletal muscle in sepsis and septic shock: comparison to limited infection and cardiogenic shock. *Infection* 19(5):317–323, 1991.
2. Rosser DM, Stidwill RP, Jacobson D, Singer M: Oxygen tension in the bladder epithelium rises in both high and low cardiac output endotoxemic sepsis. *J Appl Physiol* 79(6):1878–1882, 1995.
3. Hotchkiss RS, Swanson PE, Freeman BD, Tinsley KW, Cobb JP, Matuschak GM, Buchman TG, Karl IE: Apoptotic cell death in patients with sepsis, shock, and multiple organ dysfunction. *Crit Care Med* 27(7):1230–1251, 1999.
4. Abraham E, Singer M: Mechanisms of sepsis-induced organ dysfunction. *Crit Care Med* 35(10):2408–2416, 2007.
5. Fink MP: Bench-to-bedside review: cytopathic hypoxia. *Crit Care* 6(6):491–499, 2002.
6. Kozlov AV, van Griensven M, Haindl S, Kehrer I, Duvigneau JC, Hartl RT, Ebel T, Jafarmadar M, Calzia E, Gnaiger E, et al.: Peritoneal inflammation in pigs is associated with early mitochondrial dysfunction in liver and kidney. *Inflammation* 33(5):295–305, 2010.
7. Crouser ED: Mitochondrial dysfunction in septic shock and multiple organ dysfunction syndrome. *Mitochondrion* 4(5–6):729–741, 2004.
8. Brealey D, Karyampudi S, Jacques TS, Novelli M, Stidwill R, Taylor V, Smolenski RT, Singer M: Mitochondrial dysfunction in a long-term rodent model of sepsis and organ failure. *Am J Physiol Regul Integr Comp Physiol* 286(3):R491–R497, 2004.
9. Brealey D, Brand M, Hargreaves I, Heales S, Land J, Smolenski R, Davies NA, Cooper CE, Singer M: Association between mitochondrial dysfunction and severity and outcome of septic shock. *Lancet* 360(9328):219–223, 2002.
10. Porta F, Takala J, Weikert C, Bracht H, Kolarova A, Lauterburg BH, Borotto E, Jakob SM: Effects of prolonged endotoxemia on liver, skeletal muscle and kidney mitochondrial function. *Crit Care* 10(4):R118, 2006.
11. Crouser ED, Julian MW, Blaho DV, Pfeiffer DR: Endotoxin-induced mitochondrial damage correlates with impaired respiratory activity. *Crit Care Med* 30(2):276–284, 2002.
12. Taylor DE, Kantrow SP, Piantadosi CA: Mitochondrial respiration after sepsis and prolonged hypoxia. *Am J Physiol* 275(1 Pt 1):L139–L144, 1998.
13. Sjovall F, Morota S, Hansson MJ, Friberg H, Gnaiger E, Elmer E: Temporal increase of platelet mitochondrial respiration is negatively associated with clinical outcome in patients with sepsis. *Crit Care* 14(6):R214, 2010.
14. d'Avila JC, Santiago AP, Amancio RT, Galina A, Oliveira MF, Bozza FA: Sepsis induces brain mitochondrial dysfunction. *Crit Care Med* 36(6):1925–1932, 2008.
15. Bozza FA, D'Avila JC, Ritter C, Sonneville R, Sharshar T, Dal-Pizzol F: Bioenergetics, mitochondrial dysfunction, and oxidative stress in the pathophysiology of septic encephalopathy. *Shock* 39(7 Suppl 1):10–16, 2013.
16. Rittirsch D, Huber-Lang MS, Flierl MA, Ward PA: Immunodesign of experimental sepsis by cecal ligation and puncture. *Nat Protoc* 4(1):31–36, 2009.
17. Karlsson M, Hempel C, Sjovall F, Hansson MJ, Kurtzhals JA, Elmer E: Brain mitochondrial function in a murine model of cerebral malaria and the therapeutic effects of rhEPO. *Int J Biochem Cell Biol* 45(1):151–155, 2013.
18. Larsen S, Nielsen J, Hansen CN, Nielsen LB, Wibrand F, Stride N, Schroder HD, Boushel R, Helge JW, Dela F, Hey-Mogensen M: Biomarkers of mitochondrial content in skeletal muscle of healthy young human subjects. *J Physiol* 590(Pt 14):3349–3360, 2012.
19. Picard M, Taivassalo T, Ritchie D, Wright KJ, Thomas MM, Romestaing C, Hepple RT: Mitochondrial structure and function are disrupted by standard isolation methods. *PLoS One* 6(3):e18317, 2011.
20. Pecinova A, Drahota Z, Nuskova H, Pecina P, Houstek J: Evaluation of basic mitochondrial functions using rat tissue homogenates. *Mitochondrion* 11(5):722–728, 2011.
21. Sims NR, Finegan JM, Blass JP: Effects of postdecapitative ischemia on mitochondrial respiration in brain tissue homogenates. *J Neurochem* 47(2):506–511, 1986.
22. Hara N, Chijiiwa M, Yara M, Ishida Y, Ogiwara Y, Inazu M, Kuroda M, Karlsson M, Sjovall F, Elmer E, et al.: Metabolomic analyses of brain tissue in sepsis induced by cecal ligation reveal specific redox alterations-protective effects of the oxygen radical scavenger edaravone. *Shock* 44:578–584, 2015.
23. Singer M, De Santis V, Vitale D, Jeffcoate W: Multiorgan failure is an adaptive, endocrine-mediated, metabolic response to overwhelming systemic inflammation. *Lancet* 364(9433):545–548, 2004.
24. Sivaramakrishnan S, Ramasarma T: Noradrenaline stimulates succinate dehydrogenase through beta-adrenergic receptors. *Indian J Biochem Biophys* 20(1):16–22, 1983.
25. Ainscow EK, Brand MD: The responses of rat hepatocytes to glucagon and adrenaline. Application of quantified elasticity analysis. *Eur J Biochem/FEBS* 265(3):1043–1055, 1999.
26. Porta F, Bracht H, Weikert C, Beck M, Takala J, Brandt S, Hiltebrand LB, Jakob SM: Effects of endotoxin and catecholamines on hepatic mitochondrial respiration. *Inflammation* 32(5):315–321, 2009.
27. Kozlov AV, Staniek K, Haindl S, Piskernik C, Ohlinger W, Gille L, Nohl H, Bahrami S, Redl H: Different effects of endotoxic shock on the respiratory function of liver and heart mitochondria in rats. *Am J Physiol Gastrointest Liver Physiol* 290(3):G543–G549, 2006.
28. Glick JL, Cohen WD: Nocturnal changes in oxidative activities of rat liver mitochondria. *Science* 143(3611):1184–1185, 1964.
29. Wielgus-Serafinska E, Plewka A, Kaminski M: Circadian variation of mitochondrial succinic dehydrogenase and microsomal cytochrome P-450 dependent monooxygenase activity in the liver of sexually immature and mature rats. *J Physiol Pharmacol* 44(1):55–63, 1993.
30. Ramirez-Iniguez AL, Ortiz GG, El Hafidi M, Rincon-Sanchez AR, Macias-Rodriguez E, Pacheco-Moises FP: Acute treatment of constant darkness increases the efficiency of ATP synthase in rat liver mitochondria. *Ann Hepatol* 8(4):371–376, 2009.
31. Masri S, Patel VR, Eckel-Mahan KL, Peleg S, Forne I, Ladurner AG, Baldi P, Imhof A, Sassone-Corsi P: Circadian acetylome reveals regulation of mitochondrial metabolic pathways. *Proc Natl Acad Sci U S A* 110(9):3339–3344, 2013.
32. Sonoda J, Mehl IR, Chong LW, Nofsinger RR, Evans RM: PGC-1beta controls mitochondrial metabolism to modulate circadian activity, adaptive thermogenesis, and hepatic steatosis. *Proc Natl Acad Sci U S A* 104(12):5223–5228, 2007.
33. Diaz-Munoz M, Vazquez-Martinez O, Aguilar-Roblero R, Escobar C: Anticipatory changes in liver metabolism and entrainment of insulin, glucagon, and corticosterone in food-restricted rats. *Am J Physiol Regul Integr Comp Physiol* 279(6):R2048–R2056, 2000.
34. Otero-Anton E, Gonzalez-Quintela A, Lopez-Soto A, Lopez-Ben S, Llovo J, Perez LF: Cecal ligation and puncture as a model of sepsis in the rat: influence of the puncture size on mortality, bacteremia, endotoxemia and tumor necrosis factor alpha levels. *Eur Surg Res* 33(2):77–79, 2001.
35. Vilela SM, Santos DJ, Felix L, Almeida JM, Antunes L, Peixoto F: Are fentanyl and remifentanil safe opioids for rat brain mitochondrial bioenergetics? *Mitochondrion* 9(4):247–253, 2009.
36. Zhang Y, Xie Z: Anesthetics isoflurane and desflurane differently affect mitochondrial function, learning, and memory. *Ann Neurol* 72(4):630, 2012.
37. Protti A, Carre J, Frost MT, Taylor V, Stidwill R, Rudiger A, Singer M: Succinate recovers mitochondrial oxygen consumption in septic rat skeletal muscle. *Crit Care Med* 35(9):2150–2155, 2007.

Paper II

Experimental Neurology 271 (2015) 136–144

Contents lists available at ScienceDirect

Experimental Neurology

journal homepage: www.elsevier.com/locate/yexnr

Regular Article

Mitochondrial bioenergetic alterations after focal traumatic brain injury in the immature brain☆

Todd J. Kilbaugh [a,*,1], Michael Karlsson [b,2], Melissa Byro [c,3], Ashley Bebee [c,3], Jill Ralston [c,3], Sarah Sullivan [c,3], Ann-Christine Duhaime [d,4], Magnus J. Hansson [b,2], Eskil Elmér [b,2], Susan S. Margulies [c,3]

[a] Perelman School of Medicine at the University of Pennsylvania, Anesthesiology and Critical Care Medicine, Children's Hospital of Philadelphia, 34th & Civic Center Blvd., Philadelphia, PA 19104, USA
[b] Mitochondrial Medicine, Department of Clinical Sciences, Lund University, BMC A13, SE-221 84 Lund, Sweden
[c] Department of Bioengineering, University of Pennsylvania, 210 South 33rd Street, Philadelphia, PA 19104, USA
[d] Department of Neurosurgery, Massachusetts General Hospital, 15 Parkman Street, Boston, MA 02114, USA

ARTICLE INFO

Article history:
Received 13 January 2015
Received in revised form 12 May 2015
Accepted 13 May 2015
Available online 28 May 2015

Keywords:
Pediatric traumatic brain injury
Mitochondria
Axonal injury
Bioenergetics
Contusion
Swine

ABSTRACT

Traumatic brain injury (TBI) is one of the leading causes of death in children worldwide. Emerging evidence suggests that alterations in mitochondrial function are critical components of secondary injury cascade initiated by TBI that propogates neurodegeneration and limits neuroregeneration. Unfortunately, there is very little known about the cerebral mitochondrial bioenergetic response from the immature brain triggered by traumatic biomechanical forces. Therefore, the objective of this study was to perform a detailed evaluation of mitochondrial bioenergetics using high-resolution respirometry in a high-fidelity large animal model of focal controlled cortical impact injury (CCI) 24 h post-injury. This novel approach is directed at analyzing dysfunction in electron transport, ADP phosphorylation and leak respiration to provide insight into potential mechanisms and possible interventions for mitochondrial dysfunction in the immature brain in focal TBI by delineating targets within the electron transport system (ETS). Development and application of these methodologies have several advantages, and adds to the interpretation of previously reported techniques, by having the added benefit that any toxins or neurometabolites present in the ex-vivo samples are not removed during the mitochondrial isolation process, and simulates the in situ tricarboxylic acid (TCA) cycle by maximizing key substrates for convergent flow of electrons through both complexes I and II. To investigate alterations in mitochondrial function after CCI, ipsilateral tissue near the focal impact site and tissue from the corresponding contralateral side were examined. Respiration per mg of tissue was also related to citrate synthase activity (CS) and calculated flux control ratios (FCR), as an attempt to control for variability in mitochondrial content. Our biochemical analysis of complex interdependent pathways of electron flow through the electron transport system, by most measures, reveals a bilateral decrease in complex I-driven respiration and an increase in complex II-driven respiration 24 h after focal TBI. These alterations in convergent electron flow though both complex I and II-driven respiration resulted in significantly lower maximal coupled and uncoupled respiration in the ipsilateral tissue compared to the contralateral side, for all measures. Surprisingly, increases in complex II and complex IV activities were most pronounced in the contralateral side of the brain from the focal injury, and where oxidative phosphorylation was increased significantly compared to sham values. We conclude that 24 h after focal TBI in the immature brain, there are significant alterations in cerebral mitochondrial bioenergetics, with pronounced increases in complex II and complex IV respiration in the contralateral hemisphere. These alterations in mitochondrial bioenergetics present multiple targets for therapeutic intervention to limit secondary brain injury and support recovery.

☆ Funding information: NIH/NINDS grants: R01NS039679 and U01NS069545.

* Corresponding author.
E-mail addresses: kilbaugh@chop.edu (T.J. Kilbaugh), michael.karlsson@med.lu.se (M. Karlsson), melissa.byro@gmail.com (M. Byro), ashley.n.durban@gmail.com (A. Bebee), ralstonjm@gmail.com (J. Ralston), sarahsul@seas.upenn.edu (S. Sullivan), aduhaime@partners.org (A.-C. Duhaime), magnus.hansson@med.lu.se (M.J. Hansson), eskil.elmer@med.lu.se (E. Elmér), margulie@seas.upenn.edu (S.S. Margulies).
[1] 34th & Civic Center Blvd, Philadelphia, PA 19104, USA.
[2] Mitochondrial Medicine, Department of Clinical Sciences, Lund University, BMC A13, SE-22184 Lund, Sweden.
[3] 240 Skirkanich Hall, 210 South 33rd Street, Philadelphia, PA 19104-6321, USA.
[4] 15 Parkman Street, Boston, MA 02114-3117, USA.

http://dx.doi.org/10.1016/j.expneurol.2015.05.009
0014-4886/

1. Introduction

Estimates predict that traumatic brain injury (TBI) will become the third leading cause of death and disability in the world by 2020 (Gean and Fischbein, 2010). In the United States the Center for Disease Control (CDC) estimates nearly 500,000 emergency department visits annually for TBI in children aged 0–14 years (Faul et al., 2010). In addition, children under the age of four have the highest rate of TBI-related emergency department visits, with over 1200 per 100,000 children (Langlois et al., 2005). These staggering numbers contribute to a childhood mortality rate of approximately 33 per 100,000 children in the United States, making TBI a leading cause of death in children (Coronado et al., 2011).

TBI is a heterogeneous insult to the brain induced by traumatic biomechanical forces. TBI precipitates a complex, secondary pathophysiological process which can result in a cascade of deleterious side effects often far from the site of the initial injury, and which places tissue that survives the initial insult at risk for functional failure, neurodegeneration, apoptosis, and death (Hattori et al., 2003; Marcoux et al., 2008b; Ragan et al., 2013; Xu et al., 2010). A growing body of literature suggests that a main component of this secondary injury cascade is altered mitochondrial bioenergetics and cerebral metabolic crisis (Gilmer et al., 2009; Robertson et al., 2006). Mitochondria play a pivotal role in cerebral metabolism and regulation of oxidative stress, excitotoxicity, and apoptosis (Balan et al., 2013; Gilmer et al., 2009; Lifshitz et al., 2003; Robertson, 2004). Cerebral metabolic crisis displays regional heterogeneity, varies temporally post-injury and with gradation of injury severity, and is often sustained for a prolonged period of time (Lifshitz et al., 2003; Marcoux et al., 2008b; Ragan et al., 2013; Robertson et al., 2006, 2009; Saito et al., 2005). Unfortunately, despite evidence that such processes may vary significantly with maturation, response to cerebral metabolic and mitochondrial alterations following TBI in the immature brain is not well defined (Kilbaugh et al., 2011). Adult TBI data is difficult to extrapolate to pediatric models because critical mitochondrial characteristics are very different between young and adult animals. Differences include the number and density of complexes of the electron transfer chain, antioxidant enzyme activity and content, and lipid content (Bates et al., 1994; Del Maestro and McDonald, 1987). The immature brain's response to each type of TBI appears to change rapidly during development from infancy through adolescence (Armstead and Kurth, 1994; Duhaime et al., 2000b; Durham and Duhaime, 2007; Raghupathi and Margulies, 2002). These unique features of the developing brain make it imperative to understand the mechanisms associated with bioenergetic failure and cell death cascades following TBI in the immature brain in order to develop age-specific and injury-specific mitochondrial-directed neuroprotective and neuro-resuscitative approaches.

Previously we reported differences in the regional mitochondrial responses in infant rodent focal injury (Kilbaugh et al., 2011). Here we investigate the regional mitochondrial functional responses of a porcine model of focal cortical impact TBI in toddler-aged animals. We determined mitochondrial bioenergetics in tissue from peri-contusional and contralateral region to focal injury, by performing in-depth assessments of respiratory capacity of electron transport system (ETS) complexes utilizing high-resolution respirometry (HRR) in ex-vivo tissue homogenates obtained 24 h post-injury to analyze and pursue mechanistic insight of the bioenergetic response to TBI.

2. Materials and methods

All procedures were approved by the Institutional Animal Care and Use Committee of the University of Pennsylvania. Female, 4-week-old piglets (8–10 kg), which have comparable neurodevelopment to a human toddler, were used for the study (Armstead, 2005; Duhaime, 2006). Females were chosen to limit heterogeneity between genders based on prior work (Missios et al., 2009). Sixteen piglets were designated into a injury cohort and corresponding sham group: controlled cortical impact (CCI) at the rostal gyrus (n = 10 injured-CCI, n = 6 naïve shams-CCI). Injured animals were sacrificed 24 h after CCI.

2.1. Animal preparation

Piglets were premedicated with an intramuscular injection of ketamine (20 mg/kg) and xylazine (2 mg/kg) followed by 4% inhaled isoflurane in 1.0 fraction of inspired oxygen via snout mask, until abolishment of response to a reflexive pinch stimulus. Endotracheal intubation was followed by a decrease in fraction of inspired oxygen to 0.21 and maintenance of anesthesia with 1% inhaled isoflurane. Buprenorphine (0.02 mg/kg) was delivered intramuscularly for analgesia prior to injury. Using a heating pad, core body temperature was kept constant between 36 and 38 °C and monitored via a rectal probe. Non-invasive blood pressure, oxygen saturation, heart rate, respiratory rate, and end-tidal CO_2 were continuously monitored throughout the experiment (VetCap model 2050081; SDI, Waukesha, WI). If necessary, mechanical ventilation was utilized to maintain normoxia and normocarbia before injury, otherwise piglets maintained spontaneous ventilation.

2.2. Controlled cortical impact (CCI) injury

While maintained on isoflurane, the vertex of the head was clipped and prepped with chlorhexidine solution. After infiltration of a local anesthetic (1% lidocaine with epinephrine 1/100,000), the right coronal suture was exposed, and a craniectomy performed over the rostral gyrus allowing a 1 cm margin around the indenter tip of the cortical impact device described previously (Duhaime et al., 2000a). The exposed dura was opened in a stellate fashion to reveal the cortical surface, and the device was stabilized against the skull with screws. The spring-loaded tip rapidly (4 ms) indented to a depth of 0.7 cm of the cortical rostral gyrus (Duhaime et al., 2000a). The device was removed, the dura re-approximated, and the surgical flap sutured closed. After emergence from isoflurane, piglets were extubated when they met the following criteria: return of pinch reflex, spontaneously breathing and able to maintain oxygenation and ventilation, normotensive, and stable heart and respiratory rate. Following extubation, animals displayed initial depressed activity and gait instability, but apnea and hypotension were never observed after CCI. Animals were recovered and returned to the animal housing facility when they met the following criteria: vocalization without squealing, able to ambulate, devoid of aggression or avoidance behavior, absence of piloerection, and proper feeding and drinking behaviors. Animals were more hypoactive and spent more time recumbent than non-injured littermates following injury, but were able to drink and eat unassisted. These injuries are best described as mild-to-moderate in severity, based on parallels with human clinical severity classifications (Adelson et al., 2012; Miller et al., 2012).

2.3. Sample acquisition for mitochondrial assessments

At 24 h post-TBI, animals were re-anesthetized with 1% isoflurane. A bilateral craniectomy was performed to expose the brain, tissue was rapidly extracted from two locations of interest from the injury cohort and shams while simultaneously receiving a pentobarbital overdose. Locations of interest, included: a 2 cm^2 region of cortex of visibly viable tissue was resected immediately adjacent to the rostral edge of the contusion, along with a mirrored corresponding 2 cm^2 region from the contralateral hemisphere. Tissue was removed within seconds, and placed in ice-cold isolation buffer (320 mM sucrose, 10 mM Trizma base, and 2 mM EGTA), where the blood and blood vessels, as well as, any adherent necrotic tissue from the contused area were dissected and disposed. In addition, subcortical white matter was removed from the cortex. Following dissection tissue was placed on drying paper to

absorb excess buffer and weighed. Tissue was then gently homogenized on ice in MiR05 (110 mM sucrose, 0.5 mM EGTA, 3.0 mM $MgCl_2$, 60 mM K-lactobionate, 10 mM KH_2PO_4, 20 mM taurine, 20 mM HEPES and 1.0 g/l fatty acid-free BSA) using a 5 ml Potter–Elvehjem teflon-glass homogenizer to a concentration of 1 mg wet weight tissue/10 μl MiR05 buffer.

2.4. Mitochondrial high-resolution respirometry (HRR)

A final concentration of tissue homogenate with MiR05 analyzed was 1 mg/ml at a constant 37 °C, and the rate of oxygen consumption was measured utilizing a high-resolution oxygraph and expressed in pmols / [s ∗ mg of tissue homogenate], (OROBOROS, Oxygraph-2 k and DatLab software all from OROBOROS Instruments, Innsbruck, Austria). All experiments were performed between 75 and 220 μM of oxygen, and re-oxygenation was performed routinely prior to addition of the complex IV electron donor described below. The oxygraph was calibrated daily, and oxygen concentration was automatically calculated from barometric pressure and MiR05 oxygen solubility factor set at 0.92 relative to pure water.

A substrate, uncoupler, inhibitor titration (SUIT) protocol previously used for rodent brain tissue (Karlsson et al., 2013) was further developed and optimized in preliminary studies in porcine brain tissue. Sequential additions were used to acquire a detailed representation of mitochondrial respiration (Figs. 1a and b). Respiratory capacities with electron flow through both complex I (CI) and complex II (CII) were evaluated separately as well as the convergent electron input through the Q-junction (CI + II) using succinate and nicotinamide adenine dinucleotide (NADH)-linked substrates (Gnaiger, 2009). Plasma membranes were permeabilized with the detergent digitonin to allow non-

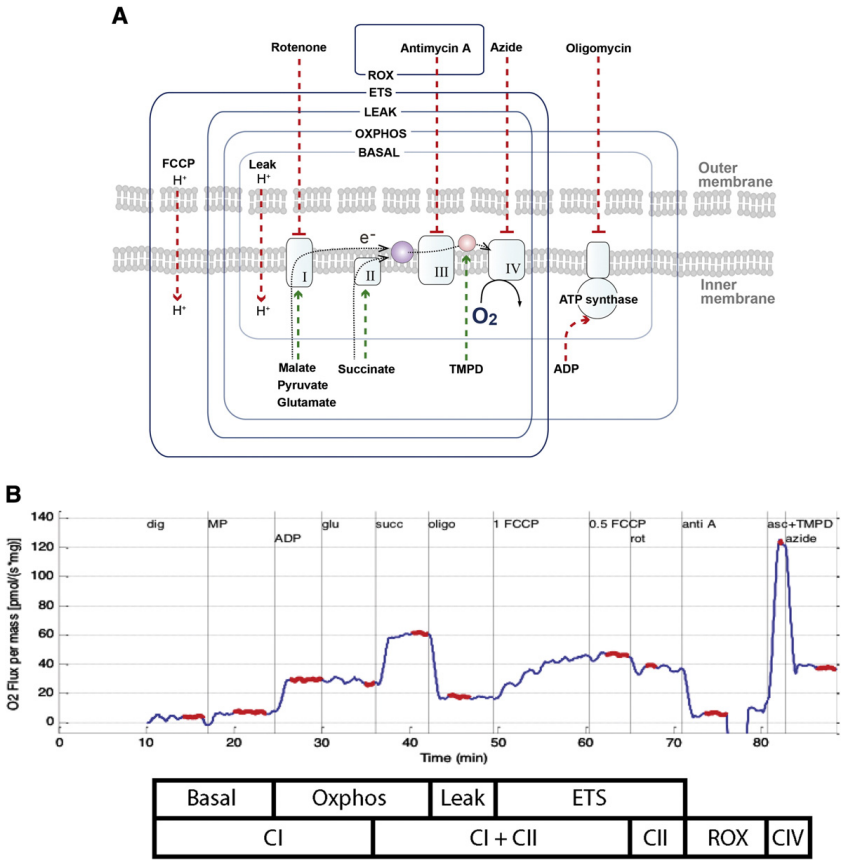

Fig. 1. Graphical representation of the substrate, uncoupler, inhibitor titration (SUIT) protocol used to study the integrated function of individual components of the electron transport system (ETS). Induced respiratory states and respiratory complexes activated are outlined by boxes: ROX, residual oxygen consumption due to non-mitochondrial respiration induced by the inhibition of the complex III by antimycin A; ETS ($ETS_{CI + CII}$), respiration that is uncoupled capacity from ATP synthase induced by the optimum titration of the protonophore FCCP; LEAK ($LEAK_{CI + CII}$), State 4_o, is the resting non-phosphorylating electron transfer across the mitochondrial inner membrane due to uncoupling of ATP synthase by Olgiomycin; OXPHOS ($OXPHOS_{CI + CII}$) coupled capacity of oxidative phosphorylation measure convergent respiration of both complex I (Malate, Pyruvate, Glutamate) and II (Succinate) substrates. The SUIT protocol employed in these experiments also utilized the complex I inhibitor, Rotenone, to measure individual complex II-driven respiration (ETS_{CII}) separately from complex I. In addition, TMPD/ascorbate and azide were administered to measure complex IV respiration.

membrane permeable substrates and ADP access to the subpopulations of mitochondria trapped within synaptosomes. Furthermore, in order to achieve similar results in brain tissue homogenates and isolated brain mitochondria, with a combination of both sub-populations, Pecinova and colleagues demonstrated that digitonin is necessary in brain homogenate preparations (Pecinova et al., 2011; Sims and Blass, 1986). Without the addition of digitonin oxidative phosphorylation capacity would likely be greatly underestimated. Thus, in preliminary experiments a careful digitonin dose titration was completed, in the presence of exogenously administered cytochrome c, which did not induce any significant effect on respiration with the digitonin dose used in the present study, indicating intact integrity of the outer mitochondrial membrane (data not shown). Routine mitochondrial respiration was established by the concomitant addition of malate (5 mM) and pyruvate (5 mM), followed by ADP (1 mM) and glutamate (5 mM), to measure the oxidative phosphorylation capacity of complex I ($OXPHOS_{CI}$), driven by the NADH-related substrates. Sequential additions followed. Succinate (10 mM) was added to stimulate maximal phosphorylating respiration capacity via convergent input through complexes I and II ($OXPHOS_{CI + CII}$). Oligomycin, an inhibitor of ATP-synthase, induced mitochondrial respiration independent of ATP production across the inner mitochondrial membrane, commonly referred to as LEAK respiration ($LEAK_{CI + CII}$) or State 4_0. Maximal convergent non-phosphorylating respiration of the electron transport system ($ETS_{CI + CII}$) was evaluated by titrating the protonophore, carbonyl cyanide p-(trifluoromethoxy) phenylhydrazone (FCCP) until no further increase in respiration was detected. Rotenone inhibited complex I-driven respiration and revealed complex II-driven respiration, the ETS capacity through complex II alone (ETS_{CII}). The complex III inhibitor antimycin-A (1 μg/ml) was added to measure the residual oxygen consumption (ROX) that is independent of the ETS. Therefore, residual value measured with antimycin-A was subtracted from each of the measured respiratory states to report ETS function devoid of ROX. Antimycin-A was chosen to measure ROX, so that in this sequential protocol, complex IV activity could also be measured at the end of the protocol. Finally, complex IV activity was determined by the addition of ascorbate (ASC, 0.8 mM) and N,N,N′,N′-tetramethyl-p-phenylenediamine (TMPD, 0.5 mM), an electron donor to complex IV. Due to the high level of auto-oxidation of TMPD, the complex IV-inhibitor sodium azide (10 mM) was added and the remaining chemical background was subtracted from the ascorbate/TMPD-induced oxygen consumption to assess complex IV activity. Integrated ETS analysis with internal normalization was generated using flux control ratios (FCR) calculated by dividing each respiratory state by the maximal, uncoupled mitochondrial respiration ($ETS_{CI + CII}$).

2.5. Citrate synthase activity

Upon completion of the HRR measurements, chamber contents were frozen for subsequent citrate synthase (CS) activity quantification. CS (μmol/mL/min) was used as a marker of brain metabolism secondary to its location within the mitochondrial matrix and importance as the first step of the tricarboxylic acid cycle (TCA). In addition, CS is used by some investigators, as a surrogate measure of mitochondrial content per mg of tissue (Bowling et al., 1993; Larsen et al., 2012). Later, samples were thawed, and a commercially available kit (Citrate Synthase Assay Kit, CS0720, Sigma) was used according to the manufacturer's instructions to determine the CS activity.

2.6. Data analysis

The oxygen flux traces were analyzed with a customized Matlab (Mathworks, Natick, MA) program designed to extract the oxygen flux plateau at each phase of the SUIT protocol (Fig. 1b), with the exception of TMPD/ASC, when the peak oxygen flux was extracted. "Side" for focal CCI was defined as ipsilateral and contralateral to the site of injury. Statistical evaluation was performed using JMP Pro (SAS Institute Inc., version 10.0, Cary, NC, USA). We compared tissue mitochondrial respiration between injured and sham subjects with an unpaired, non-parametric Wilcoxon ranked sum test with Dunn's multiple comparison test. A paired Wilcoxon ranked sum test was used to compare sides within sham and injury groups. Differences were considered significant where $p < 0.05$. All results are reported as mean ± standard error of the mean (SEM).

3. Results

3.1. Controlled cortical impact injury (CCI)

We measured CS activity per mg of tissue and found no differences between sides of the brain in the sham animals (Fig. 2). Following focal CCI injury, the ipsilateral peri-contusional side exhibited a significant reduction in CS activity, nearly 50%, compared to both ipsilateral CS activity in sham animals and contralateral tissue in injured animals.

HRR was performed on ex-vivo tissue homogenates (pmols O_2 / s * mg of tissue homogenate) in sham CCI animals to determine cerebral mitochondrial respiration. Analysis revealed no statistical difference in respiration between sides in sham animals for all measures of mitochondrial respiration ($OXPHOS_{CI}$, ETS_{CII}, $OXPHOS_{CI + CII}$, $ETS_{CI + CII}$, $LEAK_{CI + CII}$, and complex IV) (Table 1). The overall direction of the response of individual respiratory states following CCI, reported as, per mg of tissue, FCR, and CS are depicted in Table 2.

After CCI, complex I-driven respiration ($OXPHOS_{CI}$) was significantly decreased bilaterally per mg of tissue when compared to corresponding shams (Table 1). These reductions for $OXPHOS_{CI}$ remained significant when compared to maximal ETS capacity: FCR (Fig. 3A). When compared to CS (pmols O_2 / s * mg * CS), there was still a statistical trend for a decrease in $OXPHOS_{CI}$ respiration in ipsilateral tissue ($p < 0.09$); however, when compared to sham the contralateral side following CCI displayed no difference ($p = 0.55$) (Table 1).

In contrast to complex I-driven respiration, complex II-driven respiration (ETS_{CII}) per mg of tissue in the ipsilateral side was maintained at sham levels 24 h post-CCI, while the contralateral brain post-CCI was significantly increased compared to sham ($p < 0.02$) and the ipsilateral brain after injury ($p < 0.03$) (Table 1). ETS_{CII} FCR was significantly increased in both sides of the injured brain compared to corresponding shams (Fig. 3A). This bilateral increase in ETS_{CII} respiration remained significant when respiration was normalized to CS (Table 1).

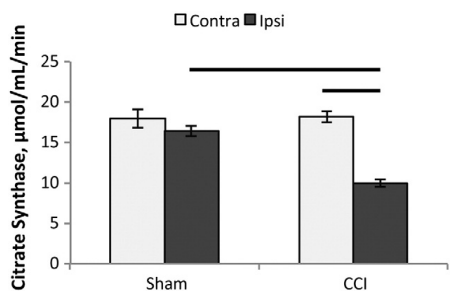

Fig. 2. Citrate synthase activity. Citrate synthase (CS) activity per mg of tissue 24 h after controlled cortical impact (CCI). There were no differences between sides of the brain in the sham animals, ($p = 0.99$). Following focal CCI injury, there was a nearly 50% reduction in CS activity in the ipsilateral peri-contusional side (9.9 ± 0.7 μmol/mL/min), compared to both the ipsilateral CS activity in sham animals, 18.2 ± 0.8 μmol/mL/min, ($p < 0.001$) and contralateral tissue in injured animals, 16.4 ± 0.6 μmol/mL/min, ($p < 0.01$). All values are mean ± SEM. Contra: contralateral side of brain, Ipsi: ipsilateral side of brain.

Table 1
Respiration of brain tissue homogenates from sham and focal controlled cortical impact TBI.
Mitochondrial respiration of brain tissue homogenates from the ipsilateral (Ipsi) and contralateral (Contra) side in two cohorts: sham and 24 h post-controlled cortical impact injury (CCI). Respiration is expressed per mg of tissue (pmols O_2 / s ∗ mg). Presented as mean ± SEM; for definitions of respiratory states and substrates utilized, please see Fig. 1.

Respiratory parameters	Per mg of tissue (pmols O_2 / s ∗ mg)				Per CS activity (pmols O_2 / s ∗ mg ∗ CS)			
	Sham (n = 6)		CCI (n = 10)		Sham (n = 6)		CCI (n = 10)	
	Ipsi	Contra	Ipsi	Contra	Ipsi	Contra	Ipsi	Contra
$OXPHOS_{CI}$	30.2 ± 1.8	28.8 ± 2.8	13.3 ± 1.8*	20.6 ± 1.8*,#	1.7 ± 0.1	1.5 ± 0.2	1.2 ± 0.2	1.3 ± 0.1
ETS_{CII}	18.6 ± 0.7	18.3 ± 1.4	17.8 ± 2.1	36.8 ± 3.5*,#	1.0 ± 0.03	1.0 ± 0.1	1.7 ± 0.2*	2.2 ± 0.2*
$OXPHOS_{CI + CII}$	47.9 ± 2.7	46.3 ± 3.7	31.6 ± 3.9*	69.8 ± 5.7*,#	2.6 ± 0.1	2.6 ± 0.2	3.2 ± 0.3	3.7 ± 0.3*,#
$ETS_{CI + CII}$	31.2 ± 1.5	30.6 ± 2.6	23.6 ± 2.9*	49.5 ± 3.9*,#	1.7 ± 0.1	1.7 ± 0.1	2.3 ± 0.2	3.0 ± 0.3*,#
Complex IV	52.9 ± 4.3	59.2 ± 3.9	51.1 ± 4.5	95.4 ± 9.3*,#	2.9 ± 0.2	3.3 ± 0.4	5.1 ± 0.1*	5.8 ± 0.7*
$LEAK_{CI + CII}$	12.4 ± 0.6	13.2 ± 0.8	7.1 ± 0.6*	13.8 ± 0.9#	0.68 ± 0.03	0.73 ± 0.02	0.70 ± 0.04	0.84 ± 0.05*,#

* $p < 0.05$ significant difference from corresponding sham side.
\# $p < 0.05$ significant difference from paired injured side.

Maximal coupled, phosphorylating respiration ($OXPHOS_{CI + CII}$) per mg of tissue, was significantly decreased ($p < 0.01$) on the ipsilateral side after injury compared to sham ($p < 0.04$) and the contralateral injured brain ($p < 0.02$) (Table 1). However, in the contralateral brain following injury, $OXPHOS_{CI + CII}$ per mg of tissue was significantly increased compared to sham ($p < 0.01$). Similar to respiration per mg of tissue, $OXPHOS_{CI + CII}$ FCR remained significantly decreased in the ipsilateral brain after injury compared to sham and the contralateral injured brain (Fig. 3A). $OXPHOS_{CI + CII}$ normalized to CS on the contralateral side post-CCI was significantly increased compared to sham animals ($p < 0.03$) and the ipsilateral brain post-CCI ($p < 0.05$), similar to respiration reported per mg of tissue (Table 1).

Maximal uncoupled, non-phosphorylating respiration ($ETS_{CI + CII}$), initiated by the protonophore FCCP following ATP synthase inhibition with oligomycin, also decreased on the ipsilateral side after CCI, and increased on the contralateral side compared to sham animals when reported per mg of tissue; as well as, when reported per CS (Table 1).

Table 2
Summary of electron transport system response to injury.
Summary of significant electron transport system (ETS) respiratory response to CCI per mg of tissue, FCR, and normalized CS compared to corresponding sham and injured sides of brain. Irrespective of normalization methods there are patterns of mitochondrial ETS response to injury. Ipsi = ipsilateral; Contra = contralateral CCI: controlled cortical impact.

		CCI Ipsi vs. Sham Ipsi	CCI Contra vs. Sham Contra	CCI Ipsi vs. CCI Contra
$OXPHOS_{CI}$				
	Per mg tissue	↓	↓	↓
	FCR	↓	↓	←→
	CS	←→	←→	←→
ETS_{CII}				
	Per mg tissue	←→	↑	↓
	FCR	↑	↑	←→
	CS	↑	↑	←→
$OXPHOS_{CI + CII}$				
	Per mg tissue	↓	↑	↓
	FCR	↓	←→	↓
	CS	←→	↑	↓
$ETS_{CI + CII}$				
	Per mg tissue	↓	↑	↓
	FCR	N/A	N/A	N/A
	CS	←→	↑	↓
Complex IV				
	Per mg tissue	←→	↑	↓
	FCR	←→	←→	←→
	CS	↑	↑	←→
$LEAK_{CI + CII}$				
	Per mg tissue	←→	←→	↓
	FCR	↓	↓	←→
	CS	←→	↑	↓

When complex IV respiration (isolated respiration of complex IV stimulated by the addition of the artificial electron donor TMPD) was analyzed per mg of tissue, the contralateral brain was altered; increased compared to both sham ($p < 0.01$) and the ipsilateral injured brain ($p < 0.01$), whereas the ipsilateral was not changed compared to sham (Table 1). Complex IV FCR was not altered post-CCI (Fig. 3B). Complex IV respiration normalized to CS was significantly increased bilaterally after CCI compared to sham (Table 1).

LEAK ($LEAK_{CI + CII}$), or State 4_o respiration, per mg of tissue was significantly decreased in the ipsilateral brain compared to sham and the contralateral injured brain (Table 1). Similarly, $LEAK_{CI + CII}$ FCR displayed a significant decrease in the ipsilateral brain compared to corresponding sham (Fig. 3B). $LEAK_{CI + CII}$ per mg of tissue in the contralateral brain post-CCI was significantly decreased compared to sham. When normalizing $LEAK_{CI + CII}$ to CS, only the contralateral brain post-CCI was altered; increasing compared to sham ($p < 0.05$) and the injured ipsilateral side ($p < 0.001$) (Table 1).

Respiratory ratios for evaluating phosphorylation coupling efficiency and the relative contributions of CI and CII to maximal respiration were calculated for sham and CCI animals (Table 3). Post-CCI contralateral $OXPHOS_{CI + CII}$/LEAK respiration was significantly increased ($p < 0.03$) compared to sham animals and the ipsilateral brain post-CCI ($p < 0.05$) (Table 3). On the ipsilateral side of the brain there was no statistical change in $OXPHOS_{CI + CII}$/LEAK after CCI compared to shams. The complex I contribution to convergent respiration of complexes I and II within the ETS post-CCI ($ETS_{CI}/ETS_{CI + CII}$) decreased bilaterally after CCI compared to sham (contralateral; $p < 0.02$ and ipsilateral; $p < 0.004$), with a corresponding increase in the complex II ($ETS_{CII}/ETS_{CI + CII}$) contribution, consistent with greater reliance on complex II after CCI in both ipsilateral and contralateral regions post-CCI (Table 3).

4. Discussion

4.1. High-resolution respirometry

Here we report the development and application of methodologies that may have several advantages over previously reported techniques to investigate mitochondrial function in the immature brain following injury (Kilbaugh et al., 2011). In this research, we used a more sensitive oxygraph, measuring pmol (10^{-12}) changes in oxygen (Oxygraph-2 k, OROBOROS, Instruments, Innsbruck, Austria), which enabled analysis of more subtle changes in mitochondrial function. In addition, we utilized whole tissue homogenates for analysis of mitochondrial bioenergetics instead of using differential centrifugation to isolate mitochondrial populations. This technique adds to the analysis of isolated mitochondria by improving ex-vivo mitochondrial health, since isolation techniques may remove greater than 60% of the total mitochondrial population compared to brain tissue homogenates, and may disrupt

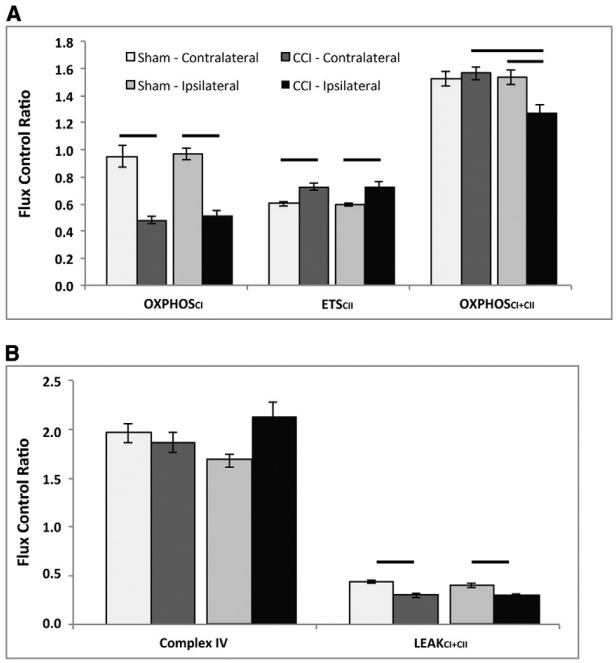

Fig. 3. Mitochondrial flux control ratios from CCI injured and shams normalized by electron transport system (ETS) capacity ($ETS_{CI + CII}$) measured 24 h post TBI. Sham contralateral (Contra) and ipsilateral (Ipsi) sides were not significantly different for any measure. A) Controlled cortical impact (CCI) injury resulted in a significant decrease in the contribution of complex I respiration ($OXHPHOS_{CI}$) to maximal electron transport ($ETS_{CI + CII}$), in injured tissue bilaterally, compared to corresponding sham regions. Complex II-driven respiration (ETS_{CII}) was significantly increased in injured tissue bilaterally, compared to corresponding sham regions. Maximal coupled, phosphorylating respiration ($OXPHOS_{CI + CII}$), stimulated by both complex I and complex II substrates, was significantly decreased post-CCI in the injured ipsilateral tissue compared to injured contralateral tissue and compared to ipsilateral sham. B) There was no significant alteration in CIV driven respiration post-CCI compared to corresponding sham in either side. State 4_o ($LEAK_{CI + CII}$) was significantly reduced in the ipsilateral and contralateral brain post-CCI compared to corresponding sham. Presented as mean ± SEM. For definitions of respiratory states and substrates utilized please see Fig. 1. Bars, $p < 0.05$. CCI: controlled cortical impact.

mitochondrial structure and function to a greater extent than permeabilization/homogenization of whole tissue (Pecinova et al., 2011; Picard et al., 2011a,b). Whole tissue homogenates also carry the added benefit that any toxins or neurometabolites present in the ex-vivo samples are not removed during the mitochondrial isolation process. Beyond the use of a more sensitive instrument and tissue homogenates, our analysis extends conventional bioenergetic protocols that utilize only complex I NADH linked substrates (pyruvate + malate + glutamate) with the addition of the complex II substrate, succinate (pyruvate + malate + glutamate + succinate). This addition maximizes oxidative phosphorylation capacity (ATP production) by simulating the in situ tricarboxylic acid (TCA) cycle and maximizing key substrates for convergent flow of electrons through complexes I and II (Gnaiger, 2009; Karlsson et al., 2013). This novel approach is directed at analyzing dysfunction in electron transport, ADP phosphorylation and leak respiration across the inner membrane (State 4_O) to provide insight into potential mechanisms and possible interventions for mitochondrial dysfunction in the immature brain in focal TBI by delineating targets within the ETS. In order to reach subpopulations of mitochondria within the synaptosome, we utilized digitonin after in our experimental protocol only after careful dose–response titration studies, but we acknowledge that it may have effect overall respiration rates (Brown et al., 2004). Currently, to our knowledge, there is limited research on biomarkers of mitochondrial content (CS activity, cardiolipin content, mitochondrial DNA content, complexes I–IV protein, and complexes I–IV) that validates these surrogates against morphologic measures following acute brain injury, such as transmission electron microscopy (Chepelev et al., 2009; Larsen et al., 2012). In order to differentiate if changes in absolute rates of respiration per amount of tissue were due to changes in global mitochondrial content and function or specific to each respiratory state, we used two strategies to normalize the values. First, we used the common approach of

Table 3
Respiratory ratios of brain tissue homogenates from sham and focal controlled cortical impact TBI.

Respiratory ratios	Sham (n = 6)		CCI (n = 10)	
	Ipsi	Contra	Ipsi	Contra
$OXPHOS_{CI + CII}$/LEAK	3.9 ± 0.2	3.5 ± 0.2	4.2 ± 0.3	5.2 ± 0.3*,#
$ETS_{CI}/ETS_{CI + CII}$	0.40 ± 0.01	0.40 ± 0.02	0.25 ± 0.03*	0.27 ± 0.02*
$ETS_{CII}/ ETS_{CI + CII}$	0.60 ± 0.01	0.60 ± 0.02	0.75 ± 0.03*	0.73 ± 0.03*
ETS_{CII}/ ETS_{CI}	1.49 ± 0.09	1.53 ± 0.12	4.04 ± 1.0*	2.94 ± 0.25*

Respiration ratios were calculated. ETS_{CI} was calculated by subtracting ETS_{CII} from $ETS_{CI + CII}$. Presented as mean ± SEM; for definitions of respiratory states and substrates utilized please see Fig. 1. Ipsi = Ipsilateral; Contra = Contralateral CCI: controlled cortical impact.
* $p < 0.05$ significant difference from corresponding sham side.
\# $p < 0.05$ significant difference from paired injured side.

measuring CS activity as a mitochondrial marker of content. However, the enzyme itself may be altered following injury devoid of any alteration in mitochondrial content (Chepelev et al., 2009). In addition, flux control ratios were assessed as an internal normalization of the respiratory states to the maximal uncoupler-induced rate of respiration within the ETS, a method that may be independent of tissue heterogeneity (Aidt et al., 2013). All of these methods have strengths and weaknesses, thus we decided to present data for each respiratory state in response to injury multiple ways: tissue mass, FCR, CS activity, as well as ratios for evaluating coupling of respiration to ATP production and the relative contribution of complex I- and II-driven respiration to maximal flux. This approach revealed distinct patterns of mitochondrial respiration 24 h after TBI in the immature brain. Because response to injury severity and time course likely varies between injury, we focused our study on regional variations in response to 24 h after TBI. Future studies are planned to identify the role of injury type, injury severity, and the post-TBI time course on regional tissue responses.

Our biochemical analysis of complex interdependent pathways of electron flow through the ETS, by most measures, reveals a bilateral decrease in complex I-driven respiration and an increase in complex II-driven respiration 24 h after focal TBI. Despite significant increase in complex II activity in the ipsilateral brain following injury, convergent complex I- and complex II-driven respiration is limited in its ability to maintain or stimulate oxidative phosphorylation compared to baseline sham mitochondrial respiration. However, surprisingly, the contralateral brain primarily relying on increases in complex II activity is able to maintain maximal oxidative phosphorylation, and for most measures, is able to increase respiration at 24 h after a focal injury. These alterations present multiple targets for therapeutic intervention to limit secondary brain injury, which we present below.

Complex I-driven respiratory dysfunction is a persistent characteristic of early mitochondrial dysfunction within 6–8 h following traumatic and ischemic injury in the brain, and even in other organ systems such as the heart (Almeida et al., 1995; Gilmer et al., 2009; Kunz et al., 2000; Lemieux et al., 2011; Niatsetskaya et al., 2012; Robertson, 2004; Singh et al., 2006; Suchadolskiene et al., 2014). Previous studies in focal TBI, in both mature and immature rodents, have shown a recovery of complex I-driven respiration to sham levels by 24 h post-CCI in the ipsilateral brain, an observation that differs from those in our study (Kilbaugh et al., 2011; Singh et al., 2006). Interestingly, Pandya and colleagues, in mature rodents showed that complex I respiration was significantly decreased at both 24 and 48 h; however, this study unlike the previously mentioned, sampled the core/penumbra while the other studies sampled the whole ipsilateral cortex (Pandya et al., 2009). These differences may be predicated by a species-related difference or to techniques of analyzing mitochondrial function, due to the fact that all previous studies utilized isolated mitochondrial preparations that select for relatively uninjured mitochondria based on density. Investigating an extended time course in tissue homogenates post-CCI, a recent study measured mitochondrial respiration at two time points and showed a reduction in complex-I driven cortical respiration at 7 days, with a recovery to sham levels at 17 days (Watson et al., 2013). Interpreting these studies and our data, creates an important time course, and we speculate that complex I-driven respiration is rapidly impaired within hours in the ipsilateral brain following CCI, and may remain significantly depressed for a minimum of 7 days. We speculate that the duration of reduction in complex I respiration and timing of recovery to maintain bioenergetic output is likely critical for neuronal survival, recovery and regeneration. In fact, chronic alterations in complex I function, loss of mitochondrial bioenergetic function, and production of ROS have been implicated in exacerbating chronic inflammation and cellular destruction in chronic traumatic encephalopathy (Navarro and Boveris, 2009; Walker and Tesco, 2013). However, the inhibition of complex I-driven respiration may be a theoretical, compensatory advantage by limiting ROS generation and improving Ca^{2+} buffering capacity by inhibiting the reversal of electron transport flow from complex II to complex I, a major source of ROS generation from the ETS, a combined process that may be an important protective process to limit secondary pathologic cascades (Loor et al., 2011; Niatsetskaya et al., 2012). Further research is needed to determine whether attenuation or supplementation of complex I as a potential therapeutic target in TBI.

Contrasting complex I-driven respiration at 24 h, ours is the first study to show an increase in complex II-driven respiration in the immature brain following TBI at any time point. In fact, our study shows that by 24 h post-CCI, complex II-driven respiration is at least maintained, if not significantly increased in peri-contusional tissue; and, interestingly is also stimulated by focal injury in regions remote from the impact in the contralateral brain. The consequence of convergent respiration, the convergence of non-linear electron flow from both complexes I and complex II to the Q-junction, and dependence on complex II respiration post-TBI is further supported by the overall decrease in $ETS_{CI}/ETS_{CI\,+\,CII}$ in both sides of the injured brain and an overall increase in $ETS_{CII}/ETS_{CI\,+\,CII}$ compared to sham. Therefore, we speculate that complex II-driven respiration may be a compensatory response to maintain an increased bioenergetic output in the face of increased demand and depressed complex I respiration following CCI, at least at 24 h post-TBI. Further support for compensatory mechanisms is the increased complex IV activity. Our study suggests similar findings to a published report in neonatal mice where global cerebral complex II FAD-linked respiration takes priority over complex I NAD-linked respiration following hypoxic ischemia (Niatsetskaya et al., 2012). In contrast, other published data available suggests that complex II-driven respiration is significantly reduced in mature brain following CCI within hours of the injury and persists up to 17 days; however, in these studies alterations in the ipsilateral brain were reported as a percent of contralateral mitochondrial respiration using the contralateral side from an injured animal as an internal control (Gilmer et al., 2009; Watson et al., 2013).; which, as our data suggest, may not be a surrogate for sham respiration due to the significant increase in complex II-driven respiration in the injured contralateral side. We speculate that the differing response is due to the developmental age of the animals studied; however, it is difficult to draw final conclusions without similar control groups. Future studies will be critical to understand an age specific time course of mitochondrial alterations following CCI, and whether supplementation of complex II-driven respiration offers a therapeutic advantage in pediatric traumatic brain injury.

As discussed, although contralateral mitochondrial respiration in the injured brain may not be comparable to shams, it may still be important to compare contralateral and ipsilateral mitochondrial bioenergetics following injury. Our results of global changes in bioenergetic function occurring in the contralateral hemisphere following focal injury in a large animal model correlates with rodent data depicting global alterations in oxidative metabolism (Scafidi et al., 2009) and neuropathology (Hall et al., 2008), as well as human imaging data utilizing positron emission tomography (Vespa et al., 2005). Compensatory increases in contralateral mitochondrial respiration post-CCI may represent an increase in mitochondrial respiration stimulated after injury that may be necessary to limit secondary cascades of TBI in face of increased metabolic demand (Marcoux et al., 2008a; Robertson et al., 2006; Wright et al., 2013). Therefore, there remains a significant difference between the contralateral and ipsilateral sides of the injured brain for maximal coupled and uncoupled oxidative phosphorylation by all measures; as well as, a significant evolving lesion volume beyond 24 h (evaluated with neuropathology and significant behavioral changes in our model; data not shown); and other limited studies in rodents (Vespa et al., 2005; Watson et al., 2013). Future research should focus on identifying and targeting mitochondrial bioenergetic demands that improve outcomes and are correlated to invasive neuromonitoring, neuroimaging, and neurobehavioral outcomes (Kilbaugh et al., 2011; Scafidi et al., 2010; Vespa et al., 2005; Watson et al., 2013). This is a critical step for the screening and development of mitochondrial-targeted therapies and the development of pre-clinical trials.

LEAK respiration, State 4_o, 24 h post-CCI of the ipsilateral side displays no difference or is significantly decreased for all measures (per mg of tissue, FCR, and CS) compared to shams and the contralateral side post-CCI. Once again this differs from reported results in mature rodent models of CCI, which displayed a significant increase in State 4_0 respiration at 24 h in isolated mitochondria from ipsilateral tissue compared to shams (Singh et al., 2006). This increase in State 4_0 respiration seen at 24 h by Singh and colleagues in mature rodents is the primary determinant of a decreased respiratory control ratio (RCR: State 3/State 4_0; an indicator of overall phosphorylation coupling efficiency), a result we do not find in the immature brain following CCI, where RCRs are similar to sham RCRs at 24 h. The increase in LEAK, State 4_o, in the contralateral brain post-CCI combined with an increase in $OXPHOS_{CI + CII}$ compared to sham likely represents an increase in coupled convergent respiration. However, a limitation to comparing our studies with conventional "Chance and Williams" State 3 and 4 respiration using only CI substrates, is that our study measures convergent input from complex I and complex II substrates which produces a higher proton motive force. The leak respiration (State 4_o) under these circumstances may differ. This could certainly affect the RCR negatively and should be taken into account when making strict comparisons between techniques. Furthermore, FCCP titration before the addition of oligomycin (OXHPOS state) would likely result in higher maximal respiration but it would also prevent the possibility of measuring LEAK respiration in the same protocol. The findings demonstrate that ATP-synthase/complex V activity is not rate limiting in immature swine brain homogenate because the FCCP-induced respiration was not higher than OXPHOS. The relative difference between the treatment groups should however not be influenced since the protocol was identical. In addition, with these pilot studies in large animals it is possible that techniques for harvesting and measuring respiration will improve over time, as will coupled respiration, and we will certainly report this in the future.

Finally, the profound reduction of citrate synthase activity within the ipsilateral tissue post-CCI, by nearly 50%, is a critical finding since CS is generally assumed to be the rate-limiting enzyme of the TCA cycle and possibly a biomarker of mitochondrial content. We speculate that decreased CS activity in the ipsilateral tissue may be associated with significant oxidative injury in the at risk peri-contusional tissue following focal impact, reflecting oxidative inactivation of CS, and/or a loss of mitochondrial content (Chepelev et al., 2009). If CS is associated with mitochondrial content, this is a staggering loss of functional mitochondria following CCI in the ipsilateral tissue. We speculate that macroautophagy or, more specifically, mitophagy may play a role in the loss of mitochondrial content seen at 24 h post-CCI, given the paucity of evidence of necrosis and cellular loss at this time point on neuropathology in this peri-contusional region (Duhaime et al., 2003; Grate et al., 2003; Weeks et al., 2014). Our findings at 24 h post-CCI are consistent with findings in cortical tissue homogenates harvested from the peri-contusional regions in adult rodents depicting significantly decreased CS activity at 7 days post-TBI. Thus, by combining our results with those previously published, we begin to delineate a time course of rapid oxidative injury and/or decreased mitochondrial content, with a rapid loss within 24 h and persisting for at least 7 days. Therefore, we propose that interventions should be instituted early to limit the reduction of CS in tissue with potential viability and increased bioenergetic demand (Watson et al., 2013).

5. Conclusion

We have evaluated the mitochondrial bioenergetic response to TBI in a unique large animal translational platform of focal impact injury and conclude that there are significant alterations in mitochondrial respiration in the immature brain 24 h after TBI that vary by location from focal injury. Alterations in complex I- and complex II-driven respiration following injury identify opportunities for therapeutic interventions in the immature brain to limit secondary injury and support post-traumatic bioenergetic demand by substrate-directed resuscitation. Finally, this translational model expands our knowledge of evolving mitochondrial techniques as well as the bioenergetic response to a spectrum of TBI pathology in the immature brain; importantly, these techniques and findings will continue to inform advanced pre-clinical trials in pediatric TBI.

Authors disclosure statement

Eskil Elmer and Magnus J. Hansson own shares in and have received salary support from NeuroVive Pharmaceutical AB, a public company active in the field of mitochondrial medicine. Michael Karlsson has received salary support from NeuroVive Pharmaceutical AB.

Acknowledgments

The authors would like to thank Albana Shahini and Saori Morota for their invaluable technical support. The Oroboros Oxygraph used in the study was a loan from NeuroVive Pharmaceutical AB, Lund Sweden. Studies were supported by the NIH UO1 NS069545, Endowed Chair of Critical Care Medicine at the Children's Hospital of Philadelphia, and Stephenson Fund Department of Bioengineering the University of Pennsylvania.

References

Adelson, P.D., Pineda, J., Bell, M.J., Abend, N.S., Berger, R.P., Giza, C.C., Hotz, G., Wainwright, M.S., Pediatric, T.B.I.D., Clinical Assessment Working G., 2012. Common data elements for pediatric traumatic brain injury: recommendations from the working group on demographics and clinical assessment. J. Neurotrauma 29, 639–653.

Aidt, F.H., Nielsen, S.M., Kanters, J., Pesta, D., Nielsen, T.T., Norremolle, A., Hasholt, L., Christiansen, M., Hagen, C.M., 2013. Dysfunctional mitochondrial respiration in the striatum of the Huntington's disease transgenic R6/2 mouse model. PLoS Curr. 5.

Almeida, A., Brooks, K.J., Sammut, I., Keelan, J., Davey, G.P., Clark, J.B., Bates, T.E., 1995. Postnatal development of the complexes of the electron transport chain in synaptic mitochondria from rat brain. Dev. Neurosci. 17, 212–218.

Armstead, W.M., 2005. Age and cerebral circulation. Pathophysiology 12, 5–15.

Armstead, W., Kurth, C., 1994. Different cerebral hemodynamic responses following fluid percussion brain injury in the newborn and juvenile pig. J. Neurotrauma 11, 487–497.

Balan, I.S., Saladino, A.J., Aarabi, B., Castellani, R.J., Wade, C., Stein, D.M., Eisenberg, H.M., Chen, H.H., Fiskum, G., 2013. Cellular alterations in human traumatic brain injury: changes in mitochondrial morphology reflect regional levels of injury severity. J. Neurotrauma 30, 367–381.

Bates, T.E., Almeida, A., Heales, S.J., Clark, J.B., 1994. Postnatal development of the complexes of the electron transport chain in isolated rat brain mitochondria. Dev. Neurosci. 16, 321–327.

Bowling, A.C., Mutisya, E.M., Walker, L.C., Price, D.L., Cork, L.C., Beal, M.F., 1993. Age-dependent impairment of mitochondrial function in primate brain. J. Neurochem. 60, 1964–1967.

Brown, M.R., Sullivan, P.G., Dorenbos, K.A., Modafferi, E.A., Geddes, J.W., Steward, O., 2004. Nitrogen disruption of synaptoneurosomes: an alternative method to isolate brain mitochondria. J. Neurosci. Methods 137, 299–303.

Chepelev, N.L., Bennitz, J.D., Wright, J.S., Smith, J.C., Willmore, W.G., 2009. Oxidative modification of citrate synthase by peroxyl radicals and protection with novel antioxidants. J. Enzyme Inhib. Med. Chem. 24, 1319–1331.

Coronado, V.G., Xu, L., Basavaraju, S.V., McGuire, L.C., Wald, M.M., Faul, M.D., Guzman, B.R., Hemphill, J.D., Centers for Disease, C., Prevention, 2011. Surveillance for traumatic brain injury-related deaths—United States, 1997–2007. Morbidity and mortality weekly report. Surveill. Summ. 60, 1–32.

Del Maestro, R., McDonald, W., 1987. Distribution of superoxide dismutase, glutathione peroxidase and catalase in developing rat brain. Mech. Ageing Dev. 41, 29–38.

Duhaime, A.C., 2006. Large animal models of traumatic injury to the immature brain. Dev. Neurosci. 28, 380–387.

Duhaime, A.C., Margulies, S.S., Durham, S.R., O'Rourke, M.M., Golden, J.A., Marwaha, S., Raghupathi, R., 2000a. Maturation-dependent response of the piglet brain to scaled cortical impact. J. Neurosurg. 93, 455–462.

Duhaime, A.C., Margulies, S.S., Durham, S.R., O'Rourke, M.M., Golden, J.A., Marwaha, S., Raghupathi, R., 2000b. Maturation-dependent response of the piglet brain to scaled cortical impact. J. Neurosurg. 93, 455–462.

Duhaime, A.C., Hunter, J.V., Grate, L.L., Kim, A., Golden, J., Demidenko, E., Harris, C., 2003. Magnetic resonance imaging studies of age-dependent responses to scaled focal brain injury in the piglet. J. Neurosurg. 99, 542–548.

Durham, S.R., Duhaime, A.C., 2007. Maturation-dependent response of the immature brain to experimental subdural hematoma. J. Neurotrauma 24, 5–14.

Faul, M., Xu, L., Wald, M.M., Coronado, V.G., 2010. Traumatic Brain Injury in the United States: Emergency Department Visits, Hospitalizations and Deaths 2002–2006.

Centers for Disease Control and Prevention, National Center for Injury Prevention and Control, Atlanta (GA).
Gean, A.D., Fischbein, N.J., 2010. Head trauma. Neuroimaging Clin. N. Am. 20, 527–556.
Gilmer, L.K., Roberts, K.N., Joy, K., Sullivan, P.G., Scheff, S.W., 2009. Early mitochondrial dysfunction after cortical contusion injury. J. Neurotrauma 26, 1271–1280.
Gnaiger, E., 2009. Capacity of oxidative phosphorylation in human skeletal muscle: new perspectives of mitochondrial physiology. Int. J. Biochem. Cell Biol. 41, 1837–1845.
Grate, L.L., Golden, J.A., Hoopes, P.J., Hunter, J.V., Duhaime, A.C., 2003. Traumatic brain injury in piglets of different ages: techniques for lesion analysis using histology and magnetic resonance imaging. J. Neurosci. Methods 123, 201–206.
Hall, E.D., Bryant, Y.D., Cho, W., Sullivan, P.G., 2008. Evolution of post-traumatic neurodegeneration after controlled cortical impact traumatic brain injury in mice and rats as assessed by the de Olmos silver and fluorojade staining methods. J. Neurotrauma 25, 235–247.
Hattori, N., Huang, S.C., Wu, H.M., Yeh, E., Glenn, T.C., Vespa, P.M., McArthur, D., Phelps, M.E., Hovda, D.A., Bergsneider, M., 2003. Correlation of regional metabolic rates of glucose with glasgow coma scale after traumatic brain injury. J. Nucl. Med. 44, 1709–1716.
Karlsson, M., Hempel, C., Sjovall, F., Hansson, M.J., Kurtzhals, J.A., Elmer, E., 2013. Brain mitochondrial function in a murine model of cerebral malaria and the therapeutic effects of rhEPO. Int. J. Biochem. Cell Biol. 45, 151–155.
Kilbaugh, T.J., Bhandare, S., Lorom, D.H., Saraswati, M., Robertson, C.L., Margulies, S.S., 2011. Cyclosporin A preserves mitochondrial function after traumatic brain injury in the immature rat and piglet. J. Neurotrauma 28, 763–774.
Kunz, W.S., Kudin, A.P., Vielhaber, S., Blumcke, I., Zuschratter, W., Schramm, J., Beck, H., Elger, C.E., 2000. Mitochondrial complex I deficiency in the epileptic focus of patients with temporal lobe epilepsy. Ann. Neurol. 48, 766–773.
Langlois, J.A., Rutland-Brown, W., Thomas, K.E., 2005. The incidence of traumatic brain injury among children in the United States: differences by race. J. Head Trauma Rehabil. 20, 229–238.
Larsen, S., Nielsen, J., Hansen, C.N., Nielsen, L.B., Wibrand, F., Stride, N., Schroder, H.D., Boushel, R., Helge, J.W., Dela, F., Hey-Mogensen, M., 2012. Biomarkers of mitochondrial content in skeletal muscle of healthy young human subjects. J. Physiol. 590, 3349–3360.
Lemieux, H., Semsroth, S., Antretter, H., Hofer, D., Gnaiger, E., 2011. Mitochondrial respiratory control and early defects of oxidative phosphorylation in the failing human heart. Int. J. Biochem. Cell Biol. 43, 1729–1738.
Lifshitz, J., Friberg, H., Neumar, R.W., Raghupathi, R., Welsh, F.A., Janmey, P., Saatman, K.E., Wieloch, T., Grady, M.S., McIntosh, T.K., 2003. Structural and functional damage sustained by mitochondria after traumatic brain injury in the rat: evidence for differentially sensitive populations in the cortex and hippocampus. J. Cereb. Blood Flow Metab. 23, 219–231.
Loor, G., Kondapalli, J., Iwase, H., Chandel, N.S., Waypa, G.B., Guzy, R.D., Vanden Hoek, T.L., Schumacker, P.T., 2011. Mitochondrial oxidant stress triggers cell death in simulated ischemia–reperfusion. Biochim. Biophys. Acta 1813, 1382–1394.
Marcoux, J., McArthur, D.A., Miller, C., Glenn, T.C., Villablanca, P., Martin, N.A., Hovda, D.A., Alger, J.R., Vespa, P.M., 2008a. Persistent metabolic crisis as measured by elevated cerebral microdialysis lactate–pyruvate ratio predicts chronic frontal lobe brain atrophy after traumatic brain injury. Crit. Care Med. 36, 2871–2877.
Marcoux, J., McArthur, D.A., Miller, C., Glenn, T.C., Villablanca, P., Martin, N.A., Hovda, D.A., Alger, J.R., Vespa, P.M., 2008b. Persistent metabolic crisis as measured by elevated cerebral microdialysis lactate–pyruvate ratio predicts chronic frontal lobe brain atrophy after traumatic brain injury. Crit. Care Med. 36, 2871–2877.
Miller, A.C., Odenkirchen, J., Duhaime, A.C., Hicks, R., 2012. Common data elements for research on traumatic brain injury: pediatric considerations. J. Neurotrauma 29, 634–638.
Missios, S., Harris, B.T., Dodge, C.P., Simoni, M.K., Costine, B.A., Lee, Y.L., Quebada, P.B., Hillier, S.C., Adams, L.B., Duhaime, A.C., 2009. Scaled cortical impact in immature swine: effect of age and gender on lesion volume. J. Neurotrauma 26, 1943–1951.
Navarro, A., Boveris, A., 2009. Brain mitochondrial dysfunction and oxidative damage in Parkinson's disease. J. Bioenerg. Biomembr. 41, 517–521.
Niatsetskaya, Z.V., Sosunov, S.A., Matsiukevich, D., Utkina-Sosunova, I.V., Ratner, V.I., Starkov, A.A., Ten, V.S., 2012. The oxygen free radicals originating from mitochondrial complex I contribute to oxidative brain injury following hypoxia–ischemia in neonatal mice. J. Neurosci. 32, 3235–3244.
Pandya, J.D., Pauly, J.R., Sullivan, P.G., 2009. The optimal dosage and window of opportunity to maintain mitochondrial homeostasis following traumatic brain injury using the uncoupler FCCP. Exp. Neurol. 218, 381–389.
Pecinova, A., Drahota, Z., Nuskova, H., Pecina, P., Houstek, J., 2011. Evaluation of basic mitochondrial functions using rat tissue homogenates. Mitochondrion 11, 722–728.
Picard, M., Taivassalo, T., Gouspillou, G., Hepple, R.T., 2011a. Mitochondria: isolation, structure and function. J. Physiol. 589, 4413–4421.
Picard, M., Taivassalo, T., Ritchie, D., Wright, K.J., Thomas, M.M., Romestaing, C., Hepple, R.T., 2011b. Mitochondrial structure and function are disrupted by standard isolation methods. PLoS One 6, e18317.
Ragan, D.K., McKinstry, R., Benzinger, T., Leonard, J.R., Pineda, J.A., 2013. Alterations in cerebral oxygen metabolism after traumatic brain injury in children. J. Cereb. Blood Flow Metab. 33, 48–52.
Raghupathi, R., Margulies, S.S., 2002. Traumatic axonal injury after closed head injury in the neonatal pig. J. Neurotrauma 19, 843–853.
Robertson, C.L., 2004. Mitochondrial dysfunction contributes to cell death following traumatic brain injury in adult and immature animals. J. Bioenerg. Biomembr. 36, 363–368.
Robertson, C.L., Soane, L., Siegel, Z.T., Fiskum, G., 2006. The potential role of mitochondria in pediatric traumatic brain injury. Dev. Neurosci. 28, 432–446.
Robertson, C.L., Scafidi, S., McKenna, M.C., Fiskum, G., 2009. Mitochondrial mechanisms of cell death and neuroprotection in pediatric ischemic and traumatic brain injury. Exp. Neurol. 218, 371–380.
Saito, A., Maier, C.M., Narasimhan, P., Nishi, T., Song, Y.S., Yu, F., Liu, J., Lee, Y.S., Nito, C., Kamada, H., Dodd, R.L., Hsieh, L.B., Hassid, B., Kim, E.E., Gonzalez, M., Chan, P.H., 2005. Oxidative stress and neuronal death/survival signaling in cerebral ischemia. Mol. Neurobiol. 31, 105–116.
Scafidi, S., O'Brien, J., Hopkins, I., Robertson, C., Fiskum, G., McKenna, M., 2009. Delayed cerebral oxidative glucose metabolism after traumatic brain injury in young rats. J. Neurochem. 109 (Suppl. 1), 189–197.
Scafidi, S., Racz, J., Hazelton, J., McKenna, M.C., Fiskum, G., 2010. Neuroprotection by acetyl-L-carnitine after traumatic injury to the immature rat brain. Dev. Neurosci. 32, 480–487.
Sims, N.R., Blass, J.P., 1986. Expression of classical mitochondrial respiratory responses in homogenates of rat forebrain. J. Neurochem. 47, 496–505.
Singh, I.N., Sullivan, P.G., Deng, Y., Mbye, L.H., Hall, E.D., 2006. Time course of post-traumatic mitochondrial oxidative damage and dysfunction in a mouse model of focal traumatic brain injury: implications for neuroprotective therapy. J. Cereb. Blood Flow Metab. 26, 1407–1418.
Suchadolskiene, O., Pranskunas, A., Baliutyte, G., Veikutis, V., Dambrauskas, Z., Vaitkaitis, D., Borutaite, V., 2014. Microcirculatory, mitochondrial, and histological changes following cerebral ischemia in swine. BMC Neurosci. 15, 2.
Vespa, P., Bergsneider, M., Hattori, N., Wu, H.M., Huang, S.C., Martin, N.A., Glenn, T.C., McArthur, D.L., Hovda, D.A., 2005. Metabolic crisis without brain ischemia is common after traumatic brain injury: a combined microdialysis and positron emission tomography study. J. Cereb. Blood Flow Metab. 25, 763–774.
Walker, K.R., Tesco, G., 2013. Molecular mechanisms of cognitive dysfunction following traumatic brain injury. Front. Aging Neurosci. 5, 29.
Watson, W.D., Buonora, J.E., Yarnell, A.M., Lucky, J.J., D'Acchille, M.I., McMullen, D.C., Boston, A.G., Kuczmarski, A.V., Kean, W.S., Verma, A., Grunberg, N.E., Cole, J.T., 2013. Impaired cortical mitochondrial function following TBI precedes behavioral changes. Front. Neuroenerg. 5, 12.
Weeks, D., Sullivan, S., Kilbaugh, T., Smith, C., Margulies, S.S., 2014. Influences of developmental age on the resolution of diffuse traumatic intracranial hemorrhage and axonal injury. J. Neurotrauma 31, 206–214.
Wright, M.J., McArthur, D.L., Alger, J.R., Van Horn, J., Irimia, A., Filippou, M., Glenn, T.C., Hovda, D.A., Vespa, P., 2013. Early metabolic crisis-related brain atrophy and cognition in traumatic brain injury. Brain Imaging Behav. 7, 307–315.
Xu, Y., McArthur, D.L., Alger, J.R., Etchepare, M., Hovda, D.A., Glenn, T.C., Huang, S., Dinov, I., Vespa, P.M., 2010. Early nonischemic oxidative metabolic dysfunction leads to chronic brain atrophy in traumatic brain injury. J. Cereb. Blood Flow Metab. 30, 883–894.

Paper III

Mitochondrion 26 (2016) 19–25

Contents lists available at ScienceDirect

Mitochondrion

journal homepage: www.elsevier.com/locate/mito

Mitochondrial response in a toddler-aged swine model following diffuse non-impact traumatic brain injury

Todd J. Kilbaugh [a,*], Michael Karlsson [b], Ann-Christine Duhaime [c,1], Magnus J. Hansson [b], Eskil Elmer [b], Susan S. Margulies [d,2]

[a] Department of Anesthesiology and Critical Care Medicine, Children's Hospital of Philadelphia, Perelman School of Medicine, University of Pennsylvania, 3401 Civic Center Blvd., Philadelphia, PA 19104, USA
[b] Mitochondrial Medicine, Department of Clinical Sciences, Lund University, BMC A13, SE-221 84 Lund, Sweden
[c] Department of Bioengineering, University of Pennsylvania, 210 South 33rd Street, Philadelphia, PA 19104, USA
[d] Department of Neurosurgery, Massachusetts General Hospital, Harvard Medical School, 15 Parkman Street, Boston, MA 02114, USA

ARTICLE INFO

Article history:
Received 12 June 2015
Received in revised form 3 November 2015
Accepted 4 November 2015
Available online 5 November 2015

Keywords:
Pediatric brain injury
Traumatic brain injury
Mitochondria
In vivo studies
Large animal model of injury

ABSTRACT

Traumatic brain injury (TBI) is an important health problem, and a leading cause of death in children worldwide. Mitochondrial dysfunction is a critical component of the secondary TBI cascades. Mitochondrial response in the pediatric brain has limited investigation, despite evidence that the developing brain's response differs from that of the adult, especially in diffuse non-impact TBI. We performed a detailed evaluation of mitochondrial bioenergetics using high-resolution respirometry in a swine model of diffuse TBI (rapid non-impact rotational injury: RNR), and examined the cortex and hippocampus. A substrate-uncoupler-inhibitor-titration protocol examined the role of the individual complexes as well as the uncoupled maximal respiration. Respiration per mg of tissue was also related to citrate synthase activity (CS) as an attempt to control for variability in mitochondrial content following injury. Diffuse RNR stimulated increased complex II-driven respiration relative to mitochondrial content in the hippocampus compared to shams. LEAK (State 4_o) respiration increased in both regions, with decreased respiratory ratios of convergent oxidative phosphorylation through complex I and II, compared to sham animals, indicating uncoupling of oxidative phosphorylation at 24 h. The study suggests that proportionately, complex I contribution to convergent mitochondrial respiration was reduced in the hippocampus after RNR, with a simultaneous increase in complex-II driven respiration. Mitochondrial respiration 24 h after diffuse TBI varies by location within the brain. We concluded that significant uncoupling of oxidative phosphorylation and alterations in convergent respiration through complex I- and complex II-driven respiration reveals therapeutic opportunities for the injured at-risk pediatric brain.

1. Introduction

Traumatic brain injury (TBI) is an important health problem and is set to become the third leading cause of death and disability in the world by 2020 (Coronado et al., 2011; Gean and Fischbein, 2010).

Diffuse TBI triggers a heterogeneous insult to the brain induced by traumatic biomechanical shearing forces when the head is rapidly accelerated and/or decelerated, such as during player-to-player contacts in sports settings, impacts after falls, or whiplash injuries in car crashes. Axonal shear stretch leads to the opening of voltage-gated calcium channels that, ultimately, precipitates mitochondrial dysfunction, bioenergetic failure, and the release of secondary messengers that end in apoptosis and death (Balan et al., 2013; Glenn et al., 2003; Lifshitz et al., 2003; Marcoux et al., 2008; Ragan et al., 2013; Xu et al., 2010).Thus, mitochondria play a central role in cerebral metabolism and regulation of oxidative stress, excitotoxicity, and apoptosis in acute brain injury; however, the mechanistic response and time course following diffuse TBI, especially in the immature brain at differing developmental stages, has limit investigation (Balan et al., 2013; Gilmer et al., 2010; Lifshitz et al., 2004; Robertson et al., 2009). Furthermore, the challenge of extrapolating adult models of diffuse TBI to pediatric models includes developmental differences in biomechanical properties and biological responses that vary in the infant, toddler, adolescent, and adult (Grate et al., 2003; Ibrahim et al., 2010; S. Sullivan et al., 2015; Weeks et al., 2014). In addition, there are critical differences in mitochondrial characteristics in the developing brain as it matures, such as the number and density of complexes of the electron transfer chain,

* Corresponding author at: Department of Anesthesiology and Critical Care Medicine, The Children's Hospital of Philadelphia, 34th & Civic Center Blvd, Philadelphia, PA, 19104, USA.
E-mail addresses: kilbaugh@chop.edu (T.J. Kilbaugh), michael.karlsson@med.lu.se (M. Karlsson), aduhaime@partners.org (A.-C. Duhaime), magnus.hansson@med.lu.se (M.J. Hansson), eskil.elmer@med.lu.se (E. Elmer), margulie@seas.upenn.edu (S.S. Margulies).
[1] 15 Parkman Street, Boston, MA 02114-3117, USA.
[2] 240 Skirkanich Hall, 210 South 33rd Street, Philadelphia, PA 19104-6321, USA.

http://dx.doi.org/10.1016/j.mito.2015.11.001
1567-7249/

antioxidant enzyme activity and content, and lipid content (Bates et al., 1994; Del Maestro and McDonald, 1987). Taken together, the immature brain's response to TBI changes during development from infancy through adolescence and differs with injury mechanism (Armstead, 2005; Duhaime, 2006; Duhaime et al., 2000; Durham and Duhaime, 2007). These unique features of the developing brain underscore the importance of characterizing the bioenergetic failure and cell death cascades following TBI in the immature brain in order to develop age-specific mitochondrial-directed neuroprotective approaches.

Previously we reported differences in the regional mitochondrial responses in neonatal piglets, age 3–5 days, following diffuse white matter injury using our large animal model (Kilbaugh et al., 2011). In our current investigation, we have expanded our investigation to the 4-week old animals with comparable neurodevelopment to a human toddler. Furthermore, we expanded our previous techniques to investigate functional mitochondrial respiration, within integrated mitochondrial networks of fresh brain tissue, to focus on pathologic metabolic pathways following TBI.

2. Materials and methods

This study was carried out in strict accordance with the recommendations in the Guide for the Care and Use of Laboratory Animals of the National Institutes of Health, and was approved by the Institutional Animal Care and Use Committee of the University of Pennsylvania (Number: 803401). Four-week old (8–10 kg) piglets, with comparable neurodevelopment to a human toddler, were studied (Armstead, 2005; Duhaime, 2006). In an effort to limit heterogeneity, only females were used based on our prior work (Missios et al., 2009). Twenty-eight piglets were randomly assigned to sham or injury cohorts, consisting of a single rapid non-impact rotational injury in the sagittal plane ($n = 18$ injured-RNR, $n = 10$ naïve sham-RNR). Animals were sacrificed 24 h after TBI.

2.1. Animal preparation

Anesthetic regimen included: 1) premedication with an intramuscular injection of ketamine (20 mg/kg) and xylazine (2 mg/kg), 2) induction: 4% inhaled isoflurane in 1.0 fraction of inspired oxygen via snout mask, until abolishment of response to a reflexive pinch stimulus, 3) maintenance: 1% inhaled isoflurane via endotracheal tube with fraction of inspired oxygen to 0.21. Buprenorphine (0.02 mg/kg) was also delivered intramuscularly for analgesia prior to injury. A circulating water blanket kept core body temperature constant between 36 and 38 °C (monitored via a rectal probe), and non-invasive blood pressure, oxygen saturation, heart rate, respiratory rate, and end-tidal CO_2 were continuously monitored throughout the experiment (Surgivet Advisor V9204; Smith Medical, Waukesha, WI).

2.2. Rapid non-impact rotational (RNR) injury

Diffuse closed head TBI was induced using an established rapid head rotation technique described previously (Eucker et al., 2011; Ibrahim et al., 2010; Raghupathi et al., 2004). While maintained on isoflurane, the head of the piglet was secured to a bite plate by a snout strap. Isoflurane was withdrawn immediately prior to injury, and the head was rotated rapidly (10–15 ms) ventral-to-dorsal in the sagittal plane with the center of rotation at the cervical spine. The peak angular velocity was nearly constant across the injured group, averaging 126 ± 0.72 rad/s.

Immediately after the RNR, the animal was removed from the injury device. At this angular velocity, rotation direction, and age animals experienced a brief period of hypoactivity, irritability and gait instability. Animals did not experience apnea or hemodynamic instability following TBI.

Following RNR, animals had significant neurologic deficits, including lethargy and longer periods of recumbancy, and unsteady gait compared to shams. However, animals eventually were able to vocalize, ambulate, maintain body temperature and exhibit proper feeding and drinking behaviors. These injuries are best described as mild-to-moderate in severity, based on parallels with human clinical severity classifications (Adelson et al., 2012; Miller et al., 2012) and neuropathology findings 6 days after RNR (Weeks et al., 2014).

2.3. Preparation of tissue homogenates

At 24 h post-RNR, a craniotomy was performed and a 2 cm^2 region of left frontal cortex was resected and both hippocampal regions extracted rapidly (less than 10 s) and combined. As a starting point for our initial large animal studies we chose 24 h as our terminal time-point for two critical reasons: 1) we have documented significant injury with neuropathology, imaging and behavior at this time point in our model of diffuse TBI (Jaber et al., 2015; Kilbaugh et al., 2011, 2015; Weeks et al., 2014), and 2) other investigators have documented bioenergetic and mitochondrial alterations in rodents following diffuse TBI at this particular time point. The hippocampus and cortex were studied as the areas of interest for two critical factors: 1) previous studies from our laboratory have documented significant neuropathology and mitochondrial dysfunction within these regions following RNR (Coats and Margulies, 2006; Eucker et al., 2011; Kilbaugh et al., 2011; Weeks et al., 2014), and 2) if our hypothesis was consistent with previous findings in adults and infants, and these areas of interest do exhibit alterations in mitochondrial functional pathways, then these findings would be instrumental in the evaluation of neurobehavioral outcomes in future studies, linking mitochondrial bioenergetics and long-term outcomes (S. Sullivan et al., 2013). Following extraction, tissue was placed immediately in ice-cold isolation buffer (320 mM sucrose, 10 mM Trizma base, and 2 mM EGTA). Blood and vasculature was dissected and 1 mg of wet weight tissue was gently homogenized on ice in MiR05 buffer (110 mM sucrose, 0.5 mM EGTA, 3.0 mM $MgCl_2$, 60 mM K-lactobionate, 10 mM KH_2PO_4, 20 mM taurine, 20 mM HEPES and 1.0 g/l fatty acid-free BSA) using a 5 ml Potter–Elvehjem teflon-glass homogenizer to a concentration of 1 mg wet weight tissue/10 μl MiR05 buffer.

2.4. Mitochondrial high-resolution respirometry (HRR)

High-resolution Oxygraph-2 k (Oroboros Instruments, Innsbruck, Austria) was used to measure mitochondrial respiration. The instrument was calibrated daily, as previously described, and respiration measurements were obtained at a constant 37 °C with the addition of tissue homogenates to a final concentration of 1 mg per ml of Mir05 buffer (Kilbaugh et al., 2015). Oxygen consumption and oxygen flux were recorded using DatLab software (5.1, Oroboros Instruments, Innsbruck, Austria).

A substrate, uncoupler, inhibitor titration (SUIT) protocol previously used was specifically designed for porcine brain tissue (Kilbaugh et al., 2015). Complex specific substrates and inhibitors allowed for the assessment of respiratory capacities of the integrated electron transport system (ETS) (Fig. 1). Complex I (CI), and complex II (CII) respiratory capacities in brain tissue were evaluated separately; as well as with pathways of convergent electron input through the Q-junction (CI + II) using succinate and nicotinamide adenine dinucleotide (NADH)-linked substrates (Gnaiger, 2009). An optimized dose of digitonin, 1 μl (50 mg/ml), necessary to achieve accurate and consistent oxidative phosphorylation capacity within synaptasomes using water-soluble substrates, and achieve similar results in brain tissue homogenates and isolated brain mitochondria (Kilbaugh et al., 2015, 2011). Exogenously administered cytochrome c did not induce a significant effect on mitochondrial respiration at the optimal digitonin dose, indicating an intact outer mitochondrial membrane (data not shown) (Brustovetsky et al., 2002; Sims and Blass, 1986). Sequential additions

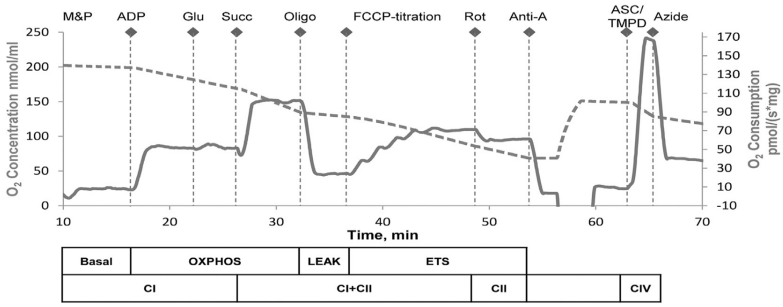

Fig. 1. Oxygen concentration and consumption example trace from SUIT protocol. The graph depicts an illustrative trace of oxygen consumption rate using a substrate, uncoupler, inhibitor titration (SUIT) protocol. Induced respiratory states and respiratory complexes activated are outlined below the x-axis. After stabilization at basal respiration with endogenous substrates, and in the presence of digitonin, the SUIT protocol was executed as indicated above the oxygen concentration trace. M&P, malate + pyruvate; Glu, glutamate; Succ, succinate; Oligo, oligomycin; Rot, rotenone; Anti-A, antimycin-A; ASC/TMPD, ascorbate and TMPD.

included: malate (5 mM) and pyruvate (5 mM), followed by ADP (1 mM) and glutamate (5 mM), measuring oxidative phosphorylation capacity of complex I ($OXPHOS_{CI}$), driven by the NADH-related substrates. Succinate (10 mM) was added to stimulate maximal phosphorylating respiration capacity via convergent input through complexes I and II ($OXPHOS_{CI+CII}$). Oligomycin, an ATP-synthase inhibitor, stopped oxidative phosphorylation, inducing LEAK respiration ($LEAK_{CI+CII}$) or State 4_o respiration. Maximal convergent non-phosphorylating respiration of the electron transport system (ETS_{CI+CII}) was evaluated by titrating the protonophore, carbonyl cyanide p-(trifluoromethoxy) phenylhydrazone (FCCP), until no further increase in respiration was detected. ETS capacity supported by succinate was measured by adding a complex I inhibitor, Rotenone, to reveal complex II-driven respiration (ETS_{CII}). ETS electron flow was inhibited by the complex III inhibitor antimycin-A (1 μg/ml), to measure the residual oxygen consumption. This residual value was subtracted from each of the measured respiratory states in the final analysis. Finally, an addition of ascorbate (ASC, 0.8 mM) and N,N,N′,N′-tetramethyl-p-phenylenediamine (TMPD, 0.5 mM), an electron donor to complex IV, measured the activity of cytochrome c oxidase. Complex IV-inhibitor sodium azide (10 mM) was added and the remaining chemical background was subtracted to assess complex IV activity, due to the high level of auto-oxidation of TMPD. The protocol was identical in timing and sequence amongst all groups, sham and injured.

2.5. Citrate synthase measurements

Following the completion of respirometry measurements, chamber contents were stored and subsequently analyzed for citrate synthase (CS) activity (μmol/mL/min) quantification (Citrate Synthase Assay Kit, CS0720, Sigma). CS was used as a marker of brain metabolism secondary to its location within the mitochondrial matrix and importance as the first step of the tricarboxylic acid cycle (TCA). In addition, some investigators use CS as a surrogate measure of mitochondrial content per mg of tissue (Bowling et al., 1993; Larsen et al., 2012).

2.6. Data analysis

Oxygen flux traces were measured automatically with a customized Matlab (Mathworks, Natick, MA) (Kilbaugh et al., 2015). Statistical evaluation was performed using JMP Pro (SAS Institute Inc., version 10.0, Cary, NC, USA). We compared tissue mitochondrial respiration between injured and sham subjects with an unpaired, non-parametric Wilcoxon ranked sum test with Dunn's multiple comparison tests. In addition, paired Wilcoxon ranked sum tests were used to compare regions within sham and injury groups. Differences were considered significant where $p < 0.05$. All results are reported as mean ± standard error of the mean (SEM).

3. Results

3.1. Mitochondrial content

We measured CS activity per mg of tissue; there were no differences between brain regions in sham animals (with cortical tissue 24.7 ± 4.5 μmol/mL/min and hippocampal 25.3 ± 6.7 μmol/mL/min, $p = 0.93$) (Fig. 2). Diffuse RNR did not stimulate a significant decrease in mitochondrial content following injury in either region (cortex 17.8 ± 0.4 μmol/mL/min, and hippocampus 16.8 ± 0.4 μmol/mL/min)

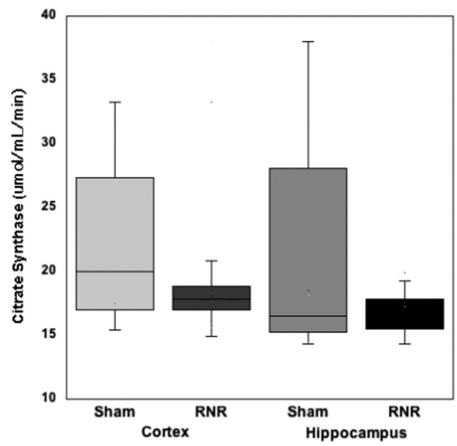

Fig. 2. Citrate synthase activity. In 24 h post-RNR there was no significant decrease in citrate synthase activity in either region compared to sham animals ($p = 0.19$ hippo and $p = 0.29$ cortex). Boxplots: Horizontal lines represent the median CS activity, with the box representing the 25th and 75th percentiles, the whiskers the 5th and 95th percentiles, and the outliers.

compared to sham animals (cortex 24.7 ± 4.5 μmol/mL/min, p = 0.1 and hippocampus 25.3 ± 6.7 μmol/mL/min, p = 0.8) (Fig. 2). All measures of respiratory capacity within the mitochondrial ETS for each animal were normalized to mitochondrial content by CS activity.

3.2. Rapid non-impact rotational (RNR) injury

We utilized a large animal model of diffuse TBI and evaluated mitochondrial respiration in two regions of interest following RNR injury: cortex and hippocampus (Table 1). In sham animals, mitochondrial respiration by all measures were consistently higher in the hippocampus compared to the cortex, and reached significance for ETS_{CII} ($p < 0.04$) and ETS_{CI+CII} ($p < 0.04$) respiration when values were normalized for mitochondrial content. Post-RNR, all measures of ETS respiration were significantly higher ($p < 0.001$) in the hippocampal region compared to cortical respiration ($OXPHOS_{CI}$, ETS_{CII}, $OXPHOS_{CI+CII}$, ETS_{CI+CII}, $LEAK_{CI+CII}$, and complex IV) following normalization for mitochondrial content (Fig. 3).

We then compared each measure per CS and per mg of tissue in sham and RNR injured animals, region by region. Complex I-linked respiration ($OXPHOS_{CI}$) did not differ between RNR and sham animals in the hippocampus ($p = 0.4$) or cortex ($p = 0.6$) when normalized by CS activity (Fig. 3); however, $OXPHOS_{CI}$ expressed per mg of tissue was significantly decreased ($p < 0.05$) in the cortex compared to sham. Complex II-linked respiration (ETS_{CII}) per CS was significantly increased by nearly 20% in the cortex ($p < 0.05$) and hippocampus ($p = 0.02$) post-RNR, compared to shams. Furthermore, unlike complex I-driven respiration in the cortex, complex II-driven respiration normalized by tissue weight was not significantly reduced following RNR in either region. Maximal phosphorylating respiration ($OXPHOS_{CI+CII}$) per CS was significantly increased in the hippocampus post-RNR compared to $OXPHOS_{CI+CII}$ in shams ($p < 0.05$), but was not altered in the cortex by RNR injury ($p = 0.3$) (Fig. 3A). Maximal uncoupled non-phosphorylating respiration (ETS_{CI+CII}) per CS post-RNR did not change from shams in either the hippocampus ($p = 0.3$) or cortex ($p = 0.6$) (Fig. 3B). Both $OXPHOS_{CI+CII}$ and ETS_{CI+CII} were significantly reduced ($p < 0.02$) per mg of tissue in the cortex post-RNR compared to sham. Following diffuse TBI, complex IV respiration per CS measured from the hippocampus ($p = 0.4$) and cortex ($p = 0.7$) was similar to complex IV respiration from corresponding regions in shams (Fig. 3B). LEAK ($LEAK_{CI+CII}$), or State 4_o respiration, was significantly increased post-RNR in hippocampal tissue when normalized by CS activity ($p < 0.03$) (Fig. 3B), and per mg of tissue ($p < 0.01$) compared to shams. Cortical tissue post-RNR also exhibited a significant increase in LEAK respiration per CS ($p < 0.02$) compared to shams; and per mg of tissue ($p < 0.05$) compared to shams.

Respiratory ratios were calculated for sham and RNR animals (Table 2). The control ratio for $OXPHOS_{CI+CII}$ ($OXPHOS_{CI+CII}$/LEAK) decreased significantly post-RNR compared to shams in the cortex ($p < 0.01$) and hippocampus ($p < 0.05$) (Table 2). ETS_{CI+CII} control ratio (ETS_{CI+CII}/LEAK) also decreased significantly post-RNR, compared to sham animals (cortex: $p < 0.006$; Hippocampus: $p < 0.01$). The complex I contribution to convergent respiration post-RNR (ETS_{CI}/ETS_{CI+CII}) was significantly decreased in the hippocampus compared to sham ($p < 0.05$), and nearly significantly decreased in the cortex following RNR compared to shams ($p = 0.08$) (Table 2). Consequently, the complex II contribution to convergent respiration (ETS_{CII}/ETS_{CI+CII}) was significantly greater in the hippocampus post-RNR compared to sham animals ($p < 0.05$), and the increase in the cortex post-RNR nearly reached significance compared to sham ($p = 0.06$).

4. Discussion

We report differences in mitochondrial respiration between the cortex and hippocampus in the uninjured immature brain. Our data differs from the uninjured mature rodents where there were no reported differences in basal mitochondria respiration in samples isolated from the striatum, cortex and hippocampus (Sauerbeck et al., 2011). Twenty-four hours after a diffuse traumatic injury to the immature brain, interesting mitochondrial bioenergetic responses emerged, with diffuse injury inducing a significant uncoupling of oxidative and non-oxidative phosphorylation in both the cortex and hippocampus. LEAK respiration, State 4_o, was significantly increased in both the injured cortical and hippocampal tissues compared to their corresponding regions in sham animals. This increase in LEAK respiration (State 4_o) in both regions is the predominant factor that influences a significant decrease in RCRs ($OXPHOS_{CI+CII}$ (State 3)/LEAK (State 4_o)), especially in the hippocampus where $OXPHOS_{CI+CII}$ is significantly increased compared to hippocampal respiration in shams. Our assessments of functional mitochondrial bioenergetics, 24 h after diffuse TBI, differs from our previously published data in focal injury at the same time-point (Kilbaugh et al., 2015). While there seems to be a common dependence on complex II-driven respiration following both focal and diffuse TBI, diffuse TBI displayed significant uncoupling of oxidative phosphorylation which was not seen in injured tissue following focal TBI (Kilbaugh et al., 2015). The differences in mitochondrial response following diffuse and focal TBI, at similar time-points, emphasizes the heterogeneity of brain injury pathology. Thus, investigations of mitochondrial metabolic pathways following differing injury mechanisms are essential to direct future mitochondrial intervention trials in TBI.

Control ratios ETS_{CI}/ETS_{CI+CII} and ETS_{CII}/ETS_{CI+II} further support the notion that complex I respiration is impaired to some degree following injury, especially in the hippocampus, while convergent respiration via complex II respiration is stimulated at 24 h post-RNR. This potential compensatory response in convergent respiration may stimulate a significant increase in maximal phosphorylating respiration and a trend toward increased maximal non-phosphorylating respiration in the hippocampus compared to hippocampal mitochondrial respiration in shams. The relative increase in complex II-driven respiration in the cortex and hippocampus when normalized for mitochondrial content may

Table 1
Respiration of brain tissue homogenates from sham and diffuse rapid non-impact rotational TBI.

Respiratory parameters	Per mg of tissue (pmols O_2/s ∗ mg)				Per CS activity (pmols O_2/s ∗ mg ∗ CS)			
	Sham (n = 10)		RNR (n = 18)		Sham (n = 10)		RNR (n = 18)	
	Cortex	Hippo	Cortex	Hippo	Cortex	Hippo	Cortex	Hippo
$OXPHOS_{CI}$	38.0 ± 2.7	39.6 ± 2.8	29.7 ± 1.8*	35.9 ± 2.8	1.6 ± 0.2	1.9 ± 0.3	1.8 ± 0.1	2.3 ± 0.1
ETS_{CII}	41.6 ± 2.1	47.3 ± 3.1	36.7 ± 2.4	47.8 ± 3.3	1.9 ± 0.1	2.4 ± 0.4	2.3 ± 0.1*	3.2 ± 0.1*
$OXPHOS_{CI+CII}$	76.0 ± 4.0	80.6 ± 6.0	67.7 ± 1.9*	82.4 ± 3.5	3.4 ± 0.4	4.0 ± 0.6	3.9 ± 0.1	5.2 ± 0.2*
ETS_{CI+CII}	61.2 ± 3.1	67.6 ± 3.9	51.2 ± 1.8*	66.1 ± 2.3	2.7 ± 0.3	3.4 ± 0.5	3.0 ± 0.1	4.1 ± 0.1*
Complex IV	106.4 ± 5.5	121.5 ± 8.3	98.3 ± 5.9	118.5 ± 3.5	5.1 ± 0.6	5.9 ± 0.9	5.7 ± 0.4	7.3 ± 0.2*
$LEAK_{CI+CII}$	13.9 ± 0.9	16.3 ± 0.8	16.1 ± 0.9*	19.2 ± 0.6*	0.67 ± 0.2	0.86 ± 0.1	0.93 ± 0.2*	1.2 ± 0.04*

Mitochondrial respiration of brain tissue homogenates from the cortex (cortex) and hippocampus (hippo) region in two cohorts: sham and 24 h post-Rapid non-impact rotational injury (RNR). Respiration is expressed per mg of tissue (pmols O_2/s ∗ mg), and per citrate synthase activity (pmols O_2/s ∗ CS) to normalize data for mitochondrial content. Presented as mean ± SEM; For definitions of respiratory states and substrates utilized, please see Fig. 1.

* $p < 0.05$ significant different from corresponding sham region.

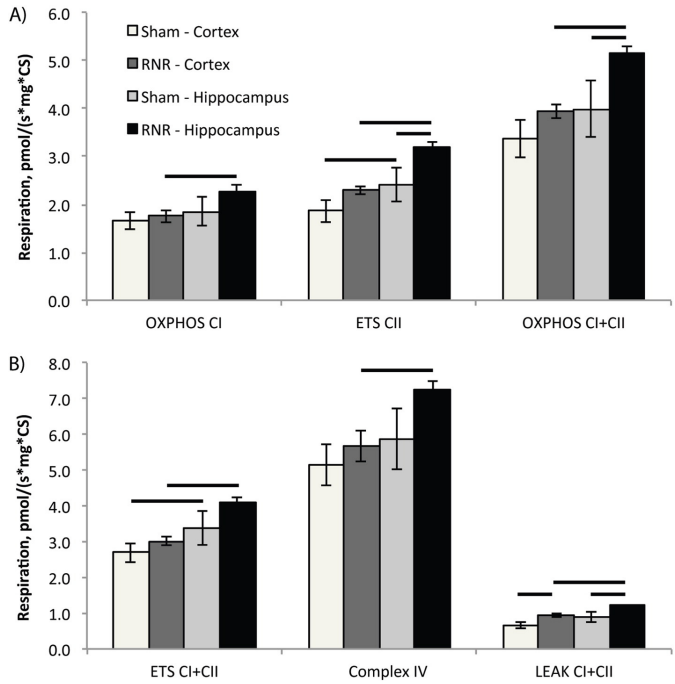

Fig. 3. Mitochondrial respiration from RNR injured and shams normalized by mitochondrial content (citrate synthase) measured 24 h post TBI. A) At 24 h post-RNR Complex II-driven respiration, ETS_{CII} and maximal, coupled phosphorylating respiration $OXPHOS_{CI+CII}$ was significantly increased compared to hippocampal respiration from sham animals. B) In addition, $LEAK_{CI+CII}$ respiration is significantly increased in both injured regions compared to corresponding regions in sham animals. Presented as mean ± SEM. For definitions of respiratory states and substrates utilized please see Fig. 1. Bars, $p < 0.05$.

be a compensatory response at 24 h in an attempt to increase mitochondrial bioenergetic output. We also speculate that the increase in regional hippocampal maximal phosphorylating mitochondrial respiration ($OXPHOS_{CI+CII}$) may be related to increased excitability of hippocampal tissue secondary to pathologic changes in inhibitory function following TBI, triggering increased bioenergetic need to compensate for ongoing secondary injury (Witgen et al., 2005). Yoshino and colleagues presented evidence in rats that hypermetabolism occurred post injury in both the cortex and hippocampus, with an especially marked response in the hippocampus (84.4–91% higher than control) compared to the cortex (30.1–46.6%); however, this hypermetabolic phase only lasted 6 h before the rodents transitioned to a hypometabolic phase lasting as long as 5 days (Yoshino et al., 1991). With limited research available, the time course and mechanistic response to a purely diffuse injury remains unclear. Future research will need to be conducted to establish correlations between alterations in mitochondrial bioenergetics and outcomes in diffuse immature brain injury.

Table 2
Respiratory ratios of brain tissue homogenates from sham and diffuse rapid non-impact rotational TBI.

Respiratory ratios	Sham (n = 10)		CCI (n = 18)	
	Cortex	Hippo	Cortex	Hippo
$OXPHOS_{CI+CII}$/LEAK	5.7 ± 0.4	5.0 ± 0.3	4.3 ± 0.2*	4.3 ± 0.2*
ETS_{CI+CII}/LEAK	4.6 ± 0.4	4.3 ± 0.2	3.3 ± 0.2*	3.4 ± 0.1*
ETS_{CI}/ETS_{CI+CII}	0.32 ± 0.02	0.31 ± 0.02	0.29 ± 0.04	0.28 ± 0.04*
ETS_{CII}/ETS_{CI+CII}	0.68 ± 0.02	0.69 ± 0.02	0.71 ± 0.01*	0.72 ± 0.04*
ETS_{CII}/ETS_{CI}	2.32 ± 0.23	2.40 ± 0.17	3.1 ± 0.34*	3.33 ± 0.33*

Respiratory ratios were also calculated. ETS_{CI} was calculated by subtracting ETS_{CI+CII} minus ETS_{CII}. Presented as mean ± SEM; For definitions of respiratory states and substrates utilized, please see Fig. 1.

* $p < 0.05$ significant different from corresponding sham region respiratory ratio.

In addition, an increase in LEAK respiration may represent mitochondrial membrane permeability transition (mPT) and a loss of functional integrity with a dissipation of the proton motive force, or a "protective" uncoupling that limits ATP production to inhibit secondary injury. State 4_o or LEAK respiration is determined mainly by proton leak across the inner membrane mediated by endogenous uncoupling proteins (UCPs), which utilize free fatty acids energy potential to translocate protons. When LEAK respiration increases, there is a resultant reduction in the mitochondrial membrane potential ($\Delta\Psi$) and ATP production; however, despite the loss of ATP production transient or mild uncoupling may confer neuroprotective properties by limiting ROS generation, mitochondrial Ca^{2+} uptake, and limiting excitotoxic neuronal death (Brand, 2000; Brookes, 2005; Mattiasson et al., 2003; Perez-Pinzon et al., 2012; P. G. Sullivan et al., 2004). This may involve the release of free fatty acids (FFA) that stimulate UCPs, especially UCP2, as a protective anti-ROS mechanism; and, future study will elucidate the mechanism and time courses involved in the immature brain. The timing and mechanism is extremely important, because this uncoupling may limit the ability of mitochondria to increase oxidative phosphorylation in response to ongoing and persistent bioenergetic

needs following TBI. Future studies will be performed to delineate the exact molecular cascades and injury timelines in response to diffuse injury.

In our previous study of 3–5-day-old infant piglets we showed that 24 h after RNR there was a significant reduction in maximal phosphorylating respiration (State 3) and a trend toward increases in State 4_o respiration compared to sham respiration in both the hippocampus and the cortex, lowering the overall respiratory control ratio (Kilbaugh et al., 2011). To compare the injury severity between these studies, the total injury volume was measured by β-APP reactivity and hematoxylin and eosin stain via histopathology in a group of N = 10 4-week-old piglets with the same RNR in the sagittal direction as the current study, which resulted in an average total injured volume of 0.79 ± 0.08%. In our previous study with 3–5-day-old piglets (n = 5), also with a sagittal RNR injury, there was a significantly higher average injured volume of 2.18 ± 0.02%. Based on these findings we postulate that a greater severity of injury post-RNR stimulates a greater reduction in mitochondrial respiration. This postulate correlates with previous work in mature rodents that shows TBI results in the disruption of brain bioenergetics and the resultant bioenergetic deficits are proportional to the degree of severity (Marklund et al., 2006). In more severe brain injury, levels of ATP and other indicators of mitochondrial bioenergetics are significantly reduced at 24 h and remain depressed for days or weeks (Tavazzi et al., 2005). Conversely, animals with mild TBI (mTBI) had the lowest value of ATP levels at 6 h with a gradual resolution near sham levels by 24 h that showed no statistical difference by 5 days post-injury with control animals (Signoretti et al., 2001). A limitation of drawing a direct comparison from our study to studies that quantified ATP levels is that respirometry provides a functional surrogate marker of ATP synthesis by measuring maximal coupled and uncoupled respiration. The difference between our current study and the previous post-RNR study may be due to developmental differences between infant and toddler, differences in methodology with isolated mitochondrial and tissue homogenates, or the possibility that it may be secondary to injury severity and its effects on mitochondrial function. Further study is critical to understand age-related alterations in mitochondrial bioenergetics, time course of mitochondrial dysfunction, and the effect of injury severity on both age and time course.

4.1. Limitations

Our pilot study of functional, integrated mitochondrial bioenergetic pathways following diffuse TBI generates questions about the complex mechanisms of secondary brain injury following diffuse TBI. Future studies will expand our molecular investigations, including isolated mitochondria and spectrophotometric analysis, to further interrogate the electron transport complex and develop a more complete understanding of the adaptive response and ongoing secondary injury. Finally, in our current experiment there is some variability in our CS measurement in the sham animals which we have not found in our previous studies (Kilbaugh et al., 2015). This was a large animal study with smaller group sizes, and although a small number of animals fell outside of the standard deviation we did not feel that it was appropriate from a rigorous scientific/statistical standpoint to exclude these animals from the sham cohort. We presented the data in multiple ways, including data measures independent of the CS, and drew our conclusions based on all measures of the data.

5. Conclusion

We conclude that there are significant alterations in mitochondrial respiration 24 h after diffuse TBI that vary by location within the brain. In addition, our data suggest that following diffuse TBI there is significant uncoupling of oxidative phosphorylation and alterations in convergent respiration through complex I- and complex II-driven respiration. Thus, the results of our immature translational large animal model suggest therapeutic benefit for strategies that support oxidative phosphorylation and bioenergetic output in the developing brain after TBI.

Authors disclosure statement

Eskil Elmer and Magnus J. Hansson own shares in and have received salary support from NeuroVive Pharmaceutical AB, a public company active in the field of mitochondrial medicine. Michael Karlsson has received salary support from NeuroVive Pharmaceutical AB. All other authors have no competing financial interests.

Animal experimentation

All procedures were approved by the Institutional Animal Care and Use Committee of the University of Pennsylvania.

Acknowledgments

The authors would like to thank Melissa Byro, Ashley Bebee, Jill Ralston, Sarah Sullivan, Albana Shahini, and Saori Morota for their invaluable technical support. The Oroboros Oxygraph used in the study was a loan from NeuroVive Pharmaceutical AB, Lund Sweden. Studies were supported by the NIH UO1 NS069545.

References

Adelson, P.D., Pineda, J., Bell, M.J., Abend, N.S., Berger, R.P., Giza, C.C., Hotz, G., Wainwright, M.S., Pediatric TBI Demographics and Clinical Assessment Working Group, 2012. Common data elements for pediatric traumatic brain injury: recommendations from the working group on demographics and clinical assessment. J. Neurotrauma http://dx.doi.org/10.1089/neu.2011.1952.

Armstead, W.M., 2005. Age and cerebral circulation. Pathophysiology 12, 5–15. http://dx.doi.org/10.1016/j.pathophys.2005.01.002.

Balan, I.S., Saladino, A.J., Aarabi, B., Castellani, R.J., Wade, C., Stein, D.M., Eisenberg, H.M., Chen, H.H., Fiskum, G., 2013. Cellular alterations in human traumatic brain injury: changes in mitochondrial morphology reflect regional levels of injury severity. J. Neurotrauma 30, 367–381. http://dx.doi.org/10.1089/neu.2012.2339.

Bates, T.E., Almeida, A., Heales, S.J., Clark, J.B., 1994. Postnatal development of the complexes of the electron transport chain in isolated rat brain mitochondria. Dev. Neurosci. 16, 321–327.

Bowling, A.C., Mutisya, E.M., Walker, L.C., Price, D.L., Cork, L.C., Beal, M.F., 1993. Age-dependent impairment of mitochondrial function in primate brain. J. Neurochem. 60, 1964–1967.

Brand, M.D., 2000. Uncoupling to survive? The role of mitochondrial inefficiency in ageing. Exp. Gerontol. 35, 811–820.

Brookes, P.S., 2005. Mitochondrial $H^{(+)}$ leak and ROS generation: an odd couple. Free Radic. Biol. Med. 38, 12–23. http://dx.doi.org/10.1016/j.freeradbiomed.2004.10.016.

Brustovetsky, N., Jemmerson, R., Dubinsky, J.M., 2002. Calcium-induced cytochrome c release from rat brain mitochondria is altered by digitonin. Neurosci. Lett. 332, 91–94.

Coats, B., Margulies, S.S., 2006. Material properties of porcine parietal cortex. J. Biomech. 39, 2521–2525. http://dx.doi.org/10.1016/j.jbiomech.2005.07.020.

Coronado, V.G., Xu, L., Basavaraju, S.V., McGuire, L.C., Wald, M.M., Faul, M.D., Guzman, B.R., Hemphill, J.D., Centers for Disease Control and Prevention (CDC), 2011. Surveillance for traumatic brain injury-related deaths—United States, 1997–2007. MMWR Surveill. Summ. 60, 1–32.

Del Maestro, R., McDonald, W., 1987. Distribution of superoxide dismutase, glutathione peroxidase and catalase in developing rat brain. Mech. Ageing Dev. 41, 29–38.

Duhaime, A.-C., 2006. Large animal models of traumatic injury to the immature brain. Dev. Neurosci. 28, 380–387. http://dx.doi.org/10.1159/000094164.

Duhaime, A.C., Margulies, S.S., Durham, S.R., O'Rourke, M.M., Golden, J.A., Marwaha, S., Raghupathi, R., 2000. Maturation-dependent response of the piglet brain to scaled cortical impact. J. Neurosurg. 93, 455–462. http://dx.doi.org/10.3171/jns.2000.93.3.0455.

Durham, S.R., Duhaime, A.-C., 2007. Basic science; maturation-dependent response of the immature brain to experimental subdural hematoma. J. Neurotrauma 24, 5–14. http://dx.doi.org/10.1089/neu.2006.0054.

Eucker, S.A., Smith, C., Ralston, J., Friess, S.H., Margulies, S.S., 2011. Physiological and histopathological responses following closed rotational head injury depend on direction of head motion. Exp. Neurol. 227, 79–88. http://dx.doi.org/10.1016/j.expneurol.2010.09.015.

Gean, A.D., Fischbein, N.J., 2010. Head trauma. Neuroimaging Clin. N. Am. 20, 527–556. http://dx.doi.org/10.1016/j.nic.2010.08.001.

Gilmer, L.K., Ansari, M.A., Roberts, K.N., Scheff, S.W., 2010. Age-related mitochondrial changes after traumatic brain injury. J. Neurotrauma 27, 939–950. http://dx.doi.org/10.1089/neu.2009.1181.

Glenn, T.C., Kelly, D.F., Boscardin, W.J., Mcarthur, D.L., Vespa, P.M., Oertel, M., Hovda, D.A., Bergsneider, M., Hillered, L., Martin, N.A., 2003. Energy dysfunction as a predictor of outcome after moderate or severe head injury: indices of oxygen, glucose, and lactate

metabolism. J. Cereb. Blood Flow Metab. 23, 1239–1250. http://dx.doi.org/10.1097/01.WCB.0000089833.23606.7F.
Gnaiger, E., 2009. Capacity of oxidative phosphorylation in human skeletal muscle: new perspectives of mitochondrial physiology. Int. J. Biochem. Cell Biol. 41, 1837–1845. http://dx.doi.org/10.1016/j.biocel.2009.03.013.
Grate, L.L., Golden, J.A., Hoopes, P.J., Hunter, J.V., Duhaime, A.-C., 2003. Traumatic brain injury in piglets of different ages: techniques for lesion analysis using histology and magnetic resonance imaging. J. Neurosci. Methods 123, 201–206.
Ibrahim, N.G., Ralston, J., Smith, C., Margulies, S.S., 2010. Physiological and pathological responses to head rotations in toddler piglets. J. Neurotrauma 27, 1021–1035. http://dx.doi.org/10.1089/neu.2009.1212.
Jaber, S.M., Sullivan, S., Margulies, S.S., 2015. Noninvasive metrics for identification of brain injury deficits in piglets. Dev. Neuropsychol. 40, 34–39. http://dx.doi.org/10.1080/87565641.2014.969733.
Kilbaugh, T.J., Bhandare, S., Lorom, D.H., Saraswati, M., Robertson, C.L., Margulies, S.S., 2011. Cyclosporin a preserves mitochondrial function after traumatic brain injury in the immature rat and piglet. J. Neurotrauma 28, 763–774. http://dx.doi.org/10.1089/neu.2010.1635.
Kilbaugh, T.J., Karlsson, M., Byro, M., Bebee, A., Ralston, J., Sullivan, S., Duhaime, A.-C., Hansson, M.J., Elmér, E., Margulies, S.S., 2015. Mitochondrial bioenergetic alterations after focal traumatic brain injury in the immature brain. Exp. Neurol. 271, 136–144. http://dx.doi.org/10.1016/j.expneurol.2015.05.009.
Larsen, S., Nielsen, J., Hansen, C.N., Nielsen, L.B., Wibrand, F., Stride, N., Schroder, H.D., Boushel, R., Helge, J.W., Dela, F., Hey-Mogensen, M., 2012. Biomarkers of mitochondrial content in skeletal muscle of healthy young human subjects. J. Physiol. Lond. 590, 3349–3360. http://dx.doi.org/10.1113/jphysiol.2012.230185.
Lifshitz, J., Friberg, H., Neumar, R.W., Raghupathi, R., Welsh, F.A., Janmey, P., Saatman, K.E., Wieloch, T., Grady, M.S., McIntosh, T.K., 2003. Structural and functional damage sustained by mitochondria after traumatic brain injury in the rat: evidence for differentially sensitive populations in the cortex and hippocampus. J. Cereb. Blood Flow Metab. 23, 219–231.
Lifshitz, J., Sullivan, P.G., Hovda, D.A., Wieloch, T., McIntosh, T.K., 2004. Mitochondrial damage and dysfunction in traumatic brain injury. Mitochondrion 4, 705–713. http://dx.doi.org/10.1016/j.mito.2004.07.021.
Marcoux, J., McArthur, D.A., Miller, C., Glenn, T.C., Villablanca, P., Martin, N.A., Hovda, D.A., Alger, J.R., Vespa, P.M., 2008. Persistent metabolic crisis as measured by elevated cerebral microdialysis lactate-pyruvate ratio predicts chronic frontal lobe brain atrophy after traumatic brain injury. Crit. Care Med. 36, 2871–2877. http://dx.doi.org/10.1097/CCM.0b013e318186a4a0.
Marklund, N., Salci, K., Ronquist, G., Hillered, L., 2006. Energy metabolic changes in the early post-injury period following traumatic brain injury in rats. Neurochem. Res. 31, 1085–1093. http://dx.doi.org/10.1007/s11064-006-9120-0.
Mattiasson, G., Shamloo, M., Gido, G., Mathi, K., Tomasevic, G., Yi, S., Warden, C.H., Castilho, R.F., Melcher, T., Gonzalez-Zulueta, M., Nikolich, K., Wieloch, T., 2003. Uncoupling protein-2 prevents neuronal death and diminishes brain dysfunction after stroke and brain trauma. Nat. Med. 9, 1062–1068. http://dx.doi.org/10.1038/nm903.
Miller, A.C., Odenkirchen, J., Duhaime, A.C., 2012. Common Data Elements for Research on Traumatic Brain Injury: Pediatric Considerations (Journal of ….).
Missios, S., Harris, B.T., Dodge, C.P., Simoni, M.K., Costine, B.A., Lee, Y.-L., Quebada, P.B., Hillier, S.C., Adams, L.B., Duhaime, A.-C., 2009. Scaled cortical impact in immature swine: effect of age and gender on lesion volume. J. Neurotrauma 26, 1943–1951. http://dx.doi.org/10.1089/neu.2009-0956.
Perez-Pinzon, M.A., Stetler, R.A., Fiskum, G., 2012. Novel mitochondrial targets for neuroprotection. Journal of cerebral blood flow & amp. Metabolism 32, 1362–1376. http://dx.doi.org/10.1038/jcbfm.2012.32.
Ragan, D.K., McKinstry, R., Benzinger, T., Leonard, J.R., Pineda, J.A., 2013. Alterations in cerebral oxygen metabolism after traumatic brain injury in children. J. Cereb. Blood Flow Metab. 33, 48–52. http://dx.doi.org/10.1038/jcbfm.2012.130.
Raghupathi, R., Mehr, M.F., Helfaer, M.A., Margulies, S.S., 2004. Traumatic axonal injury is exacerbated following repetitive closed head injury in the neonatal pig. J. Neurotrauma 21, 307–316. http://dx.doi.org/10.1089/089771504322972095.
Robertson, C.L., Scafidi, S., McKenna, M.C., Fiskum, G., 2009. Mitochondrial mechanisms of cell death and neuroprotection in pediatric ischemic and traumatic brain injury. Exp. Neurol. 218, 371–380. http://dx.doi.org/10.1016/j.expneurol.2009.04.030.
Sauerbeck, A., Pandya, J., Singh, I., Bittman, K., Readnower, R., Bing, G., Sullivan, P., 2011. Analysis of regional brain mitochondrial bioenergetics and susceptibility to mitochondrial inhibition utilizing a microplate based system. J. Neurosci. Methods 198, 36–43. http://dx.doi.org/10.1016/j.jneumeth.2011.03.007.
Signoretti, S., Marmarou, A., Tavazzi, B., Lazzarino, G., Beaumont, A., Vagnozzi, R., 2001. N-acetylaspartate reduction as a measure of injury severity and mitochondrial dysfunction following diffuse traumatic brain injury. J. Neurotrauma 18, 977–991. http://dx.doi.org/10.1089/08977150152693683.
Sims, N.R., Blass, J.P., 1986. Expression of classical mitochondrial respiratory responses in homogenates of rat forebrain. J. Neurochem. 47, 496–505.
Sullivan, P.G., Springer, J.E., Hall, E.D., Scheff, S.W., 2004. Mitochondrial uncoupling as a therapeutic target following neuronal injury. J. Bioenerg. Biomembr. 36, 353–356. http://dx.doi.org/10.1023/B:JOBB.0000041767.30992.19.
Sullivan, S., Eucker, S.A., Gabrieli, D., Bradfield, C., Coats, B., Maltese, M.R., Lee, J., Smith, C., Margulies, S.S., 2015. White matter tract-oriented deformation predicts traumatic axonal brain injury and reveals rotational direction-specific vulnerabilities. Biomech. Model. Mechanobiol. 14, 877–896. http://dx.doi.org/10.1007/s10237-014-0643-z.
Sullivan, S., Friess, S.H., Ralston, J., Smith, C., Propert, K.J., Rapp, P.E., Margulies, S.S., 2013. Improved behavior, motor, and cognition assessments in neonatal piglets. J. Neurotrauma 130613004306008. http://dx.doi.org/10.1089/neu.2013.2913.
Tavazzi, B., Signoretti, S., Lazzarino, G., Amorini, A.M., Delfini, R., Cimatti, M., Marmarou, A., Vagnozzi, R., 2005. Cerebral oxidative stress and depression of energy metabolism correlate with severity of diffuse brain injury in rats. Neurosurgery 56, 582–589 (discussion 582–9).
Weeks, D., Sullivan, S., Kilbaugh, T.J., Smith, C., Margulies, S.S., 2014. Influences of developmental age on the resolution of diffuse traumatic intracranial hemorrhage and axonal injury. J. Neurotrauma 31, 206–214. http://dx.doi.org/10.1089/neu.2013.3113.
Witgen, B.M., Lifshitz, J., Smith, M.L., Schwarzbach, E., Liang, S.-L., Grady, M.S., Cohen, A.S., 2005. Regional hippocampal alteration associated with cognitive deficit following experimental brain injury: a systems, network and cellular evaluation. Neuroscience 133, 1–15. http://dx.doi.org/10.1016/j.neuroscience.2005.01.052.
Xu, Y., Mcarthur, D.L., Alger, J.R., Etchepare, M., Hovda, D.A., Glenn, T.C., Huang, S., Dinov, I., Vespa, P.M., 2010. Early nonischemic oxidative metabolic dysfunction leads to chronic brain atrophy in traumatic brain injury. J. Cereb. Blood Flow Metab. 30, 883–894. http://dx.doi.org/10.1038/jcbfm.2009.263.
Yoshino, A., Hovda, D.A., Kawamata, T., Katayama, Y., Becker, D.P., 1991. Dynamic changes in local cerebral glucose utilization following cerebral conclusion in rats: evidence of a hyper- and subsequent hypometabolic state. Brain Res. 561, 106–119.

Paper IV

nature COMMUNICATIONS

ARTICLE

Received 16 Apr 2016 | Accepted 21 Jun 2016 | Published 9 Aug 2016

DOI: 10.1038/ncomms12317 OPEN

Cell-permeable succinate prodrugs bypass mitochondrial complex I deficiency

Johannes K. Ehinger[1,2,3], Sarah Piel[1,2], Rhonan Ford[4], Michael Karlsson[1,2], Fredrik Sjövall[1,5], Eleonor Åsander Frostner[1,2], Saori Morota[1], Robert W. Taylor[6], Doug M. Turnbull[6], Clive Cornell[4], Steven J. Moss[7], Carsten Metzsch[8], Magnus J. Hansson[1,2], Hans Fliri[9] & Eskil Elmér[1,2,10]

Mitochondrial complex I (CI) deficiency is the most prevalent defect in the respiratory chain in paediatric mitochondrial disease. This heterogeneous group of diseases includes serious or fatal neurological presentations such as Leigh syndrome and there are very limited evidence-based treatment options available. Here we describe that cell membrane-permeable prodrugs of the complex II substrate succinate increase ATP-linked mitochondrial respiration in CI-deficient human blood cells, fibroblasts and heart fibres. Lactate accumulation in platelets due to rotenone-induced CI inhibition is reversed and rotenone-induced increase in lactate:pyruvate ratio in white blood cells is alleviated. Metabolomic analyses demonstrate delivery and metabolism of [^{13}C]succinate. In Leigh syndrome patient fibroblasts, with a recessive *NDUFS2* mutation, respiration and spare respiratory capacity are increased by prodrug administration. We conclude that prodrug-delivered succinate bypasses CI and supports electron transport, membrane potential and ATP production. This strategy offers a potential future therapy for metabolic decompensation due to mitochondrial CI dysfunction.

[1] Mitochondrial Medicine, Department of Clinical Sciences Lund, Faculty of Medicine, Lund University, BMC A13, 221 84 Lund, Sweden. [2] NeuroVive Pharmaceutical AB, Medicon Village, 223 81 Lund, Sweden. [3] Department of Otorhinolaryngology, Head and Neck Surgery, Department of Clinical Sciences Lund, Lund University, Skåne University Hospital, 221 85 Lund, Sweden. [4] Selcia Ltd, Fyfield Business and Research Park, Fyfield Road, Ongar CM5 0GS, Essex, UK. [5] Department of Intensive Care and Perioperative Medicine, Skåne University Hospital, 205 02 Malmö, Sweden. [6] Wellcome Trust Centre for Mitochondrial Research, Institute of Neuroscience, The Medical School, Newcastle University, Newcastle upon Tyne NE2 4HH, UK. [7] Isomerase Therapeutics Ltd, Chesterford Research Park, Cambridge CB10 1XL, UK. [8] Anaesthesiology and Intensive Care, Department of Clinical Sciences Lund, Faculty of Medicine, Lund University, 221 85 Lund, Sweden. [9] Mitopharm Ltd, Fyfield Business and Research Park, Fyfield Road, Ongar CM5 0GS, Essex, UK. [10] Clinical Neurophysiology, Department of Clinical Sciences Lund, Lund University, Skåne University Hospital, 221 85 Lund, Sweden. Correspondence and requests for materials should be addressed to J.K.E. (email: johannes.ehinger@med.lu.se).

Paediatric mitochondrial disease due to complex I (CI) deficiency is a heterogeneous group of disorders, and can be due to alterations in either the nuclear or mitochondrial genome. It is the most prevalent defect in the respiratory chain in paediatric patients and often leads to serious or fatal neurological presentations, such as Leigh syndrome[1]. There are currently very limited evidence-based treatment options directed towards mitochondrial respiratory chain dysfunction[2,3]. Succinate is a mitochondrial substrate metabolized through complex II (CII). It is not cell membrane-permeable and exogenously given succinate has limited uptake into cells.

Here we describe that cell membrane-permeable prodrugs of succinate provide increased ATP-linked mitochondrial oxygen consumption in CI-deficient human cells and tissues, which offers a potential future intervention for patients with metabolic decompensation due to mitochondrial CI dysfunction.

Results

Drug development and screening. In a drug discovery program, >50 different prodrugs of succinate[4] were designed, synthesized and evaluated for cell permeability and ability to support respiration independent of CI in human peripheral blood cells from healthy donors (platelets and mononuclear cells (PBMCs)) using an Oroboros O2k respirometer. Three compounds were selected for further evaluation: NV101-118 (NV118, diacetoxymethyl succinate), NV101-189 (NV189, bis-(1-acetoxy-ethyl) succinate) and NV101-241 (NV241, 1-acetoxyethyl acetoxymethyl succinate) (Fig. 1a). This article focuses on NV189, but qualitatively the results for all three prodrugs were similar and data on the other compounds are presented as Supplementary Figs.

Increased CII-linked respiration. At 100 μM, NV189 increased mitochondrial oxygen consumption in intact platelets with CI inhibition induced by the mitochondrial toxin rotenone (2 μM). Neither succinate nor monomethyl succinate, a monoester of succinate previously reported to be cell permeable[5], increased mitochondrial respiration (Fig. 1b; Supplementary Fig. 1a). In cells with normal CI function, oxygen consumption was also increased upon addition of 100 μM NV189 (Fig. 1c; Supplementary Fig. 1b). To exclude the possibility that increased respiration was due to an induction of proton leak through the mitochondrial inner membrane (uncoupling), the platelets were treated with the ATP synthase inhibitor oligomycin. This prompted a significant decrease in oxygen consumption, which indicates the extent of respiration linked to ADP phosphorylation (Fig. 1c; Supplementary Fig. 1b). Increased substrate supply, rather than uncoupling, was further demonstrated by measuring mitochondrial inner membrane potential with the positively charged membrane-permeable probe tetramethylrhodamine methyl ester (TMRM) in non-quench mode using fluorescence-activated cell sorting. TMRM fluorescence was increased in CI-inhibited human platelets upon addition of 250 μM NV189 and fluorescence increased further with ATP synthase inhibition, indicating mitochondrial membrane hyperpolarization (Fig. 1d). Cells with maximal uncoupled respiratory chain activity via titration of the protonophore carbonyl cyanide *p*-(trifluoromethoxy) phenylhydrazone (FCCP) increased oxygen consumption even more with addition of 250 μM NV189, further indicating increased substrate supply to the respiratory chain (Fig. 1e; Supplementary Fig. 1c). In blood cells, pre-permeabilized with the detergent digitonin, 250 μM NV189 did not induce any increase in respiration, while succinate control did, showing the need for intracellular metabolism for succinate to be released and made available to the mitochondria (Fig. 1f; Supplementary Fig. 1d). To confirm that the increase in respiration is specifically due to respiration through CII, a cell-permeable prodrug of the CII inhibitor malonate, NV01-161, (NV161, diacetoxymethyl malonate, Fig. 1h) was designed, synthesized and evaluated (Supplementary Fig. 2). Intact cells exposed to succinate prodrugs were treated with NV161 with ensuing decrease in respiration (Fig. 1g; Supplementary Fig. 1e). The applicability of the platelet data to other cell types was evaluated by assessing respiration in PBMCs treated with NV189 with or without CI inhibition with similar results to those in platelets (Fig. 1i,j; Supplementary Fig. 1f,g).

Paediatric mitochondrial diseases primarily display symptoms from energy intense organs such as the liver, brain, muscles, retina and cochlea. In some reports, 30–40% of paediatric patients with respiratory chain CI dysfunction present with cardiomyopathy[6,7], a condition that is linked to higher mortality[8]. Human atrial heart muscle biopsies from elective surgery were acquired and the fibres gently separated using forceps. The fibres were incubated with the CI inhibitor rotenone and subsequently treated with succinate prodrug, eliciting an increase in oxygen consumption (Fig. 1k; Supplementary Fig. 1h).

Attenuated lactate production. A hallmark of mitochondrial disease is lactic acidosis. When the mitochondrial energy production fails to comply with demand, pyruvate is converted to lactate to maintain the NAD^+ pool, causing increased lactate levels and decreased pH in blood and cerebrospinal fluid in the patients. About 80% of patients with mitochondrial disease show signs of lactate accumulation[6,8,9]. We incubated human platelets with or without 2 μM rotenone and measured lactate accumulation in media over time. With CI inhibition, the cells displayed a significantly higher lactate production than control, 4.30 ± 0.24 μmol lactate per 10^9 cells per hour compared with control level 1.73 ± 0.5 (regression slope ± s.d.), but with incubation with NV189 the rotenone-induced lactate production was similar to control level (1.26 ± 0.19). To verify the viability of the cell preparation, the glycolytic pathway upon drug addition and the specificity of CII-mediated ATP supply, cells were incubated with NV189, rotenone and an inhibitor of the downstream respiratory chain complex III (antimycin A, 1 μg ml^{-1}), eliciting lactate production at the level of that of rotenone alone (4.44 ± 0.19; Fig. 1m,n; Supplementary Fig. 1i).

Metabolomics confirms metabolism of delivered succinate. To elucidate the intracellular metabolism of NV189, a metabolomic assay was performed on PBMCs from four healthy donors. Cells were incubated with or without rotenone and with or without NV189 for 20 min. Using quantitative capillary electrophoresis mass spectrometry (CE-MS), the concentrations of 116 metabolites were determined. Delivery of intracellular succinate and anaplerosis of tricarboxylic acid (TCA) cycle intermediates were confirmed (Fig. 2a; Supplementary Fig. 3). The lactate:pyruvate ratio was increased when cells were inhibited with rotenone and normalized when the cells were treated with NV189 (Fig. 1l). No conclusive alterations due to drug treatment in metabolism of succinyl-CoA-related amino acids or glycolysis could be shown. Levels of cysteine were decreased, which could indicate oxidative stress. To investigate the time course of intracellular metabolism of delivered succinate, [1, 2, 3, 4-$^{13}C_4$]NV118 was synthesized, whereby the carbon atoms in NV118 that upon release would comprise the four carbon atoms in succinate were enriched with the stable isotope ^{13}C. This distinguishes between endogenous TCA cycle intermediates and metabolites originating from the prodrug-delivered succinate. NV118 rather than NV189 was used due to relatively less complex synthesis. Human platelets were then

incubated with [1, 2, 3, 4-$^{13}C_4$]NV118 for 7.5, 15, 30, 120 and 240 min. Even at the first time point, [$^{13}C_4$]malate and [$^{13}C_4$]citrate were observed, demonstrating rapid entry of [$^{13}C_4$]succinate into the TCA cycle (Fig. 2b). There was also [$^{13}C_6$]citrate present, which indicates that [^{13}C]oxaloacetate or [^{13}C]malate had converted to pyruvate and through acetyl-CoA formed citrate with [$^{13}C_4$]oxaloacetate (Fig. 2b; Supplementary Fig. 4), demonstrating continuous metabolism in the TCA cycle. The ratio of labelled species gradually declined with time but still after 240 min, there was a supply of labelled succinate available.

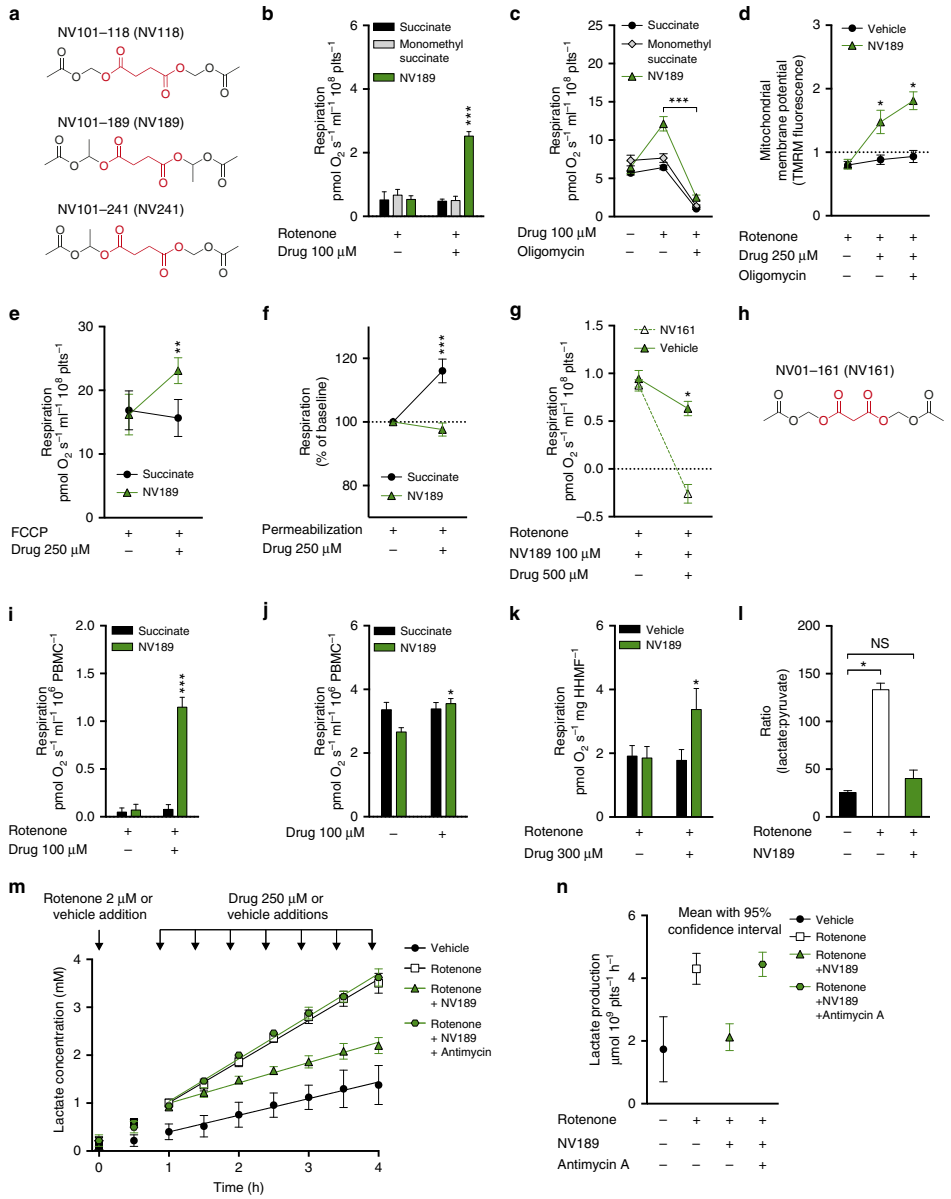

Figure 1 | Effects of mitochondrial complex II stimulation by the succinate prodrug NV189. (**a**) Structures of NV118, NV189 and NV241, succinate highlighted in red. (**b**) Respiration in platelets (plts) with rotenone-induced mitochondrial complex I (CI) inhibition. (**c**) ATP-generating respiration in platelets. (**d**) Mitochondrial membrane potential in complex I-inhibited platelets, ratio of basal TMRM fluorescence, $n=4$. (**e**) Respiration in platelets with FCCP-induced uncoupling. (**f**) Respiration in digitonin-permeabilized platelets. (**g**) Effect on respiration in platelets with addition of the cell-permeable complex II inhibitor NV161, * indicate significant difference between NV161 and vehicle, $n=4$. (**h**) Structure of NV161, malonate highlighted in red. (**i**) Respiration in peripheral blood mononuclear cells (PBMCs) with rotenone-induced CI inhibition, $n=4$. (**j**) Convergent respiration in PBMCs, $n=4$, * indicate significant difference between pre and post dosing. (**k**) Respiration in human heart muscle fibres (HHMFs), $n=5$. (**l**) Lactate:pyruvate ratio in PBMCs at baseline, after rotenone CI inhibition and after treatment with NV189, $n=4$. * indicates significant difference using Friedmans non-parametric paired test with Dunn's multiple comparisons test of all groups against control. For three data points, pyruvate was below detection limit and the estimated lower-quantification limit was used for calculating the ratio. (**m**) Lactate accumulation in 2 ml buffer containing 400×10^6 platelets, incubated with or without rotenone, antimycin A and NV189, $n=5$. (**n**) Lactate production in platelets, data quantification from previous panel. Mean with 95% confidence interval. All respirometric experiments in human platelets were performed with $n=6$ individuals donors if not otherwise stated. All data presented as mean and s.e. if not otherwise stated. In all experiments, blood cells from separate donors are used for each *n*. $^*P<0.05$, $^{**}P<0.01$, $^{***}P<0.001$ (two-tailed paired or unpaired Student's *t*-test as appropriate, difference between test compound and control if not otherwise stated).

Respiration increased in Leigh syndrome patient fibroblasts. To evaluate the effect of NV189 on patient cells, fibroblasts from a patient with Leigh syndrome due to recessive nuclear DNA mutations in the structural CI gene *NDUFS2* and three control cell lines were investigated using a Seahorse Bioscience XF^e 96 Extracellular Flux Analyzer (Fig. 3; Supplementary Fig. 5). The patient fibroblasts have previously been shown to exhibit severely decreased activity of CI, decreased CI assembly and lower expression of CI structural proteins[10]. Pooled data from all experiments (Fig. 3c,d; Supplementary Fig. 5c,d) revealed a 25% decrease in basal oxygen consumption rate (OCR) and a 42% reduction in maximum uncoupled respiration in the Leigh syndrome patient cells compared with the mean of the control cell lines. After addition of NV189, the OCR was similar between

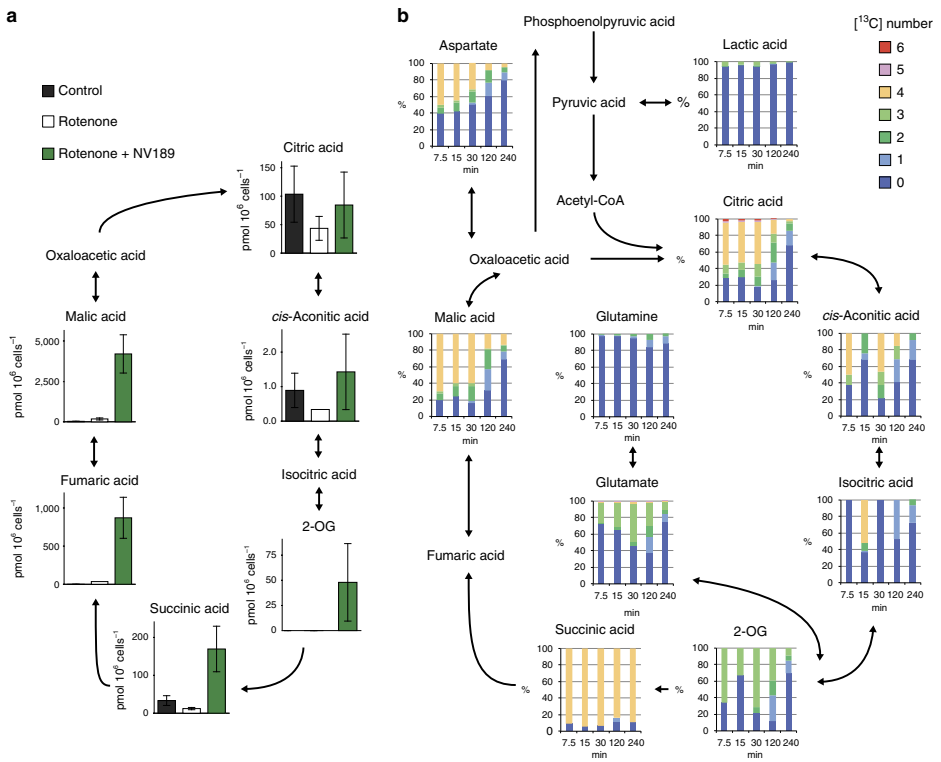

Figure 2 | Intracellular metabolism of exogenous prodrug-delivered succinate. (**a**) TCA cycle intermediates in peripheral blood mononuclear cells after 20 min incubation with or without rotenone and NV189 quantified using capillary electrophoresis mass spectrometry, $n=4$. Data presented as mean and s.d. (**b**) Fraction of [^{13}C] isotope labelled carbons in TCA cycle intermediates and related metabolites in human platelets incubated with [1, 2, 3, 4-$^{13}C_4$]NV118 for 7.5, 15, 30, 120 or 240 min. Mean of $n=2$. 2-OG, 2-oxoglutaric acid.

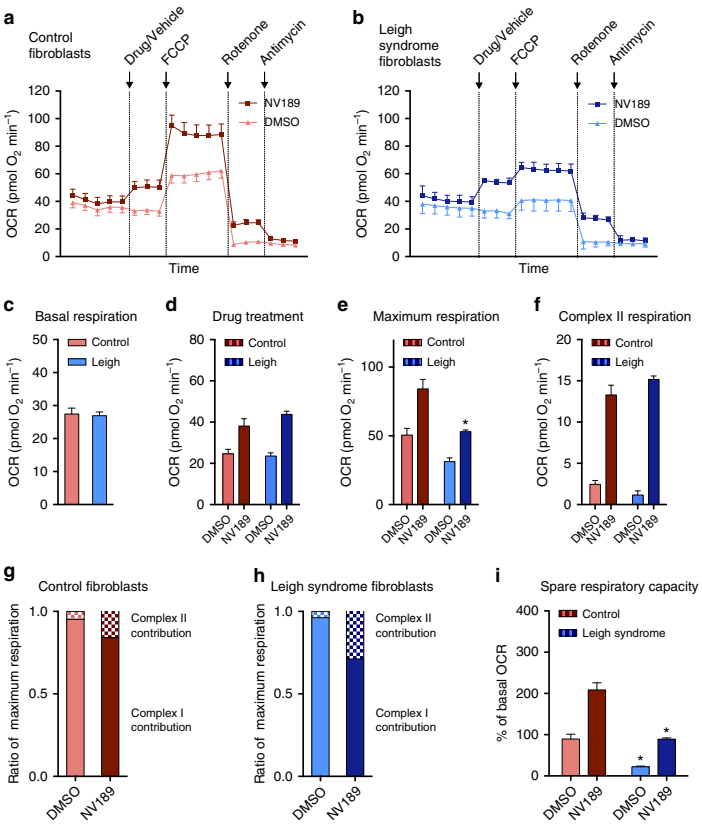

Figure 3 | Succinate prodrug treatment of mitochondrial complex I-deficient Leigh syndrome patient fibroblasts. (**a**,**b**) Oxygen consumption rate (OCR) in three control fibroblast cell lines and a mitochondrial complex I-deficient cell line (recessive *NDUFS2* mutation) treated with NV189 or vehicle. (**c**–**f**) Quantification of OCR in control and patient fibroblasts for each respiratory state. (**g**,**h**) Relative contribution of complex I- and complex II-linked respiration to maximum uncoupled respiration in patient cells and control cell lines. (**i**) Spare respiratory capacity, defined as per cent increase from endogenous baseline to maximum uncoupled respiration. Data presented as mean and s.e. of $n=3$ experiments from separate cell culture flasks performed with eight technical replicates each time for each cell lines. Data from the three control cell lines are pooled. $^*P<0.05$ (two-tailed unpaired Student's *t*-test, difference between Leigh and control cell lines).

patient and controls (Fig. 3d; Supplementary Fig. 5d). The patient cells had lower maximum respiration compared with control cells, but in the presence of NV189 the OCR of patient cells was similar to that of untreated control cells (Fig. 3e and Supplementary Fig. 5e). After rotenone inhibition of CI, both cell types elicited clear remaining respiratory activity in cells treated with NV189 (Fig. 3f; Supplementary Fig. 5f). The relative contribution of flux through CII to maximum uncoupled respiration for NV189 was 4.8% in the control cell lines and 3.8% in the Leigh syndrome cells. With treatment, this increased to 15.9% in control cells and to 28.8% in patient cell (Fig. 3g,h; Supplementary Fig. 5g,h), illustrating the dependence of CII substrates in the patient cells to reach normal respiratory function. When patient cells were treated with the prodrugs, the spare respiratory capacity (respiratory reserve, the ability of the cells to increase respiration from the endogenous baseline) as percentage of the endogenous baseline was similar to that of the control cell lines (Fig. 3i; Supplementary Fig. 5i). Succinate or dimethyl succinate (an ester previously suggested to be cell permeable[11,12]) did not exert any effects on either cell type (Supplementary Fig. 6).

Discussion

Mitochondrial disorders frequently present early in life with failure to thrive, myopathy and neuropathy, but the symptoms are very diverse[13]. At least 1 in 8,000 births will develop a mitochondrial disease[14]. Mitochondrial diseases are usually progressive and have a fluctuating clinical course. Periods of deterioration, such as during an intercurrent viral infection, are prompted by the increase in metabolic demand that the mitochondria cannot compensate for, resulting in metabolic

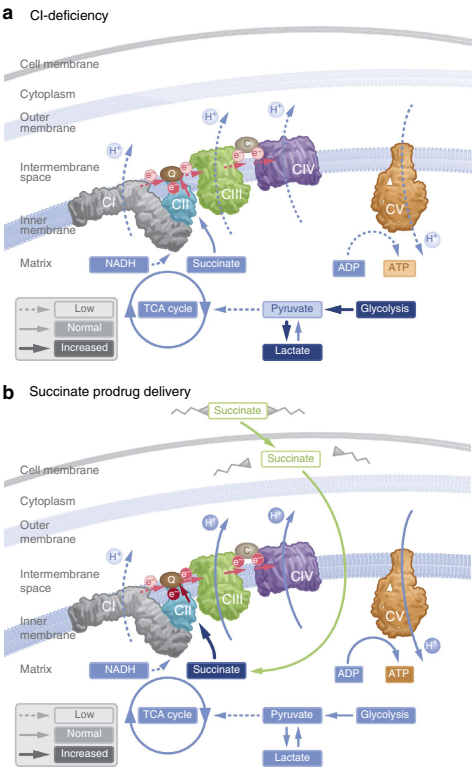

Figure 4 | Delivery of succinate to the intracellular space via a prodrug strategy. (**a**) Dysfunction in mitochondrial complex I reduces electron flow through the respiratory chain, shift metabolism towards glycolysis, induce lactate accumulation and limit ATP production. (**b**) Cell membrane-permeable prodrugs of succinate access the intracellular space and release succinate, enabling increased electron transport, respiration and ATP production through complex II, thus bypassing the deficiency in mitochondrial complex I.

decompensation[15]. It is an area of large unmet medical need as few evidence-based treatment options are available[2]. We describe here three model compounds of the first generation of a new pharmacological strategy to metabolically support these patients during time of metabolic decompensation. The current compounds lack sufficient plasma stability to be suitable for *in vivo* use. A cell-permeable prodrug of succinate can enter the cell independent of active uptake and subsequently release succinate. By supplying the mitochondria with substrates for CII, cells that are unable to comply with metabolic demand due to limitations at CI, or upstream thereof, may increase ATP production through oxidative phosphorylation, demonstrated here by the normalization of spare respiratory capacity in metabolically defect patient cells (Fig. 3i). By supporting aerobic metabolism, the relative dependence on glycolysis for ATP generation is alleviated and lactate production is attenuated (Figs 1n and 4). Utilizing a cell-permeable prodrug strategy to deliver a TCA cycle intermediate to the intracellular space is a feasible pharmacologic strategy with potential benefit in conditions affecting mitochondrial function, such as CI dysfunction or TCA cycle intermediate depletion in organic acidemias. Here we demonstrate that prodrug-delivered succinate can alleviate metabolic decompensation due to CI-related mitochondrial dysfunction.

Methods

Human peripheral blood cells. The blood cell protocols were approved by the regional ethics committee of Lund University, Sweden (permit no. 2013/181), and written informed consent was acquired from each participant. From healthy volunteers, venous blood was drawn to K_2EDTA tubes (Vacutainer, BD, Franklin Lakes, USA) via venous puncture. Platelets were isolated with consecutive centrifugation steps as previously described[16]. Peripheral blood mononuclear cells (PBMCs) were isolated using Lymphoprep (Axis-Shield, Dundee, Scotland). Erythrocytes and PBMCs were loosely pelleted by 10 min centrifugation at 500*g*. The pellet was resuspended in saline, layered on a Ficoll gradient and centrifuged at 800*g* for 20–30 min. The resulting leukocyte layer was collected, resuspended in saline and pelleted by 5 min centrifugation at 250*g*. The supernatant was removed and the pellet resuspended in 100–200 µl of saline. Blood cells were counted using an automated hematocytometer (SweLab Alfa, Boule Diagnostics, Sweden). The number of biological replicates (blood cells derived from different individual donors) are provided in the respective figure legends for all experiments.

Human cardiac muscle samples. Biopsies of human cardiac muscle were obtained at the Department of Cardiothoracic Surgery, Skåne University Hospital, Lund, Sweden. Pre-surgery informed consent was obtained from patients undergoing planned open-heart surgery such as mitral valve repair or maze procedure for treatment of atrial fibrillation. Only superfluous tissue that otherwise would have been discarded or located behind the suture line for the cannulation catheter was collected (up to 2 g was collected, 50–100 mg used for each experiment). Ethical permission was granted by the regional ethical review board of Lund, Sweden (permit no. 2013/271, 2013/701). The biopsy was immediately transferred to ice-cold preservation solution (BIOPS; 10 mM Ca-EGTA buffer, 0.1 µM free calcium, 20 mM imidazole, 20 mM taurine, 50 mM K-MES, 0.5 mM dithiothreitol, 6.56 mM $MgCl_2$, 5.77 mM ATP and 15 mM phosphocreatine, pH 7.1). It was thereafter dissected under microscope using forceps to gently separate the fibres and remove any fat and connective tissue. Biopsy wet weight was obtained before respiratory measurements (Precisa 40SM-200A, Abbot, USA).

Cultured fibroblasts. Permit for research on fibroblasts was granted by the Newcastle and North Tyneside 1 NRES Committee (REC reference 2002/205). A cultured skin fibroblast cell line from a patient with clinical Leigh syndrome due to a deficiency in the nuclear encoded structural mitochondrial CI protein *NDUFS2* (p.Arg118Gln; p.Met292Thr mutations), and relevant control cell lines from healthy donors were provided by the Wellcome Trust Centre for Mitochondrial Research at Newcastle University, UK[10]. The fibroblasts were cultured in minimum essential medium (MEM) supplemented with 10% fetal bovine serum, 1% MEM vitamins, 1% MEM non-essential amino acids, 2 mM L-glutamine, 50 µg ml^{-1} streptomycin, 50 U ml^{-1} penicillin, 50 µg ml^{-1} uridine and 1 mM sodium pyruvate at 37 °C and 5% CO_2. Cells were collected using trypsin and split or used for analysis at ~70–80% confluence and counted using an automated cell counter (TC20, Bio-Rad, Hercules, USA).

Respirometry. For cells in monolayers, the Seahorse Bioscience XF^e 96 Extracellular Flux Analyser (Seahorse Bioscience, North Billerica, USA) was the instrument of choice, and for cells in suspension such as blood cells the Oroboros O2k (Oroboros Instruments, Innsbruck, Austria) was used. Respiratory measurements using Oroboros O2k were performed in stirred (750 r.p.m.) 2 ml glass chambers at 37 °C. The media MiR05 (sucrose 110 mM, HEPES 20 mM, taurine 20 mM, K-lactobionate 60 mM, $MgCl_2$ 3 mM, KH_2PO_4 10 mM, EGTA 0.5 mM and bovine serum albumin 1 g l^{-1}, pH 7.1) was used in all experiments[16,17]. Data were recorded using the DatLab software version 4, 5 or 6 (Oroboros Instruments). Correction for instrumental background and air calibration was performed according to the manufacturer's instructions.

All experiments with platelets were performed with cell concentrations of 200×10^6 cells per ml and all experiments with PBMCs with 5×10^6 cells per ml. In experiments with human heart fibres, ~10 mg of tissue was used in each run. To inhibit mitochondrial CI, rotenone (2 µM) was used and to inhibit mitochondrial complex III, antimycin A (1 µg ml^{-1}) was used. ATP synthase was inhibited using oligomycin (1 µg ml^{-1}), evaluating the contribution of respiration independent of ADP phosphorylation. Maximum uncoupled respiration of the electron transport system was induced by titration of the protonophore carbonyl cyanide FCCP until no further increase in respiration was detected. The test compound or control substances (succinate, dimethyl succinate, monomethyl succinate, malonate, dimethyl malonate or dimethylsulphoxide (DMSO)) were dosed as indicated in each figure.

Respirometric measurements in fibroblasts were performed using a Seahorse Bioscience XF^e 96 Extracellular Flux Analyzer. The day before the experiment, fibroblasts were seeded out at 25,000 cells per well in cell growth medium in collagen-coated 96-well plates and kept at 37 °C and 5% CO_2 overnight. Before the experiment, the growth medium was replaced by XF-Base Medium containing 2 mM L-glutamine, 5 mM sodium pyruvate and 10 mM glucose (pH 7.4) and the cells were kept at 37 °C 1 h at atmospheric O_2 and CO_2. Oxygen consumption was measured at routine state and after addition of 500 µM of NV241 or NV189, its vehicle DMSO, dimethyl succinate or disodium succinate, followed by different concentrations of FCCP (0.125, 0.5, 1.0 and 1.5 µM), 2 µM rotenone and 1 µg ml^{-1} antimycin A. After FCCP and drug addition, the first data point was generally used, if not another data point was clearly higher, and for the remaining states the last data point before the subsequent addition was used. The FCCP dosing resulting in the highest uncoupled respiration was chosen for analysis for each experiment with each cell line and treatment.

All respirometric measurements, with the exception of the human heart fibre data, were corrected for non-mitochondrial oxygen consumption, obtained after the addition of antimycin A.

Lactate. Platelets ($n = 5$ individual donors, 200×10^6 cells per ml) were incubated in PBS for 4 h with rotenone (2 µM), rotenone and antimycin A (1 µg ml^{-1}) combined or the vehicle for rotenone (DMSO). At $t = 60$ min, additions of 250 µM NV118, NV189, NV241 or vehicle (DMSO) were initiated and repeated every 30 min throughout the experiment. Lactate levels were determined every 30 min using a Lactate ProTM 2 blood lactate meter (Arkray, Alere AB, Lidingö, Sweden)[18]. Incubation was performed at 37 °C at a stirrer speed of 750 r.p.m.

Mitochondrial membrane potential. Mitochondrial membrane potential in isolated human platelets (200×10^6 ml^{-1}) was measured using a flow cytometer FACSAria III (BD, Franklin Lakes, USA) with Diva version 7.0 acquisition and analysis software, using the probe TMRM (Life Techologies, Ref: T668), in non-quench mode (30 nM)[19] excited by 561 nM 40 mW laser and collected on 582/15 band pass filter. CD41a-APC (BD Pharmingen, Clone HIP8, Ref: 559777) at 18 times dilution was used to assess platelet activation. Samples were incubated with the probes in MiR05 for 30 min at room temperature. CI was inhibited using 2 µM rotenone. NV189 (250 µM) or DMSO control was added to the samples, followed by oligomycin (1 µg ml^{-1}), FCCP (20 µM) and antimycin A (1 µg ml^{-1}), the two latter additions as internal controls. Data software used was FlowJo 10 (Tree Star, Ashland, USA). Statistical analyses were performed, and all figures were generated using Prism 6 (GraphPad Software).

Metabolomics. Isolated human PBMCs ($16–25 \times 10^6$ ml^{-1}) were incubated at 37 °C in 2 ml MiR05 with 5 mM glucose and with rotenone 2 µM or DMSO control. NV189 (250 µM; 0.5 mM total) or DMSO control was added in two subsequent additions. Samples were centrifuged at 4,600g for 4 min and the supernatant discarded in two cycles with resuspension of pellet in 1.5 ml of 5% mannitol solution before the second run. To each sample, 800 µl of methanol and 550 µl of solution of the internal standard (H3304-1002, Human Metabolome Technologies Inc., Tsuruoka, Japan) were added and 1 ml of the extracted solution was taken for centrifugation at 2,300g at 4 °C for 5 min. Thereafter, 400 µl of the supernatant was filtered at 9,100g at 4 °C until no liquid remained. The extract was dried in a centrifugal evaporator (1,500 r.p.m., 1,000 Pa) and put in −80 °C until analysis. Samples were analysed using capillary electrophoresis time-of-flight mass spectrometry (CE-TOFMS) for cationic compounds and capillary electrophoresis tandem mass spectrometry (CE-MS/MS) for anionic compounds (Agilent Technologies, Santa Clara, USA), as previously described[20]. Peaks detected in CE-TOFMS analysis were extracted using automatic integration software (MasterHands ver.2.16.0.15 developed at Keio University) and those in CE-MS/MS analysis were extracted using automatic integration software (MassHunter Quantitative Analysis B.06.00, Agilent Technologies) to obtain peak information including m/z, migration time and peak area. The peak area was then converted to relative peak area. The peaks were annotated based on the migration times in CE and m/z values determined by TOFMS. Putative metabolites were then assigned from Human Metabolome Technologies (HMT) metabolite database on the basis of m/z and migration time. All the metabolite concentrations were calculated by normalizing the peak area of each metabolite with respect to the area of the internal standard and using standard curves, which were obtained by three-point calibrations. The lactate:pyruvate ratio was analysed using Friedman's non-parametric paired test for comparison between three groups or more with Dunn's multiple comparisons test of all groups against control. For three data points (one data point in the group treated with only rotenone and two data points in the group treated with rotenone and NV189), pyruvate was below the quantification limit. The estimated lower-quantification limit for pyruvate was between 16.96 and 20.55 pmol per 10^6 cells and a mean of these two values was used for calculating the lactate:pyruvate ratio for the missing data points. Experiments were performed by the service provider Human Metabolome Technologies Inc. (Tsuruoka, Japan). Cells from the same four healthy volunteers were used for each experimental group.

Isotope labelling. NV118 was synthesized incorporating all four carbons in the central succinate structure of the molecule with [^{13}C] isotopes. Isolated platelets (800×10^6 ml^{-1}) were kept at 37 °C in 2 ml MiR05 containing 5 mM glucose. [1, 2, 3, 4-$^{13}C_4$]NV118 was added in two boluses to a final concentration of 0.5 mM and the samples were incubated for 15, 30, 120 or 240 min. Extracts were prepared as described above. Metabolome measurements were carried out through Human Metabolome Technology Inc., Tsuruoka, Japan. Target metabolites and their isotopomers were annotated based on their theoretical m/z value and migration time[21]. Cells from the same two healthy volunteers were used for each experimental group.

Statistics. Statistical analyses were performed, and all figures generated, using Prism 6 (GraphPad Software, La Jolla, USA) if not otherwise stated. A P value of <0.05 was considered statistically significant. No blinding or randomization was performed, except for the metabolomics assays, where the lab performing the analyses was blinded to the intervention allocated to the samples. Data from blood cell respirometry have previously been reported to be normally distributed and parametric tests were used[16].

Data availability. All relevant data are contained within the paper and Supplementary Information files or available from the authors upon request.

References

1. Distelmaier, F. *et al.* Mitochondrial complex I deficiency: from organelle dysfunction to clinical disease. *Brain* **132,** 833–842 (2009).
2. Pfeffer, G., Majamaa, K., Turnbull, D. M., Thorburn, D. & Chinnery, P. F. Treatment for mitochondrial disorders. *Cochrane Database Syst Rev* **4,** CD004426 (2012).
3. Lightowlers, R. N., Taylor, R. W. & Turnbull, D. M. Mutations causing mitochondrial disease: What is new and what challenges remain? *Science* **349,** 1494–1499 (2015).
4. Fliri, H. *et al.* Protected succinates for enhancing mitochondrial ATP-production. Patent WO2014053857 A1 (2014).
5. MacDonald, M. J., Fahien, L. A., Mertz, R. J. & Rana, R. S. Effect of esters of succinic acid and other citric acid cycle intermediates on insulin release and inositol phosphate formation by pancreatic islets. *Arch. Biochem. Biophys.* **269,** 400–406 (1989).
6. Loeffen, J. L. *et al.* Isolated complex I deficiency in children: clinical, biochemical and genetic aspects. *Hum. Mutat.* **15,** 123–134 (2000).
7. Robinson, B. H. Human complex I deficiency: clinical spectrum and involvement of oxygen free radicals in the pathogenicity of the defect. *Biochim. Biophys. Acta* **1364,** 271–286 (1998).
8. Diogo, L. *et al.* Pediatric mitochondrial respiratory chain disorders in the Centro region of Portugal. *Pediatr. Neurol.* **40,** 351–356 (2009).
9. Kirby, D. M. *et al.* Respiratory chain complex I deficiency: an underdiagnosed energy generation disorder. *Neurology* **52,** 1255–1264 (1999).
10. Tuppen, H. A. *et al.* The p.M292T NDUFS2 mutation causes complex I-deficient Leigh syndrome in multiple families. *Brain* **133,** 2952–2963 (2010).
11. Selak, M. A. *et al.* Succinate links TCA cycle dysfunction to oncogenesis by inhibiting HIF-alpha prolyl hydroxylase. *Cancer Cell* **7,** 77–85 (2005).
12. Chouchani, E. T. *et al.* Ischaemic accumulation of succinate controls reperfusion injury through mitochondrial ROS. *Nature* **515,** 431–435 (2014).
13. DiMauro, S. Mitochondrial diseases. *Biochim. Biophys. Acta* **1658,** 80–88 (2004).
14. Skladal, D., Halliday, J. & Thorburn, D. R. Minimum birth prevalence of mitochondrial respiratory chain disorders in children. *Brain* **126,** 1905–1912 (2003).
15. Chinnery, P. F. & Turnbull, D. M. Clinical features, investigation, and management of patients with defects of mitochondrial DNA. *J. Neurol. Neurosurg. Psychiatry* **63,** 559–563 (1997).
16. Sjovall, F. *et al.* Mitochondrial respiration in human viable platelets--methodology and influence of gender, age and storage. *Mitochondrion* **13,** 7–14 (2013).
17. Gnaiger, E. *et al.* in *Life in the Cold.* (eds Heldmaier, G. & Klingenspor, M.) 431–442 (Springer, 2000).
18. Tanner, R. K., Fuller, K. L. & Ross, M. L. Evaluation of three portable blood lactate analysers: Lactate Pro, Lactate Scout and Lactate Plus. *Eur. J. Appl. Physiol.* **109,** 551–559 (2010).
19. Perry, S. W., Norman, J. P., Barbieri, J., Brown, E. B. & Gelbard, H. A. Mitochondrial membrane potential probes and the proton gradient: a practical usage guide. *BioTechniques* **50,** 98–115 (2011).
20. Soga, T. *et al.* Quantitative metabolome analysis using capillary electrophoresis mass spectrometry. *J. Proteome Res.* **2,** 488–494 (2003).
21. Kami, K. *et al.* Metabolomic profiling rationalized pyruvate efficacy in cybrid cells harboring MELAS mitochondrial DNA mutations. *Mitochondrion* **12,** 644–653 (2012).

Acknowledgements

E.E., M.J.H., J.K.E., S.P., F.S., E.Å.F. and M.K. are funded by Swedish Research Council (2011-3470), Swedish government project and salary funding for clinically oriented medical research (ALF grants), Regional research and development grants (Southern healthcare region, Sweden), The Crafoord Foundation, The Royal Physiographic Society in Lund and the Linnéa and Josef Carlsson foundation. R.W.T. and D.M.T. are supported by The Wellcome Trust Centre for Mitochondrial Research (G906919), Newcastle University Centre for Ageing and Vitality (supported by the Biotechnology and Biological Sciences Research Council and Medical Research Council (G016354/1)), MRC Centre for Neuromuscular Disease (G000608-1), The MRC Centre for Translational Research in Neuromuscular Disease Mitochondrial Disease Patient Cohort (UK) (G0800674), The Lily Foundation, the UK NIHR Biomedical Research Centre in Age and Age Related Diseases award to the Newcastle upon Tyne Hospitals NHS Foundation Trust, and UK NHS Specialist Commissioners 'Rare Mitochondrial Disorders of Adults and Children' Service. The authors thank Per Wierup, Per Paulsson, Henrik Bjursten and Johan Sjögren at the Department of Cardiothoracic Surgery at Skåne University Hospital for providing tissue samples. The authors also thank David Nicholls for constructive discussions.

Author contributions

E.E., M.J.H., F.S. and J.K.E. conceived the study. R.F., C.C., H.F. and S.J.M. designed new chemical entities. R.W.T. and D.M.T. provided cell lines. S.M., S.P., J.K.E., M.K., C.M., R.W.T., D.M.T., S.J.M. and E.Å.F. evaluated the properties of the compounds. J.K.E., S.P. and M.K. performed the statistical analysis. J.K.E. drafted the manuscript. J.K.E., S.P., M.J.H. and M.K. prepared figures. J.K.E., M.J.H. and E.E. directed the study. All authors critically reviewed the manuscript and approved of the final version.

Additional information

Supplementary Information accompanies this paper at http://www.nature.com/naturecommunications

Competing financial interests: This study is partly funded by NeuroVive Pharmaceutical AB and Selcia Ltd, companies active in the field of mitochondrial medicine. J.K.E., S.M., E.E., M.J.H., M.K., S.P., F.S., S.J.M. and E.Å.F. have or have had salary from and/or equity interest in NeuroVive Pharmaceutical. H.F., R.F. and C.C. have or have had salary from and/or equity interest in Selcia Ltd/Mitopharm Ltd.

Reprints and permission information is available online at http://npg.nature.com/reprintsandpermissions/

How to cite this article: Ehinger, J. K. *et al.* Cell-permeable succinate prodrugs bypass mitochondrial complex I deficiency. *Nat. Commun.* 7:12317 doi: 10.1038/ncomms12317 (2016).

Paper V

Mitochondrion 31 (2016) 56–62

Contents lists available at ScienceDirect

Mitochondrion

journal homepage: www.elsevier.com/locate/mito

Changes in energy metabolism due to acute rotenone-induced mitochondrial complex I dysfunction – An *in vivo* large animal model

Michael Karlsson [a,b,*,1], Johannes K. Ehinger [a,b,1], Sarah Piel [a,b], Fredrik Sjövall [a], Johanna Henriksnäs [c], Urban Höglund [c], Magnus J. Hansson [a,b], Eskil Elmér [a,b]

[a] Mitochondrial Medicine, Department of Clinical Sciences, Lund University, BMC A13, SE-221 84 Lund, Sweden
[b] NeuroVive Pharmaceutical AB, Medicon Village, Scheelevägen 2, SE-233 81 Lund, Sweden
[c] Adlego Biomedical AB, P.O. Box 42, SE-751 03 Uppsala, Sweden

ARTICLE INFO

Article history:
Received 16 December 2015
Received in revised form 6 October 2016
Accepted 13 October 2016
Available online 18 October 2016

Keywords:
Animal model
Mitochondria
Complex I
Metabolic crisis
Energy metabolism

ABSTRACT

Metabolic crisis is a clinical condition primarily affecting patients with inherent mitochondrial dysfunction in situations of augmented energy demand. To model this, ten pigs received an infusion of rotenone, a mitochondrial complex I inhibitor, or vehicle. Clinical parameters, blood gases, continuous indirect calorimetry, *in vivo* muscle oxygen tension, *ex vivo* mitochondrial respiration and metabolomics were assessed. Rotenone induced a progressive increase in blood lactate which was paralleled by an increase in oxygen tension in venous blood and skeletal muscle. There was an initial decrease in whole body oxygen utilization, and there was a trend towards inhibited mitochondrial respiration in platelets. While levels of succinate were decreased, other intermediates of glycolysis and the TCA cycle were increased. This model may be suited for evaluating pharmaceutical interventions aimed at counteracting metabolic changes due to complex I dysfunction.

1. Introduction

NADH:ubiquinone oxidoreductase, more commonly referred to as Complex I (CI), is the largest complex of the mitochondrial electron transport chain (ETC) (Carroll et al., 2006). CI dysfunction is a common pathophysiological mechanism involved in several mitochondrial disorders. Various other inborn errors of metabolism (IEM) may also cause secondary inhibition of CI (Brusque et al., 2002). Further, in a general patient population drug-induced CI dysfunction may occur, for example in metformin-induced lactic acidosis (Brunmair et al., 2004; Dykens et al., 2008; Piel et al., 2015; Protti et al., 2012b). CI dysfunction is also implicated in the pathophysiology of several other conditions, including neurodegenerative disorders such as Parkinson's disease, cardiac ischemia-reperfusion injury, traumatic brain injury and sepsis (Kilbaugh et al., 2015; Paradies et al., 2004; Protti et al., 2007; Schapira et al., 2014).

Even though our knowledge about the pathophysiology underlying mitochondrial respiratory chain disorders in recent years has increased considerably, this has not been paralleled by the development of new pharmaceutical treatment options (Dimauro and Rustin, 2009). In a Cochrane review from 2012 it is concluded that there is presently no evidence supporting the use of any pharmacological intervention in mitochondrial disorders (Pfeffer et al., 2012).

A cornerstone of effective pharmaceutical development is a relevant and reliable animal model. A few models related to mitochondrial respiratory diseases exists, for instance transgenic mice (Koene et al., 2011; Kruse et al., 2008; Tyynismaa and Suomalainen, 2009; Wallace and Fan, 2009), among them specific CI models such as the WB NDUFS4$^{-/-}$ KO mouse, the CWB NDUFS4$^{-/-}$ KO mouse (Roestenberg et al., 2012) and the NDUFS6$^{-/-}$ KO mouse with cardiac specific defects (Ke et al., 2012). There is also the *Harlequin* mouse, where the phenotype of the natural mutant has been attributed to CI dysfunction (Vahsen et al., 2004). In order to allow for adequate clinical monitoring with invasive measurements and control of the ventilation, resembling an intensive care unit, a large-animal model is preferable. Further, a larger animal also grants the possibility of collecting multiple blood samples, where the blood volume of a rodent would be insufficient. A pig model of metformin-induced lactic acidosis has recently been published (Protti et al., 2012a), where inhibition of mitochondrial CI respiration by metformin is likely a major mechanism for lactate accumulation (Piel et al., 2015).

In general, mitochondrial disorders affect organs with high energy requirements. The development of lactic acidosis is a common feature related to the shift from aerobic mitochondrial respiration to anaerobic glycolysis as the cells strive to uphold ATP production (Jackson et al.,

* Corresponding author at: Mitochondrial Medicine, Department of Clinical Sciences, Lund University, BMC A13, SE-221 84 Lund, Sweden.
E-mail addresses: michael.karlsson@med.lu.se (M. Karlsson), johannes.ehinger@med.lu.se (J.K. Ehinger), sarah.piel@med.lu.se (S. Piel), fredrik.sjovall@med.lu.se (F. Sjövall), johanna.henriksnas@adlego.se (J. Henriksnäs), urban.hoglund@adlego.se (U. Höglund), magnus.hansson@med.lu.se (M.J. Hansson), eskil.elmer@med.lu.se (E. Elmér).
[1] Contributed equally.

http://dx.doi.org/10.1016/j.mito.2016.10.003
1567-7249/

1995; Sue et al., 1998). Lactate overproduction can be due to either hypoxia or dysoxia, with the former representing true lack of oxygen in the tissue regardless of cause and the latter representing abnormal tissue oxygen metabolism in the presence of normal tissue oxygen supply (Robin, 1977).

The objective of this study was to establish an *in vivo* pig model of acute mitochondrial CI dysfunction with associated changes in metabolism to be used to evaluate pharmaceutical interventions aimed at counteracting these changes, and to show that the detected systemic effects, and specifically the increase in lactate, were primarily due to a shift towards non-mitochondrial metabolism and not only due to tissue hypoperfusion or other secondary cardiovascular effects of rotenone. The model aims at mimicking a clinical situation of acute metabolic crisis involving CI dysfunction.

2. Material and methods

2.1. Animals and rotenone infusion

The regional animal experimental ethics committee of Stockholm approved the study (N29/13). Ten female Yorkshire/landrace hybrid pigs (mean body weight 37.8 kg range 30.4–46 kg, age 12–14 weeks) were included. Before transportation to the test facility the animals were pre-medicated with intramuscular administration of Zoletil (tiletamine; 1.5 mg/kg and zolazepam; 1.5 mg/kg), Domitor (medetomidine hydrochloride; 0.06 mg/kg) and atropin (0.033 mg/kg).

The pigs were anaesthetized by a combination of pentobarbital (120 mg bolus) and fentanyl (100 μg bolus). Thereafter the animals were intubated and supplied with assisted ventilation. The rate and tidal volume of the ventilator was kept constant during the experiment. $ETCO_2$ and SaO_2 were measured continuously and recorded every 15 min. Arterial blood pO_2 was kept constant at approximately 13 kPa by regulating the inspired oxygen concentration, measurements were done every 15 min and FiO_2 was adjusted accordingly. A urine catheter with a temperature sensor was placed in the urine bladder and a pulse-oximeter was positioned on either lip or auricle to monitor oxygen saturation. Anesthesia was maintained with continuous intravenous infusions of pentobarbital 7–18 mg/kg/h and fentanyl 2–3 μg/kg/h. Ringer-Acetate was infused at a rate of 300–1000 mL/h, adjusted according to the clinical assessment of urinary output and MAP. Heparin (5000 IE) bolus doses was administered hourly.

In five of the pigs, after stabilization, the rotenone infusion was initially 0.25 mg/kg/h for 3 h, thereafter at 0.5 mg/kg/h for 1 h through a single lumen catheter in the left jugular vein. The remaining five pigs were infused with vehicle (71% H_2O, 25% *N*-methylpyrrolidone, 4% polysorbate). The selected rotenone dosing regiment and tolerability of the vehicle were determined in a prior set of dose-escalation experiments in a total of ten pigs with a rotenone dose starting at 0.3 μg/kg/h (data not shown).

2.2. Hemodynamic parameters and blood gases

Arterial blood pressure was measured continuously through a catheter in the femoral artery. A Swan-Ganz catheter (CCOmbo V, Edwards Life sciences, Irvine, USA) was inserted through the right external jugular vein into the pulmonary artery. Pulmonary artery pressure and central venous pressure were recorded every 15 min; pulmonary wedge pressure was measured every 30 min. Cardiac output (CO) was measured by thermo-dilution from the Swan-Ganz catheter and recorded every 15 min. Animals were also monitored by ECG during the experiment to detect serious arrhythmias.

Arterial blood samples were collected from the femoral artery and venous blood samples were collected from the Swan-Ganz catheter in the pulmonary artery. Blood gases were analyzed every 15 min (ABL725 blood gas analyzer, Radiometer Medical Aps, Brønshøj, Denmark) measuring pH, pCO_2, pO_2, HCO_3, sO_2, tCO_2(B), tHb, Hct, K^+, Na^+, Ca^{2+}, Cl^-, glucose, lactate and base excess.

2.3. Continuous indirect calorimetry

Continuous indirect calorimetry was performed using a Quark RMR ICU (Cosmed, Rome, Italy) measuring whole animal oxygen consumption (VO_2) and carbon dioxide production (VCO_2). The Quark RMR ICU measures VCO_2 and VO_2 using a breath-by-breath technique through an infrared CO_2 and paramagnetic O_2 analyzer. The gas is sampled through a tube attached to the ventilator. Minute ventilation is measured by a turbine flow meter attached to the ventilator expiratory port. The Quark software detects any bias flow from the ventilator and compensates for this when calculating VCO_2 and VO_2 (Sundstrom et al., 2013). Data was recorded every 15 min.

2.4. Oxygen tension in skeletal muscle in vivo

Measurement of oxygen tension was conducted with large area surface (LAS)™ oxygen-sensing luminescent optodes (0.7 mm diameter; 8 mm^2) in *m. pectineus* and *m. sternocleidomastoideus* for continuous monitoring of tissue PO_2 with data recorded every 15 min. The skin incisions for placement of probes were sutured. The probes were pre-calibrated by the manufacturer (Oxylite Pro, Oxford Optronic Ltd, Abingdon, UK). These fiber optic probes send pulses of light to a luminophore at the tip of the cable and the emitted light is then carried back to a monitoring system with automatic temperature compensation (Dyson et al., 2012).

2.5. Mitochondrial respiration ex vivo

In four pigs per treatment group mitochondrial respiratory function was analyzed *ex vivo* in platelets and skeletal muscle biopsies using high-resolution respirometry (Oxygraph-2k, Oroboros Instruments, Innsbruck, Austria). Oxygen flux was monitored and recorded in real-time using DatLab 5.1 software (Oroboros Instruments, Innsbruck, Austria). Samples were collected and analyzed both immediately prior to infusion and after 3 h.

Using the catheter in the femoral artery, 20 mL of blood was collected in K_2EDTA tubes (Vacuette®, Greiner Bio-One GmbH, Kremmünster, Austria). Platelets were isolated using sequential centrifugation steps, as previously described (Sjovall et al., 2013). Mitochondrial function of intact platelets was analyzed in both the animal's own plasma and MiR05 solution (0.5 mM EGTA, 3 mM $MgCl_2$, 60 mM *k*-lactobionate, 20 mM taurine, 10 mM KH_2PO_4, 20 mM HEPES, 110 mM sucrose, 1 g/L BSA, pH 7.1). Analysis was executed using an adapted version of a previously published protocol (Sjovall et al., 2010). After stabilization of routine respiration with endogenous substrates, carbonyl cyanide *p*-(trifluoromethoxy) phenylhydrazone (FCCP) was titrated until no further respiratory increase. Rotenone (2 μM) was added to completely inhibit CI and lastly antimycin-A (1 μg/mL), a mitochondrial complex III inhibitor, was added to reveal residual oxygen consumption.

Muscle biopsies were obtained using a 14 G micro-biopsy needle from the *m. pectineus* (contralateral to the *in vivo* oxygen tension probe described above). The samples were instantaneously transferred to ice-cold biopsy preservation solution (BIOPS) (10 mM *Ca*-EGTA buffer, 0.1 μM free calcium, 20 mM imidazole, 20 mM taurine, 50 mM K-MES, 0.5 mM DTT, 6.56 mM $MgCl_2$, 5.77 mM ATP, 15 mM phosphocreatine, pH 7.1) and thereafter gently dissected using forceps to remove any fat and connective tissue. The mitochondrial function was then analyzed in MiR05 (Pesta and Gnaiger, 2012). A titration protocol was implemented specified at detecting complex I (CI) dysfunction using NADH-linked substrates at concentrations that were semipermeable in muscle biopsies. First malate (5 mM), pyruvate (5 mM) and glutamate (5 mM) were added, thereafter, FCCP was titrated until no further

increase in respiration was achieved (mean concentration 1.5 μM). Subsequently rotenone (2 μM) and finally antimycin-A (1 μg/mL) was added.

Citrate synthase activity was used as a biomarker for mitochondrial content, as a complement to cell-count and tissue weight for normalization of respiration (Larsen et al., 2012). Citrate synthase activity was measured using a commercially available kit according to the manufacturer's instructions (Citrate Synthase Assay Kit, CS0720, Sigma).

2.6. Metabolomics in muscle biopsies

Assessment of metabolomics profile was performed in a subset of three control samples and two rotenone treated samples. Muscle biopsies were collected as described in the previous section after 3 h of rotenone or vehicle infusion.

A targeted quantitative analysis of 116 metabolites was performed using capillary electrophoresis time-of-flight mass spectrometry (CE-TOFMS) for cationic compounds and capillary electrophoresis tandem mass spectrometry (CE-MS/MS) for anionic compounds. Focus was on metabolites involved in glycolysis, pentose phosphate pathway, TCA cycle and the urea cycle, as well as polyamine, creatine, purine, glutathione, nicotinamide, choline, and amino acid metabolism. The analysis (CARCINOSCOPE™) was carried out by Human Metabolome Technologies Inc. (HMT), Tsoruka, Japan. Samples were handled according to their instructions and sent to HMT in frozen condition. At HMT the samples were mixed with 750 μL of 50% acetonitrile in water (v/v) containing internal standards (40 μM for cation and 10 μM for anion measurement) and homogenized. Then 750 μL of 50% acetonitrile in water (v/v) was added and subsequently centrifuged. The supernatant was filtrated through a 5-kDa cut-off filter (ULTRAFREE-MC-PLHCC, HMT) The filtrate was once again centrifuged and thereafter resuspended in 50 μL of ultrapure water before metabolome analysis using CE-MS. All the metabolite concentrations were calculated by normalizing the peak area of each metabolite with respect to the area of the internal standard and by using standard curves, which were obtained by three-point calibrations.

2.7. Statistical analysis

Statistical analyses of hemodynamic parameters and blood gases (means, SD, and 2-way repeated measures (RM) ANOVA of interaction between time and drug) were performed using Prism 7 (GraphPad Software, San Diego, USA). In the repeated measures analysis missing values were replaced by carrying forward (or backward) the last sampled data. Data of indirect calorimetry revealed that parameter values differed substantially between animals at start of the sampling periods and data was normalized group-wise to the highest initial value. A running median with a window of 3 min was used to filter drastic spikes in data caused by adjustments of the inspired oxygen concentration. Statistical analyses for mitochondrial respiration were performed using paired *t*-test. In the analysis of platelet respiration one value was excluded due to evident laboratory error. A p-value <0.05 was considered significant. As the magnitude of changes in evaluated parameters were not pre-specified, power calculation for sample size was not applicable in the present study.

3. Results

3.1. Hemodynamic parameters

All animals survived the 4 h infusion period. In both the rotenone and vehicle treated groups, the major hemodynamic parameters such as body temperature, oxygen saturation (SaO_2), heart rate (HR) and cardiac output (CO) remained stable throughout the first 3 h of rotenone infusion at 0.25 mg/kg/h. There was a trend of decreased mean arterial pressure (MAP) with time for both groups for the first 3 h. With the higher infusion rate at 0.5 mg/kg/h, the clinical status of the pigs treated with rotenone rapidly became unstable in regards to vital hemodynamic parameters (Table 1).

3.2. Lactate, pH and oxygen tension

Rotenone infusion induced a progressive increase in lactate concentration up to 6.1 mmol/L (range: 4.9–7.6 mmol/L) during the first 3 h ($p < 0.05$ at 45 min) and up to 10.5 mmol/L (range: 9.4–11.4 mmol/L)

Table 1
Clinical parameters. Rot – Rotenone, Temp – Temperature, SaO_2 – Oxygen saturation, HR – Heart rate, MAP – Mean arterial pressure, CO – Cardiac output, CVP – central venous pressure, MPAP – Mean pulmonary arterial pressure, PCWP – Pulmonary wedge pressure. Data presented as mean (SEM).

		Start of infusion (0.25 mg/kg/h)						Increased rate (0.5 mg/kg/h)			
Time (min)		0	30	60	90	120	150	180	210	240	270
Temp °C	Control	38.8 (0.29)	38.8 (0.37)	38.8 (0.33)	38.8 (0.31)	39.0 (0.33)	39.0 (0.42)	39.1 (0.46)	39.2 (0.45)	39.3 (0.42)	39.4 (0.42)
	Rot	39.3 (0.36)	39.3 (0.43)	39.1 (0.45)	39.2 (0.46)	39.5 (0.41)	39.6 (0.39)	39.6 (0.38)	39.7 (0.33)	39.6 (0.33)	39.5 (0.33)
SaO_2%	Control	97.4 (0.81)	98.2 (0.49)	98.0 (0.55)	98.0 (0.77)	96.8 (0.86)	97.2 (0.49)	96.6 (0.75)	96.2 (1.46)	97.0 (1.05)	96.6 (0.93)
	Rot	98.4 (1.12)	98.0 (1.14)	98.2 (1.32)	97.4 (1.86)	98.6 (0.68)	98.4 (0.87)	97.8 (0.73)	98.0 (0.84)	96.8 (1.02)	92.8 (2.06)
HR Beats/min	Control	118.6 (9.91)	116.2 (13.3)	104.0 (9.47)	103.2 (5.44)	101.0 (4.39)	103.6 (3.26)	103.8 (3.18)	105.8 (3.48)	106.0 (3.62)	109.8 (4.87)
	Rot	114.0 (8.44)	114.8 (6.85)	104.4(8.39)	107.8 (6.34)	109.0 (10.5)	114.4(7.09)	119.2 (5.83)	122.8 (5.96)	173.6 (5.22)	185.0 (16.1)
MAP mm Hg	Control	101.4 (5.36)	109,2 (4.42)	102.2 (5.36)	96.2 (6.60)	91.0 (6.51)	87.0 (7.08)	84.2 (6.89)	81.2 (7.66)	77.4 (7.38)	80.2 (7.78)
	Rot	109.2 (4.13)	105.6 (4.01)	94.60 (3.98)	94.4 (2.71)	82.8 (5.81)	77.6 (4.13)	75.2 (4.73)	71.6 (3.91)	97.4 (4.17)	63.5 (10.1)
CO L/min	Control	5.18 (0.46)	5.38 (0.23)	4.93 (0.36)	4.80 (0.43)	4.83 (0.53)	4.88 (0.50)	4.88 (0.45)	4.88 (0.46)	4.78 (0.48)	4.98 (0.47)
	Rot	4.50 (0.41)	4.62 (0.24)	4.12 (0.36)	4.44 (0.26)	4.70 (0.18)	4.70 (0.22)	4.92 (0.29)	5.16 (0.43)	6.26 (0.50)	5.88 (0.63)
CVP mm Hg	Control	7.0 (0.63)	7.8 (0.37)	7.8 (0.37)	8.2 (0.49)	8.2 (0.58)	8.2 (0.58)	8.2 (0.66)	8.6 (0.40)	8.0 (0.63)	7.8 (0.66)
	Rot	10.6 (2.93)	7.2 (0.80)	7.8 (0.73)	7.0 (0.55)	7.4 (0.75)	7.0 (0.63)	6.8 (0.80)	6.8 (0.80)	6.0 (1.00)	6.2 (0.97)
mPAP mm Hg	Control	18.7 (0.93)	19.7 (1.38)	19.9 (1.06)	20.0 (0.66)	21.1 (0.79)	20.5 (0.87)	22.1 (1.16)	21.9 (0.98)	21.3 (0.91)	21.5 (0.56)
	Rot	24.1 (1.41)	21.3 (1.88)	23.7 (1.71)	20.6 (1.43)	19.1 (1.47)	19.6 (1.47)	19.2 (1.31)	17.7 (1.11)	27.1 (1.37)	22.4 (3.17)
PCWP mm Hg	Control	8.2 (0.73)	10.8 (1.88)	9.0 (0.63)	9.2 (0.58)	9.0 (0.45)	8.8 (0.49)	8.8 (0.58)	9.0 (0.63)	9.0 (0.45)	8.8 (0.37)
	Rot	11.0 (3.07)	11.0 (2.37)	11.0 (2.61)	11.4 (2.29)	10.4 (2.44)	10.4 (2.73)	7.8 (0.86)	8.0 (0.63)	11.6 (3.59)	7.6 (1.29)

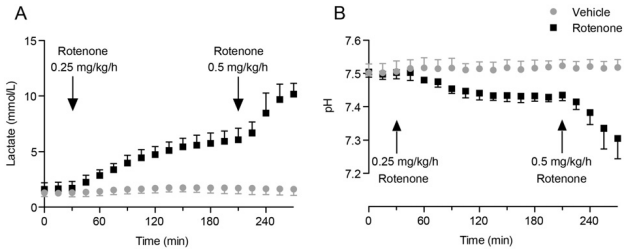

Fig. 1. Lactate and pH. Rotenone infusion induced a progressive increase in blood lactate (A) concentration up to 6.1 mmol/L during the first 3 h, reaching 10.5 mmol/L following the higher infusion rate of rotenone. Parallel to the lactate increase, arterial pH (B) progressively decreased. In control animals lactate and pH did not change significantly. $p < 0.0001$ with 2-way RM ANOVA for interaction between time and drug for both figures. Mean ± SD (one-sided shown in figure). $n = 5$ animals in each group.

following the higher infusion rate (Fig. 1A). Parallel to the lactate increase, arterial pH progressively decreased as illustrated in Fig. 1B ($p < 0.05$ at 60 min). Simultaneously, the rotenone treated pigs demonstrated an increased oxygen saturation in venous blood (Fig. 2A) and an increase in oxygen tension in skeletal muscle *in vivo* (Fig. 2B). There was a biphasic change in blood glucose levels with an initial increase (9.7 mmol/L at 75 min, $p < 0.05$) that was followed by a later decrease (3.5 mmol/L at 270 min, $p < 0.05$) compared to control (Fig. 3).

3.3. Continuous indirect calorimetry

Continuous indirect calorimetry showed that rotenone caused a decrease in whole body oxygen consumption and initially a decrease in carbon dioxide production as illustrated in Fig. 4A and B. During the first 30 min of rotenone infusion the oxygen uptake decreased by a mean of 8.7% ($p < 0.0001$) (range: −3.5% to −13.3%).

3.4. Oxygen delivery

Oxygen delivery remained steady during the lower infusion rate and increased with the higher infusion rate (Fig. 5).

3.5. Mitochondrial respiration ex vivo

Analysis of mitochondrial function *ex vivo* in viable intact platelets from rotenone treated animals displayed a statistically non-significant inhibition ($p = 0.059$) of phosphorylating capacity after 3 h of rotenone infusion. Platelets from the vehicle treated animals on the other hand displayed a non-significant increase (Fig. 6A–B). This trend was consistently present when platelets were analyzed in both the animals' own plasma and buffer solution (MiR05) (data not shown). These changes were seen regardless if respiration was normalized per cell or citrate synthase activity (data not shown). The trend seen in platelets was not detected in muscle fibers (Fig. 6C–D).

3.6. Metabolomics

In muscle biopsies from rotenone-treated animals pyruvic acid, the end product of glycolysis, was increased by 50% and lactic acid levels were almost doubled (Fig. 7); the resulting mean lactate-to-pyruvate ratio was increased from 21.9 in the controls (range 19.6–24.5) to 27.7 in the rotenone treated group (range 25.2–30.2). In the analysis of the tricarboxylic acid (TCA) cycle metabolites, succinic acid was the only intermediate that was decreased, while the others displayed increased levels. Citric acid levels were doubled and cis-aconitic acid, an intermediate in the isomerization of citrate to isocitrate, was increased several fold (Fig. 7). There was a trend towards higher levels of glycolysis intermediates in the rotenone treated group. Glucose 6-phosphate (G6P), fructose 6-phosphate (F6P) and glyceraldehyde 3-phosphate (G3P) were all several fold increased (Fig. 7). The trend was similar but less pronounced for metabolites downstream of glyceraldehyde 3-phosphate. Markers of energy state such as ATP, products of ATP hydrolysis and phosphocreatine were not altered significantly by rotenone treatment (Supplementary Table 1). The complete metabolomics data is available as supplementary material (Supplementary Table 1).

4. Discussion

The composite data indicates that intravenous rotenone infusion decreases mitochondrial utilization of oxygen and causes a switch from

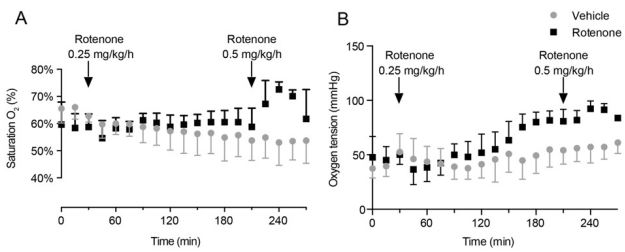

Fig. 2. Oxygen tension. The development of lactic acidosis in the rotenone treated animals was paralleled by an increase in oxygen saturation in venous blood (A) and oxygen tension in skeletal muscle (B). Measurements illustrated in Fig. 2B were acquired from *m. sternocleidomastoideus*. p < 0.0001 with 2-way RM ANOVA for interaction between time and drug for both figures. Mean ± SD (one-sided shown in figure). $n = 5$ animals in each group.

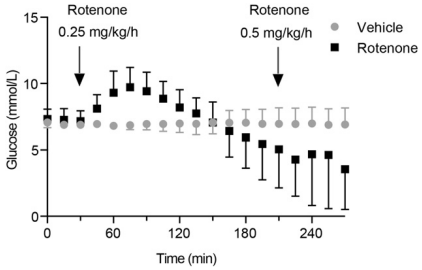

Fig. 3. Blood glucose. Rotenone infusion initially increased blood glucose levels ($p < 0.05$ at 45 min), however over time the blood glucose dropped and approached hypoglycemic levels towards the end of the experiment. $p < 0.0001$ with 2-way RM ANOVA for interaction between time and drug. Mean ± SD (one-sided shown in figure). $n = 5$ animals in each group.

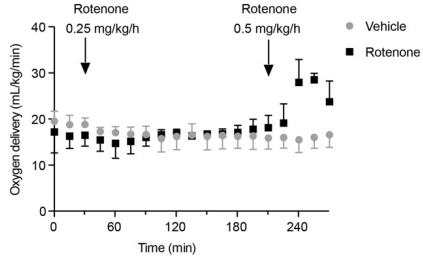

Fig. 5. Oxygen delivery. Oxygen delivery calculated as cardiac output (CO) multiplied by oxygen content ($1.39*Hb*O_2Sat/100$) + ($0.003*PO_2$). Mean ± SD (one-sided shown in figure). $n = 5$ animals in each group.

aerobic to anaerobic metabolism with a subsequent rise in arterial blood lactate and decrease in pH. With the start of rotenone infusion, the global oxygen consumption rapidly decreased and in the initial phase, the amount of expired carbon dioxide decreased. Venous and skeletal muscle oxygen tension displayed a progressive increase throughout the experiment, indicating a decreased oxygen extraction through decreased mitochondrial respiration. These results, together with the observed metabolic changes *in vivo* and the trend towards inhibition of mitochondrial respiration in platelets *ex vivo* suggest that the increased blood lactate levels are triggered by a mitochondrial inhibition and not secondary to decreased tissue perfusion and cellular hypoxia. The alternative interpretation that the increased tissue oxygen saturation may be due to vasodilation cannot be excluded. After the first 3 h there is no manifest energy decompensation, most likely due to accelerated glycolysis.

The increased blood lactate concentration indicates an accelerated glycolysis, a compensatory mechanism to mitigate decreased ATP production by the mitochondria. Metabolomics data demonstrates a trend towards higher levels of glycolysis intermediates in the rotenone treated group. This trend was more prominent upstream of G3P and can be related to the metabolism of G3P which is the first redox step in glycolysis as NAD+ is reduced to NADH, which can either be oxidized back to NAD+ at CI or by lactate dehydrogenase coupled to the conversion of pyruvate to lactate. There was also a trend towards an increased lactate-to-pyruvate ratio in the rotenone treated group indicating accelerated glycolysis and increased lactate production with a metabolic shift from mitochondrial respiration to glycolysis (Huckabee, 1958). Furthermore, the decrease in aspartic acid could be related to its role in the mitochondrial matrix and cytosolic redox of NADH and NAD+. All detected TCA cycle intermediates were trending towards increased levels except succinic acid, which was slightly decreased. Succinate is oxidized by complex II of the respiratory chain, which is not inhibited by rotenone. The limited group size of the metabolomics data is a limitation to the interpretation of the data.

In the *ex vivo* analyses of mitochondrial respiration, a trend towards inhibition was detected in platelets while analysis of peripheral skeletal muscle did not detect such a trend. The discrepancy between the metabolomic and respiration data of skeletal muscle could possibly be related to technical aspects of preparing the samples. As the muscle biopsies were rinsed in MiR05 buffer in preparation of respiration measurements, the rotenone was perhaps removed. The platelets, on the other hand, were suspended in plasma during the preparatory steps of the protocol and added to the final analysis as platelet-rich plasma, thereby decreasing the risk of altering the rotenone exposure during the *in vivo - ex vivo* transition. It may also be that the mitochondrial respiration in skeletal muscle was in fact not inhibited by rotenone *in vivo* and that the increase in lactate production primarily comes from other organs.

Due to the successive decrease in pH during rotenone infusion, expired VCO_2 overestimates the metabolic CO_2 production as it also encompasses the release of stored CO_2 due to a continuous leftward shift in the CO_2 - carbonic acid – bicarbonate equilibrium. The metabolic respiratory quotient (RQ) ranges from 0.7 to 1.0 depending on the relative

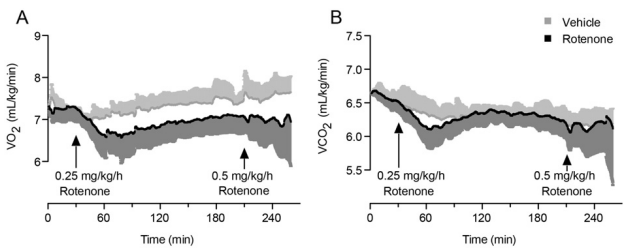

Fig. 4. Continuous indirect calorimetry. Determination of VO_2 (A) and VCO_2 (B) using indirect calorimetry demonstrated that rotenone caused a decrease in oxygen uptake and initially a decrease in carbon dioxide production which resulted in subsequent calculated increased respiratory quotient and decreased energy expenditure. During the first 30 min of rotenone infusion the oxygen uptake decreased by a mean of 8.7% ($p < 0.0001$). Data was normalized group-wise and a running median with a window of 3 min was used. Mean ± SD (one-sided shown in figure). $n = 5$ animals in each group.

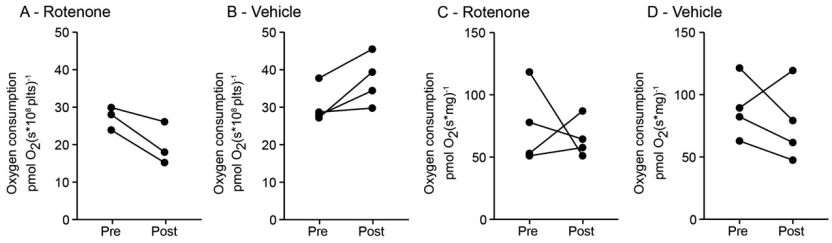

Fig. 6. Mitochondrial respiration. Mitochondrial respiration of viable platelets analyzed *ex vivo* indicated a trend towards decreased aerobic function following 3 h of rotenone infusion ($p = 0.059$) (A), compared to before start of infusion, when suspended in their own plasma. The vehicle treated group indicated a trend in the opposite direction (B). This trend was not detected in skeletal muscle fibers analyzed *ex vivo* (C–D). Individual values are shown. Paired *t*-test.

proportions of carbohydrate and fat metabolism (Krogh and Lindhard, 1920). The measured respiratory exchange ratio (RER, VCO_2/VO_2) was above 1.0 in the rotenone treated group demonstrating a partial increase in elimination of CO_2 not related to production of CO_2 in the mitochondria. As there was no steady state metabolism the decrease in energy expenditure cannot be accurately determined, but the corresponding decrease in VO_2, was as previously stated, 8.7% during the first 30 min after start of rotenone infusion.

This *in vivo* large animal model would be suitable for evaluating pharmaceutical therapies for changes in energy metabolism involving mitochondrial CI dysfunction. Our group recently published a paper presenting the concept of succinate prodrugs as a potential treatment for mitochondrial CI deficiency (Ehinger et al., 2016). It has also been suggested that standard succinate can recover mitochondrial function in septic skeletal muscle (Protti et al., 2007). Methyl succinate and heptanoate, a short odd-chain fatty acid, has also been evaluated for the treatment of CI dysfunction (Doctor et al., 1994; Hinke et al., 2007). Furthermore, methylene blue has been shown to bypass complex I and II inhibition in models of drug-induced mitochondrial dysfunction (Lee et al., 2015). These different potential pharmacological strategies have been tested *in vitro* and in small animal *in vivo* models. A potential next step in the development could be a large-animal *in vivo* model. More refined models are warranted for specific diseases, but the model presented here may be suitable for initial testing.

5. Conclusions

In conclusion, rotenone infusion decreases whole animal extraction of oxygen due to mitochondrial CI inhibition and causes a switch from mitochondrial metabolism to glycolysis. Interestingly the rather dramatic increase in lactate corresponded to a moderate decrease in VO_2. This model may be well suited for future studies of pharmacological interventions aiming at counteracting acute changes in energy metabolism due to inherited as well as drug-induced mitochondrial CI dysfunction.

Authors disclosure statement

The study was in part funded by NeuroVive Pharmaceutical AB. The listed authors, as indicated by their affiliation, have received salary

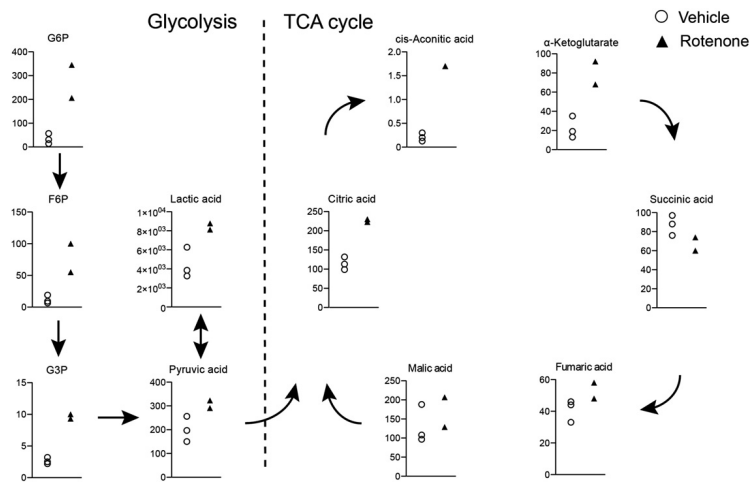

Fig. 7. Metabolomics. Analysis performed in muscle biopsies after 3 h of vehicle ($n = 3$) or rotenone ($n = 2$) infusion. G6P – Glucose 6-phosphate, F6P – Fructose 6-phosphate, G3P – Glyceraldehyde 3-phosphate. Y axis: concentration (nmol/g). Individual values shown.

support from and have equity interests in NeuroVive Pharmaceutical AB, a public company developing pharmaceuticals in the field of mitochondrial medicine.

Supplementary data to this article can be found online at http://dx.doi.org/10.1016/j.mito.2016.10.003.

Acknowledgments

The authors would like to thank Eleonor Åsander Frostner for administrative and laboratory support. The study was funded by NeuroVive Pharmaceutical, the Swedish Research Council (2012/5164), the Crafoord Foundation (2015-0879) and Swedish government project and salary funding for clinically oriented medical research (ALF-grants, M 2011/1636, M 2012/1789).

References

Brunmair, B., Staniek, K., Gras, F., Scharf, N., Althaym, A., Clara, R., Roden, M., Gnaiger, E., Nohl, H., Waldhausl, W., Furnsinn, C., 2004. Thiazolidinediones, like metformin, inhibit respiratory complex I: a common mechanism contributing to their antidiabetic actions? Diabetes 53, 1052–1059.

Brusque, A.M., Borba Rosa, R., Schuck, P.F., Dalcin, K.B., Ribeiro, C.A., Silva, C.G., Wannmacher, C.M., Dutra-Filho, C.S., Wyse, A.T., Briones, P., Wajner, M., 2002. Inhibition of the mitochondrial respiratory chain complex activities in rat cerebral cortex by methylmalonic acid. Neurochem. Int. 40, 593–601.

Carroll, J., Fearnley, I.M., Skehel, J.M., Shannon, R.J., Hirst, J., Walker, J.E., 2006. Bovine complex I is a complex of 45 different subunits. J. Biol. Chem. 281, 32724–32727.

Dimauro, S., Rustin, P., 2009. A critical approach to the therapy of mitochondrial respiratory chain and oxidative phosphorylation diseases. Biochim. Biophys. Acta 1792, 1159–1167.

Doctor, R.B., Bacallao, R., Mandel, L.J., 1994. Method for recovering ATP content and mitochondrial function after chemical anoxia in renal cell cultures. Am. J. Phys. 266, C1803–C1811.

Dykens, J.A., Jamieson, J., Marroquin, L., Nadanaciva, S., Billis, P.A., Will, Y., 2008. Biguanide-induced mitochondrial dysfunction yields increased lactate production and cytotoxicity of aerobically-poised HepG2 cells and human hepatocytes in vitro. Toxicol. Appl. Pharmacol. 233, 203–210.

Dyson, A., Simon, F., Seifritz, A., Zimmerling, O., Matallo, J., Calzia, E., Radermacher, P., Singer, M., 2012. Bladder tissue oxygen tension monitoring in pigs subjected to a range of cardiorespiratory and pharmacological challenges. Intensive Care Med. 38, 1868–1876.

Ehinger, J.K., Piel, S., Ford, R., Karlsson, M., Sjovall, F., Frostner, E.A., Morota, S., Taylor, R.W., Turnbull, D.M., Cornell, C., Moss, S.J., Metzsch, C., Hansson, M.J., Fliri, H., Elmer, E., 2016. Cell-permeable succinate prodrugs bypass mitochondrial complex I deficiency. Nat. Commun. 7.

Hinke, S.A., Martens, G.A., Cai, Y., Finsi, J., Heimberg, H., Pipeleers, D., Van de Casteele, M., 2007. Methyl succinate antagonises biguanide-induced AMPK-activation and death of pancreatic beta-cells through restoration of mitochondrial electron transfer. Br. J. Pharmacol. 150, 1031–1043.

Huckabee, W.E., 1958. Relationships of pyruvate and lactate during anaerobic metabolism. I. Effects of infusion of pyruvate or glucose and of hyperventilation. J. Clin. Invest. 37, 244–254.

Jackson, M.J., Schaefer, J.A., Johnson, M.A., Morris, A.A., Turnbull, D.M., Bindoff, L.A., 1995. Presentation and clinical investigation of mitochondrial respiratory chain disease. A study of 51 patients. Brain 118 (Pt 2), 339–357.

Ke, B.X., Pepe, S., Grubb, D.R., Komen, J.C., Laskowski, A., Rodda, F.A., Hardman, B.M., Pitt, J.J., Ryan, M.T., Lazarou, M., Koleff, J., Cheung, M.M., Smolich, J.J., Thorburn, D.R., 2012. Tissue-specific splicing of an Ndufs6 gene-trap insertion generates a mitochondrial complex I deficiency-specific cardiomyopathy. Proc. Natl. Acad. Sci. U. S. A. 109, 6165–6170.

Kilbaugh, T.J., Karlsson, M., Duhaime, A.C., Hansson, M.J., Elmer, E., Margulies, S.S., 2015. Mitochondrial response in a toddler-aged swine model following diffuse non-impact traumatic brain injury. Mitochondrion 26, 19–25.

Koene, S., Willems, P.H., Roestenberg, P., Koopman, W.J., Smeitink, J.A., 2011. Mouse models for nuclear DNA-encoded mitochondrial complex I deficiency. J. Inherit. Metab. Dis. 34, 293–307.

Krogh, A., Lindhard, J., 1920. The relative value of fat and carbohydrate as sources of muscular energy: with appendices on the correlation between standard metabolism and the respiratory quotient during rest and work. Biochem. J. 14, 290–363.

Kruse, S.E., Watt, W.C., Marcinek, D.J., Kapur, R.P., Schenkman, K.A., Palmiter, R.D., 2008. Mice with mitochondrial complex I deficiency develop a fatal encephalomyopathy. Cell Metab. 7, 312–320.

Larsen, S., Nielsen, J., Hansen, C.N., Nielsen, L.B., Wibrand, F., Stride, N., Schroder, H.D., Boushel, R., Helge, J.W., Dela, F., Hey-Mogensen, M., 2012. Biomarkers of mitochondrial content in skeletal muscle of healthy young human subjects. J. Physiol. 590, 3349–3360.

Lee, K.K., Imaizumi, N., Chamberland, S.R., Alder, N.N., Boelsterli, U.A., 2015. Targeting mitochondria with methylene blue protects mice against acetaminophen-induced liver injury. Hepatology 61, 326–336.

Paradies, G., Petrosillo, G., Pistolese, M., Di Venosa, N., Federici, A., Ruggiero, F.M., 2004. Decrease in mitochondrial complex I activity in ischemic/reperfused rat heart: involvement of reactive oxygen species and cardiolipin. Circ. Res. 94, 53–59.

Pesta, D., Gnaiger, E., 2012. High-resolution respirometry: OXPHOS protocols for human cells and permeabilized fibers from small biopsies of human muscle. Methods Mol. Biol. 810, 25–58.

Pfeffer, G., Majamaa, K., Turnbull, D.M., Thorburn, D., Chinnery, P.F., 2012. Treatment for mitochondrial disorders. Cochrane Database Syst. Rev. 4, CD004426.

Piel, S., Ehinger, J.K., Elmer, E., Hansson, M.J., 2015. Metformin induces lactate production in peripheral blood mononuclear cells and platelets through specific mitochondrial complex I inhibition. Acta Physiol (Oxford) 213, 171–180.

Protti, A., Carre, J., Frost, M.T., Taylor, V., Stidwill, R., Rudiger, A., Singer, M., 2007. Succinate recovers mitochondrial oxygen consumption in septic rat skeletal muscle. Crit. Care Med. 35, 2150–2155.

Protti, A., Fortunato, F., Monti, M., Vecchio, S., Gatti, S., Comi, G.P., De Giuseppe, R., Gattinoni, L., 2012a. Metformin overdose, but not lactic acidosis per se, inhibits oxygen consumption in pigs. Crit. Care 16, R75.

Protti, A., Lecchi, A., Fortunato, F., Artoni, A., Greppi, N., Vecchio, S., Fagiolari, G., Moggio, M., Comi, G.P., Mistraletti, G., Lanticina, B., Faraldi, L., Gattinoni, L., 2012b. Metformin overdose causes platelet mitochondrial dysfunction in humans. Crit. Care 16, R180.

Robin, E.D., 1977. Special report: dysoxia. Abnormal tissue oxygen utilization. Arch. Intern. Med. 137, 905–910.

Roestenberg, P., Manjeri, G.R., Valsecchi, F., Smeitink, J.A., Willems, P.H., Koopman, W.J., 2012. Pharmacological targeting of mitochondrial complex I deficiency: the cellular level and beyond. Mitochondrion 12, 57–65.

Schapira, A.H., Olanow, C.W., Greenamyre, J.T., Bezard, E., 2014. Slowing of neurodegeneration in Parkinson's disease and Huntington's disease: future therapeutic perspectives. Lancet 384, 545–555.

Sjovall, F., Morota, S., Hansson, M.J., Friberg, H., Gnaiger, E., Elmer, E., 2010. Temporal increase of platelet mitochondrial respiration is negatively associated with clinical outcome in patients with sepsis. Crit. Care 14, R214.

Sjovall, F., Ehinger, J.K., Marelsson, S.E., Morota, S., Frostner, E.A., Uchino, H., Lundgren, J., Arnbjornsson, E., Hansson, M.J., Fellman, V., Elmer, E., 2013. Mitochondrial respiration in human viable platelets–methodology and influence of gender, age and storage. Mitochondrion 13, 7–14.

Sue, C.M., Lipsett, L.J., Crimmins, D.S., Tsang, C.S., Boyages, S.C., Presgrave, C.M., Gibson, W.P., Byrne, E., Morris, J.G., 1998. Cochlear origin of hearing loss in MELAS syndrome. Ann. Neurol. 43, 350–359.

Sundstrom, M., Tjader, I., Rooyackers, O., Wernerman, J., 2013. Indirect calorimetry in mechanically ventilated patients. A systematic comparison of three instruments. Clin. Nutr. 32, 118–121.

Tyynismaa, H., Suomalainen, A., 2009. Mouse models of mitochondrial DNA defects and their relevance for human disease. EMBO Rep. 10, 137–143.

Vahsen, N., Cande, C., Briere, J.J., Benit, P., Joza, N., Larochette, N., Mastroberardino, P.G., Pequignot, M.O., Casares, N., Lazar, V., Feraud, O., Debili, N., Wissing, S., Engelhardt, S., Madeo, F., Piacentini, M., Penninger, J.M., Schagger, H., Rustin, P., Kroemer, G., 2004. AIF deficiency compromises oxidative phosphorylation. EMBO J. 23, 4679–4689.

Wallace, D.C., Fan, W., 2009. The pathophysiology of mitochondrial disease as modeled in the mouse. Genes Dev. 23, 1714–1736.